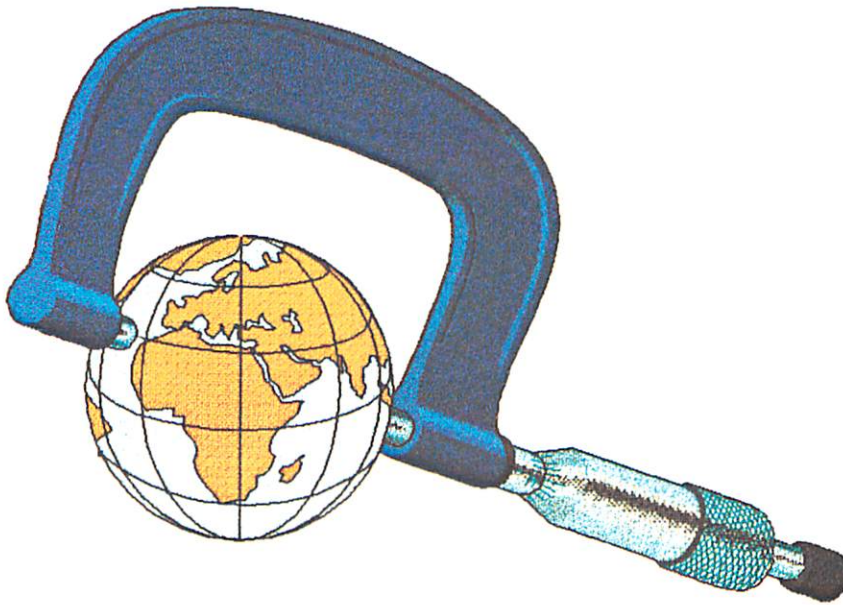


PROCEEDINGS OF THE 10th WORKING MEETING ON EUROPEAN VLBI FOR GEODESY AND ASTROMETRY



HELD AT
Centro di Geodesia Spaziale "G. Colombo"
MATERA, ITALY
on MAY 24-25, 1995

Edited by R. Lanotte and G. Bianco



PROCEEDINGS OF THE 10th WORKING MEETING ON EUROPEAN VLBI FOR GEODESY AND ASTROMETRY

HELD AT
Centro di Geodesia Spaziale "G. Colombo"
MATERA, ITALY
ON MAY 24-26, 1995

Edited by R. Lanotte and G. Bianco

Contents

- The EUROPE 1994/95 experiments: A status report from the Bonn Correlator
K. Standke, 1
- Correlator Operations at the Max-Planck-Institut für Radioastronomie in Bonn
A. Müskens and W. Alef, 11
- Medicina Station: status and policy report
F. Mantovani, A. Orfei and P. Tomasi, 16
- Radioastronomy at the NASA Madrid Deep Space Communications Complex during the year 1994.
A. Alberdi, J.A. Perea and A. Rius, 22
- Geodetic VLBI studies with the Yebes radiotelescope.
Yebes VLBI team, 27
- VLBI at Ny-Ålesund Space Geodetic Observatory: Station Report 1993-1995
B.R. Pettersen, 29
- Geodesy VLBI at the Onsala Space Observatory: Station Report, 1994-1995
G. Elgered, T.R. Carlsson, T.M. Carlsson, R.T.K. Jaldehag, P.O.J. Jarlemark, J.M. Johansson, B.I. Nilsson, B.O. Rönnäng and H.G. Scherneck, 32
- Station Report for Effelsberg - May 1995
R.W. Porcas, 38
- The Radioastronomical Station of Noto Geodetic status report
V. Tornatore, 39
- A description of the Medicina 32m dish upgrade
A. Orfei, G. Maccaferri, S. Mariotti, M. Morsiani and G.P. Zacchiroli, 45
- Matera VLBI station: Status report
G. Bianco, A. Cenci, G. Colucci, D. Del Rosso and L. Garramone, 49
- A concept for real-time VLBI
H. Schuh, 51
- The Use of the Datahighway for Real-Time Correlation of VLBI-Data
H. Hase, 57
- Status Report ERS/VLBI Station O'Higgins Antarctica
A. Reinhold and R. Wojdziak, 66
- Status Report VLBI - calculations at IfAG, Agency Leipzig
V. Thorandt and D. Ullrich, 68
- Temperature Stability of the Onsala 20-m Antenna and Its Impact on Geodetic VLBI
G. Elgered and T.R. Carlsson, 69

- Managing Geodetic VLBI in Europe: The European Crustal Motion Network
J. Campbell, 79
- Analysis of the European Geodetic VLBI Experiments with a Free Network Concept
N. Zarraoa, J. M. Juan and A. Rius, 87
- Geodynamical Parameters Determined by VLBI
R. Haas, J. Campbell and H. Schuh, 91
- VLBI in the Far North. A closer look
N. Zarraoa, 103
- Present status of the VLBI data analysis activities at the Matera Space Geodesy Center
R. Lanotte, G. Bianco and M. Fermi, 109
- Investigations of Thermal Height Changes of Geodetic VLBI Radio Telescopes
A. Nothnagel, M. Pilhatsch and R. Haas, 121
- Tropospheric delays estimated from VLBI, WVR and GPS. A comparative study
A. Rius, G. Elgered, J.M. Johansson, S. Keihm and N. Zarraoa, 134
- GPS as a tool for estimating the ionospheric effects on the VLBI observables
A. Rius, J.M. Juan, M. Hernández-Pajares, E. Sardón and A. Alberdi, 141
- External wet tropospheric corrections during a two-week-long VLBI campaign
T.R. Carlsson, G. Elgered and J.M. Johansson, 148
- A VLBI Survey with the European Geodetic Network: preliminary results
F. Mantovani, W. Alef, M. Bondi and D. Dallacasa, 154
- A "Cluster-Cluster" VLBI experiment
M.J. Rioja, L.I. Gurvits, R.T. Schilizzi, A. van Ardenne, A.-J. Boonstra, J. Bergman, H.R. Butcher, A.R. Foley, H. Kalmann, T.A.Th. Spoelstra, H. van S. Greve, W. Alef, M.J. Claussen, E.B. Fomalont, Y. Asaki, T. Sasao, 160
- Success and Limitations of X- and S/X-band Astronomical Observations with the EVN and The Geodetic VLBI Network
W. Alef and M. Rioja, 164
- Structure and Astrophysics of Geodetic VLBI Sources
S. Britzen and T.P. Krichbaum, 172
- Absolute proper motion in the quasar 4C39.25
J.C. Guirado, A. Alberdi and J.M. Marcaide, 181
- Gravitational lens image astrometry
R.W. Porcas and A.R. Patnaik, 188
- Did the Matera Radiotelescope Really Observe the Jupiter/SL9 "T" impact ?
G. Bianco, L. Garramone and R. Lanotte, 193

INTRODUCTION

This book is made of the written version of all the communications presented at the 10th Working Meeting on European VLBI for Geodesy and Astrometry, held at the Italian Space Agency's Centro di Geodesia Spaziale "Giuseppe Colombo", Matera, Italy, from 24 to 26 May, 1995.

In about 200 pages, 32 papers describe the state of the art of the VLBI activities in Europe, going from the operational aspects to the scientific results in the fields of Geodesy and Astronomy.

As a matter of fact, the results presented at the meeting demonstrate without any doubt the great power of VLBI: inter-station baseline evolution is routinely monitored with a precision consistently better than 1 mm/y, while earth orientation parameters are being solved for with a precision consistently better than 0.001 arcsec; a similar precision in the observation of the radio source structure is the base of a number of astrophysical research projects, such as gravitational lens monitoring.

On the contrary, by looking at the management aspects, it turns out that the international VLBI network is seriously jeopardized by lack of funds and other growing difficulties, first of all as a consequence of the dramatic budget cuts that NASA is continuing to force with respect to its VLBI projects. This, in turn, results in a more and more important role of the European network with respect to the worldwide community, which should be properly sustained both by the national Agencies and by the European Union.

The message is clear: the European Geodetic community should relentlessly look for innovating techniques and research projects devoted to the monitoring of global parameters for which the VLBI technique is unique in terms of reliability, precision and coverage. Moreover, a growing effort is needed to effectively merge all the available space geodetic techniques, taking in proper account each one's advantages and drawbacks, with an eye constantly kept on the evolving technology.

Giuseppe Bianco
Matera, November 1995

The EUROPE 1994/95 experiments: A status report from the Bonn Correlator

Kurt STANDKE^{1,2}

¹ *Geodetic Institute of the University of Bonn (GIUB), Germany*

² *Max-Planck-Institut für Radioastronomie, Bonn, Germany*

Abstract. The EUROPE experiments are now being performed in their 4th year. This has resulted in a long and well sampled data base for studying crustal motion within Europe. The amount of data has grown rapidly:

- In 1994 and 1995 six experiments were scheduled: two more than in 1993.
- The participation of Crimea and Ny Ålesund increased the number of participating antennas to a maximum of 9. Yebes plans to join in mid 1995. Thus the typical number of baselines per experiment has increased from 15 to 28.

The total amount of data increased in 1994 by a factor of 2.44 with respect to 1993.

Some problems had to be solved in the '94 experiments:

- The S band interference in Matera and Medicina could be avoided with a new EUR-SX frequency setup.
- The Noto Data Acquisition Rack had only 6 BBCs. Therefore a special sub-group of 4 X-band and 2 S-band frequencies was chosen. With the help of a special fringe fitting technique it was possible to correct for the ionospheric delay and obtain a reasonable data quality.

Data analysts (at Greenbelt, Bonn, Matera, Bologna, and recently also St.Petersburg) gave the EUROPE experiments good ratings once more.

1 EUROPE's Statistics 1990 – 1995

The EUROPE experiments have been performed since the end of 1990. The purpose of these experiments is to measure the baselines between the cooperating European stations with the highest precision possible. The number of stations taking part has increased during this period. The network first consisted of six antennas: Wettzell, Onsala, Matera, Noto, Medicina and DSS65 near Madrid. In 1-2 experiments per year Effelsberg participated also. In 1994 two new stations were included: Crimea and Ny Ålesund. In EUROPE3-95 Yebes will take part for the first time.

In Figure 1 the increasing number of participating antennas and therefore baselines from 1990 – 1995 is shown.

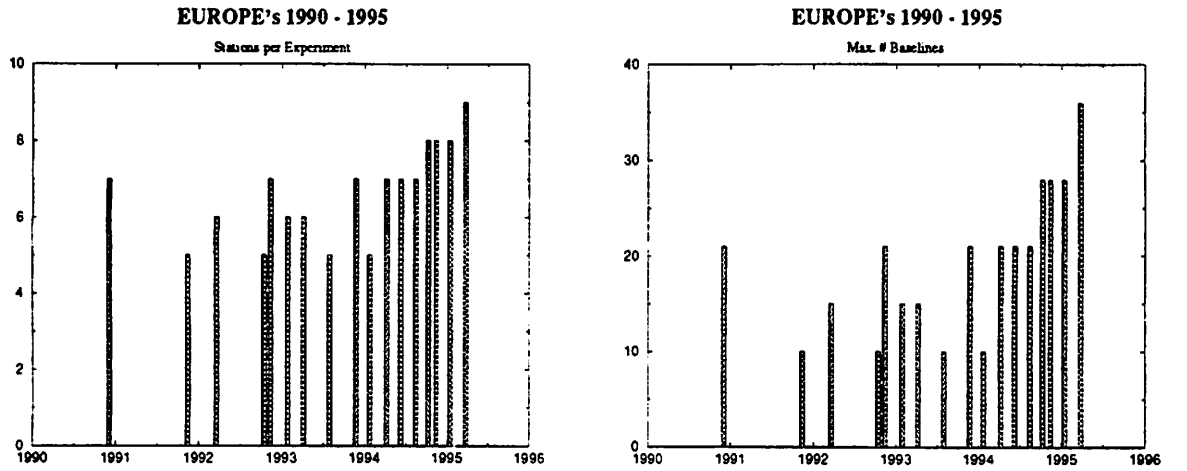


Figure 1: *Number of stations and baselines in the EUROPEs 1990 – 1995*

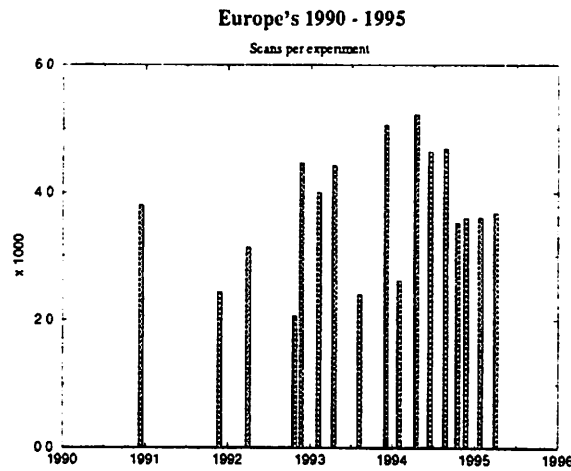


Figure 2: *Number of observations per experiment in the EUROPEs 1990 – 1995*

The total number of observations per experiment shows a different trend (see Figure 2). Due to the increased number of stations spread over an area ranging from Sicily to Crimea and Spitzbergen, scheduling has become more complex. To create a uniform sky distribution many scans with only a subnet of the total configuration have to be scheduled. Thus the

total number of scans per experiment has decreased (Figure 2).

The load on the correlator is mainly determined by the number of 'passes' needed for an experiment. To get acceptable low tape synchronization times at the Bonn correlator, in one pass a maximum of 11 baselines can be correlated with a maximum of 7 play back drives in use. (Status: spring 1995; see also report of A. Müskens and W. Alef). In order to find the best compromise between the network size and efficient correlator use, the optimal number is 8 antennas per experiment! The addition of a 9th station would increase the amount of work at the correlator by 1/3, as an additional 4th pass becomes necessary! (see equation ??). Therefore the goal of the EUROPE scheduling is to use 8 antennas for each experiment, but exceptions from this like e.g. in EUROPE2-95 and EUROPE3-95 have been made.

2 Modification of S-Band Frequency Setup

A major problem in the geodetic experiments before 1994 at Matera and Medicina was interference in several S-band frequency channels. This was presumably caused by TV links, which in Italy work in the affected frequency range, but a precise determination of the origin was not possible. So the only solution for this problem was a change of the S-band frequency setup, which had to be done with regards to the delay resolution function. Since in Medicina S1 (2217.99 MHz) and in Matera S6 (2302.99 MHz) were spoiled, these frequencies were changed as shown in Figure 3. This solved the interference problems completely.

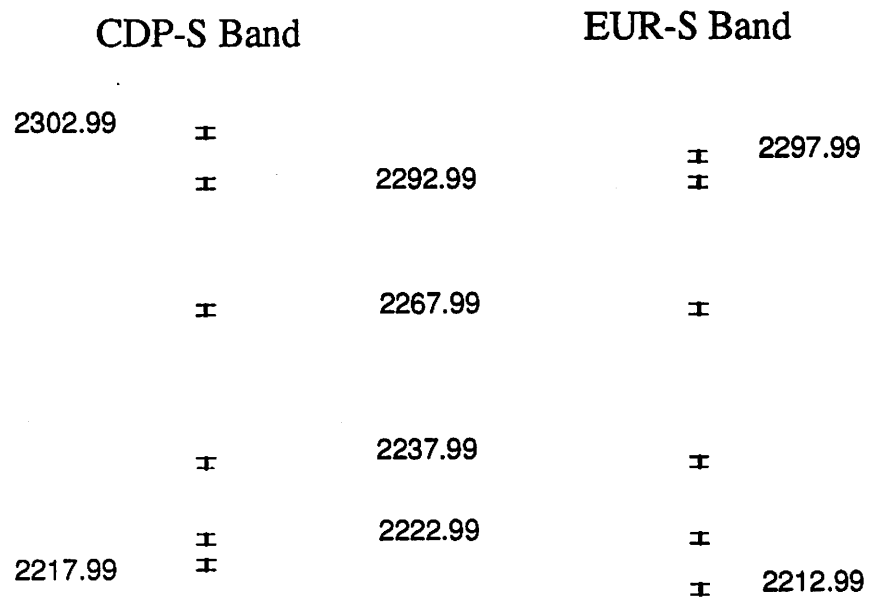


Figure 3: *CDP and EUR-S Band frequency setup; (Frequencies in MHz)*

3 Noto Frequency Setup

In July 1993 the Mark III Data Acquisition Rack (DAR) from Noto was brought to the new antenna in Ny Ålesund. Noto was left with an incomplete VLBA DAR with only 6 Base Band Converters (BBC's) (since March 1995: 8 BBC's). So the original EUR-SX frequency setup, which needs 14 BBCs had to be modified for Noto, again with regards to the delay resolution function. Due to the small ionospheric contributions to the delay at that time, it was possible to get the ionospheric path length corrections from S-band with only 2 recorded frequencies. The other 4 BBCs were used for X-band.

	8 BBC's	4 BBC's	6 BBC's
8570.99	-	-	-
8550.99	-		-
8500.99	-		-
8420.99	-	-	
8310.99	-		-
8250.99	-	-	
8220.99	-		-
8210.99	-	-	-

Figure 4: *Noto X-Band frequency setups (Frequencies in MHz); 8 BBCs: Standard setup*

To avoid the fitting of the 'fringe peak' on a sidelobe of the delay resolution function, the fringe fitting was done only within small multi-band delay windows covering only the main peak of the delay resolution function. The use of the new Haystack program FOURFIT, which runs on UNIX machines, made the necessary refringing possible within an acceptable amount of time ($\sim 30 \times$ faster than FRNGE on the old HP 1000/A990 computer).

For the first experiments, Noto was scheduled in 'tag-along' mode, but the results from these

test were so promising that Noto was scheduled again as a full station since EUROPE6-94. In EUROPE2-95 8 (6 X-band; 2 S-band) BBCs have been available and in EUROPE3-95 hopefully 12 (8 X-band; 4 S-band) BBCs will be usable. The different setups are shown in Figure 4 and 5.

6 BBC's		2 BBC's	4 BBC's
2297.99	I		I
2292.99	I	I	
.			
2267.99	I		I
.			
2237.99	I		
.			
2222.99	I	I	I
.			
2212.99	I		I

Figure 5: *Noto S-Band frequency setups (Frequencies in MHz); 6 BBCs: Standard setup*

4 The individual experiments

The histogram in Figure 6 shows the number of observations loaded into the Calc&Solve databases relative to the scheduled number of observations (in %). The values vary between ~55% (very poor!) and 97 %. The reasons for these differences are given in the following sections, each referring to one experiment.

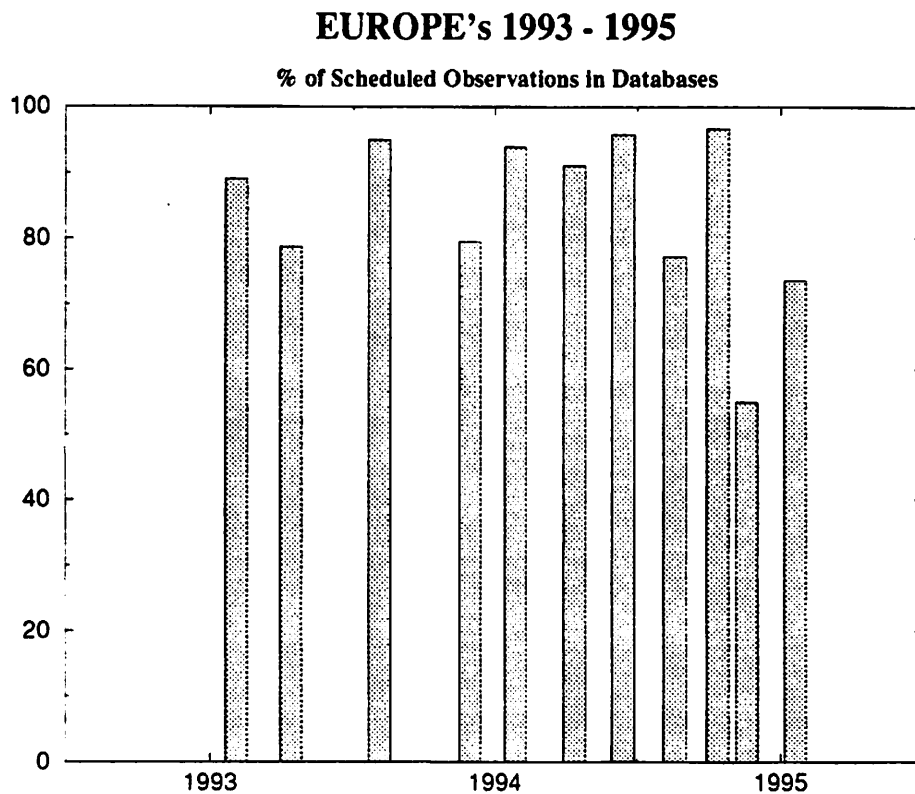


Figure 6: *Percentage of observations in the EUROPE databases*

- EUROPE1-94: Start: February 9th, 20:00 U.T.; 5 antennas: Wettzell, Matera, Medicina, Madrid, Noto:
 - Madrid showed no fringes. Presumably the formatter reset button was not pushed after last power on;
 - Matera and Medicina again had strong interferences in S-band. Thus the S-band data had to be refringed without the frequency channels S1 and S6;
 - Noto observed for the first time with the reduced frequency setup (6 BBC's);

All data were refringed with the new Haystack fringe fitting program 'FOURFIT'. The comparison of these data with the output from the old 'FRNGE' software showed almost identical results. Differences in the CALC&SOLVE solutions were not detectable.

- EUROPE2-94: Start: April 27th, 20:00 U.T.; 7 antennas: Wettzell, Madrid, Effelsberg, Matera, Medicina, Onsala, Noto
 - Madrid showed no fringes in the first hour of the experiment. After 7 hours the subreflector moved into a limit and stuck there. This resulted in serious pointing problems which affected mainly X-band, due to the smaller antenna beam at that frequency. In the following experiments the subreflector was kept in a fixed position.
 - In Effelsberg the antenna control system had been changed. This resulted in a longer time offset between commanding and start of slewing than that used for the creation of the schedule. In many scans the antenna was ~ 20 sec late on source. But this did not give problems for data analysis, because the minimal SNR's (X-band: 20; S-band: 15) could be achieved nevertheless, due to the large collecting area of the Effelsberg dish.
 - Again strong interference spoiled the S-band data from Matera and Medicina. In Medicina the spare BBC was used for the affected frequency S1. Since the interference still occurred, instrumental effects could be excluded. It was decided that the next experiment should be done with the modified S-band setup.
- EUROPE3-94: Start: June 29th, 14:00 U.T.; 7 antennas: Wettzell, Madrid, Crimea, Matera, Medicina, Onsala, Noto
 - With the new EUR-SX setup the interference problems in Medicina and Matera could be solved completely.
 - Crimea participated in a EUROPE experiment for the first time. Fringes could be detected in $\sim 4\%$ of the observations only. The malfunction presumably was caused by pointing problems.
- EUROPE4-94: Start: August 31st, 20:00 U.T.; 7 antennas: Wettzell, Madrid, Crimea, Matera, Medicina, Onsala, Noto
 - Crimea participated successfully in a EUROPE experiment for the first time.
 - In Wettzell the write head was totally worn out. The data recorded in reverse direction could not be used, thus leading to 50% data loss. Shortly after the experiment the head was replaced.
 - The Noto weather data shows a strange behaviour. Constant offsets in temperature, pressure and humidity exist between consecutive measurements.

- EUROPE5-94: Start: October 26th 31, 20:00 U.T.; 8 antennas: Wettzell, Ny Alesund, Madrid, Crimea, Matera, Medicina, Onsala, Noto
 - Ny Alesund participated for the first time. The data quality was o.k.
 - Crimea showed clock instabilities. This was visible during the correlation and in the data analysis as well.
 - The Noto humidity data showed values between 85 % and 140 %

- EUROPE6-94: Start: December 28th, 20:00 U.T.; 8 antennas: Wettzell, Ny Alesund, Madrid, Crimea, Matera, Medicina, Onsala, Noto

This was the worst experiment since 1993. Only ~ 55 % of the scheduled scans could be used for the analysis.

 - Crimea did not observe because they could not get the schedule in time. To avoid problems like these in the future a second directory for the schedule distribution was created at the MPIfR.
 - Of three tapes recorded in Noto only the first one arrived at the correlator. At present now it is not clear whether the two missing tapes disappeared in transit or at the MPIfR. Thus about 60 % of the Noto recordings were lost.
The phase calibration signal was used now in Noto.
 - In Matera ~ 30 % of the scans showed no data for unknown reasons. This problem was not investigated further, because it did not occur again in the next experiment.
 - Shortly before the experiment an ‘antenna runner’ problem occurred in Madrid. This made a reduction of the maximal antenna slew velocities necessary. In a modified schedule Madrid was ‘tagged along’ with new, lower values for the slew speed.

- EUROPE1-95: Start: February 1st, 20:00 U.T.; 8 antennas: Wettzell, Ny Alesund, Madrid, Crimea, Matera, Medicina, Onsala, Noto
 - In Noto ~ 2/3 of the observations were lost mainly due to bad weather conditions.
 - In Crimea X-band freq. X6 (8500.99 MHz) was missing.
 - In Medicina the humidity data was not measured.

- EUROPE2-95: Start: April 12th, 20:00 U.T.; 9 antennas: Wettzell, Effelsberg, Ny Alesund, Madrid, Crimea, Matera, Medicina, Onsala, Noto
 - Noto used the frequency setup with 8 BBCs. The assignment of frequency channels to the recorded tracks was different from standard. Tracks were re-ordered during playback via the MK4 recorder cross- point switch. The resulting data looked fine.

- In Madrid no Log file was recorded. The missing tape footage information thus were ‘faked’ values from the schedule.
- On May 18th (about 5 weeks after the experiment!) the tapes from Crimea arrived in Bonn.

After correlation the Calc&Solve databases are created and calibrated. They are put on an anonymous ftp account at the MPIfR in order to make them accessible to the community of analysts. At the moment the data gets analysed at 5 different locations: Greenbelt, Bonn, Matera, Bologna, and recently also St.Petersburg. The EUROPE experiments normally get good records from those places, so that it can be called a successful campaign (see also J. Campbell, this issue). A continuation of these experiments for coming the next years therefore is most desirable.

Correlator Operations at the Max-Planck-Institut für Radioastronomie in Bonn

Arno MÜSKENS, Walter ALEF

*Geodetic Institute of the University of Bonn (GIUB), Germany
Max-Planck-Institut für Radioastronomie, Bonn, Germany*

Abstract

The correlators at the Max-Planck-Institute for Radioastronomy (MPIfR), Bonn have played an important role in European VLBI since the mid-seventies catering to the needs of astronomers and geodesists. The operation at Bonn has been supported additionally by the Geodetic Institute of the University of Bonn (GIUB) and later by the Institute for Applied Geodesy in Frankfurt (IFAG). In the period 1993–94 the backlog at the correlator increased due to the size and the number of experiments observed in MK3 mode. With the arrival of three new VLBA/MK4 style playback drives and the completion of the re-built old MK3 correlator this backlog has now been significantly reduced, although the demand for correlator time both from astronomy and geodesy remains high. The present MK3 processor configuration at the MPIfR in Bonn is shown and the short and medium-term plans are presented. A summary of the correlator usage by astronomers and geodesists is also presented.

The last few years

In its first years the MK3 processor consisted of three tape drives and six correlator crates. At the end of 1989 four playback drives were available and two of these playback units were equipped with narrow track heads.

In 1990 the MK3A processor became operational with 12 correlator crates and 5 MK3A (narrow track) playback recorders — doubling the correlator capacity. The MK3A correlator design of Haystack had been modified by MPIfR from the expensive wire-wrap technique to the cheaper and more reliable multi-wire boards. The old MK3 correlator was mothballed.

EC funds were used to buy a 6th playback drive. This as well as an existing drive were successfully upgraded to the VLBA/MK4 standard and have been integrated into the processor. The playback quality of the VLBA/MK4 drives is nearly 2 orders of magnitude better than that of the original Mk3A drives. From the same EC funds a VLBA/MK4 prototype had been developed by Penny&Giles. It was tested in Bonn and increased the number of available playback drives at the processor to 7.

In 1992 MPIfR, IFAG and GIUB agreed to resurrect the old MK3 correlator and since early 1994 it is fully operational. IFAG provided 3 new VLBA/MK4 playback drives and the Bonn geodesists contributed their HP1000/F computer and some peripherals. The cooling system as well as the manpower was provided by MPIfR. As part of the agreement 40% of the total correlator time has been reserved for geodetic correlation since early 1994. In order to enable correlation with MK4 drives on the old MK3 correlator, an improved MK4 speed control was developed at MPIfR and has been installed in all MK4 drives more than a year ago. This speed self-calibration also improves the speed of tape synchronisation on both correlators. Thus data loss due to tape synchronisation could be reduced, which is especially important for geodetic and astrometric observations with short scans and many stations.

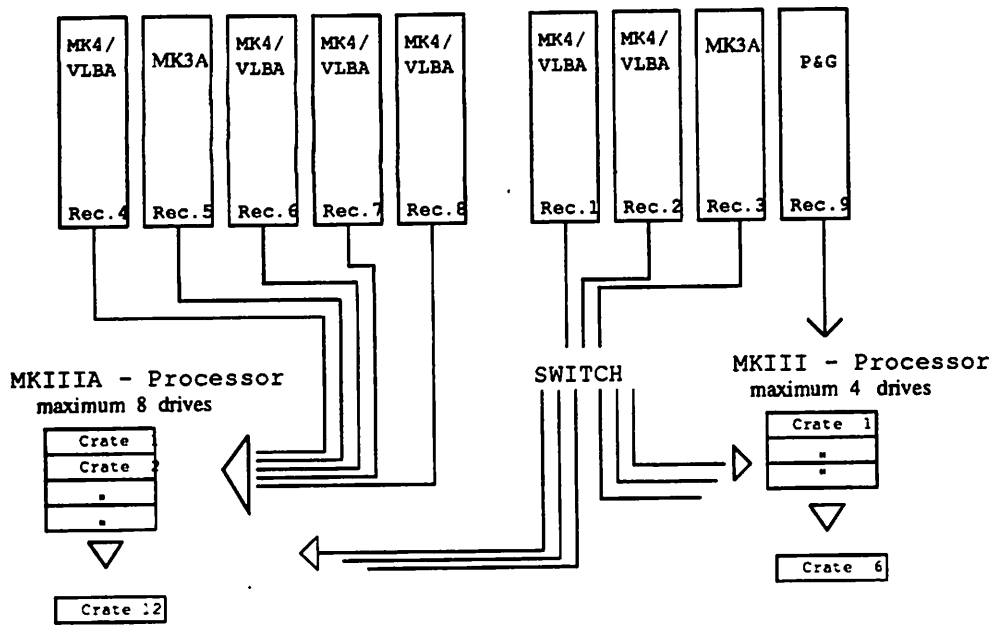


Fig.1: Processor diagramm

Present status

After the very successful modification of a MK3A style playback unit to VLBA/MK4 standards, it was decided to upgrade all the remaining MK3A tape drives. The improved playback quality and the superior speed control would make the correlation process significantly more robust. At the time of this meeting only 2 of the 8 correlator tape drives are still of the original MK3A design. One tape drive is being upgraded in the lab.

The European correlator centre at MPIfR operates both correlators in parallel (Fig. 1). Six VLBA/MK4, 2 MK3A, and one Penny&Giles tape drive are connected to both correlators and can be assigned to either correlator with some flexibility.

After extensive re-building the old MK3 correlator has been successfully integrated into the processor centre. It is mainly used for fringe search, tests and for correlation of small experiments and spectral line observations.

number of stations	4	5	6	7	8	9	10	11	12
baselines	6	10	15	21	28	36	45	55	66
Mode A (56MHz)	1	2	3	4	5	6	8	10	11
Mode B/C (28MHz)	1	1	2	2	3	4	5	5	6
Mode E (14MHz)	1	1	2	2	3	3	4	4	5

Table 1: number of passes needed for correlation

The bigger MK3A processor is used for production correlation with typically 5 to 7 tape drives for nearly 18 hrs/day (6570 hrs/year), except for occasional maintenance. Table 1 summarizes the current capabilities of the MK3A processor in Bonn. The MK3 processor is used for production correlation mostly during the night and on weekends depending on how many tape drives are not being used on the MK3A correlator.

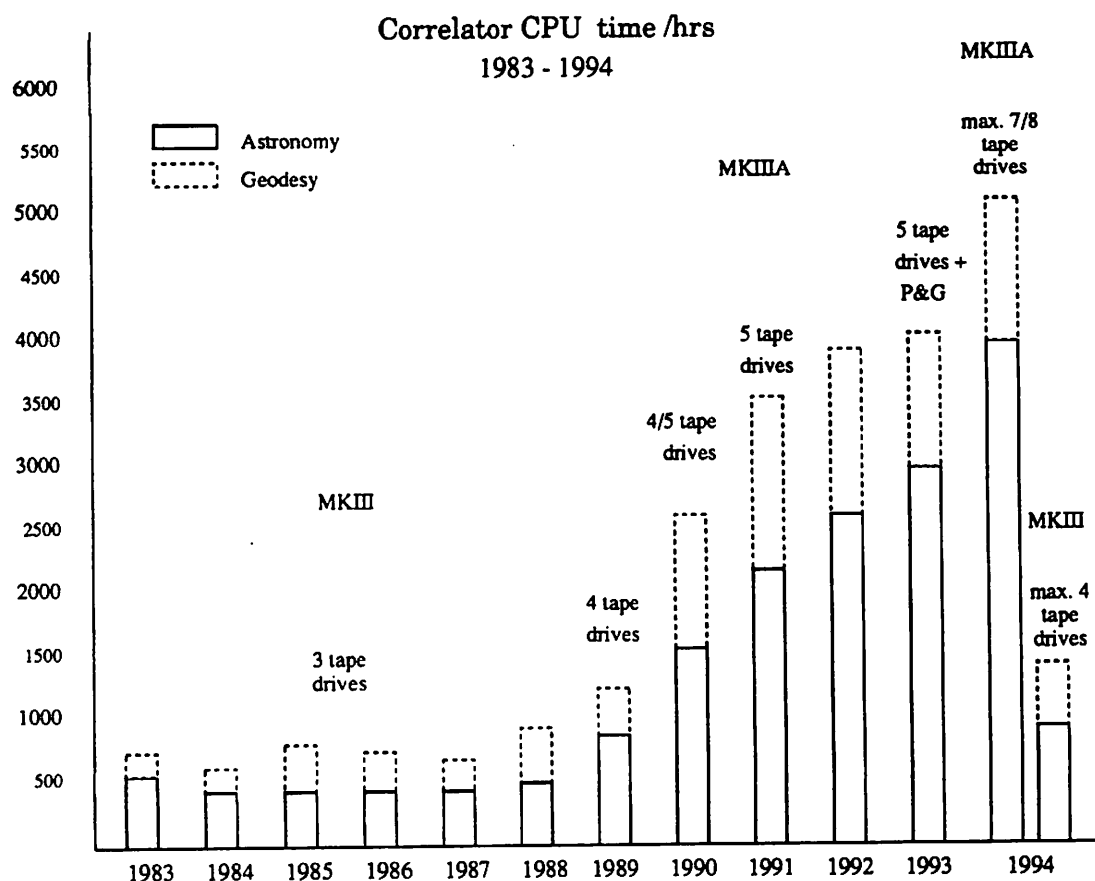


Fig.3: correlator usage time of astronomy and geodesy

Statistics

The histogram (Fig.2) of the annual correlator usage shows an increase since the early eighties. The re-installed MK3 correlator helped to increase the throughput by about 20%, as in addition the daytime working hours can now also be used for production correlation.

In 1994 the correlation of astronomical data profitted most from the 3 new tape drives and the increased amount of available correlation time for production. This was mostly due to a 6 months backlog for astronomical observations at the beginning of 1994, which was reduced to nearly zero in March 1995, and more rapid correlation of geodetic observations.

VLBI Software

The follwing software is presently installed on various computers:

- Schedule preparation:
 - SKED/DRUDG (mostly for Geodesy) on several HP9000/7xx computers under HP-UX.
 - PC-SCHED (only for Astronomy) for MS-DOS. runnig under SoftPC on several HP9000/7xx computers

- Correlation:
 - (Not quite) latest version running on HP1000/F (2×) and HP1000/A990¹.
- Postprocessing:
 - Latest version of Haystack software and MPIfR antenna based fringe fitting software on HP1000/A990.
 - Nearly latest version of Haystack's UNIX based MK3 software (HOPS) on several HP9000/7xx computers. MPIfR's antenna based fringe fitting software is being ported to UNIX as well. Standard fringe fitting and archiving will be moved from the HP1000/A990 to UNIX in the near future.
 - CALC/SOLVE on several HP9000/7xx computers.
 - Very latest NRAO AIPS 'TST' version ("Midnite" Job) for astronomical analysis

Personel

The increased number and size of observations was processed by unchanged personel. The processor group is led by a scientist. Two operators are responsible for running the correlator and tape handling. One engineer and two technicians are in charge of upgrading the MK3A tape drives as well as maintaining them including the correlator hardware. One scientist devotes more than half of his time to supervise the MPIfR in-house correlation and to maintain the correlator and system software. One scientist supported by JIVE is responsible for supervising all non MPIfR-based EVN experiments. Four students operate the correlator during weekends and nights (15hrs/week/student).

The EVN quality monitoring 'CAL' observations are processed with high priority supported by one additional scientist from JIVE. These 'CAL' observations, which are being run during standard network sessions since 1993, have helped to improve the performance of the EVN significantly.

The Bonn geodesists have operated their correlation independently of the astronomers from the very beginning. They have 1.5 scientists who are responsible for all geodetic experiments processed on the MPIfR correlator. An additional scientist supported by the EC is in charge of all the EUROPE campaigns. The tasks of these 2.5 people are:

- Schedule preparation of all experiments correlated in Bonn
- Preparation of correlator control files.
- Fringe search.
- Supervise correlation
 - Organizing ten trained students (7.5hrs/week/student) who do the actual correlation process.
 - Verification of the correlation results and setting up possible re-correlation.
- Management and tape logistics (logistics are organized together with MPIfR staff).

¹The dribble mode is not yet implemented at Bonn.

As a great benefit it turned out that three of the four main geodetic VLBI tasks (*Schedule preparation, Recording, Correlation and Analysis*) are done by one group — the Bonn Geodesists. This allowed a tight feedback loop and resulted in high motivation of the people involved, complemented by the excellent work done at the participating geodetic stations.

Outlook

In 1993 it has been agreed between the MPIfR (Bonn), IFAG (Frankfurt) and the geodetic group of the Bonn University to jointly buy and operate a MK4 correlator. As part of this agreement IFAG has ordered a correlator from Haystack/NASA for delivery in 1997. MPIfR will provide the housing, the cooling system, the manpower and its 6 tape drives upgraded to MK4 standard. IFAG will provide upgrades for its 3 tape drives. MPIfR and the geodetic community will use this new correlator on a 50/50 basis.

MK4 is the new data acquisition system which will increase today's recorded bandwidth by a factor of about 18 to over 1 Gigabit/sec. The factor 4 increase in sensitivity will permit the use of smaller antennas and weaker radio sources to fill in the celestial reference frame and will provide additional observations for improved geodetic analysis. The new MK4 correlator design and bandwidth will significantly improve VLBI data processing capacity and speed.

The successful collaboration between astronomers and geodesists in the recent years have shown that this should be a good way forward for both branches of science also in the future, in order to guarantee and maintain the high standard of scientific work from which both sides are able to benefit.

Medicina Station: status and policy report

F. Mantovani¹, A. Orfei¹ and P. Tomasi^{1,2}

¹ Istituto di Radioastronomia del CNR, Bologna, Italy

² Istituto di Tecnologie Informatiche Spaziali del CNR, Matera, Italy

Abstract

In this report we like to briefly present the observing activities at the Medicina Station in VLBI and as a single dish during the last couple of years. The Medicina antenna is in operation since 1985. It is the time for a plan which makes the station management more easy, safe and as much as automate as possible.

The presentation will be divided in three sections: observing activities, upgrading and activities more related with geodynamics.

Observing activities

The Medicina Antenna is one of the dishes of the European VLBI Network. As such, it takes part to the observations scheduled by the network itself and/or with the VLBA along the year. This means that the dish is involved in coordinated observations for **~100 days** (and nights) a year, generally planned for source imaging on the milli-arcsecond scale.

Besides, there are observations scheduled by the Geodetic Network for **~10 days** a year which are mainly devoted to accurate measurements of the baseline length between stations and polar motion.

There have been also cases in which the VLBI observations were organized outside the EVN on 'ad hoc' bases. The main projects have been: *a)* monitoring observations of the SN1993J in M81, of the quasars 3C273 and 3C345; *b)* surveys of H₂O and OH masers for candidates for Space VLBI and imaging of a sample of BLac objects and radio galaxies.

The remaining time available on the antenna was dedicated to *single dish* observations. These observations were mainly spectral lines. The main aim was to produce a catalogue of H₂O masers (see for example Brand et al. 1994) at 22 GHz and to make a list of methanol masers at 6 GHz and 12 GHz. Observing time was also dedicated to special astronomical events like the impact of the Shömaker-Levy9 comet with Jupiter and the tracking of the Ulysses probe for investigations on gravitational waves (Bertotti et al. 1995).

Upgrading of the Station

The upgrading of the Medicina Station concerns the instrumentation (acquisition terminals), the antenna, the driving computer.

Instrumentation

The terminal used till now in VLBI is a Mark3A terminal. This terminal is going to be upgraded to MarkIV, which means mainly to record radio signal faster and with a wider bandwidth. Spectral lines observations are done using an 1024 autocorrelator. Recently a spectrum analyzer with 128,000 channels has become available at the station.

A polarimeter have also been built for palarization measurements of the galactic background (Cortiglioni et al. 1995). This new equipment will also provide very useful information on the performances of the receivers. Infact, polarization VLBI data recorded at the Medicina Station seem to suffer by cross-talk between the LHC and the RHC polarization at $\lambda 18$, $\lambda 6$ and $\lambda 3.6\text{cm}$.

Antenna

At present, there are two sets of receivers available on the antenna. They have two different locations. In the primary focus of the dish we have a 'box' containing cooled, dual channel receivers at 8.4/2.3 GHz, 22 GHz and 1.6 GHz. These receivers are under computer control and the observing frequency can be changed in a few minutes. The remaining receivers are located in the secondary focus. The vertex room (secondary focus of the dish) is organized in such a way that the following receivers, 5 GHz, 6 GHz, 12 GHz, 15 GHz (under construction) and 43 GHz can be operative one at a time. The observing frequency in this configuration can be changed manually in ~ 3 hours. A more heavy work is required to pass from observing frequencies that are in the primary focus to those that are in the secondary focus. In that case one has to dismount the 'heavy' subreflector from the antenna.

As it appears clear from the above description, the antenna is not really flexible in changing the observing frequency. The modern radioastronomical observations do require dishes that are *flexible in changing frequency*. The plan for upgrading the Medicina antenna will be presented in more detail by Orfei et al. (these proceeding; see also Orfei et al. 1993). Summarizing, the two sets of receivers above will be located in both the primary and secondary focus, as it is at present. However, the set of receivers located in the secondary focus will be permanently mounted in the vertex room and kept cooled. The subreflector will have a new designed. It will be lighter and it can automatically be tilted and focused pointing the feeds of the receivers round-located in the vertex room. Moreover, the subreflector shall be shifted from its position in case one likes to pass from primary to secondary focus receivers. All the operations will be under computer control and a single operator will be able to change the observing frequency in a few minutes.

We mentioned that a 43 GHz receiver is now available at Medicina. Actually, fringes were found during the February 1995 EVN Session. However, the dish was built with specification in order to observe up to 22 GHz with a good efficiency. To be able to observe at 43 GHz with a reasonable efficiency, we need to improve the antenna pointing changing the encoder electronics and using a pointing model which takes care of thermal effects on the antenna structure.

Station Management

All the operation briefly described above will be under computer control. The computer in charge is a PC486 which mounts the Field System version 8.27 under the VENIX operating system (Linux in the near future). This computer will be connected via Internet. Thus the operator can load directly an observing schedule from a remote computer (ASTBO1 in Bologna, Istituto di Radioastronomia, in case of VLBI observations), run the observations and deposit the observing logs immediately after the observations where requested. Information useful at the VLBI correlators like the station clock offset (Formatter-GPS) will be automatically loaded and send to the archive computer ASTBO1.

Geo-activities

The Medicina Station is deeply involved in geodetic activities. The main duty is of course to take part to the VLBI projects for Geodynamics. The dish do observe the experiments planned for the projects EUROPE, POLAR and GLOBAL-TRF. The data sets from these projects, together with the existing data in the VLBI data base, can be analysed at the Istituto di Radioastronomia. The geodetic group runs CALC 8.1 and SOLVE 5.022 on a HP9000/715. A HP9000/380 in cluster with the previous one is also available. In total, the space on disk available on these workstations is of 11 Gbytes with ~ 100 databases already stored. The plan is to install the whole set of VLBI experiments as soon as possible. The geodetic group is regularly running global solutions on European databases spanning from 1988 up to 1994. Informations up to April 1994 on position and station velocities in Europe were recently presented (Tomasi et al. 1995). Including experiments up to December 1995, for many european baselines it has been found that the baselines length related to the last six months experiments are off the previous linear fitting (see Fig. 1). This problem is under investigation.

Nearby the antenna a Laser Ranging pad is available. The station was visited twice by Mobile Laser Ranging in the frame of the Wegener project. Only during the second visit good data were taken. The next mobile SLR mission to Medicina is planned for the Autumn 1995. A monument for a permanent GPS receiver (Turbo Rogue) has been founded by the Italian Space Agency (ASI) and the receiver will be operative quite soon. The station is also involved as a reference point in projects like SELF which aims to measure the mean sea level variation. Several measurements were performed with a gravimeter and a well for measuring the water table has been digged.

References

- Bertotti B. et al. (1995) *A&A*, **296**, 13. .
- Brand J. et al. (1994) *A&A.Suppl.Series*, **103**, 541.
- Cortiglioni et al. (1995) *Il Nuovo Cimento*, submitted
- Orfei et al. (1993) Proceeding of the URSI/IAU Symposium on *VLBI Technology Progress and Future Observational Possibilities*, Kyoto, in press
- Tomasi P. et al. (1995) Proceeding of the *St. Petersburg Wegener Meeting*, ed. M.Pearlman, pag. 344

Vector baseline plots for NOTO -WETZELL

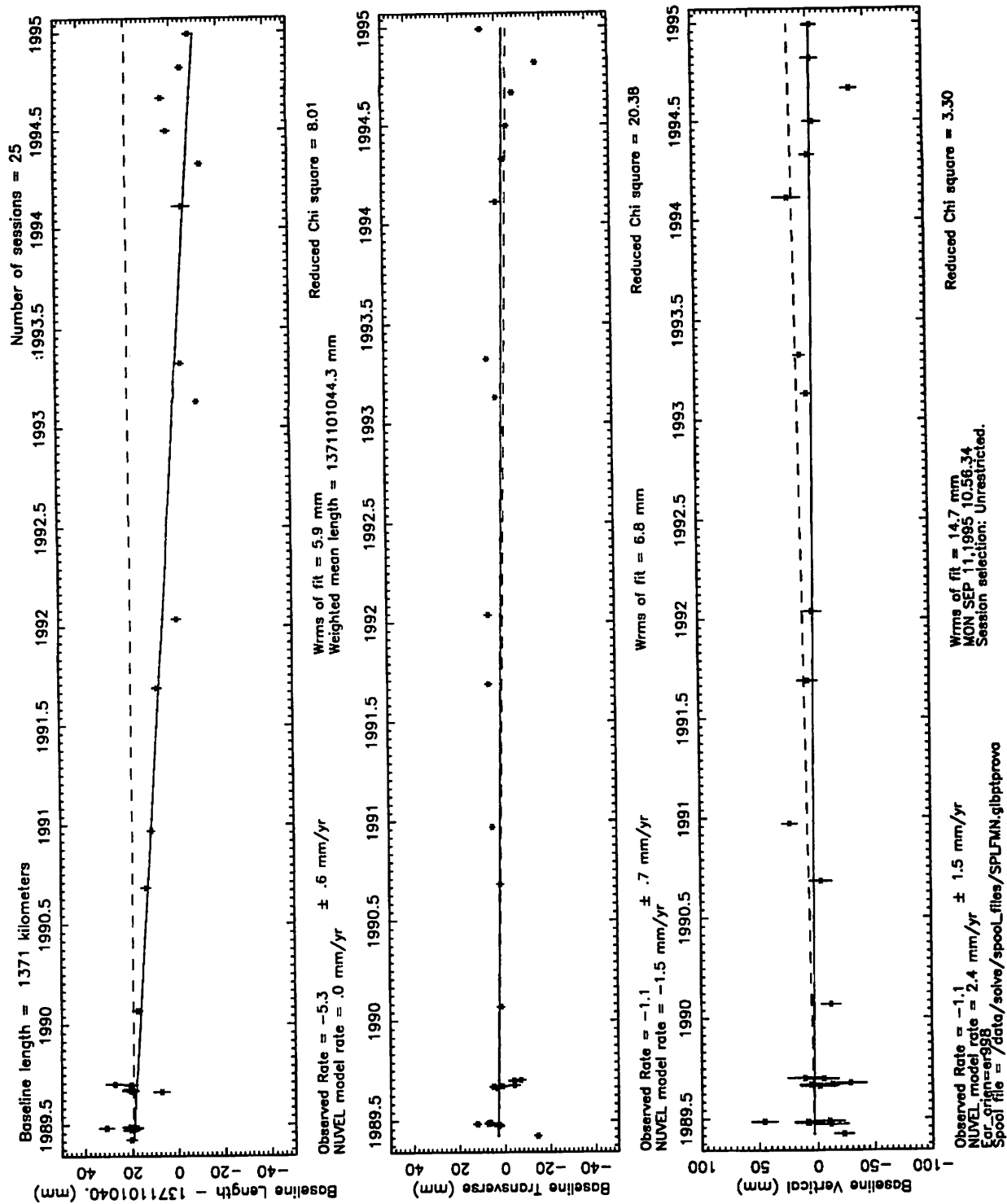


Figure 1.

Vector baseline plots for MATERA –WETZELL

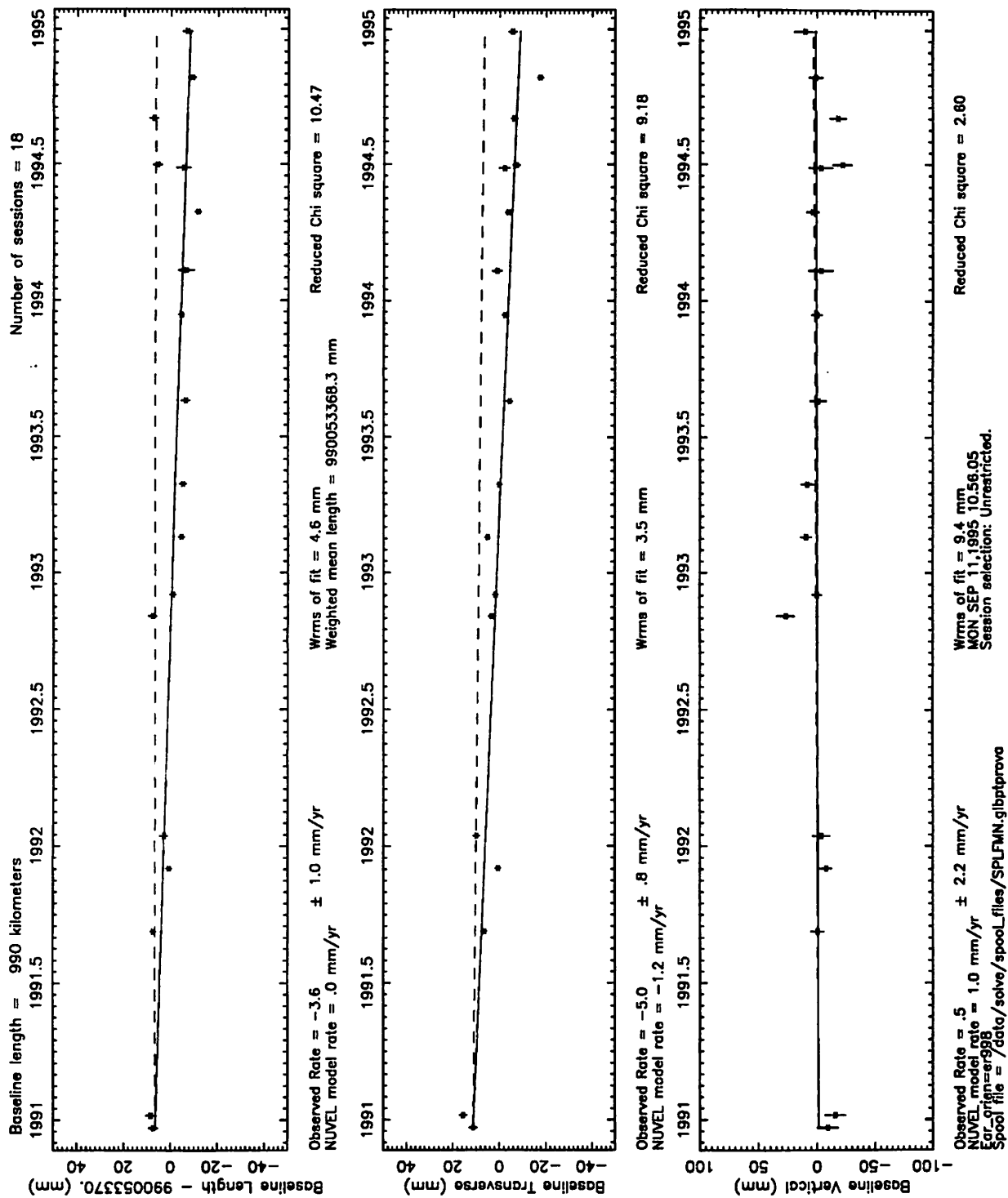


Figure 1 cont.

Radioastronomy at the NASA Madrid Deep Space Communications Complex during the year 1994

By A. ALBERDI^{1,2}, J.A. PEREA³, A. RIUS^{1,4}

¹ Laboratorio de Astrofísica Espacial y Física Fundamental, Apdo. 50727, 28080 Madrid, Spain

² Instituto de Astrofísica de Andalucía, CSIC, Apdo. 3004, 18080 Granada, Spain

³ Madrid Deep Space Communications Complex, Madrid, Spain

⁴ Centre d'Estudis Avancats de Blanes, CSIC, Blanes, Spain

The purpose of this report is to summarize the radioastronomical activities performed during the year 1994 using the facilities provided by the *NASA Madrid Deep Space Communications Complex (MDSCC)*. The projects which have been performed at the *MDSCC* require the unique resources and capabilities available at the *DSN*: large antennas, precise and accurate clocks, low noise receivers and high sensitivity ... and its geographical location. The scientific objectives included VLBI differential astrometry, observation of variable radio stars and exploding supernovae, observations of the parsec-scale radio jets of Quasars and Active Galactic Nuclei, applications of VLBI to the Geodynamics and applications of GPS observations to the study of the ionosphere and its effect on the proper calibration of the radioastronomical observations.

We note that the reported activities have been performed in a specific environment: a *NASA* spacecraft tracking station. The positive action of many individuals at the *Jet Propulsion Laboratory (JPL)* and at the *MDSCC* have been necessary for the accomplishment of this work.

1. The Radio Astronomy Program in the *DSN*

The Radioastronomy Program in the *DSN* can be divided in the following different segments of activity:

- Applied Radio Astronomy: it is made in support of the *DSN (Deep Space Network)* activities.
- Support of the *NASA Office of Space Sciences and Applications, OSSA*: These activities include observations of the atmospheres and magnetospheres of the planets, observations of a catalogue of radio sources placed around the ecliptic, etc.
- Host Country Observations: This observing time is available for the spanish community. A proposal must be presented to a Local Program Committee which will allocate the available time. Both, single dish and VLBI projects have been performed. The astrophysical goals which have been studied include: i) study of the absolute motion of the superluminal components of the parsec-scale radio jets of compact radio sources with respect to an external reference source, via VLBI differential astrometry; ii) study of the structure of SgrA*, an unique and compact radio source at the very Centre of the Milky Way, with VLBI at $\lambda 1.3$ cm and $\lambda 3.6$ cm; iii) study of the shape, angular expansion rate and distance of the supernova SN 1993J through VLBI observations at $\lambda 1.3$ cm, $\lambda 3.6$ cm and $\lambda 13$ cm; iv) study of the periodicity of the light curve of Cygnus X-3, between others.

- Radio Astronomical Observations which require the unique capabilities of the *DSN*: The proposals must be submitted to the *European VLBI Network (EVN)* and the *VLBA Program Committee* where they will be evaluated. Those proposals which are highly rated will be observed with the participation of the *DSN*-dishes.

2. Experiments performed at the *MDSCC* during 1994

In this section, we summarize the main radioastronomical observations performed at the *MDSCC* during 1994, both in Geodesy and Astrophysics:

2.1. Geodesy Experiments

- Europe 1* - February 9th.
- Europe 2** - April 27th.
- Europe 3 - June 29th.
- RDSAT 1 - July 28th.
- Europe 4 - August 31st.
- RDSAT 2 - October 13th.
- Europe 6 - December 28th.

2.2. Astronomy Experiments

- RAES SN1993J - Bartel/Rupen - January 27th - X-Band.
- GM17D - Marcaide - February 20th - X-Band.
- RAES SN1993J - Bartel/Rupen - March 14th - X-Band.
- MAH7 - Space VLBI Pre-Launch Survey - March 27th - L-Band.
- RAES SN1993J - Bartel/Rupen - April 21st - X-Band.
- GM17E - Marcaide - May 29th - X-Band.
- BR27 - Bartel/Rupen - June 1st - X-Band.
- GR04L*** - Bartel/Rupen - June 21st - X-Band.
- GR04M*** - Bartel/Rupen - August 29th - X-Band.
- MAH9 - Space VLBI Pre-Launch Survey - Sept. 3rd - L-Band.
- GM17F - Marcaide - September 24th - S-Band.
- GM17G - Marcaide - October 23rd - S-Band.
- MAH11 - Space VLBI Pre-Launch - October 25th - L-Band.
- GR04N* - Bartel/Rupen - October 31st - X-Band.
- GR04O - Bartel/Rupen - December 21st - X-Band.

* No fringes were obtained. ** Pointing Problems. *** Problems with the Continuous Recording Mode.

3. The problems with the antenna DSS65

During 1994, it was found that the track of the 34m radiotelescope (DSS65) presented severe deformations. Consequently, the azimuth speed of the telescope has been limited in order to preclude further degradation of structure, hardware and/or equipment. It has been found that when the antenna is driven in AZ at 0.800 degrees/sec (normal azimuth speed), the wheels going over the runner joints pivot and hit the mechanical

limits producing a bump.

The limiting azimuth speed has been defined as the speed at which the pivoting movement as measured at the mechanical stops of the wheel assemblies is no more than 5 millimetres from the neutral position when the wheel assembly traverses any runner point; this limiting speed has been found to be 0.250 degrees/sec.

A number of repair procedures have been considered and applied in order to save the foundation of the telescope. The epoxy injection of the walls has been considered the last of these procedures. Sometime in Autumn-November 1995 the final procedures for track rellevelling after the epoxy injection will be performed.

4. Publications in Refereed Journals in 1994 with data from DSS63-65

- (a) Bartel, N., Bietenholz, ..., Rius, A. *et al.* 1994, "The shape, expansion rate, and distance of supernova 1993J from VLBI measurements", *Nature* 368, 610-613
- (b) Cotton, W.D., Feretti, L., ..., Lara, L., Marcaide, J.M. *et al.* 1994, "VLBI Observations of a Complete Sample of Radio Galaxies. IV- 3C346 and 4C31.04: Two Unusual CSS Sources", *Astrophysical Journal*, in press
- (c) Giovannini, G., Feretti, L., ..., Lara, L., Marcaide, J.M. *et al.* 1994, "VLBI Observations of a Complete Sample of Radio Galaxies: IV-The Radio Galaxies NGC2484, 3C109 and 3C382", *Astrophysical Journal* 435, 116
- (d) Gómez, J.L., Alberdi, A., Marcaide, J.M. 1994, "Synchrotron Emission from Bent Shocked Relativistic Jets. II: Shock Waves in Helical Jets", *Astronomy & Astrophysics*, 284, 51-64
- (e) Gómez, J.L., Alberdi, A., Marcaide, J.M., Marscher, A.P., Travis, J. 1994, "Synchrotron Emission from Bent Shocked Relativistic Jets. III: Aberration of light and time delay effects", *Astronomy & Astrophysics*, 292, 33
- (f) Guirado, J.C., Marcaide, J.M. *et al.* 1995, "VLBI Differential Astrometry of the Radio Sources 1928+738 and 2007+777 at 5 GHz", *Astronomy & Astrophysics* 293, 613
- (g) Lara, L., Alberdi, A., Marcaide, J.M., Muxlow, T.W.B. 1994, "The Superluminal Quasar 3C 395 revisited: New VLBI Observations and Numerical Simulations", *Astronomy & Astrophysics*, 285, 393-403
- (h) Marcaide, J.M., Elósegui, P., Shapiro, I.I. 1994, "On the Relative Proper Motion of Quasars 1038+528 A,B", *Astronomical Journal* 108, 2
- (i) Marcaide J.M., Alberdi, A. *et al.* 1994, "Radio-Size Estimates of SN1993J", *Astrophysical Journal* 424, L25-L29
- (j) Marcaide, J.M., Alberdi, ..., Rius, A. *et al.* 1994, "Discovery of Shell-like Radio-Structure in SN1993J", *Nature* 373, 44-45
- (k) Peracaula, M., Paredes, J.M., ..., Rius, A. *et al.* 1994, "A 21-hour period in the quiescent radio emission of Cygnus X-3", *Astronomy & Astrophysics* 285, 547-550
- (l) Sardón E., Rius, A., Zarraoa, N. 1994, "Ionospheric calibration of single frequency VLBI and GPS observations using dual GPS data", *Bulletin Geodesique* 68, 230-235
- (m) Sardón E., Rius, A., Zarraoa, N. 1994, "Estimation of the transmitter and receiver differential biases and the ionospheric total electron content from Global Positioning System observations", *Radio Science* Vol 29, Number 3, 577-586
- (n) Standke, K.J., Quirrenbach, A., ..., Alberdi, A. *et al.* 1994, "The Intraday Variable Quasar 0917+624: VLBI and X-Ray Observations", *Astronomy & Astrophysics*, in press
- (o) Zarraoa, N., Rius, A., Sardón, E., Ryan, J.W. 1994, "Relative motions in Europe

studied with a geodetic VLBI network", *Geophysical Journal International* 117, 763-768, No.3

5. Instrumentation

(See the 'Radio Astronomy and the Deep Space Network' reports generated yearly by the *JPL* Telecommunications and Data Acquisition Science Office, M/S 303-401, Pasadena, California 91109, for details on the available instrumentation).

Telescopes	5.1. <i>Front End Areas</i>				DSS65	
	DSS63					
Diameter	70 m				34 m	
Bands	L	S	X	K	S	X
Efficiency	.6	.7	.7	.4	.6	.7
System T(K)	35	20	20	60	55	21/40
Surface RMS (mm)	6-7				5	

5.2. *Time and Frequency*

2 Redundant Hydrogen MASERS.

5.3. *Recording Terminals*

1 Mark III A DAT (with two recorders).

It is controlled through the DSP-V System. For the Host-Country observations and some other experiments, the Bonn MkIII VLBI PC-Field System has been used.

5.4. *Other equipment*

- SNR-8 ROGUE GPS Receiver.
- Pressure, humidity and temperature sensors integrated in the system.
- Water Vapour Radiometre: Method to estimate the wet delay.

5.5. *Software*

The permanent availability of the Mark III data acquisition terminal at the *MDSCC* and the need of improving existing observational capabilities, not specifically oriented towards the astronomy, prompted us to develop a set of programs, generically called RA-Tools, which, together with the Bonn MarkIII VLBI PC-Field System, allowed the host country community to use efficiently the *NASA* resources for radioastronomical observations. This effort is still continuing towards producing a reliable interface with the TMC/SMC software developed at the Madrid Complex, the next major step in this development.

Since 1 December 1994, the new automatic "dr2dsn" procedure has been tested and used to produce the antenna predicts for VLBI experiments. For the moment, we will continue to use the Bonn PC Field System, but it is our intention to move towards the GSFC solution (see next Section).

6. Future Plans and Hopes

6.1. Upgrade to MkIV

The actual recording system for VLBI (MkIII) will be upgraded to MkIV, increasing substantially the sensitivity of the observations, in order to be compatible with the other antennas of the *European VLBI Network* and to be able to participate in the Space-VLBI campaigns. *JPL* has planned the upgrade to MkIV at the end of 1996 in Goldstone, and in the middle of 1997 for the complexes in Madrid and Canberra.

6.2. K-band HEMT Receiver

A new wide-band (18-26.5 GHz Modules) K-band HEMT receiver will be installed. A second down-converter chain in the MMS will be installed permitting to observe two polarisations or two spectral lines simultaneously.

6.3. 22 GHz Tunable Maser

A new 22 GHz tunable maser is planned to be installed at the end of 1997.

6.4. Remote Monitoring

The *JPL*-engineers are working in the remote control of both the *DSN*-Radioastronomy antenna and the recorders. A Course demonstration is planned at Goldstone for the Summer of 1995.

6.5. Space-VLBI Co-observing

NASA, with *JPL*, is participating in the Space-VLBI missions by providing *VSOP* spacecraft tracking and orbit determination. A new antenna of 12 m will be built for telemetry. Moreover, the *NASA*'s 70-meter antennas will co-observe with the space VLBI satellites. Although it has not been finally decided, the intention is that the antenna DSS63 will participate in 4 space-VLBI experiments per week.

6.6. New VLBI Field System

The actual Bonn PC-Field System which controls the MkIII terminal will be replaced by the Goddard PC-Field System running under Linux. Since the Field System does not have any hard real-time requirements –it requires real time support of around a few tens of milliseconds– Linux is appropriate most of the time. The new Field System will be installed as soon as possible.

6.7. Digital Espectrometre

The digital espectrometre, which was previously installed at the *Canberra Deep Space Communications Complex (CDSCC)*, will be installed at the *MDSCC*. This digital espectrometre consists of a 1024 channels correlator with a bandwidth up to 16 MHz. It will be of special interest for the study of i) the *OH*-masers with the L-band receiver and ii) the *H₂O*-masers with the K-band receiver.

Geodetic VLBI studies with the Yebes radiotelescope

Yebes VLBI team^{1,2}

¹ *Centro Astronómico de Yebes, Apartado 148, E-19080 Guadalajara, Spain*

Abstract. We report on the status of the technical improvements being produced on our radiotelescope for its immediate participation in geodetic VLBI campaigns.

The *Observatorio Astronómico Nacional* of Spain (OAN-IGN) has participated in successful VLBI astronomical observations at 7 millimeter wavelength (43 GHz) since 1990 (e.g. Colomer *et al.* 1992). Our radome-enclosed 13.7-m radiotelescope at Yebes is now equipped with a VLBA DAR (with 14 BBCs) and recording system (compatible with MK IIIa), a GPS receiver, and an H-maser clock lent by the French CNRS.

In the last months, we have designed and built a S/X band receiver and optical system (subreflector and dual frequency horn). Table 1 shows their performance, together with the values for the Q band receiver. The S/X system has been installed on the telescope, and full characterization tests (pointing, focus, gain, etc) have been performed.

Table 1: Available receivers at the Yebes 13.7-m radiotelescope

Band	Tunable range (GHz)	Bandwidth (MHz)	T _{rec} (K)	T _{sys} (K)	η_A (%)	Sensitivity (Jy/K)	SEFD (Jy)	Pol	Rec ^J
Q	41.0 – 49.0	400	110 ^a	250	40 – 20 ^d	70 ^d	17500	LCP	CS
S	2.21 – 2.35	140	65 ^b	87 ^c	38 ^e	49 ^e	3800 ^e	RCP	HEMT
X	8.13 – 8.63	500	40 ^b	77 ^c	50 ^e	37 ^e	3300 ^e	RCP	HEMT

^a T_{rec} = 110 K is DSB and includes the polarizer; without the polarizer is 75 – 90 K.

^b These values include horns, polarizers, and transmission lines. Noise temperatures at the cryostat window are T_{rec} = 15 K for S-band, and 20 K for X-band.

^c We believe that the increase in system noise temperature is in part due to radome effects.

^d Elevation dependent (the sensitivity value quoted is for 45°). All numbers include radome effects.

^e Measured using Tau A with an assumed flux of 810 Jy in S band, and 563 Jy in X band.

^J Receiver: CS = Schottky diode. HEMT = High Electron Mobility Transistor amplifier. All cooled to 20 K.

²The VLBI team at Yebes is presently formed by (in alphabetical order): Javier Alcolea, Alberto Barcia, Francisco Colomer (*friend of VLBI*), Pablo de-Vicente, Juan Daniel Gallego, Juan Eusebio Garrido, Jesús Gómez-González (OAN Director), Stella Liehti, and Isaac López-Fernández. This communication was presented by F. Colomer. (Email: vlbi@cay.es)

We are presently studying several ways of improving the sensitivity (efficiency) of our telescope. On one hand, we are patching the millimeter subreflector surface according to the results of holographic measurements (so the values for the Q-band system in Table 1 will improve soon). On the other hand, we are considering the reinforcement of the telescope backstructure following the procedure that has resulted so successful on the 20-m telescope at Onsala Space Observatory (Sweden). We will upgrade as well our telescope control system in the near future, because the impossibility of controlling the antenna movements from the PC computer that controls the DAR and recorder units is a limitation of our present system for VLBI observations. We have recently purchased a H-maser, that will be installed in the following months.

We have participated in the EUROPA experiment performed on June 8th to 9th, 1995. First fringes have been already detected between Yebes and Onsala telescopes (Mueskens, priv.comm.). Our goal is to participate regularly in the next geodetic VLBI EUROPA experiments, and in the GLOBAL TRF experiments from November, 1995.

Acknowledgements: We thank Pere Planesas for his help with the telescope computer control program. We also thank Fermín Raluy, and Miguel Pérez for their help during the geodetic VLBI observations.

References

- [1] Colomer F., Graham D.A., Krichbaum T.P., *et al.* 1992. A&A 254, L17.

VLBI at Ny-Ålesund Space Geodetic Observatory Station Report 1993-1995

Bjørn R. PETTERSEN

Geodetic Institute, Norwegian Mapping Authority, N-3500 Hønefoss, Norway

Abstract. The Ny-Ålesund VLBI facility went into regular operation in January 1995, after having conducted several test observations in late 1994. The Space Geodesy group of the Geodetic Institute in Hønefoss has analyzed VLBI and GPS data. The last two years have seen particular focus on results from mobile campaigns in Norway and continental Europe.

Observations and Instruments

Following planning and construction work in 1992-94, the first test observations of the VLBI facility at Ny-Ålesund Space Geodetic Observatory were carried out on September 14, 1994. Further adjustment work and modifications were made in the following months, but the 20 m antenna was able to participate in 9 VLBI experiments in October-December 1994 as part of its technical testing program. We have faced several technical challenges, especially during the most severe weather conditions. However, the observatory has now made the transition into regular operations. A resident staff of 3 persons has been contracted and is supplemented by engineering support from the Geodetic Institute in Hønefoss. Table 1 lists the experiments with Ny-Ålesund participation to date, including one EVN astronomy experiment. A description of the VLBI facility is found in Pettersen (1994).

Monuments for a geodetic network for local control of the VLBI antenna and for establishing ties between the VLBI, GPS, and Sirius-A instruments of the observatory was established in 1994 and will be measured annually. Prare may be added in connection with the recent launch of ERS-2. Upgrade of the VLBI data aquisition system (on long term loan from NASA) to Mark IV is planned for 1995-96.

Data Analysis

NOAA's mobile VLBI observatory MV-2 was operated by the Norwegian Mapping Authority in 1991-93 and produced time series data for the presumed maximum uplift site in Norway; Trysil. During field campaigns it also secured a first epoch position for Höfn, Iceland, and a second epoch position for Tromsø, Norway. A number of sites in continental Europe and the Azores were measured in collaboration with IfAG and NOAA. These observations have been analyzed with the OCCAM software (Zarraqa and Danielsen, 1993; Zarraqa et al. 1994a) and compared to GPS results (Kristiansen and Zarraqa 1994) and VLBI results from European permanent observatories (Zarraqa 1994, Zarraqa et al. 1994 b).

Ionospheric effects are presumed to be significant at the Arctic location of Ny-Ålesund. A collaborative effort to understand this phenomenon has begun, and initial results were published by Sardon et al. (1994).

A new approach is being tested to evaluate if simultaneous analysis of VLBI and GPS data improve global solutions, and involves the Geosat-software developed by Andersen (1995).

Table 1: VLBI observations from Ny-Ålesund

Date	Program
14 Sept 1994	Fringe test
4 Oct 1994	NEOS-A-75
24 Oct 1994	NAVEX-44
26 Oct 1994	EUROPE 94-5
31 Oct 1994	C-ASIA-1
12 Dec 1994	POLAR-N2
13 Dec 1994	NEOS-A-85
20 Dec 1994	NAVEX-45
28 Dec 1994	EUROPE 94-6
29 Dec 1994	R&D 94-10
1 Feb 1995	EUROPE 95-1
2 Feb 1995	R&D 95-2
12 Feb 1995	ern1 (astro-EVN)
13 Feb 1995	C 95x1n (astro-cal)
6 Mar 1995	GLOBAL TRF-2
13 Mar 1995	X-ATLANTIC 1
12 Apr 1995	EUROPE 95-2
13 Apr 1995	C-ASIA 1
18 Apr 1995	NEOS-A-103
19 Apr 1995	POLAR-N1

Initial Results for Ny-Ålesund

Baseline lengths between Ny-Ålesund and other VLBI sites have been repeatedly measured since October 1994. At the time of writing, analysis results for experiments up to February 1995 are available. An examination of the repeatability reveals no simple relationship with baseline length, but all rms values are less than ± 16 mm. Four sites with 3 to 5 observations each have rms errors less than ± 5 mm.

No systematic motion of Ny-Ålesund can be detected within the initial 6 month observing interval. However, GPS data have been collected since 1991 in Ny-Ålesund and a data base spanning more than 4 years is now available. These data reveal a north-easterly motion of 16 mm/year, with a repeatability of half that value. No vertical motion has been detected with certainty. This is not expected from theoretical models either. Calculations by Tom James (1993) of post-glacial rebound radial velocities based on the ICE-3G model shows Ny-Ålesund to be located very near the null motion line.

References

- Andersen, P.H., 1995, *High Precision Station Positioning and Satellite Orbit Determination*, Ph.D. dissertation, University of Oslo.
- James, T., A. Lambert, 1993, *A Comparison of VLBI Data with the ICE-3G Glacial Rebound Model*, Geophys. Research Lett. **20**, 871.
- Kristiansen, O., N. Zarraoa, 1994, *Comparison of the GPS and VLBI Geodetic Results at Tromsø (Norway)*, presented at XIX General Assembly of EGS, Grenoble, April 1994.
- Pettersen, B.R., 1994, *Very Long Baseline Interferometry in the Arctic*, Teletronikk **90**, 29.
- Sardon, E., A. Rius, N. Zarraoa, 1994, *Ionospheric Calibration of Single Frequency VLBI and GPS Observations using Dual GPS Data*, Bull. Geod. **68**, 230.
- Zarraoa, N., 1994, *Determination of Vertical Displacements in Active Tectonic Areas in Europe using VLBI*.
- Zarraoa, N., J. Danielsen, 1993, *Analysis of the European Mobile VLBI Campaigns*, Proc. IX European VLBI Meeting (eds. J. Campbell and A. Nothnagel), Univ. Bonn Geod. Publ. **80**, 60.
- Zarraoa, N., S. Rekkedal, O. Kristiansen, B. Engen, 1994 a, *The Mobile VLBI Campaigns in Norway (1989-1993)*, Bull. Geod., in press.
- Zarraoa, N., A. Rius, E. Sardon, J.W. Ryan, 1994 b, *Relative Motions in Europe Studied with a Geodetic VLBI Network*, Geophys. J. Int. **117**, 763.

Geodesy VLBI at the Onsala Space Observatory: Station Report, 1994–1995

G. Elgered, T.R. Carlsson, T.M. Carlsson, R.T.K. Jaldehag, P.O.J. Jarlemark,
J.M. Johansson, B.I. Nilsson, B.O. Rönnäng, and H.-G. Scherneck

Onsala Space Observatory, Chalmers University of Technology
S-439 92 Onsala, Sweden
phone +46 31 7725500, fax +46 31 7725590
e-mail: geo@oso.chalmers.se

Abstract. We summarize the performed and planned geodesy VLBI activities at the Onsala Space Observatory for the period 1994–1995. The period is characterized mainly by observations, typically 2–3 days per month. Results from the continuously operating Swedish GPS network are now comparable to VLBI data in terms of demonstrated reproducibility of estimated geodetic parameters. We discuss, for example, the Onsala–Wettzell baseline length. Only small changes in the VLBI equipment have been made during the last two years. Plans for the upgrade to the Mark-IV data acquisition system will be discussed briefly.

1. VLBI Observations

In spite of the fact that this report covers the 1994–1995 period it is interesting to view the experimental activities of geodetic VLBI at the Onsala site over a longer perspective. Figure 1 shows the number geodetic VLBI experiments at Onsala since the introduction of the Mark-III data acquisition system in 1980. It is seen how the number of experiments reaches a first maximum in 1986. The following decrease occurred because the slewing speed of the Onsala antenna made it relatively less attractive to be used in geodetic VLBI experiments when new antennas, with faster slew rates, were built, allowing for more observations during an experiment and thereby better modelling of clocks and atmospheric effects. After the antenna upgrade in 1991–1992 there were again an increase in the number of experiments per year. While studying long term trends we should ignore the years of 1989 and 1992 because of the extra activities due to the European mobile VLBI campaigns. We can now, after the recently announced cut of NASA activities in 1995, only speculate if there will be less experiments per year, or if the activities at Onsala will stabilize at a level of 10–20 experiments per year.

The pure European network

The Onsala 20-m antenna participates regularly in the experiments of the European network. This network typically include the antennas at Noto, Matera, Medicina, Madrid, Wettzell, and Onsala. Occasionally the Effelsberg antenna is

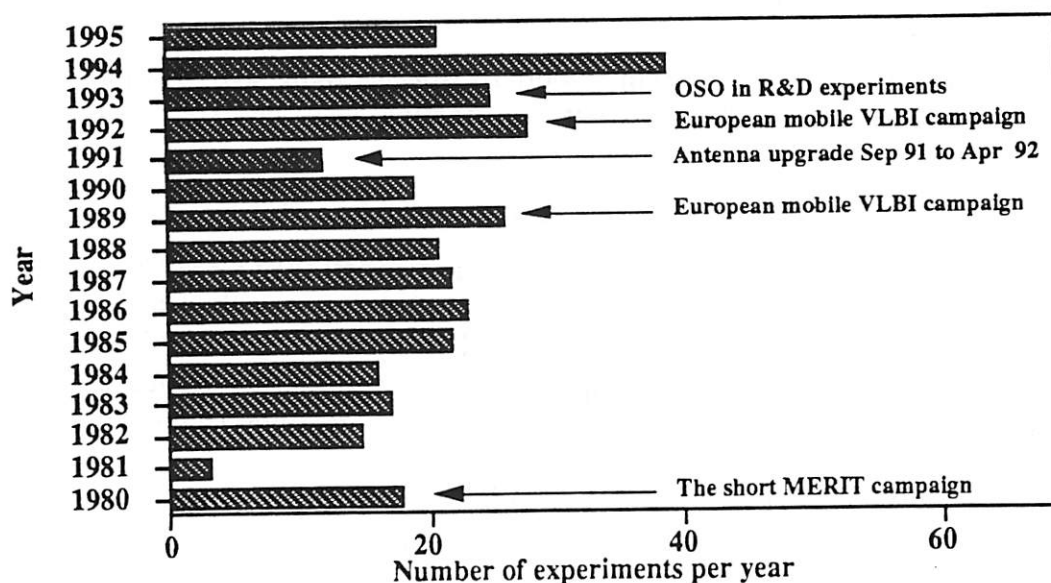


Figure 1. Number of geodetic Mark-III VLBI experiments per year using the Onsala 20-m radio telescope.

included and more recently the Crimea and Ny Ålesund radio telescopes have been added to the network. Five experiments were scheduled and performed at Onsala during 1994; an additional six experiments are planned for 1995.

NEOS-B

The NEOS-B network observed at approximately one month intervals during 1994. Onsala participated in nine experiments. The stations used have been: Algonquin Park, Fairbanks, Green Bank, Matera, Onsala, and Wettzell. The NEOS-B experiment series was ended with the November 6-7 experiment 1994.

The Research and Development (R&D) network

Monthly observations including Onsala in the R&D network, coordinated by GSFC, NASA, started in 1993. This network consists of Fairbanks, Fort Davis (VLBA), Kokee Park, Los Alamos (VLBA), Onsala, Westford, and Wettzell. The same network was used in the CONT-94 measurement campaign 12-25 of January 1994. The total number of observation days was 22 during 1994 and an additional 12 experiments are planned for 1995.

Polar-N and Crimea experiments

The Polar-N experiments have been carried out twice during 1994 and once during 1995. The antenna sites are: Fairbanks, Haystack, Kashima, Madrid, Medicina, and Onsala. One "dedicated" Crimea experiment, including Crimea, Medicina, and Onsala, was carried out on June 28-29, 1994.

2. Technical developments during 1994–1995

PC Field System

The new PC based Field System (Goddard Space Flight Center standard) replaced the older HP A-400 based software starting with the experiments in October 1994.

Measurements of antenna tower temperatures

A PC-based system for data acquisition of the temperature measured at twenty different places in the concrete tower of the 20-m antenna has been designed and constructed. The data archive starts in December of 1994 and is planned to continue for, at least, the next couple of years. More details about the results obtained so far are presented by *Elgered and Carlsson* [1995, this volume].

The Onsala Water-Vapor Radiometer (WVR)

The WVR has been operating more or less continuously during 1994 and 1995. Malfunctioning cables and the following replacements have, however, implied that data were not acquired during a couple of experiments. The impact of using WVR data for wet delay corrections has been studied in detail by *Carlsson et al.* [1995, this volume].

Data from the WVR have also been used to study the influence of the atmospheric water vapor on geodetic observations using the Global Positioning System (GPS). The results from four dedicated GPS campaigns on the Swedish west coast during 1992 show that water vapor variability is a dominating error source in the estimated geodetic parameters [*Dodson et al.*, 1995]. More recently it has been found that residuals of the GPS analysis occasionally correlate well with horizontal gradients in the wet propagation delay observed by the WVR [*Jarlemark et al.*, 1995].

3. Plans for the Future

The future activities in the space geodesy group at Onsala is aimed towards an integration of the different activities. The work towards improvement of both GPS and VLBI for geodetic applications will continue. This will necessarily include further studies of atmospheric effects. We will here try to summarize the plans for these areas in the near future.

Future improvements of the VLBI system

The upgrade to the Mark-IV system will be carried out within the plan by the Joint Institute for VLBI in Europe (JIVE). The main improvement for geodetic VLBI is the possible bandwidth expansion from the present maximum of 4 MHz to 16 MHz per recorded track. The implication is that integration times may be reduced with a factor of two so that more scans can be made during an experiment. This means that the estimates of clock instabilities and atmospheric variations could be improved. It could also mean that weaker, but more point like, sources can be observed. This will reduce the influence of source structure on the estimated geodetic parameters and/or make it possible to obtain a better geometry of the observations.

An additional improvement of the sensitivity within the next couple of years is being investigated. A study aiming for new feed systems for all receivers used in the 20-m telescope is underway. The present feed uses a tertiary reflector for S-band which is equipped with a dichroic surface which has low transmission loss at X-band [Jaldehyag *et al.*, 1993]. A possible new solution is to use a tertiary reflector for both S- and X-band which is illuminated by a dual-band horn. The horn will use aperture controlled beam widths which implies an efficient, and simultaneous, illumination of both the subreflector and the primary reflector at both bands.

SWEPOS, the Swedish GPS network

SWEPOS, presently consisting of 20 stations within Sweden, has been established in cooperation with the National Land Survey of Sweden. The 20 continuously operating GPS receivers produce data which are analyzed together with data from global IGS-stations on a daily basis. These IGS-stations are in many cases colocated with VLBI-sites. Of special interest for our European VLBI activities is the comparison of the Onsala–Wettzell baseline. The results obtained for a time period slightly larger than one year is shown in Figure 2. The reproducibility of 2.5 mm is comparable with the VLBI result for the CONT-94 campaign [Carlsson *et al.*, 1995, this volume].

One major application of this network is to study the postglacial rebound in Fennoscandia. Strong indications for a general vertical uplift have been obtained. As an example, the estimated three-dimensional coordinates of the Sundsvall site are presented in Figure 3. The results from the two years of operation are presently summarized by Johansson *et al.*, [in preparation 1995].

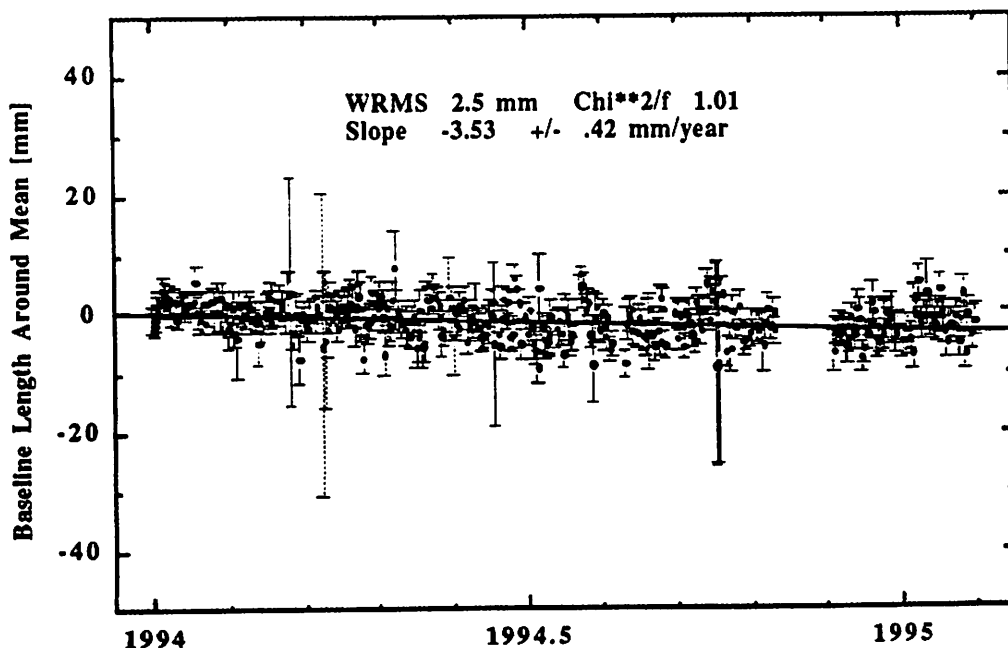


Figure 2. Estimates of the Onsala–Wettzell baseline obtained from the GPS analysis of the continuously operating SWEPOS network. The mean is 919697.273 \pm 0.004 (1- σ formal error). Each estimate is based on data from one day.

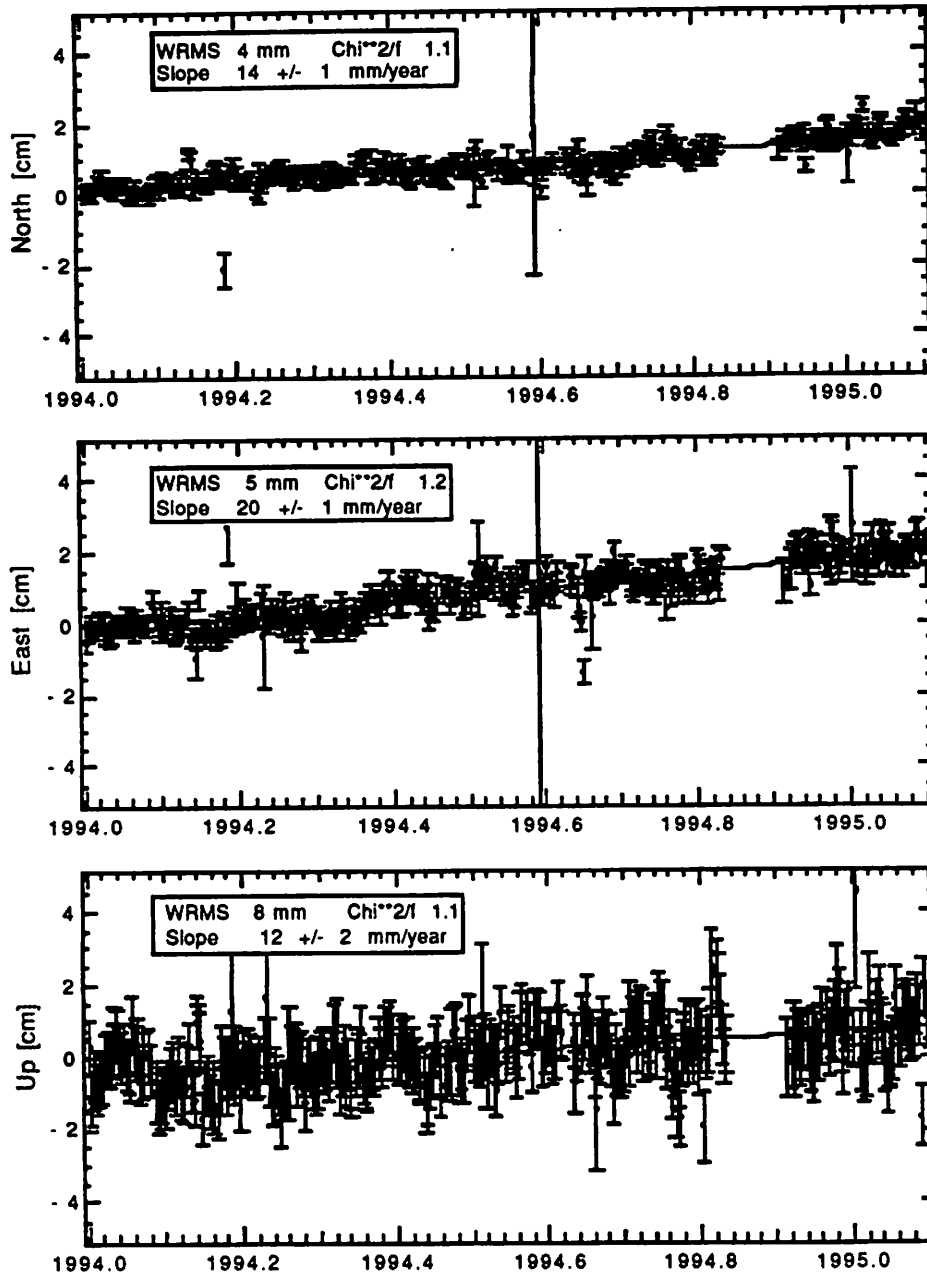


Figure 3. The estimated position of the Sundsvall site in the ITRF-92 coordinate system [IERS, 1993].

Atmospheric studies

We have already mentioned the applications of microwave radiometry for studies using both VLBI and GPS data. Another ongoing project is the evaluation of the possibility to use the continuously operating Swedish GPS network for meteorological applications (see, *e.g.*, Bevis *et al.* [1992]).

Horizontal gradients in the refractive index have been identified as one potential error source in geodetic VLBI [Davis, 1986]. In order to investigate possible gradients we have initiated *in situ* measurements using an aircraft. A first attempt was made during the last part of the Europe-2 experiment in April 1995. Unfortunately, no significant horizontal gradients were seen in the airplane data (see Figure 4). This was supported by the simultaneously operating WVR,

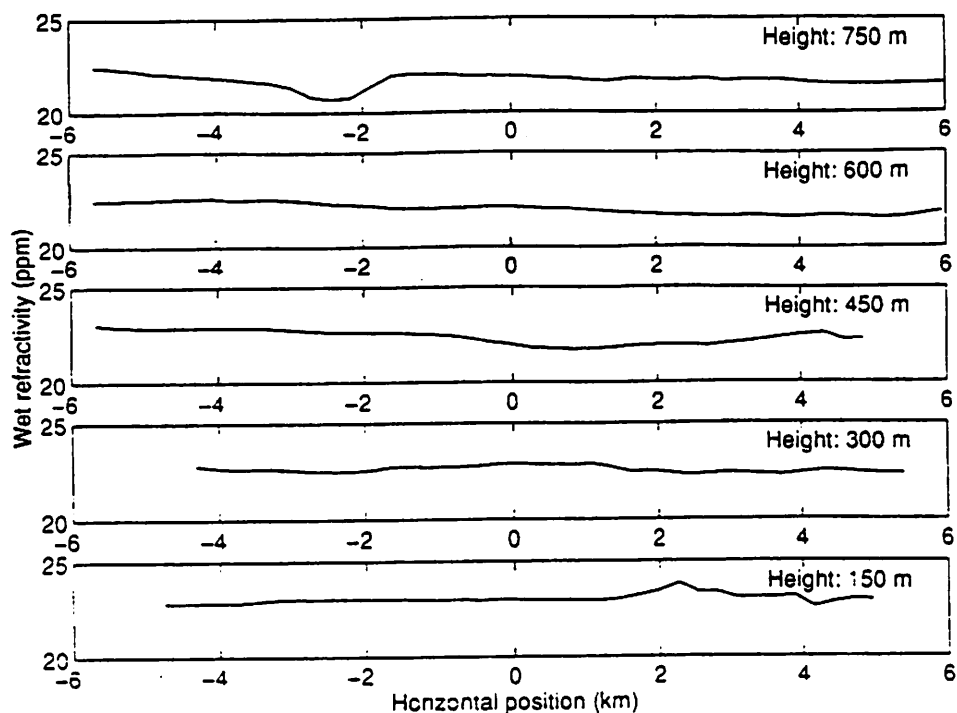


Figure 4. Inferred wet refractivity from temperature and humidity measurements during five east-west flights at different altitudes. The horizontal coordinate has east in the positive direction; zero is at the observatory site. The equivalent zenith integrated excess propagation path due to water vapor will only differ with <1 mm for elevation angles above 10° .

which detected no significant variations in the sky emission while scanning along the azimuth coordinate at an elevation angle of 30° . We plan to continue to use aircraft for *in situ* measurements with the goal to fly when the meteorological conditions for horizontal gradients to develop are favorable.

References

- Bevis, M., S. Businger, T.A. Herring, C. Rocken, R.A. Anthes, and R.H. Ware, GPS Meteorology: Remote Sensing of Atmospheric Water Vapor Using the Global Positioning System, *J. Geophys. Res.*, **97**, 15787-15801, 1992.
- Carlsson, T.R., G. Elgered, and J.M. Johansson, External Wet Tropospheric Corrections During a Two-Week-Long VLBI Campaign, 10th Working Meeting on European VLBI for Geodesy and Astrometry, *this volume*, 1995.
- Davis, J.L., Atmospheric Propagation Effects on Radio Interferometry, Ph.D. Thesis, Massachusetts Inst. of Tech., 1986.
- Dodson, A.H., P.J. Shardlow, L.C.M. Hubbard, G. Elgered, and P.O.J. Jarlemark, Wet Tropospheric Effects on Precise Relative GPS Height Determination, *Bulletin Geodesique*, *in press*, 1995.
- Elgered, G., and T.R. Carlsson, Temperature Stability of the Onsala 20-m Antenna and Its Impact on Geodetic VLBI, 10th Working Meeting on European VLBI for Geodesy and Astrometry, *this volume*, 1993.
- IERS, 1992 *International Earth Rotation Service Annual Report*, Observatoire de Paris, Paris, 1993.
- Jaldehyag, R.T.K., P.-S. Kildal, and B.O. Rönnäng, Dual Band Reflector Feed Systems for Classical Cassegrain Radio Telescopes, *IEEE Trans. Antennas Propagat.*, **AP-41**, 325-332, 1993.
- Jarlemark, P.O.J., G. Elgered, and J.M. Johansson, Remote Sensing of Temporal and Spatial Gradients of the Wet Refractivity, *IGARSS'95 Digest*, *in press*, 1995.
- Johansson, J.M., *et al.*, Geodynamics with the Global Positioning System: First Two Years of Observations From a Continuous Network in Sweden. 1. Results, *in preparation*, 1995.

STATION REPORT FOR EFFELSBURG - MAY 1995

R.W.Porcus

Max-Planck-Institut für Radioastronomie, Auf dem Hügel 69, D-53121, Bonn, Germany.

The 100m radio telescope at Effelsberg is used for about 90 days per year for VLBI observations, mostly for astronomical projects scheduled together with the EVN or the VLBA. Recently, however, it has taken part in a few geodetic VLBI experiments. A few recent developments which may be of interest to the geodesy community are listed below.

- 1) In late summer this year, the antenna will be out of action for 2 to 3 months, while a replacement azimuth track is installed.
- 2) We now have a VLBA record terminal (with 4 BBCs), controlled by a Motorola computer in a manner almost identical to that at VLBA sites. The prime purpose is for joint Effelsberg-VLBA observing.
- 3) In common with the EVN observatories at Onsala, Westerbork, Medicina and Jodrell Bank, we will upgrade the Effelsberg MK3a terminal to Mk4 in the course of the next 12 months. Initially this involves adding 8 and 16 MHz filters to the video-converter units and changing the ssb circuitry. Installation of a MK4 formatter and final fitting out for MK4 observing will occur later. During this period we will replace our old, home-grown PC field system with the new FS9 running under Linux.
- 4) We have a Motorola GPS timing receiver for continuous monitoring of the H-maser, via the VLBA formatter.
- 5) To meet the input requirements of the VLBA terminal, the X-band receiver now also has 500-1000 MHz IF outputs.
- 6) We are working hard on "frequency agility", the ability to change between the secondary focus receivers entirely in software, and hence allowing them to be schedule driven.

The Radioastronomical Station of Noto

Geodetic Status Report

Vincenza Tornatore

Istituto di Radioastronomia, C.N.R. Stazione Radioastronomica, Noto, Italy

Abstract. An overview of the activities of the station for geodesy and astronomy is presented. As an update of the present performances in the geodetic VLBI field we describe the status and the planned improvements concerning receivers, data acquisition and timing systems, and experiments analysis. An outline on other spatial geodetic measurements will be also discussed.

INTRODUCTION

Since the last presentation of the station held in Bad Neuenahr, FRG [Tomasi, 1993] the Staff operating at Noto is almost doubled. This big increase has occurred thanks to a certain number of employments for the formation of the personnel : five of the eight new positions are scholarships and three of these are for only ten months.

The tasks of the station can be subdivided in three big categories : technological, astrophysical and geodynamical.

The bulk of the efforts is turned since the beginning of the activity of the Observatory [Tomasi, 1989] to the technological field and partly to the astrophysical. Anyway with the increasing of the staff the interests of research in the astrophysical and the geodynamical sectors are having also chances to grow.

TECHNOLOGICAL ACTIVITY

Most of the work dedicated to the station involves maintenance and all that it implies to carry out good observations. Since the announcement of Tom Clarck of the new 'TAC' (Totally Accurate Clock) people are working to introduce it, so Noto will have a GPS timing receiver instead of a Loran-C. This will increase the timing accuracy from about 1 microsec to values that typically are of about 100 nanoseconds. To improve the antenna pointing it is in progress a study to produce a model of the antenna behaviour as function of the legs temperature.

Projects on a longer time scale and of big engagement of people and investments intend to make possible the fast switching among receivers, and the automatic change from the primary to the

secondary focus. These projects are very similar to those described in detail for the Medicina antenna by Orfei et al [1995] (this volume)

Very important for the technological activity is the development. Some people participate to the project of the correlator (JIVE) and to the development, now in final stage, of the spectrometer autocorrelator and of its management software in collaboration with the Arcetri Observatory. Moreover it is at the attention of the technical team the feasibility evaluation for a small correlator having high performances with respect to present MKII standards.

ASTROPHYSICAL ACTIVITY

The research in the astrophysical field plays an important role for the Noto Station. The principal interests of researchers involved in the astrophysical field cover the GALACTIC and EXTRAGALACTIC RADIOASTRONOMY. In particular the Galactic radioastronomy is turned to study RS CVn and Algol stellar binary systems. These studies include single dish monitoring of the systems, VLBI ad hoc with antennas of European, American, Australian networks in case they reveal during the monitoring an increase of the activity of the systems. Some studies are carried out using VLA observations too. Researches of correlation with the emission in other spectrum regions, statistical analysis of flares, development of softwares for single dish acquisition are effected. The radio emission of peculiar chemical stars and the masers in Stars of Mira type are also followed.

Subjects for the extragalactic area are the compact radio source GPS and CSS and the BLAC selected in the Radio band. Examinations about their morphology at different VLBI frequencies with a milliarcsecond scale are performed. The polarization on an arcsec scale is also investigated.

GEODYNAMICAL ACTIVITY

It's well known that Noto has had a very deeply-felt course before it was equipped with a VLBA recorder and a VLBA terminal [Tomasi 1993]. The present configuration misses two BBCs to be completed. We have just received the 'DELAY CAL' module on loan by the Haystack Observatory till the end of '95. We are making plans to build or to buy it as soon as possible. The field System and the software for the antenna driving are running on PCs computers 486. More detailed characteristics of the Noto VLBI system can be found in figure 1. The objectives pursued in the geodynamic field have been turned in the last months to improve the quality of the VLBI observations and to make possible the analysis of the data. The first point has been reached in part by the introduction of the phase delay calibration in december '94, and the increase of the number of BBCs. Then the tests carried out before the experiments have been enlarged, checks on the values of the antenna velocity have been performed (Antenna velocity measured in azimuth is 43 deg/min instead of the expected 48 deg/min). The availability of the ground unit will give the opportunity to include cable calibration for the first time in the next Global TRF-3 experiment on July 24. Plans to build a new multifeed S/X/L receiver with better System Temperature of the present 110K and 120K in the X and S band respectively and of wider bandwidths are under consideration.

As concerns the analysis of the data the installation of Calc 7.6 and Solve 4 under Sunos on a SparcStation LX and of OCCAM 3.3 on PC 486 are in progress.

Some projects in which the station can give a scientific contribute are also becoming clear. They concerns with the study of geodynamic problematics with reference to the eastern Sicily using VLBI, GPS and seismic methodologies in collaboration with the Institute of Geophysics of Catania. A strong interest is also bound to the evaluation of the position of Noto not only in front of the Euroasiatic Plate but also respect to the African one since Noto occupies a particular position respect the two plates. Then thanks to the strong astrophysical characterization of the station, we believe that this experience can be used to contribute to the studies of the influence of Source structures and variability on the geodetic VLBI data [S. Britzen et al. 1993] beginning from sourses observed during the Europe campaigns.

OBSERVATIONAL ACTIVITY

The histograms in the figure 2 show the observations, subdivided for different programs, held in '93 and '94. The observations are counted in unit of 24 hours. Nearly all the days of activity are dedicated to programs of astrophysical character above all galactic (ad hoc + single dish + part of EVN) then extragalactic (EVN). A special program Jupiter was effected in '94 for the impact with the Shoemaker-Levy9 comet. The experiments of geodetic interest cover only 6 days in '94 (Europe program) and 4 days in '93 (3 Europe, 1 Navex-PA). The figure 3 shows the geodetic experiments performed at Noto since the first partecipation of the station in campaigns of geodynamic character. The first year of activity has been the richest with 12 experiments (EATL, IRIS-A, EUROMOB), the poorest the '92 with only 2 Europe experiments because a MKIII terminal was available only at the beginning of the year. The rule is as of today to take part to the Europe experiments [J. Campbell 1991]. This partecipation is very important since the station occupies a very interesting position from the geodynamic point of view in the Mediterranean area.

OTHER SPATIAL TECHNIQUE MEASUREMENTS

Noto is equipped with a permanent Turbo Rouge receiver managed by Italian Space Agency (ASI) since the beginning of February '95.

GPS Campaigns occurred after the '92 concern with different projects :

SELF (SEa Level Fluctations: geophysical interpretation and environmental impact) in March '93 and '94,

WHAT_A_CAT (West Hellenic Arc Tectonics and Calabrian Arc Tectonics) in September '94, TYRGEONET (TYRhenian GEOdetic NETwork) in october '93 and in June '94,

STRAITS OF MESSINA in September '94,

CEE-SCIENCE project "Volcanic Deformation and Tidal Gravity Effects at the Mount Etna" in September '94.

No SLR measurements have been made after the '93.

NOTO VLBI SYSTEM

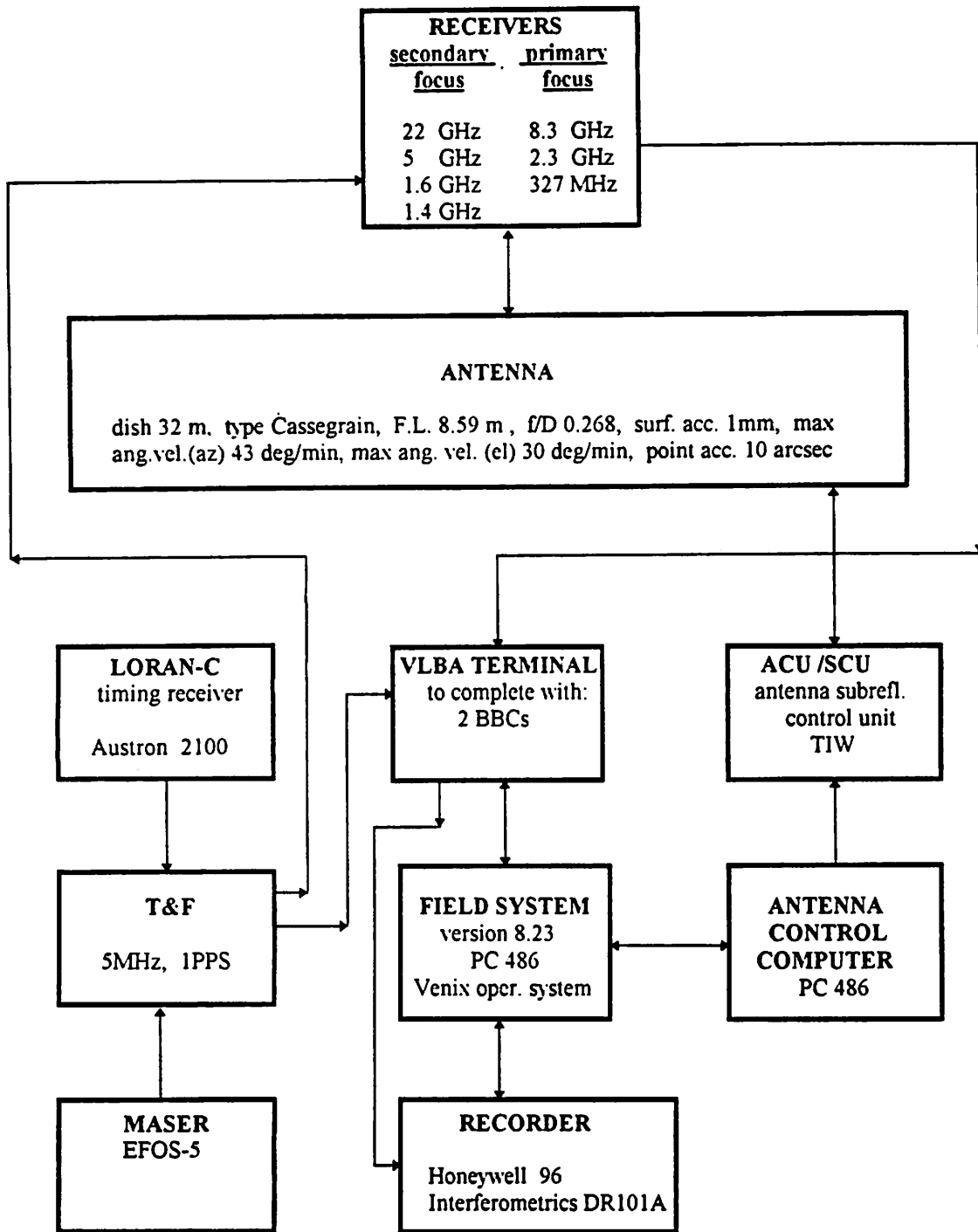


Fig. 1

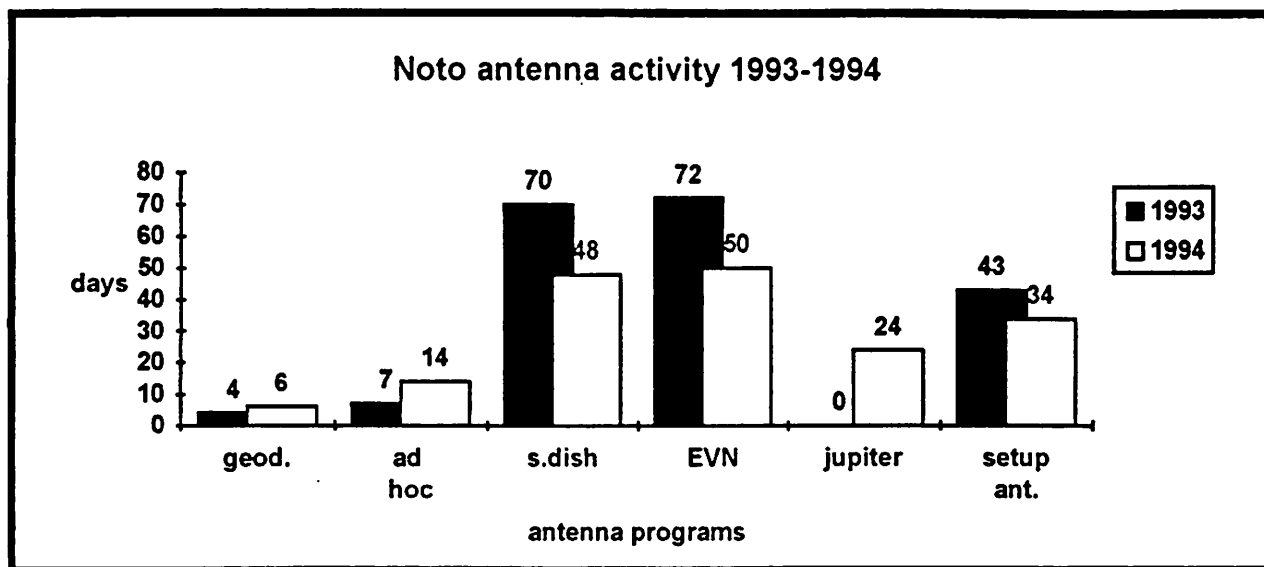


Fig. 2

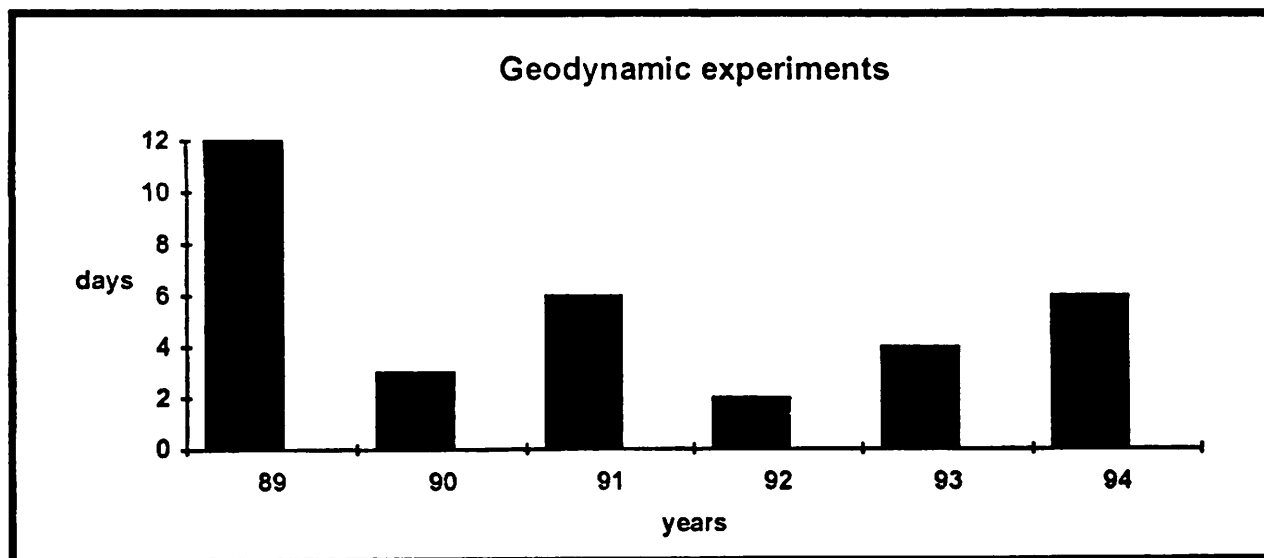


Fig. 3

Acknowledgement

The author would like to thank the colleagues of the Noto Station and P. Tomasi to have provided comments, informations, suggestions, critics, etc..., very constructive for the realization of this report; thanks to G. Nicotra for the collaboration to plot graphs of the figures.

References

- Britzen S., Gontier A.-M., Witzel A., Schalinski C. J., Campbell J., Radio Source structure and its influence on the accuracy of geodetic VLBI analysis, Proc. of the 9th Working Meeting on European VLBI for Geodesy and Astrometry, Bad Neuenahr, FRG p. 157, 1993.*
- Campbell J., The European Geodetic VLBI-Network - Status report, Proc. of the 8th Working Meeting on European VLBI for Geodesy and Astrometry, Dwingeloo, The Netherlands, 1991.*
- Orfei A., Maccaferri G., Mariotti S., Morsiani M., Zacchioli G.P., A description of the Medicina 32m dish upgrade, 10th Working Meeting on European VLBI for Geodesy and Astrometry, this volume, 1995.*
- Tomasi, P., Un anno di attivita` alla stazione di Noto, Rapporto interno 122/'89.*
- Tomasi, P., Noto Statio Status Report, Proc. of the 9th Working Meeting on European VLBI for Geodesy and Astrometry, Bad Neuenahr, FRG p. 11, 1993.*

A DESCRIPTION OF THE MEDICINA 32M DISH UPGRADE

A. ORFEI, G. MACCAFERRI, S. MARIOTTI, M. MORSIANI, G. ZACCHIROLI

C.N.R. - Istituto di Radioastronomia, Bologna, Italy

Abstract. A description of the upgrade project for the VLBI Medicina antenna is presented. Solutions regarding subreflector movement and secondary focus receivers arrangement are showed as well as expected efficiency enhancement at higher frequency and fast switching among receivers. In addition we mention new facilities for single dish observations, and personal computer use for station management.

1. Introduction

In this paper we give some technical details about the upgrade of Medicina antenna and news at the station. Very important for us is to create a receivers arrangement such that a fast and completely automatic switching among frequencies comes available. This is one of the VLBI requirements for the years to come and this is also the need of the Medicina people in order to save valuable time.

Another task is to enhance the antenna efficiency, mostly at the highest usable frequencies. In the last february Medicina took part at the 43GHz session and first results was good. However the antenna efficiency is very poor, simply because our antenna was not designed to work at that frequency.

2. Fast switching

About fast and automatic receivers switching much work has been done but much remain to do. Basically three are the key points,

1) provide space into the vertex room, the place where the cassegrain receivers are located. This was prevented by the huge L-band receiver, therefore we have designed a new 1.4/1.6 GHz receiver to be placed on the primary focus. This one has been integrated in an already existing receiver box, containing the S,X and K bands, so some mechanical constraints had to be taken. Due to lack of enough space inside the box the feed is very compact, 25mm of the illuminator diameter and a total length of 400mm. For the same reason concerning the dewar the preamplifiers were not cooled. That job is now completed and thus we could arrange for the step 3. Anyway, the current movement length of the subreflector axis does not match with the requested shift of the secondary receivers therefore a redesign of its mechanical strokes is necessary. So the achievement of the step 3 needs the step 2 be carried out before.

2) The most uncomfortable job about receiver switching is the removal or mounting of the subreflector. This is a huge mirror, 3m in diameter and 800kg in weight. Its management needs many people and a crane, further that job is weather dependent. Thus, a complete redesign of the subreflector mechanics is needed to avoid the mounting and dismounting. The new mechanics will allow to shift laterally the mirror when primary focus receiver have to be used, it will point all the secondary feeds and also will allow to perform beam switching at the highest frequencies by fastly tilting the subreflector. This design is not an easy job, principally because of constraints due to the existing quadrupode structure. Anyway, the design is in an advanced stage and most of the commercial parts are ordered, such that new motors, new electronic driving and control boards, mechanical moving pieces and so on.

In fig.1 the present status about the receivers at Medicina and the time needed to switch among them is showed. It takes some minutes among primary focus receivers, due to the very slow speed of the present mechanics. It takes some hours among secondary focus receivers, due to the dismounting of one receiver and the mounting of the other one to be used; but this is not weather dependent because all operations are done inside the vertex room.

Mounting and dismounting the subreflector takes two or more hours and above all involves a big logistics.

The goal of the upgrade proposed is to switch among frequencies at a maximum of a minute. This will be only due to the speed of the mechanics because, from a control point of view, already now we are able to do a receiver setup by typing a snap command only. This performs cables switching, set proper local oscillator value, set procedure files, command the right focus position, set proper pointing parameters and whatever is needed to use that frequency.

3) Place all secondary focus receivers permanently mounted into the vertex room. The idea is to place the phase center of each feed in the plane containing the focus of the antenna but shifted respect to this last. In this way many receivers could be located and each one will be pointed by the subreflector using its five moving axis.

3. Improving antenna efficiency

The antenna efficiency is affected by many causes, such that

- a) rms surface accuracy of the panels making up the primary mirror
- b) primary mirror deformation due to gravity as the elevation changes
- c) rms surface accuracy of the subreflector
- d) pointing errors

All of these, although with different amount, affect antenna efficiency but not all give the same technical difficulties. In fact, items a and c are "only" matter of money, much money, because the state of the art is able to provide surface with rms accuracy needed, typically 0.1mm or so, made by aluminium for panels and plastic reinforced fiberglass for subreflector.

Item b is a very attractive technical challenge because to overcome it the idea should be to arrange a system for moving all affected panels to restore a parabolic shape of the primary mirror as the antenna elevation changes. The gravity deformation of our antenna was measured and the results were that a panel displacement of some millimeters at a maximum arises when the antenna looks at horizon or zenith. At this purpose the system involves a mechanical actuator and an electronic control system to command the panels at the pre-established position and to read the actual one. The heart of the system is the actuator; it needs a stroke of ± 5 mm, a compact manufacture, low cost and above all high reliability. About two hundred of these ones are needed, they will be mounted under the panels, in an hard environment and so failures have to be avoided as much as possible. We have designed and made two prototypes of mechanical actuator, and they are ready to undergo heavy tests to prove reliability and functioning. In a box of 240x165x65mm are contained the moving parts, the motor, the sensor position and the control electronics. In the final release all actuators should be connected by a network to communicate with a personal computer located into the station control room. Overcoming all these causes should bring the antenna efficiency at its maximum value, 50%, at 43GHz.

About item d we can say that Medicina rms pointing error is around 18-20 arcsec in normal operative conditions. If this is yet an acceptable value respect to our 22GHz HPBW, equal to 2 arcminutes, it isn't respect to an HPBW around 60 arcsec such that of our 43GHz receiver. So the antenna efficiency loss should be about 30%, only due to pointing errors. Therefore some way to correct them is necessary.

Since four years two electronic levelmeters and related measurement system are mounted onto Medicina antenna and can detect alidade deformation, for example due to wind and thermal effects. They were used to learn about solar heating effects on the antenna structure and the results matched with a finite elements structural analysis, they also were used to measure the azimuth plane tilt and the results matched with the estimated parameter obtained by an usual pointing calibration run. Further, stability tests on electronics was performed for over a year on daily basis. So the system is well tested and reliable and moreover all hardware and software needed to perform measurements is available. Therefore our aim is to try to use the system for a real time correction of the pointing errors, at least those ones due to the alidade deformations. Antenna time have to be allotted to start the tests.

4. News

Besides of the upgrade project many other development tasks were done at the station in the last year. The summary of them are as following.

- The pointing antenna control software have been integrated with the new PC Field System so this one is fully on line as the first step towards the MK4 upgrade. Last two geodetic experiments have already been done with it as well as the May 95 VLBI session.

- In incoming summer new filters and components will be mounted in the videoconverters so upgrading their bandwidth up to 16MHz. The new read/write electronics for the tape unit has been delivered. This complete the present status of the MK4 upgrade at Medicina.

- The old and obsolete electronic position converters of the antenna encoders have been changed with new ones designed at Medicina laboratories. The new design provides lower cost, easier maintenance, more performance.

- In the last years Medicina clock performance has suffered of a large day variation, outside the usable range. The cause was fixed in a inadequate conditioning system. So a new one has been implemented. The ambient temperature of the H-Maser room is now within $\pm 0.1^\circ\text{C}$.

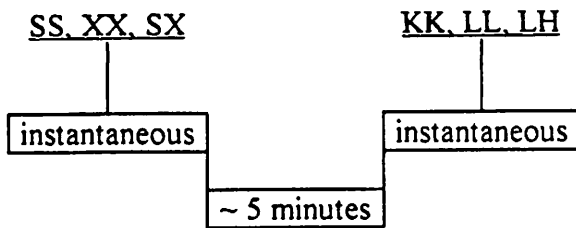
-Finally, a new generation of spectrum analyzer, usable for single dish spectral lines observations is available at Medicina. That is a high time and frequency resolution digital spectrometer capable to perform the fast fourier transform directly to the incoming analog signal in 33msec up to 20MHz bandwidth. After the FFT the boards compute the power spectrum and average up to thousands of these spectra. The averaged signal is then available for display or for further processing.

A lot of molecular and maser lines was measured and during the Jupiter-SL9 comet crash observations the high time resolution was exploited to compensate the fast Doppler shift between Earth and Jupiter and as a result a water line emission in the microwave region was detected.

Next month an upgrade of the machine will be completed and the choice to use both polarization channels will be available so two 20MHz bandwidth signals could be explored at the same time.

MEDICINA RECEIVERS FAST SWITCHING: PRESENT STATUS

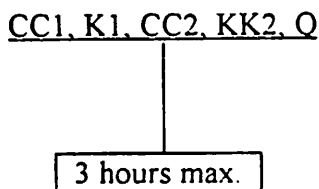
❶ PRIMARY FOCUS CONFIGURATIONS



SS= 2GHz dual channel
XX= 8GHz dual channel
SX= 2/8GHz single channel
KK= 22+24GHz dual channel
LL= 1.6GHz dual channel
LH= 1.4GHz dual channel

Note about switching: COMFORTABLE

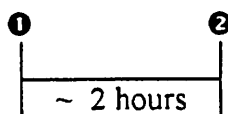
❷ SECONDARY FOCUS CONFIGURATIONS



CC1= 5GHz dual channel
K1= 22GHz single channel
CC2= 6, 6.6GHz dual channel
KK2= 12GHz dual channel
Q= 43GHz single channel

Note about switching: UNCOMFORTABLE

❸ SWITCHING BETWEEN PRIMARY/SECONDARY FOCUS RECEIVERS



Note about switching: VERY UNCOMFORTABLE

Fig. 1

MATERA VLBI STATION: STATUS REPORT

**G. Bianco
ASI - Matera**

**A. Cenci, G. Colucci, D. Del Rosso, L. Garramone
Nuova Telespazio S.p.A. - Matera**

1. INTRODUCTION

This report summarizes the present status (to May 1995) of the operational VLBI activities at the Matera Space Geodesy Center (CGS).

In the first part the main characteristics of the VLBI system and the operating activities are described.

In the second part the future plans for the Matera VLBI system are reported.

2. VLBI SYSTEM CHARACTERISTICS

The Matera VLBI system consists of a 20 meter diameter radiotelescope, designed and built in Italy, a Mark III Data Acquisition Terminal and a Time and Frequency System based on Cesium beam frequency standards and on a Hydrogen MASER.

Radiotelescope's main characteristics are:

- Cassegrain configuration;
- 2 meter subreflector;
- altazimuth mount with crossing axes;
- 2 deg/s max angular velocity (both axes);
- dual band, S/X conical horn feed;
- two stages, helium cooled FET low-noise RF receiver;
- wide band down converter.

The Data Acquisition Terminal is equipped with a VLBA narrow track tape recorder and is controlled by a 486 Personal Computer.

The Time and Frequency System was designed in order to meet the requirements for both SLR and VLBI systems. It consists of three frequency sources (two Cesium beam and one H-MASER) and three independent clock chains. The H-MASER is used also as frequency source for VLBI. Synchronization to UTC is guaranteed by a GPS receiver. In order to minimize the effect of environmental conditions, in particular for the H-MASER, the frequency standards are hosted in a dedicated room. This room has been built into the rock about 5 meter below the equipment room. Temperature measurements from May 1990 to May 1995 show variations in temperature less than 1°C/month with no active air conditioning.

2.1 VLBI Observations

Since May 1990 (starting of the VLBI acquisitions) up to May 1995 Matera participated to 160 VLBI sessions (total time of acquisition: 3353.5 hours) organized by NASA, USNO, NOAA, MPIfR and CNR (Istituto di Radioastronomia di Bologna). The time lost during the acquisitions for technical reasons was on the order of 1%.

The Matera system is affected by RF interferences in S-band due to TV relays. The effect is significant on two channels.

3. FUTURE PLANS

In September 1994 the upgrade process of the Matera VLBI system began. This process foresees the modifications of both the receiver chains (X and S) following the indications of NASA on the R&D VLBI systems. Allied Technical Services Corporation (ATSC) will supply the new receiver within this year. ATSC will perform also the holographic measurement of the VLBI antenna in order to check the surface quality.

A concept for real-time VLBI

HARALD SCHUH

Deutsches Geodätisches Forschungsinstitut (DGFI), Abt.I, Marstallplatz 8, D-80539 München, Germany, Tel.: +49/89-23031-214, Fax: +49/89-23031-240, e-mail: schuh@dgfi.badw-muenchen.de

1. Introduction

VLBI is an extremely precise modern geodetic technique for monitoring the Earth rotation and for the realization of the global reference system. However, the costs are relatively high and there is still a delay of one week minimum between the time of observation and the availability of the results. If this gap could be shortened to a few hours this would allow to monitor the relative station motions and the Earth rotation parameters in near real-time. This could be very useful for an earthquake warning programme, for monitoring the Earth rotation parameters needed for high precision positioning and navigation and as references for other "on-line" observing methods.

2. Present status of geodetic VLBI

VLBI is the only geodetic space technique which allows to simultaneously monitor *all* parameters which determine the orientation of the Earth, i.e. polar motion x_p, y_p , Universal Time UT1 and the nutation parameters $\Delta\epsilon, \Delta\psi$. VLBI is important for the realization of the global terrestrial reference system because it is based on the quasi-inertial reference system of extragalactic radio sources. Thus, it is much less depending on hypotheses than geodetic satellite techniques. In the past one and a half decades the accuracy of the results of VLBI measurements has improved considerably due to improvements of the VLBI technology and due to refinements of the models used for data analysis. However, the VLBI procedure with four independent steps:

- preparation
- observation
- correlation
- data analysis

has not changed since the end of the seventies. As can be seen on fig. 1, efforts and costs and also the time till availability of final results mainly depend on the procedure itself rather than on the technology or on the models.

Very Long Baseline Interferometry (VLBI)

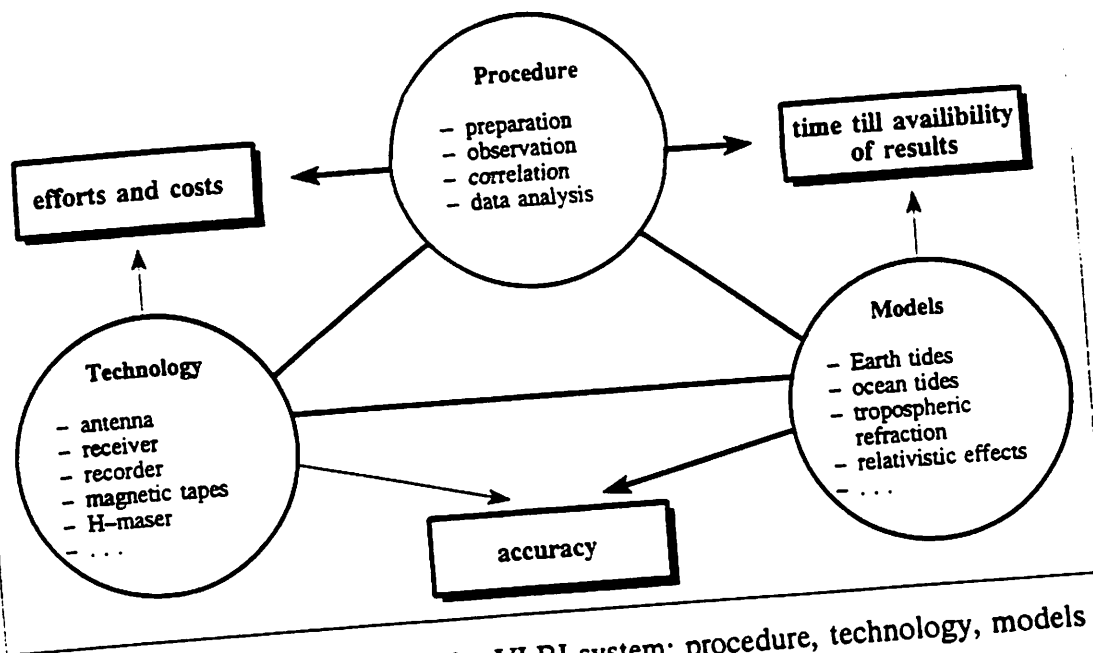


Fig. 1: The three components of the VLBI system: procedure, technology, models

In the last years information and communication technologies made rapid progress with respect to computer power and data transmission rates. The knowledge of special remote control techniques based on world-wide computer networks and of the application of modern software tools to process large amounts of data has increased, too. There is a strong need to make use of these recent developments in information and communication technologies and to innovate the VLBI procedure.

The concept for VLBI in near real-time will be presented in the next chapter. It is mainly the aspect of automation which will "automatically" streamline and accelerate the VLBI procedure. Further general remarks concerning the future of geodetic VLBI have been given by *Schuh and Campbell (1993)*.

3. A concept for VLBI in near real-time

All means which will contribute to an automation and acceleration of the VLBI process are briefly given below. These are the "glue" between the four steps of "classical" VLBI.

Steps of VLBI means for automation and acceleration

1. Scheduling
 - a) "automatic" scheduling by optimization methods
 - b) schedules by e-mail to stations
2. Observation
 - a) by teleoperation, i.e. remote control of radiotelescopes (in remote areas)
 - b) direct data transmission to correlator

3. Correlation
 - a) software correlation and fringe on parallel computers
 - b) supported by AI methods (artificial intelligence)
 - c) feedback to radiotelescopes
 - d) results of correlation directly transmitted to VLBI analysis centres
4. Analysis
 - a) supported by AI methods
 - b) global solution on parallel computers
 - c) continuous update of global data base (Kalman filter)
 - d) automatic transfer of results to Earth observation centres (IERS, Earthquake research centres,)

An important component of the concept for real-time VLBI is to directly transmit the received signals from the radiotelescopes to the correlator or to a central computer for further processing (2a). High bandwidth communication networks using optical fiber or communication satellites will soon allow intra- and intercontinental transmission of signals at hundreds of Mbits/sec.

The main advantages of the direct transmission of data are the following:

- no tape recording and playback of the observed radio signals is needed. This avoids degradation and loss of data,
- the check of the quality of the recorded data during the time of observation will be possible. Errors and failures can be reported back immediately from the correlation centre to the radiotelescopes,
- the efforts for purchasing, handling and transporting the large number of big magnetic tapes can be saved and the cost-effectiveness could be improved.


The correlation process itself could be done by software only, rather than by special processors (3a). First successful correlation runs by software only using a transputer based parallel computer have been reported by *Fayard et al.* (1993). But this requires high computer power as the MkIII correlator performance is equivalent to 1 Gflops/baseline and that of the MkIV correlator to 10-100 Gflops/baseline.

In the final data analysis many steps which are carried out manually can be supported by artificial intelligence (AI) methods (4a). First examples have been shown by *Schuh* (1993). In a semi-automated data analysis more data can be processed faster and at lower costs. Many parts of the data analysis software can be parallelised, and by using highly parallel computers the time for a global solution combining many hundreds of VLBI sessions will be reduced from presently 8 hours and more to just a few minutes (4b). In the future, a global data base of VLBI observables can be updated permanently (4c) and by Kalman filter methods a solution for monitoring of the Earth rotation parameters and of geodynamic effects in near real-time with 1 mm accuracy will be done in a few seconds.

Table 1 gives a short overview about the current status and examples of activities which have already been carried out with respect to the different parts of the concept, i.e. 1a-4d, presented above. The table contains also estimates on how much research and how much technical development (rating from 0 to 3) is needed for the final realization of each

component and on the possible time frame till finalization. The latter mainly depends on the efforts which are made for each of the components of the total concept. It can be seen that all of the proposed innovations of the VLBI procedure could be finished in five to eight years.

Real-time VLBI: Status and work to be done					
steps	status and activities	research needed	technical development needed	realization [years]	
1. Scheduling					
a)	working				
b)					
2. Observation					
a)	work by japanese groups (Showa, Key Stone) VLBA	1	2	2 - 4	
b)	Key Stone Project EU proposal by Schuh/Hase	1	3	3 - 5	
3. Correlation					
a)	G. Petit, IGN Paris	1	2	5 - 8	rating: 0 - none 1 - low 2 - medium 3 - high
b)	—	3	1	3 - 5	
c)	see 2.a)	1	3	3 - 5	
d)	working				
4. Analysis					
a)	work by Schuh	3	1	3 - 6	
b)	contacts with HPC groups	3	1	1 - 2	
c)	Herring et al. and others	2	1	1 - 2	
d)	—	0	1	4 - 8	



DGF



Table 1: The concept for next generation VLBI: current status and work to be done in each step explained in this chapter

4. Benefits of the new VLBI concept

As mentioned in chapter 2 there is a good chance to make use of the rapid progress in modern information and communication technologies to obtain a considerable innovation of the VLBI progress.

The main advantages will be:

1.) High degree of automation

- to reduce the costs
- to be able to process large amount of data
- to be more independent
- to be safer against failures and data losses

2.) Results in near real-time, i.e. in 12-24 hours after the VLBI session

- to provide the ERPs
 - for high precision terrestrial navigation and positioning
 - for space tracking
 - as references for continuous "on-line" observing methods of ERPs (e.g. laser gyro, supra-fluid helium gyro, ...)
- to monitor crustal deformations in near real-time. Then local/regional measurements by terrestrial geodetic instruments or by GPS could be referred to the independent high-order VLBI network which starts to observe in the near real-time mode when "suspicious" regional deformations have been monitored. This would be an important contribution to an international Earthquake warning system because so-called precursors usually occur between 6 and 0 days before the Earthquake in a distance of up to 1000 km from the epicentre.
- On the astrophysical side, real-time VLBI will have an impact on astronomy as transient phenomena in radio sources (e.g. super novae, rapid intra-day variations of the flux density of active galactic nuclei, ...) will be observable. After having detected such effects in quasi real-time by scanning on known candidates, the network of radiotelescopes could immediately start intensive observation of the specific phenomenon.

5. Conclusions

There is a good chance for basic innovations of the VLBI procedure which are necessary to obtain a higher degree of automation. This will decrease the time till availability of the final results considerably, i.e. to 12-24 hours after the VLBI session. Each part of the concept has a different potential concerning cost and time reduction and should be elaborated in parallel. An integration of similar developments in other techniques, for instance automation in GPS, is necessary. Besides the innovation of the VLBI *procedure* further improvements of the VLBI *technology* and of the *models* used for data analysis should be aimed at.

6. References

Fayard, T.; Petit, G.; Noel, J.; Moueza, J.: The New CNES Soft-Correlator, proceedings of the 9th Working meeting on European VLBI for Geodesy and Astrometry, Sept. 1993, Mitteil. a.d. Geodätischen Instituten der Rhein. Friedr. Wilh. Univ. Bonn, Nr. 81, pp.123-128, 1993.

Schuh, H.; Campbell, J.: The Future of Geodetic VLBI, Proceedings of the 9th Working meeting on European VLBI for Geodesy and Astrometry, Sept. 1993, Mitteil. a.d. Geodätischen Instituten der Rhein. Friedr. Wilh. Univ. Bonn, Nr. 81, pp. 189-193, 1993

Schuh, H.: An Expert System for the Selection of Parameters in Solve, proceedings of the 9th Working meeting on European VLBI for Geodesy and Astrometry, Sept. 1993, Mitteil. a.d. Geodätischen Instituten der Rhein. Friedr. Wilh. Univ. Bonn, Nr. 81, pp. 79-86, 1993.

The Use of the Datahighway for Real-Time Correlation of VLBI-Data

Hayo HASE

*Institut für Angewandte Geodäsie
Fundamentalstation Wettzell
D-93444 Kötzing
Germany
hase@wettzell.ifag.de*

Abstract. The "information age" is based on wider bandwidth for data exchange through the networks. In the near future the bandwidth of networks will be higher than the data output rate of a standard MkIII VLBI experiment. Therefore the real-time-correlation of VLBI-data using the datahighways between the stations and the correlator becomes possible. Some technical background informations and ideas for its realization are given.

1 Introduction

Very Long Baseline Interferometry (VLBI) is the only technique which can measure all three Earth orientation parameters (EOP) independently. Therefore VLBI is the primary technique for the determination of EOP at the International Earth Rotation Service (IERS) [1]. VLBI plays a major role in the production of Celestial and Terrestrial Reference Frames.

The condition to achieve the high accuracy of a few ten picoseconds for the group delay is to deal with a number of models for various long and short periodic effects in the appropriate manner. Doing so it became possible to monitor with VLBI subdaily EOP variations [2]. In order to use those informations e.g. for the navigation of space vehicles or for improved Earth models the availability of EOP has to be closer to real-time. The recent developments in global datahighways illuminate the possibility of Real-Time-VLBI [6].

2 Typical VLBI Operation

The necessary steps for VLBI operation are executed sequential. They are

- scheduling of the observation program,
- execution of the observation program synchronously at different sites with production of data.
- transmission of the data to a correlator for the correlation and determination of the observables.

- post-processing of the data according to the scientific goals and publication of the results.

The time needed for each step is depending of the degree of automatization and the distance of data transportation. In order to achieve faster results the automatization and the speed of data transportation have to be increased in the future.

The scheduling was almost automated with the optimization algorithms of Steufmehl [7].

The execution of the observation requires still manpower to put new tapes onto the recorder and observe necessary devices for usually 24 hours.

The transportation of the data takes at minimum another 24 hours.

The correlation and post-processing needs in the ideal case about 27 hours, usually 48 hours or more.

That means that the results are in total by 4 days delayed before they can be used.

Accurate EOP are of interest for any satellite technique and high speed space navigation. Other geodetic techniques like GPS and Satellite Laser Ranging (SLR) are able to determine EOP also. The difference between VLBI derived EOP and satellite derived EOP are, that VLBI determines all three parameter and the nutation independently of any other technique. GPS and SLR cannot determine nutation and need after a couple of days a set of VLBI derived EOP in order to compensate drifts between the satellite orbits and the Earth itself. Further on accurate EOP are necessary for SLR in order to be able to track the satellite.

From the theoretical point of view the use of measured values instead of modeled values promise higher accuracy, when the measures are consistent and available. Fundamental stations can reach a higher degree of integration of the different techniques. Part of it will be Real-Time VLBI.

3 The concept of Real-Time VLBI

The concept of Real-Time VLBI is to parallelize the sequential steps of the typical VLBI operation. The ideal case would be to have an automated dataflow from the station formatters directly into the correlator using highspeed data networks. The data are correlated in one pass only and fed into a post-processing software, which computes one solution after each new scan. The results will be distributed over highspeed data networks to the user.

In other words: While the radiotelescope is moving towards the next source, the previous scan is already transformed into a result.

The correct term for this ideal case would be "Near-Real-Time-VLBI", since the group-delay itself, the data transmission, the computations need time also. But in comparison to the minimum of 4 days in order to achieve results, any result produced within a few minutes or seconds after the observation is here for simplicity described with the term "Real-Time VLBI".

The hardware key to Real-Time VLBI is the data network infrastructure; the software key is a new post-processing software design.

4 The Data Output at VLBI-Sites

In the geodetic VLBI community the Mk3 standard is widely used. The Mk3 hardware for the data acquisition terminal (DAT) was developed in the late 70's. In the end of the 80's newer components were used to built VLBA-data acquisition terminals, which can be used for Mk3 observations with minor modifications. Nowadays we find Mk3 and VLBA equipment at the stations. Within the next years the new Mk4 standard will become effective, which requires upgrades at the Mk3 and VLBA-DATs in order to meet the Mk4 specs.

The data output rate in a geodetic standard Mk3 mode C VLBI experiment is 56Mbit/s at a Mk3-DAT and 63Mbit/s at a VLBA-DAT. The difference between both output rates is due to the different formatters of the Mk3 and the VLBA systems. Mk3 uses a data-replacement-mode, while VLBA uses a data-insertion-mode. That means that the Mk3 formatter overwrites some source data with time-information and parity and sync bits, while the VLBA formatter inserts those bits into the source data-stream.

The new Mk4 standard will be based on the data-replacement-mode. Upgradekits will replace the formatter in both Mk3 and VLBA equipment. Upgraded Mk3 and VLBA terminals will then produce at all stations the same amount of data.

The Mk4 data output rate will depend on the observation mode. Mk4 was designed for data output rates up to 1Gbit/s, but it will also work on the Mk3 level of 56Mbit/s. Mk4 exists only on a prototype level and until it will be the adopted standard at each station a few more years will pass by.

Therefore I focus the Mk3 standard mode C operation with an output rate of 56Mbit/s. For bandwidth consideration in the next chapter one should keep in mind, that at the correlator side the bandwidth has to be n -times the data output rate of one station in order to correlate with no delay (n =number of stations in an experiment).

5 The Data Network Infrastructure

Worldwide available is the 'plain old telephone system' (POTS) based on copper wires. The bandwidth corresponds to the bandwidth of natural speech, hence it is limited to 3000Hz or expressed in digital terms used for computer modems it is 2.4kbit/s. With quadrature amplitude modulations the limitation of POTS can be overcome and reach 9.6kbit/s and with additional quadrature phase modulation even 28.8kbit/s. In a noisy connection the transmission rates drops down to 2.4kbit/s.

The next development is the 'integrated services digital network', which is based on three copper wires and reaches a bandwidth of 128kbit/s. ISDN isn't available in all countries and is installed on special request only e.g. in Germany.

The next higher bandwidth technique is called T1, based on 24 copper wires with 64kbit/s each. A bandwidth of 1540kbit/s can be reached. Those lines exist for long-distance phone links and for Internet connections.

Much higher bandwidth can be realized with optical fibres instead of copper wires. One existing technique is called T3, based on optical fibre with a bandwidth of 45Mbit/s. T3 is used for wide area networks (WAN) like the Internet.

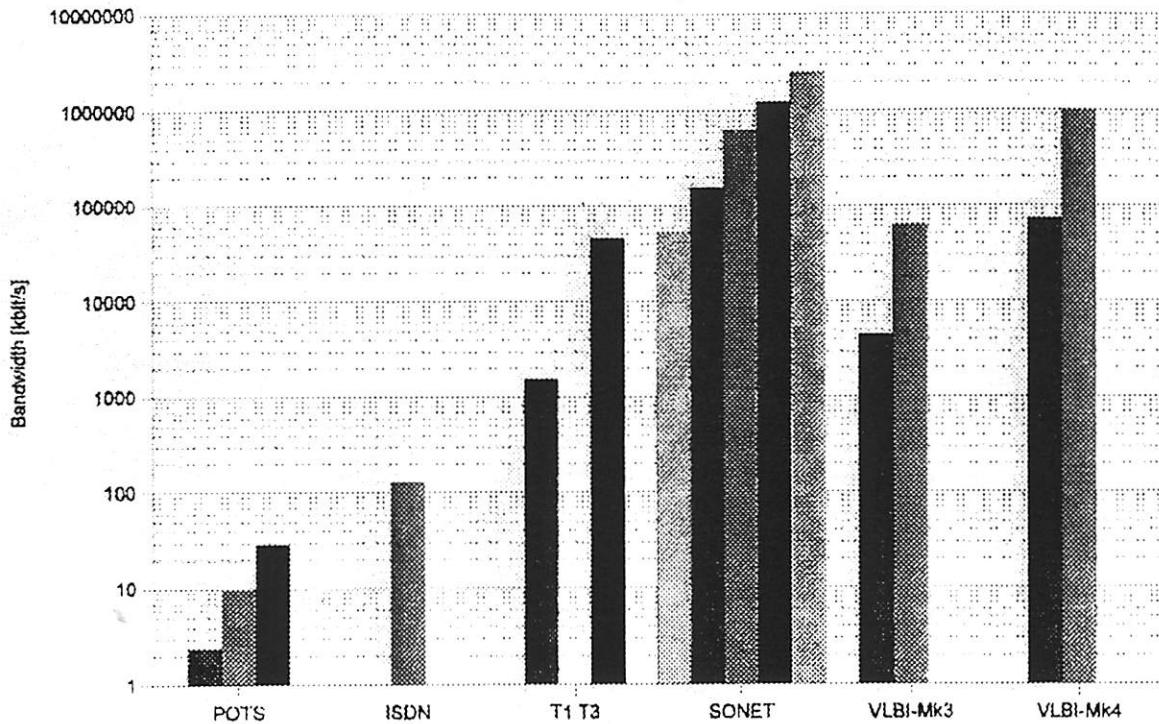
A new family is 'synchronous optical network' (SONET) also based on optical fibres on which different bandwidth standards using the connection-oriented 'asynchronous transfer mode' (ATM) can be installed. According to CCIT STM-1 the bandwidth is 155Mbit/s. In Germany this mode is currently in a pilot phase and is announced to become effective in the end of 1995. The future standards will be multiples of 155.520Mbit/s. The CCIT STM-4 has a bandwidth of 622Mbit/s. A network with 622Mbit/s will be the future network of the National Science Foundation in the US [8]. During 1996 a pilot phase for 622Mbit/s is scheduled by the German Telekom. The availability will be in the end 1996.

Name	max.Band-width [kbit/s]	Technique	Availability
POTS 'plain old telephone system'	2.4	telephone line	worldwide
	9.6	quadrature amplitude modulation	with noisy links the bandwidth decreases to 2.4kbit/s
	28.8	quadrature phase modulation	
ISDN 'integrated services digital network'	128	2*64 kbit/s + 1*16 kbit/s, twisted pair	partly
T1	1540	24*64 kbit/s, copper wires	long-distance phone links, Internet
T3	45000	optical fiber	existent: WAN, Internet
SONET 'synchronous optical network'	51480	optical fiber	
	155520	optical fiber CCIT STM-1	announced for 1994 by US telephone companies, end of 1995 in Germany
	622080	optical fiber CCIT STM-4	future network of NSF, end of 1996 in Germany
	1244160	optical fiber CCIT STM-8	under development
	2488320	optical fiber CCIT STM-16	

All copper wire based techniques have insufficient bandwidth to transport the Mk3 56Mbit/s in real-time. Only with optical fibers at the correlator and to the stations Real-Time VLBI will become possible. From the view of offered bandwidth it will be possible to run a 2 station VLBI experiment on real-time base in the end of 1995 and a normal 8 station Europe VLBI experiment in the end of 1996. Technologically we are close to the turning point in which the embarrassment in VLBI to record data on tapes at the stations and to play the data back at the correlator can be overcome.

The development of available bandwidth is exponential. In the future also Mk4 experiments could be treated in real-time.

Data Transmission Systems vs. VLBI Data Output



The first column of VLBI-Mk3 indicates the data output rate of one channel (4Mbit/s) which is interesting for test purposes before an experiment, while the second indicates the amount of all 14 channels (56Mbit/s). VLBI-Mk4 respectively.

6 Advantages of Real-Time VLBI

Numerous advantages can be predicted, if data highways will be used for Real-Time-VLBI.

- Immediate results. Real-Time EOP, station coordinates, baselines, etc., (with relevance also for space VLBI projects).
- No delay in the correlation. With the first observation the performance of each station can be determined. If necessary an experiment can be postponed until a station is up.
- No losses of bits. The bits reach the correlator 100% errorfree, while the process of write-to-tape and read-from-tape is noisy. Up to 50% of the data from tapes fed into the correlator have been seen to be wrong due to old heads.
- Data networks are safe. The best achievable data-quality at the correlator will lead to shorter scans at the sources and better geometrical distribution with an scientific gain for subdaily EOP variation studies.
- Refracting will not be necessary.
- No backlog of correlation at the correlator.
- No recorder means less maintenance at the station.

- One pass correlation saves correlator resources.
- Remote control of stations becomes possible. Nobody needs to change tapes.
- If stations with and without access to the datahighway observe together, data of linked stations can be recorded at the correlator and played back on the same recorder, when remote tapes have arrived. This will decrease the loss of data from tape.
- High speed datalink at the station for other purposes (e.g. video aided assistance from the community in case of technical problems at the station, video working meetings on European VLBI for geodesy and astrometry).
- Interactive monitoring of highly structure variable sources opens a new research field in radioastronomy.

7 Costs

Besides the costs for hardware and software developments one has to consider the transmission costs. The situation may vary from country to country.

Today the German Telekom offers a Datex-M service, which has a bandwidth of 34Mbit/s, the highest available bandwidth up to now. Datex-M uses the DQDB as connectionless transportation technique. Prices are depending on the transmitted volume. In future services based on connection-oriented ¹ ATM instead of connectionless ² DQDB prices will depend on the distance and transmission time, not on the volume.

Further on from 1996 the monopol of the German Telekom will fall. In competition with other service provider prices will be subject of the market situation. In addition other companies like the energy supplier and the railroad company will be able to offer own network infrastructures. It is impossible to estimate the concrete costs for using broad bandwidth for VLBI-data since many parameters are not known precisely enough yet. Nevertheless all experts expect for the future that the prices will decrease with the acceptance of the information technology by the population.

Further it is worth to push for free access to and the free use of a European (global) science network.

Needless to mention that money for tapes (Mk4 thintape: 1100USD) and their transportation as well as money for recorder heads will be saved in the case of Real-Time VLBI.

¹Connection-oriented is similar to make a telephone call. Before data packages are transmitted, the line between transmitter and receiver needs to be established. Connection-oriented ATM has the advantage of "bandwidth on demand" and "quality of service", which are necessary for time-sensitive traffic such as Real-Time VLBI.

²Connectionless is similar to send a letter, where the route is not fixed when sending information. Data packages are given to the network without a clear routing description (e.g. Ethernet, Token Ring, DQDB).

8 What is to do?

Work at the stations:

- Connection to the national datahighway with optical fiber.
- Development and installation of an highspeed interface between VLBI-formatter and datahighway.

Work at the correlator:

- Connection to the national datahighway with optical fiber(s).
- Development and installation of an highspeed interface between datahighway including a data buffer with a capacity of a few ten milliseconds of data.
- Construction and installation of the data buffer, which can compensate for group delay, transmission delay and device dependent delays.
- Correlator interface for the databuffer and control software which can deal with data from buffer instead of tapes.
- Software interface for the post-processing software.

Work at the computation centers:

- Software interface for scanwise correlator output.
- Reorganisation of the software packages for continous processing.

Some research work in relation to the application of data(de)compression algorithms to VLBI rawdata needs to be investigated in order to save network (and also tape!) resources.

If all steps are seen under the aspect of an automated data flow with the support of expert systems an unattended "VLBI-Machine" or "EOP-Watcher" can be realized.

9 Where to start with?

First it needs to be said, that all the necessary parts and tools for gigabitlinks resp. to perform the steps above are already available [4].

The action items above need a common effort from the different groups at the stations, correlators and the post-processing groups. For the realization of the big idea a few smaller projects can be carried out. This will give the opportunity to collect experiences with reliability of the datatransmission and means to move slowly towards the Real-Time-VLBI.

The most likely approach will be to start with using the existing data network infrastructure, which is based on the Internet or DECnet. The VLBI data can already travel through that network to the correlator. The transmission speed depends on the local access interface to the datahighway and on the amount of traffic on the datahighway. The bottleneck will be the access to and exit from the datahighway.

3 minute scan = $180s * 56\text{Mbit/s} / 8 = 1260\text{Mbyte VLBI data/station}$	
Interface to datahighway	Netto Transmission Time for 3min scan
9.6 kbit/s	12.4 days
64 kbit/s	1.8 days
2 Mbit/s	1.4 hours
155 Mbit/s	1 min 5 s
622 Mbit/s	16 s

The table above shows the netto transmission times (only VLBI data - no header, no delays) for a 3 minute scan of one source. The amount of data is about 1260Mbyte which could be buffered at the station on a 2 GByte harddisk instead of magnetic tape [9]. From the harddisk the data could travel in small packages through the network to the correlator, where another harddisk receives the data. From the harddisk buffer the correlator will be supplied as soon as the scan has completely arrived. A second harddisk at the sites and the correlator for each station will be necessary, when correlation/sending of a previous scan and data reception of following scan should happen at the same time. The delay with the fixed disk buffers can be expected to be a few minutes.

The 9.6kbit/s interface is to slow in order to accelerate the data transmission. A tape can be mailed quicker.

The 64kbit/s interface enables 2-4 days in advance at least a fringe test e.g. with a critical station to verify a new setup before an experiment. The amount of time is more or less the same than to mail a tape. But if only one channel is send for fringe tests (similar Mk2) the transmission time is $1.8d/14 = 3.2$ hours. This is interesting for stations which exchange receivers often in order to make a test just before the experiment starts. This might be an interesting option according to the 'Recommendations to reduce EVN downtime' [5].

The 2Mbit/s interface enables the stations to check the complete setup on the day before the experiment, which is faster than to record and send tapes. At the moment 2Mbit/s is e.g. the highest available speed at the German science network (DFN-WiNet, provider of Wettzell).

The future possible interfaces at 155Mbit/s resp. 622Mbit/s will enable the Real-Time VLBI, perhaps without any buffer at the sites. The delay between observation and arrival of the data at the correlator should decrease to fractions of seconds.

10 Conclusion

The challenging data infrastructure enables to set up Real-Time-VLBI as an advanced technique for Earth orientation and geodynamic research. The VLBI community has the chance to take advantage of the "information age" for their own goals and needs. In the concert of all space geodesy techniques VLBI cannot be replaced for EOP research due to its relation to the quasi-inertial system of the quasars. But VLBI also is with its delay for results of at least 4 days the slowliest technique, while the GPS and SLR communities push towards real-time results.

References

- [1] Boucher, C., Altamimi, Z., Duhem, L.: Results and Analysis of the ITRF93, IERS Technical Note 18, Observatoire de Paris, October 1994
- [2] Haas, R., Campbell, J., Schuh, H.: Geodynamical Parameters Determined by VLBI, this proceedings
- [3] Hase, H., Schlüter, W., Dassing, R., Kilger, R.: Echtzeitkorrelation von VLBI-Beobachtungen für Erdrotationsbestimmung, Proposal for the German VLBI Meeting, Bonn, 13.12.95
- [4] Hewlett Packard: The 1995 Digital Communications Design Symposium, Technical Papers. München, 1995
- [5] Sanghera, H.S., Rioja, M.J., Dallacasa, D.: EVN Downtime 1993-94, Report presented at EVN Directors Meeting, December 1994
- [6] Schuh, H., Campbell, J.: The Future of Geodetic VLBI, Proceedings of the 9th Working Meeting on European VLBI for Geodesy and Astrometry, Mitteilungen aus den Geodätischen Instituten der Universität Bonn, 1993
- [7] Steufmehl, H.: Optimierung von Beobachtungsplänen in der Langbasisinterferometrie (VLBI), DGK Reihe C Nr.406, Verlag des Instituts für Angewandte Geodäsie, Frankfurt am Main, 1994
- [8] Swadley, R.K.: The Internet Unleashed. SAMS Publishing, 1994
- [9] Whitney, A.: private communication, 1995

Status Report ERS/VLBI Station O'Higgins Antarctica

Andreas Reinhold, Reiner Wojdziak
Institut für Angewandte Geodäsie
Außenstelle Leipzig
Karl-Rothe-Str. 10-14
04105 Leipzig

Since 1993 four VLBI observation campaigns have been performed under participation of the ERS/VLBI station O'Higgins which comprised altogether 18 experiments with 24 hours observation time each. All experiments carried out delivered results in the following correlation and so are available for further scientific evaluation and interpretation.

Besides the VLBI activities further geodetic measurement equipment was installed and series of measurements were performed to enable a more comprehensive geodetic, geologic and geomorphologic interpretation of the area around the station O'Higgins.

1. VLBI Experiments

O'Higgins forms together with stations in South America, Africa, Australia and Oceania the VLBI network "Southern Hemisphere" and is integrated into various projects.

Within the project "Dynamic of Solid Earth" (DOSE) POLAR-S experiments (NASA GSFC) were performed from 1993 to 1995 and SHS experiments (NOAA NGS) in 1993/94. To improve the accuracy of coordinate determination from sources of the Southern Hemisphere O'Higgins participated in the SOREF experiments of the US Naval Research Laboratory in 1993 and in the SURVEY experiments (NASA GSFC) until 1994.

The development in the VLBI community brought also for O'Higgins far-reaching changes in 1995. So with the start of the planned observation campaign in September/October 1995 only experiments within the Southern Terrestrial Reference Frame (STRF) will be performed.

2. Problems with VLBI Equipment

Accuracy and reliability of VLBI data from O'Higgins are affected by some technical problems.

Cable Delay:

The cable delay data are still useless because they are too instable. The cable measures vary by about 30 us during the experiment and contain jumps. Various special investigations haven't brought any conclusions for reason yet.

Formatter jumps:

For not yet known reasons the formatter time jumps uncontrollable by one second forward or backward - several times within one experiment. This complicates the correlation and should be removed during the next observation campaign.

Parity errors:

Track 14 and 25 show parity and sync-errors. Investigations show that the error could be in the Analog Drive Module. This effect is at present eliminated by shifting the tracks to free VLBA tracks.

3. Extension of Geodetic Data Registration at O'Higgins

In the area of the station O'Higgins two further geodetic measuring systems were installed in February 1995:

a) permanent GPS registrations with a Turbo Rogue receiver:

The receiver was permanently installed on a special pillar and protected with a radom. The registered data are automatically transferred to Wettzell via INMARSAT every day. So data from this station in Antarctica have been available to IGS since February 1995.

b) automatic gauge measuring station:

In a water depth of about 4 to 5 m and 20 m away from the shore an automatically working pressure sensor was permanently installed for registration of data for derivation to tide. The data are at present registered on the spot on a ROM. Data for evaluation are available until 10 March 1995 at our institute.

c) GPS projectes

O'Higgins was in 1993 integrated into the SCAR GPS project and 1995 into the German Antarctic GPS project.

The geometric relations between radiotelescope and excentric sites of geodetic measuring equipment are determined terrestrial with high accuracy.

For the stay in September/October 1995 the following tasks are planned besides the VLBI experiments and works at VLBI equipment:

- stabilization of data registrations for the Turbo Rogue,
- integrating the measuring data of the gauge system and of the local wheather station into the daily data transfer via INMARSAT,
- installation of a PRARE Ground Unit for orbit tracking of ERS2.

Status Report

VLBI - calculations at IfAG, Agency Leipzig

Volkmar Thorandt, Dieter Ullrich
Institut für Angewandte Geodäsie
Außenstelle Leipzig
Karl-Rothe-Str. 10-14
04105 Leipzig

The VLBI evaluation group of IfAG in Leipzig has consolidated at present. After a phase of getting into the CALC/SOLVE software - where we were essentially supported by the VLBI group Bonn and by NASA GSFC - we now independently evaluate experiments and exchange results with other VLBI groups. According to an agreement between IfAG and the Geodetic Institute of the University Bonn (GIUB) we are responsible for generating standard databases from correlator data and distributing the magnetic tapes among the stations and for electronically providing the databases to GIUB, USNO and NASA GSFC and to other interested institutions on request.

At present the evaluation of experiments comprises generating separate solutions of all IRIS-S experiments and of all experiments in which O'Higgins participated and still participates.

Objectives for the result of evaluating the experiments have been so far the determination of earth's rotation parameters and the derivation of coordinates of the station O'Higgins.

We lately started the computation of global solutions for longer time periods.

For the future it is planned that the IfAG VLBI group generates its own global solutions which are equally sent to IERS. Together with the group working at the Geodetic Institute of the University Bonn the results shall be published.

Temperature Stability of the Onsala 20-m Antenna and Its Impact on Geodetic VLBI

G. Elgered and T.R. Carlsson

Onsala Space Observatory, Chalmers University of Technology

S-439 92 Onsala, Sweden

phone +46 31 7725500, fax +46 31 7725590

e-mail: geo@oso.chalmers.se

Abstract. The demonstrated repeatability of the height component of a site estimated from geodetic Very-Long-Baseline-Interferometry (VLBI) observations is at the mm-level. Based on anticipated seasonal temperature variations of the antenna concrete foundation we have estimated the position of the reference point to vary with an amplitude of a few mm. Therefore, continuous temperature measurements of the concrete pedestal started in December 1994. We will report on the data acquired up to the middle of May 1995. The maximum seasonal effect of the height of the reference point is estimated to be 4 mm between summer and winter. Horizontal displacements, as well as height changes during a 24-hour experiment, inferred from the data obtained so far, is estimated to always be less than 1 mm.

1. Background

The geodetic Very-Long-Baseline-Interferometry (VLBI) antenna is typically a rather large piece of equipment, which is not moved around too easily. This is especially true for the 20-m radio telescope at the Onsala Space Observatory. A basic requirement, however, is that the geodetic reference point, the intersection of the azimuth and the elevation axes, is stable over short as well as long time scales. In order to quantify this requirement we use the demonstrated state of the art reproducibility of the estimated coordinates based on geodetic VLBI data. Twelve 24-hour experiments were carried out with NASA's R&D-network during two weeks in January 1994. The campaign is referred to as the CONT-94 campaign and results using these data have also been presented by *Carlsson et al.* [1995, this volume]. Figure 1 shows the estimated vertical coordinate of the Onsala antenna. We note that both the formal ($1\text{-}\sigma$) error bar for a 24-hour experiment and the observed weighted root-mean-square (wrms) scatter about the mean are approximately 5–6 mm. Furthermore, we may use all experiments to calculate the $1\text{-}\sigma$ uncertainty of the mean. This uncertainty is hence only 2 mm. Therefore, given that we have VLBI data of this quality, we require that the variations in the position of the geodetic reference point, relative to the underlying granite rock, must be significantly smaller than these numbers in order to be neglected. If not, corrections must be made, *e.g.*, based on a model using measured temperature variations as input data.

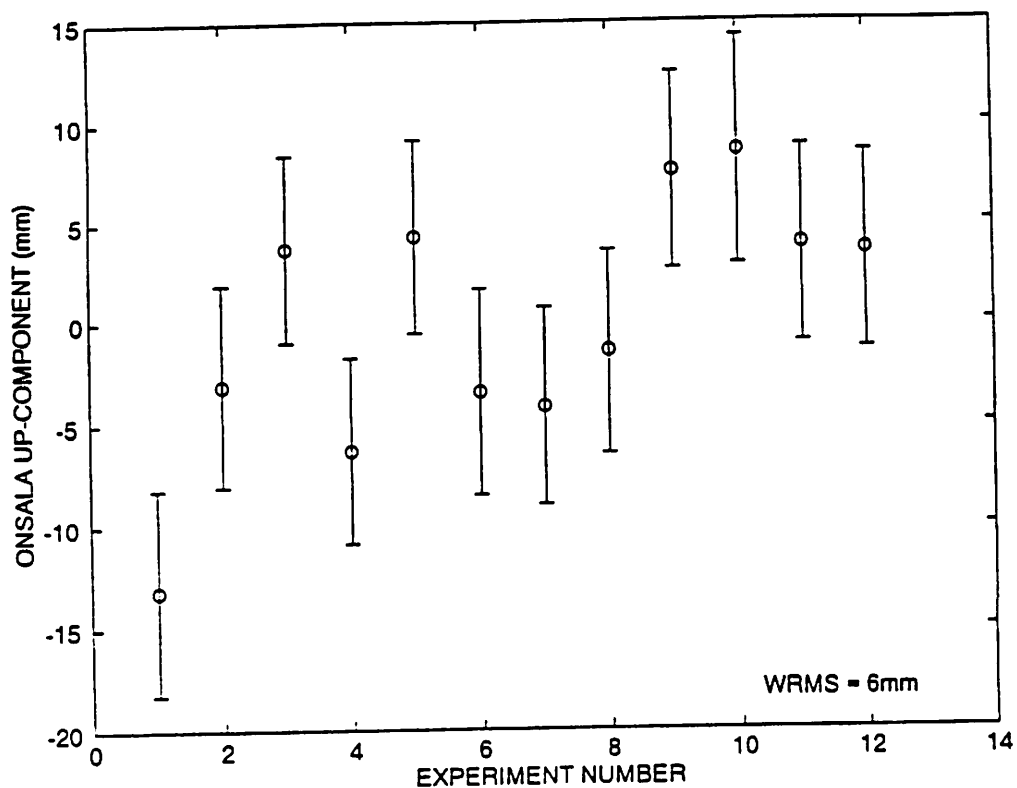


Figure 1. The repeatability of the estimated local vertical coordinate of the reference point of the Onsala VLBI antenna during the CONT-94 campaign.

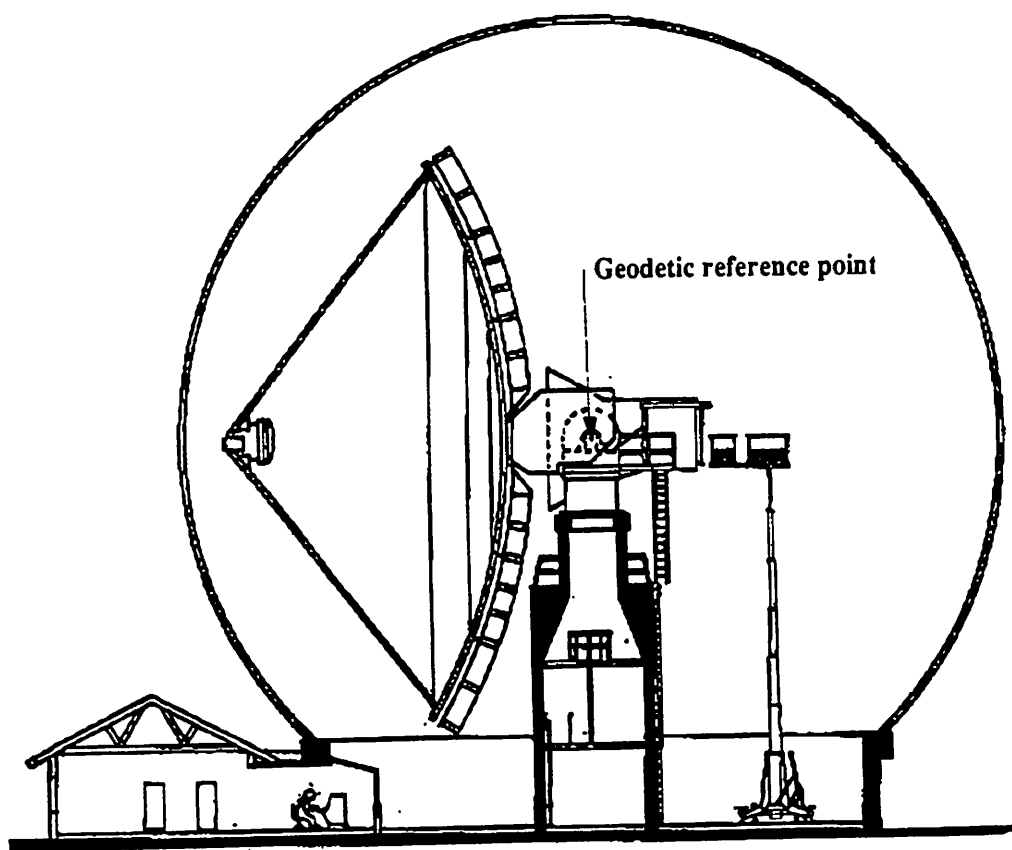


Figure 2. Drawing of the Onsala 20-m radio telescope. The radome diameter is 30 m.

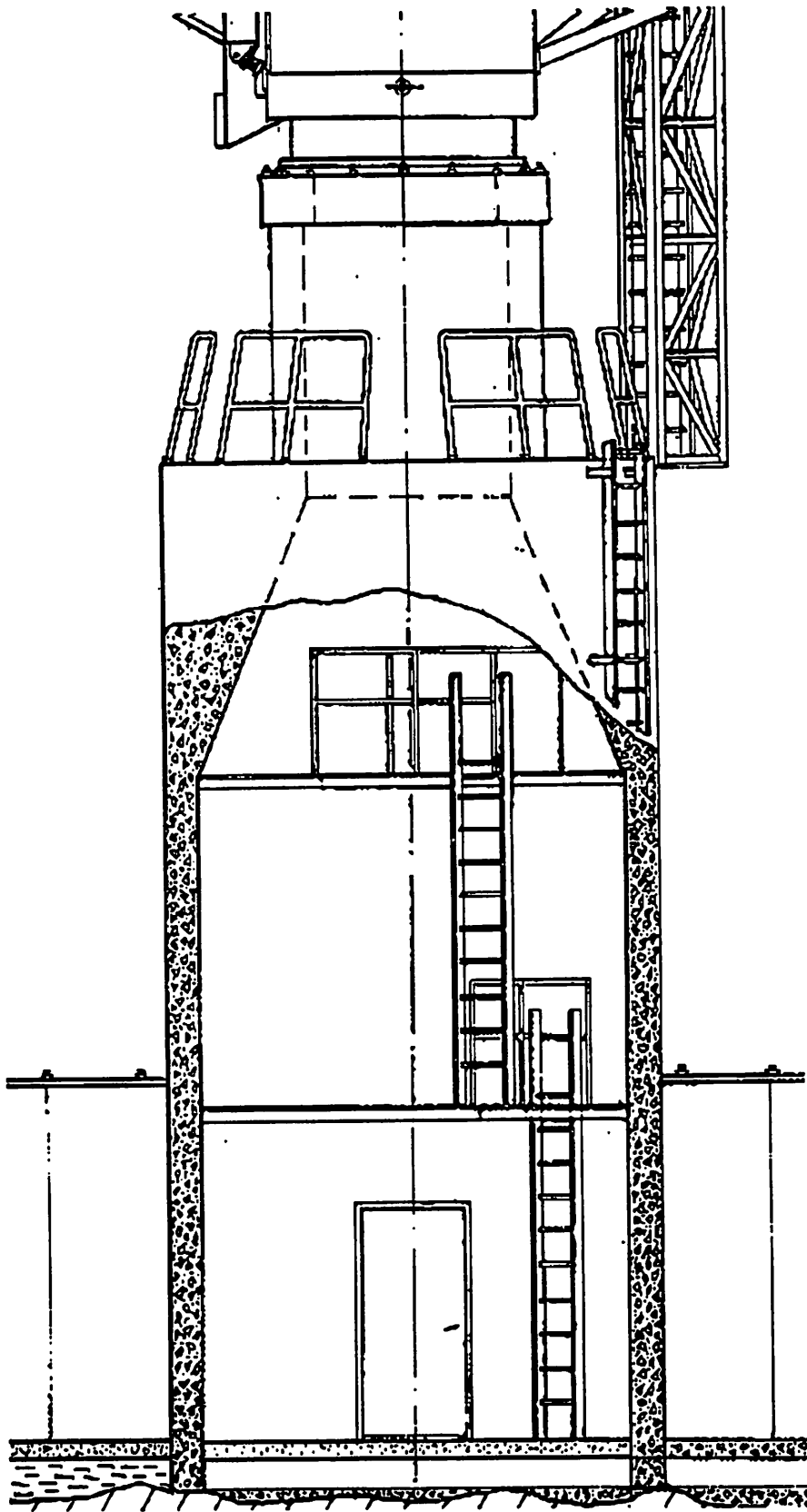


Figure 3. A closer look at the antenna foundation of the Onsala 20-m radio telescope. The top of the concrete foundation is 11.29 m above the ground floor. The distance from the ground floor to the geodetic reference point (located above the top of this drawing) is 14.20 m. The thickness of the concrete wall is 30 cm.

A drawing of the radome enclosed 20-m antenna is shown in Figure 2, where also the approximate location of the geodetic reference point is indicated. A close-up of the concrete foundation is shown in Figure 3.

In order to evaluate the importance of temperature variations on the stability of the VLBI reference point the following questions should be answered:

- (i) What is the range of the temperature variations during a one day long geodetic VLBI experiment?
- (ii) What is the range of the temperature variations over a year?
- (iii) What is the relation between the temperature of the concrete and the outside temperature (which is approximately the same as the temperature of the air inside the radome because the radome material provides poor insulation)?
- (iv) How large are vertical and horizontal temperature gradients in the tower?
- (v) How large is the temperature effect caused by the four heaters used to prevent condensation on the outside of the radome?
- (vi) Do we need to carry out measurements of displacements of the antenna foundation in addition to the acquisition of temperature data described in this paper?

In this paper, which can be seen as a status report, we will try to answer these questions using the data acquired from December 1994 to May 1995.

2. Data acquisition system

The aim of the study is to collect temperature data more or less continuously for a long time period (>1 year). By using a personal computer (PC) connected to InterNet it is easy to acquire continuous observations and, thereafter, transfer the data to other computers, where analysis as well as archival of the data is performed.

The locations of the sensors are shown in Figure 4. In total twenty sensors are used to measure the temperature at different points of the antenna foundation. The sensors #1–16 (as indicated in Figure 4) are in the middle (depth 15 cm) of the concrete walls. The drilled holes were well insulated after that the sensors had been installed. Sensor #17 measures the air inside the tower, #18 is taped on the inside wall, and #19 and #20 measure the air temperature inside the radome, some 20 cm away from the tower.

The sensors are of the type LM35 and are specified to have an absolute accuracy of $<0.5^{\circ}\text{C}$ at 25°C . It has a typical nonlinearity of $\pm 0.25^{\circ}\text{C}$ from -55°C to $+150^{\circ}\text{C}$. The self-heating is 0.08°C in still air. An experimental verification of the reproducibility between the twenty used sensors, prior to the installation, showed an agreement better than 0.1°C over a period of ten hours during which the temperature varied between 20 and 25°C . (We will see later, when the results are presented, that the internal consistency of the measured temperatures using different sensors remains at this level.)

The software used to acquire the data runs continuously and each sensor is sampled once approximately every 4 s. These samples are used to form 5 minute averages which are stored on the PC hard disk. This means that in total 5760 temperature measurements are archived per day during normal operation.

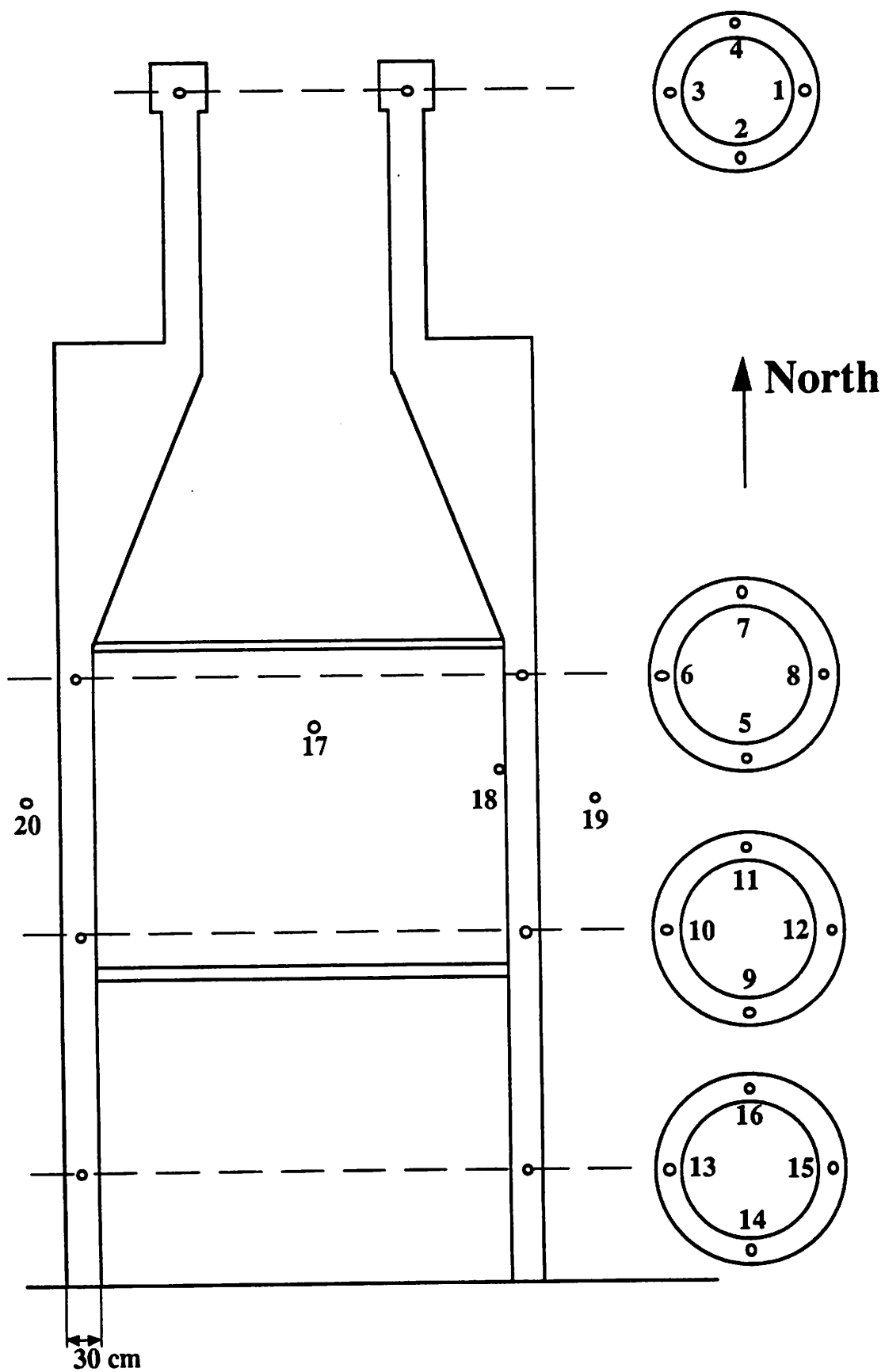


Figure 4. A drawing showing the approximate location of the temperature sensors.

3. Results

We will study the acquired data for the entire time period from December 9, 1994, to May 21, 1995. In total there are 44003 samples of 5 minute averages, from each sensor. There were two major interruptions of the data acquisition during this period, January 13–18 and March 28–April 1. In both cases the PC was halted for some unexplained reason.

Relation between air and concrete temperatures

In Figure 5 we present the observed temperatures for the entire time period of the air outside the tower (sensor #19), the air inside the tower (sensor #17), on the inside of the wall (sensor #18), and in the middle of the wall (sensor #15). We clearly see how the daily amplitudes of the variations in the air temperature are reduced as we measure temperatures at locations that have a better insulation from the outside temperature. We note that the maximum variation in the concrete temperature over the time period is approximately 20°C. It is, however, clear that if the air temperature would have remained low for some more days after day 60 and continued to be high after day 150, this range would have been significantly larger.

Through a cross-correlation analysis we determine the lag time between the temperature of the concrete tower and the outside air temperature to be approximately 6 hours but some dependence on the sensor location is seen. For example, the lag time for sensor #1 is 5.5 hours while it is 7.0 hours for sensor #15.

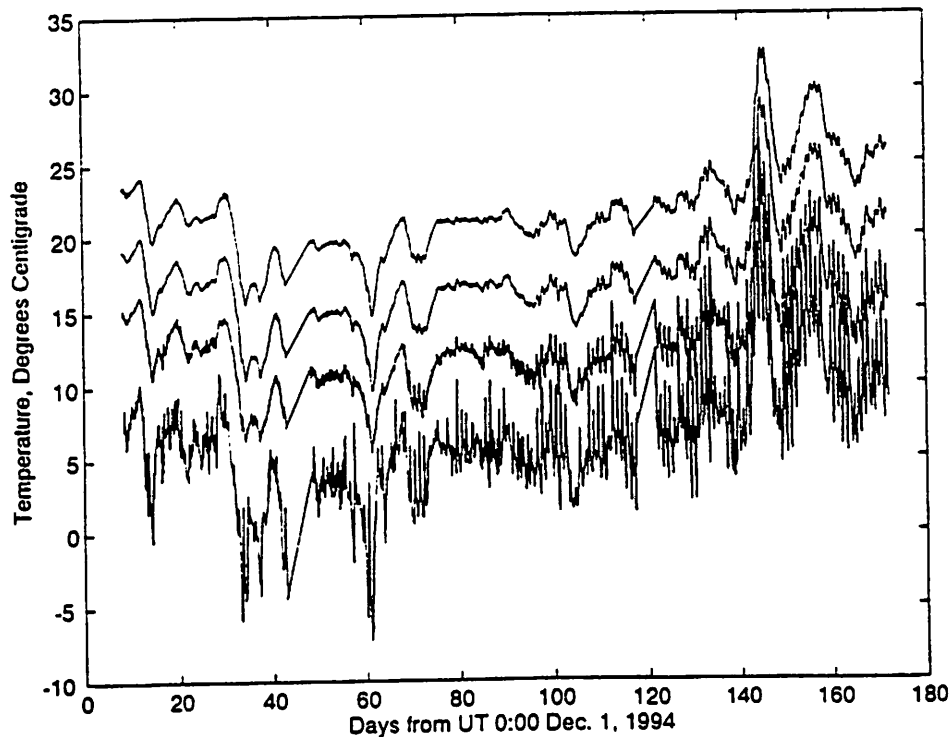


Figure 5. Temperature measurements: The bottom curve shows the air temperature outside the tower (but inside the radome) (correct y-scale); the 2nd curve from the bottom shows the air temperature inside the tower (+5°C for improved visibility); the 2nd curve from the top shows the inside wall temperature of the tower (+10°C); and the top curve shows the temperature in the middle of the concrete wall (+15°C).

Vertical temperature gradients

In Figure 6 we study vertical temperature gradients using the sensors mounted in the north direction. When the sensor located at the highest level is excluded, the other three measure temperatures which agree within approximately 1°C . The reason for the excess temperature at the top is that a heater with a maximum power of 1 kW is used to regulate the temperature of the azimuth encoder and its associated electronics mounted at the top center of the tower. We will return to this issue when we study the horizontal temperature gradients at this level.

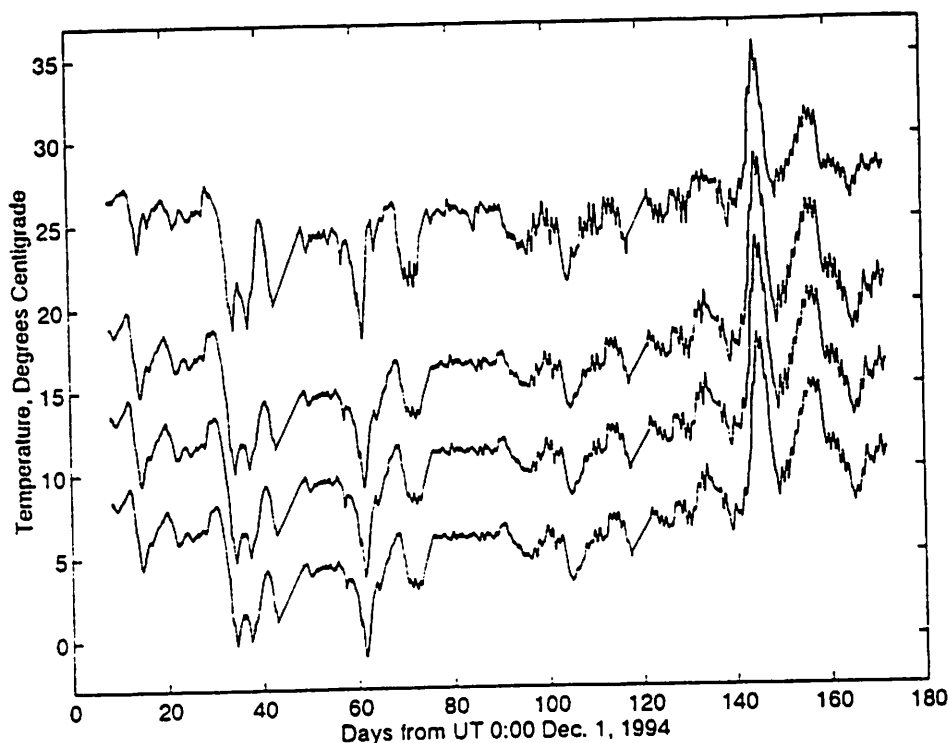


Figure 6. Temperature measurements using the sensors mounted in the middle of the concrete wall in the north direction at the four different levels of the antenna tower (see Figure 4). From the bottom to the top the curves show the temperature at: the bottom level (correct y-scale); the low of the two middle levels ($+5^{\circ}\text{C}$); the high of the two middle levels ($+10^{\circ}\text{C}$); the top level ($+15^{\circ}\text{C}$).

Horizontal temperature gradients

In addition to overall temperature variations, which mainly will cause a variation in the vertical coordinate, possible horizontal gradients may introduce a horizontal displacement of the reference point. Figures 7 and 8 show the gradients at the bottom and at the top levels. The gradients observed at the two middle levels are not presented because they were always less than 1°C . Note the different scale of Figure 8! The cause for the large negative gradient in the east direction is the previously mentioned heater which is mounted approximately 1 m below the sensor in the west direction (sensor #3). In order to study these gradients a little better Figure 9 shows the April 1995 data only. Here it is clearly seen that when the air temperature increases on day 143 the heater is no longer turned on and the gradient vanishes. A very rough calculation indicates that the pointing of the antenna will change with 5–10 arcsec during these couple of days which could introduce problems while observing at 100 GHz with a full width half power beam

width of approximately 40 arcsec. We can, however, conclude that the size of the observed horizontal gradients correspond to horizontal displacements of the reference point which are significantly less than 1 mm.

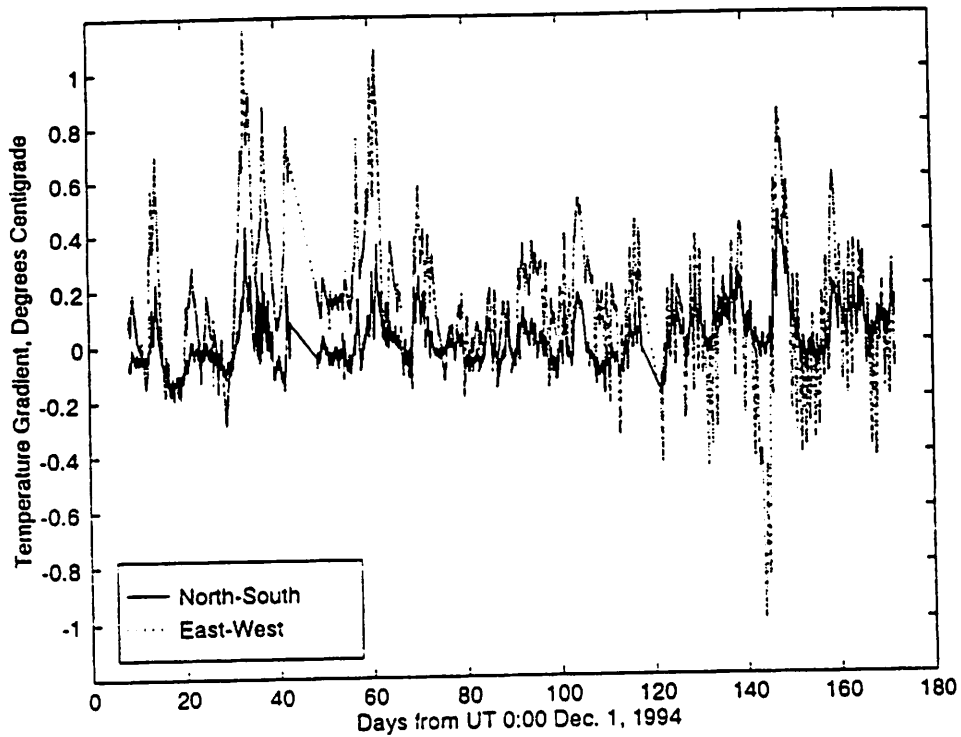


Figure 7. Temperature gradients at the bottom level of the tower. East-west means temperature measured in the east direction minus the temperature measured in the west direction, in this case sensor #15 - sensor #13.

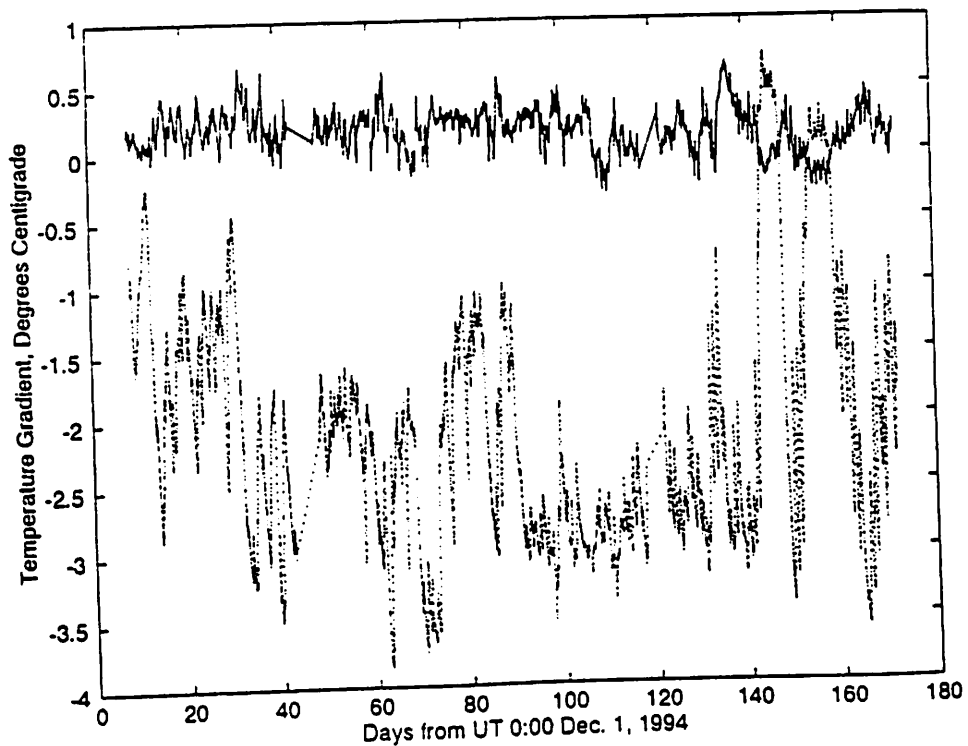


Figure 8. Temperature gradients at the top level (see legend of Fig. 7). The large gradient in the east-west direction is discussed in the text.

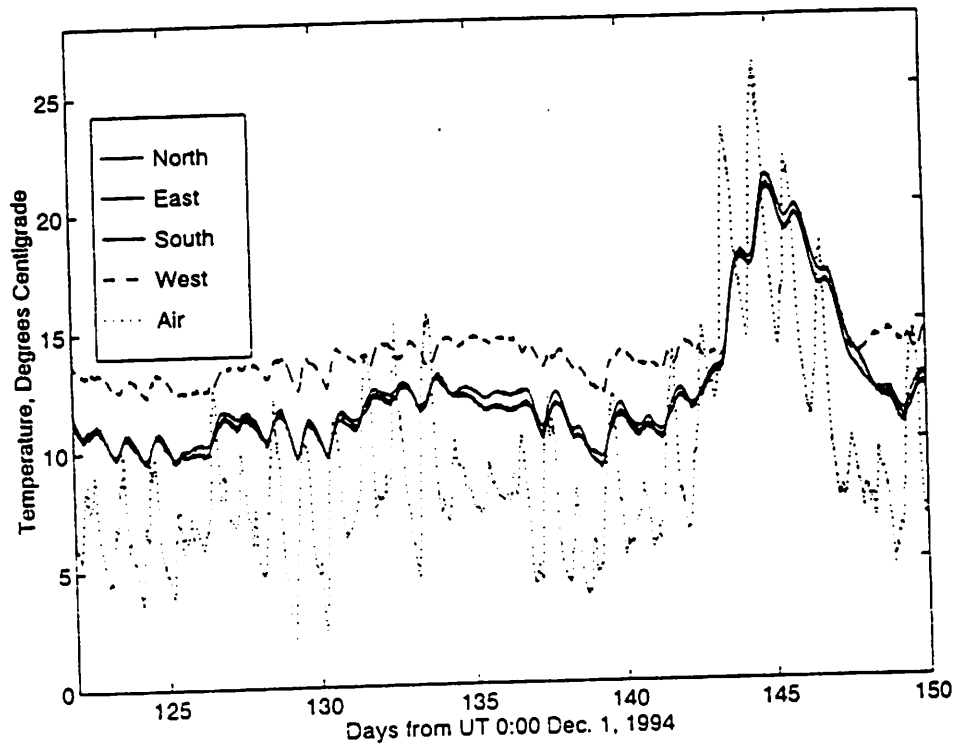


Figure 9. The measured temperatures in the concrete wall at the top level together with the air temperature during the month of April 1995. The excess temperature measured in the west direction is not seen when the outside temperature increase (see text). The average value of 6 hours for the lag time between concrete and air temperature seems to be a reasonable value also for this subset of data.

Effect of radome heaters

Four heaters are used to prevent condensation on the radome. These heaters are (in difference to the previously mentioned heaters inside the tower) symmetrically mounted on the top of the outer concrete wall for the radome support. At many occasions, especially during the winter months, these heaters were turned on. The total power used was 60 kW. Their effect on the air temperature inside the radome (sensors #19 and #20) is clearly visible and amounts to an excess temperature of approximately 1–2°C. However, this change is much less than the typical temperature variations due to the weather and no large or unusual effects were detected in the observed concrete temperatures which could be traced to the heaters being turned on or off.

4. Conclusions

The maximum variation in temperature so far observed is approximately 20°C. This implies that the height of the 11 m concrete tower varies with approximately 3 mm between the summer and the winter. We note, however, that the last winter was not extremely cold, and that the warmest period of the summer has not yet

been observed, meaning that we can make a rough estimate that the typical winter to summer variation is 3–4 mm. We regard the need for complementary length measurements of the tower to be of second priority, even though it would be desirable to verify these estimated movements.

We note that the observed temperature variations during a 24 hour period, the typical length of a geodetic VLBI experiment, correspond to variations in the position of the geodetic reference point much less than 1 mm. This is also true for the anticipated effects caused by the observed variations in the vertical and the horizontal temperature gradients. However, by making the heating of the tower more symmetric it should be possible to significantly reduce the size of the horizontal temperature gradients. This may be important in order to obtain more stable pointing models for single dish observations at high frequencies since the observed gradients may introduce pointing effects on the order of 5–10 arcsec.

Finally, we must remember that our study has been limited to measurements of the antenna concrete tower. The steel structure from the top of the tower to the intersection of axes will of course also be affected by temperature variations. These have not been addressed in this study. However, because the additional distance is only 2.91 m it is anticipated that they will have a smaller influence on the stability of the reference point.

Acknowledgement. We thank Karl-Åke Johansson at the Onsala Space Observatory for the careful design and the realization of the data acquisition system.

References

- Carlsson, T.R., G. Elgered, and J.M. Johansson, External Wet Tropospheric Corrections During a Two-Week-Long VLBI Campaign, 10th Working Meeting on European VLBI for Geodesy and Astrometry, *this volume*. 1995.

Managing Geodetic VLBI In Europe : The European Crustal Motion Network

James CAMPBELL

Geodetic Institute of the University of Bonn (GIUB), Bonn, Germany

Abstract. An overview is given of the status of the European Geodetic VLBI network after a first phase of operational funding under the European Commission's Framework Programme has been brought under way. In the beginning of the 90's, the European VLBI groups gradually took over the responsibilities from NASA whose guidance and support gave the cue to the strong commitment of a number of European countries to build up geodetic or shared astro-geodetic VLBI facilities. Currently, a core network of six stations is observing regular experiments at a rate of six per year and several new stations are joining in the campaigns. For the second project phase, a follow-up proposal under the Training and Mobility scheme has been submitted to the EC, which is designed to ensure another four years of VLBI operations. In this proposal the main scientific objectives are concentrated on the determination of vertical crustal motions, which require longer time spans to detect than the horizontal motions.

1 Introduction

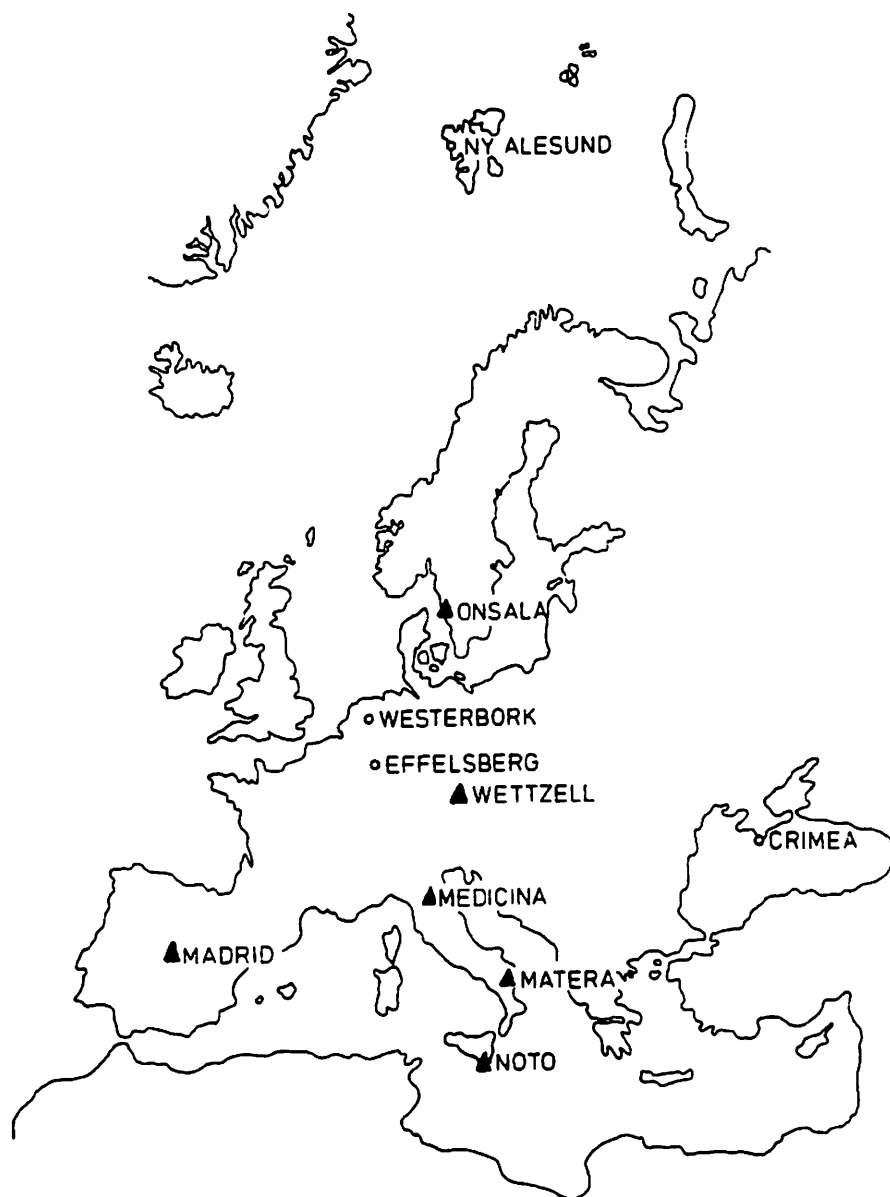
Since the early eighties, the European Geodetic VLBI-Group, a community formed by members of the organisations involved in the carrying out of VLBI observations and data processing, has been striving for the realization of a program of regular VLBI-campaigns among the fixed VLBI-stations in Europe, with the aim of determining relative site motions to study regional crustal motions and to provide a stable reference network for the other geodetic techniques used in this area.

At first, the campaigns were organized by the NASA/GSFC VLBI group as part of the Crustal Dynamics Program. From 1990 onwards, the European VLBI-groups have gradually taken on the responsibility to ensure the continuation of regular observations with the Geodetic Institute of the University of Bonn in cooperation with the correlator center of the Max-Planck-Institute for Radio Astronomy (MPIfR) in charge of the organisation, scheduling and processing of the geodetic experiments. Operational funding has been secured by means of the European Commission to provide a sound financial basis for the pursuit of European involvement in geodetic VLBI.

In recent years the number and distribution of geodetic VLBI observatories in Europe has improved considerably. The telescopes of the Onsala Space Observatory in Sweden and of the Wettzell Geodynamic Fundamental Station in Germany were the first to participate in international VLBI projects. When the Medicina facility was completed in 1987 the foundation was laid for a purely European geodetic VLBI network. Madrid, Noto and Matera

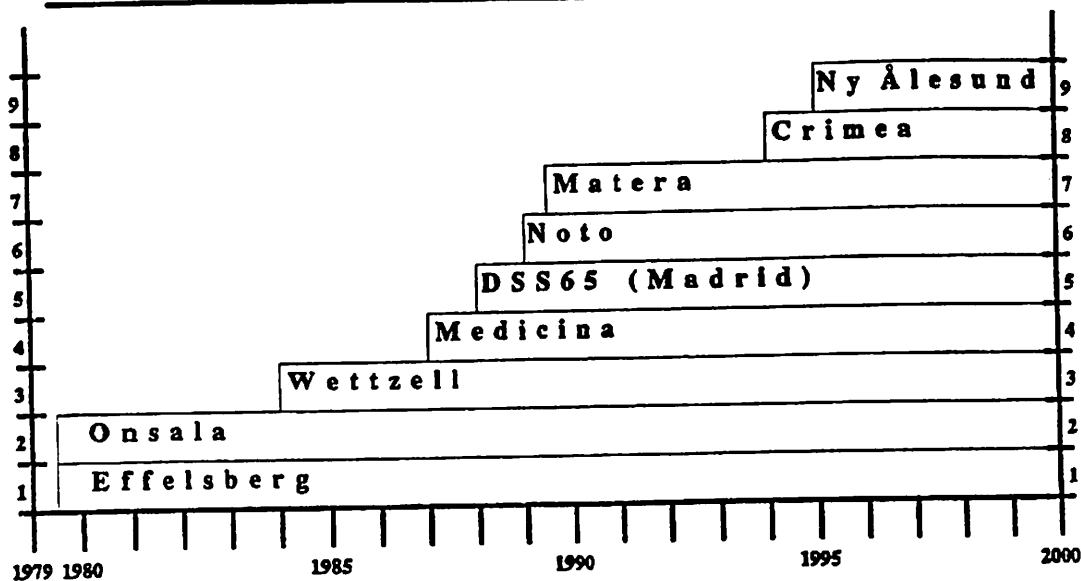
joined in the following years.

At present, the European Geodetic VLBI Network consists of six core stations (filled triangles in figure below) and several new stations have just become operational, such as the 20m antenna erected at Ny Ålesund on Spitsbergen. Also, the astronomical station of Simeis on Crimea has been able to join the geodetic network with a VLBI terminal on loan from NASA in 1994.



The European Geodetic VLBI Network

Euro-VLBI stations with MkIIIa, S/X, H-Maser



Developement of European VLBI stations for high precision geodetic measurements

2 Scientific background

The geotectonic situation in central and southern Europe is currently understood to consist of an essentially 'stable' central part north of the Alpine system belonging to the Eurasian plate while the South, i.e. the Mediterranean, is dominated by complex geotectonic motions, both horizontal and vertical. In a plausible plate tectonic scenario the African plate has been moving northward on a collision course with Eurasia. During this collision, which involved also the smaller plates of Arabia, the Apennine and the Iberian peninsula, the Alpine system was thrown up, a process which is believed to be still in progress today. The associated compression and subduction processes along the complex fault lines are a major cause for the frequent and strong earthquakes occurring in this region. In contrast, the northern part of Europe, i.e. Fennoscandia, is characterized by a vertical postglacial rebound (Mueller, Kahle 1993).

In trying to model the pattern of observed horizontal crustal motions in the Mediterranean, two approaches (among many others) are being discussed: the microplate mosaic with deformable boundary zones and the smooth deformation model covering the entire region. In order to be able to discriminate between these models direct geodetic measurements of site motions are forming an evidence of increasing importance (Drewes 1992).

In most cases, vertical crustal motions caused by isostatic and/or tectonic processes in the

earth's crust are much smaller than horizontal motions, i.e. at most about 10 mm/year. Man-induced vertical changes (i.e. by withdrawal of natural gas, oil or groundwater) may be larger but are locally confined. Volcanic activities are often associated with local height changes of considerable size (e.g. Pozzuoli near Naples). In this situation it will be difficult to interpret any vertical station motions in a meaningful way without relying on a combination of GPS- and levelling data.

While the scientific goal of the first phase has been the detection of horizontal crustal motions, the second phase of the European VLBI project stresses the vertical crustal motions because their detection requires much longer observational periods. The question of sea level rise and land subsidence, which is vital for the flat countries around the North Sea, will profit from increasingly precise determinations of height changes (Diamante et al. 1987).

3 Observing methods

In order to measure crustal motions as small as a few cm or even mm per year, geodesists have carried out measurement campaigns using the most advanced geodetic techniques such as Satellite Laser Ranging (SLR), Very-Long-Baseline Interferometry (VLBI) and the Global Positioning System (GPS). VLBI has the advantage of a true inertial reference and not being influenced by orbital errors. There is at present no other technique than VLBI able to provide such a stable reference frame. GPS, on the other hand, readily provides the means for a much denser network of points, thus permitting to monitor crustal movements with a better spacial resolution. Therefore, in the present state of the project GPS data collection and analysis are being included in the activities.

In 1992 permanent GPS-receivers have been installed at VLBI/SLR-stations and at other geodynamically interesting sites. The network is being operated globally under the IGS network but data are available for regional studies as well. In addition, denser regional networks are being set up, such as in Scandinavia, where a permanent network of GPS stations has started operating with the aim of determining the Fennoscandian post-glacial uplift. Similarly, in the Netherlands and other European countries networks are created with the aim of connecting tide gauges to primary GPS sites and to the levelling networks.

The modelling of the atmospheric path delays, the prime error source in geodetic VLBI measurements, has seen considerable progress lately. This has led to a progressive improvement of the rms scatter between repeated experiments. Still, the fact remains that the vertical component is inherently weaker in the solutions.

In view of the slow progress made on the water vapour radiometer front, it is interesting to note that tropospheric refraction data derived from GPS-measurements may be useful to correct the VLBI group delay observations, a possibility that resides in the fact that GPS can sample the atmosphere over a wide elevation range at every observation epoch.

4 Technical aspects

In the past decade, the MKIIIA VLBI system developed in Haystack (NEROC/MIT) and introduced by NASA has set the standard for geodetic VLBI in Europe. With the implementation of the high density recording system, the ease of operation of this tape-based system has substantially improved and the tape transport costs have gone down considerably. Nevertheless, the system is basically technology of the seventies and cannot be maintained indefinitely. This is why a new system based on the most advanced technology of the nineties is under development: the MKIV-system. This new system is being developed jointly by the VLBI groups in Haystack and in Dwingeloo using financial contributions from both the US and Europe. It is still tape-based but uses a wider bandwidth and a new station-oriented concept of the correlator design. The basic correlator configuration which is planned to be set up at the MPIfR in Bonn, will allow simultaneous correlation of up to eight stations (see also Alef and Müskens in this volume).

Ideas to eventually replace the tape recording system by on-line data links to the correlator are being discussed more seriously again since the development of high data rate communications links is making considerable progress. A proposal to the EC Telematics programme has been prepared and will be revised and improved for resubmission in 1996 (see also Schuh and Hase in this volume).

5 Organisational aspects

The organisation of a programme of regular observations in the European VLBI Network involves interactions between all the participating agencies and institutions in order to arrive at an agreement on the use of the VLBI facilities for the proposed campaigns. At the start of the first project phase the understanding has been agreed that the required time for carrying out six 24-h experiments per year would be available at all participating stations (except for the 100m telescope of Effelsberg which can be used for geodesy only once or twice a year). It was also agreed, that the network management should be handled by the VLBI group of the Geodetic Institute in Bonn. The actual organizational structure (see diagram) has evolved during the first years of European VLBI and has proved to be entirely satisfactory.

In close cooperation with the VLBI group at NASA/GSFC, who handles the global VLBI activities, the annual time tables for the European campaigns are negotiated. The Bonn VLBI group acts as a coordination and processing center for the European geodetic VLBI network. The network management is performed by the VLBI group at the Geodetic Institute. A data quality feedback from the central correlator to the observatories is organised by members of the team.

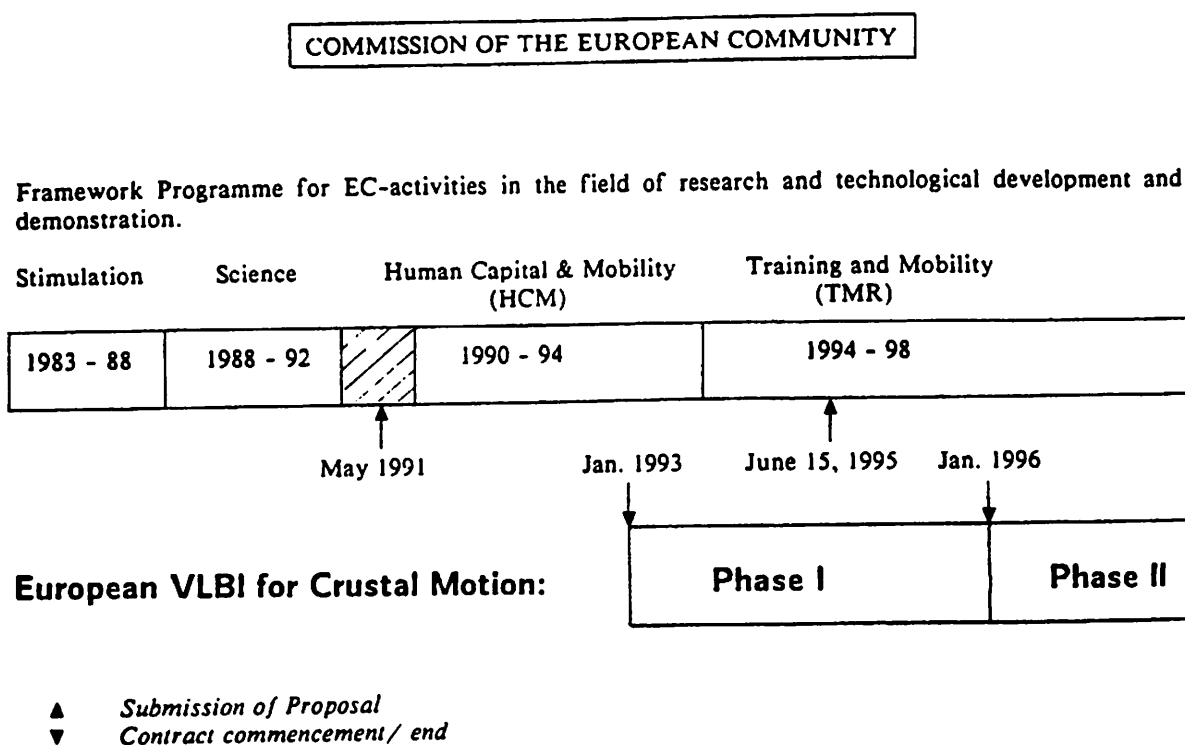
In view of the involvement of the European VLBI observatories (shared as well as dedicated geodetic) in NASA's global VLBI program, the transition of MkIIA to MkIV will be made in coordination with all parties concerned.

Communication among the participants in the network has now been entirely geared to the E-mail/INTERNET data link. The connections to the participants and the telescopes have

been implemented and are being used throughout. Apart from regular messages, a great deal of data (observing schedules, log sheets etc.) and also software modules are being transferred via INTERNET.

6 Funding scheme

In Europe, the big investment in the VLBI technique at the national level has been encouraged by the successful global VLBI campaigns under NASA's Crustal Dynamics Project and NOAA's IRIS Earth Rotation Program. In contrast, the running costs of a multinational network have been more difficult to institutionalize. The organization, scheduling and processing, the sending out of tapes etc. create a need for additional funding that cannot be met by any one of the participating institutions alone.



The European VLBI project within the EC Framework Programme

At this point, the benefit of the Framework Programme for Research and Technical Development of the European Community (since 1994 the European Union) has become evident. Since 1988 three overlapping 4-year programmes have been implemented, the Science Plan (1988-1992), the Human Capital and Mobility (HCM) (1990-1994) and the Training and Mobility of Researchers (TMR) (1994-1998). In the final year of the Science Plan a first proposal under the title "European VLBI for Crustal dynamics" was accepted and has provided funding for the current operational phase of the European geodetic VLBI Network

(1993-1995). The second project phase is now being proposed under the Training and Mobility program. The TMR program emphasises the training aspect, which is of particular importance in the many-faceted field of geodetic VLBI.

The Research Networks funding scheme of the TMR program provides in an optimal way for the costs incurred by operating a VLBI network including tape transport and consumables. The training scheme will be implemented chiefly through temporary employment of visiting young post-doctoral researchers from the participating countries, but students in their final years will also be recruited on part-time basis in order to stimulate the interest of young talents in the new developments in the geosciences. This adds an element of flexibility in the creation of man power resources.

7 . Outlook

Looking at the future development of the European VLBI network, a critical factor still remaining is the correlator capacity, both in terms of the number of stations that can be processed simultaneously and in terms of the available manpower to supervise the correlation. At present the optimum size of the network is 5 to 6 stations. With more stations the number of runs at the 'old' Mk IIIA correlator increases rapidly. In this situation the ongoing development of the MkIV-system will improve the matter significantly. It is expected that after the delivery of the new MkIV correlator in two years from now 8 stations can be processed as efficiently as 5 stations are handled now.

Another aspect of the future is the emergence of the permanent GPS network, which provides an enormous amount of daily data that will allow to monitor position changes on much shorter time scales and enable us to carry out regional and local studies. It will be one of the challenges of the near future to determine the role and the optimal combination of both techniques in the coming campaigns as well as in the processing strategies.

It is hoped that the proposal for the second EC funding phase will be successful in order to be able to ensure the continuity of the geodetic VLBI operations in Europe.

8 References

- Campbell, J., A. Nothnagel, N. Zarraoa, P. Tomasi** ; The European Regional VLBI Network for Crustal Motion Measurements: Proceedings of the International Workshop for Reference Frame Establishment and Technical Development in Space Geodesy, iRiS '93. Communications Research Laboratory, Tokyo, pp. 263-268, January 18-21, 1993
- Campbell, J., H. Hase, A. Nothnagel, H. Schuh, N. Zarraoa, A. Rius, E. Sardon, V. Tornatore, P. Tomasi** : First Results of European Crustal Motion Measurements with VLBI: AGU Geodynamics Series. Vol. 23. Contributions of Geodesy to Geodynamics: Crustal Dynamics. ISBN 0-87590-523-4, AGU Washington. 1993

- Campbell, J., H. Hase, A. Nothnagel, H. Schuh, N. Zarraoa, A. Rius, E. Sardon, V. Tornatore, P. Tomasi** ; First Results of European Crustal Motion Measurements with VLBI; in Geodesy and Physics of the Earth, Geodetic Contributions to Geodynamics, Proceedings of IAG Symposium No. 112, Potsdam, October 5-10, 1992, ISBN 3-540-56572-2, Springer-Verlag, 1993
- Diamante, J.M., T.E. Pyle, W.E. Carter, W. Scherer** ; Global Change and the Measurement of Absolute Sea-Level. Progress in Oceanography, Vol. 18, pp. 1-21, 1987
- Drewes, H.** ; A Deformation Model of the Mediterranean from Space Geodetic Observations and Geophysical Predictions, Proc. 7th Sympos. on Geodesy and Physics of the Earth, IAG-Sympos. No. 112, Eds. H. Montag, Ch. Reigber, Springer-Verlag, Berlin 1993, pp. 373-378
- Mueller, St. , H.-G. Kahle** ; Crust-Mantle Evolution. Structure and Dynamics of the Mediterranean-Alpine Region, in: Smith. D.E., D.L. Turcotte (Eds.), Contribution of Space Geodesy to Geodynamics: Crustal Dynamics, AGU Geodynamics Series, Vol. 23, Washington, pp. 249-298. 1993

Analysis of the European Geodetic VLBI Experiments with a Free Network Concept

Néstor Zarraoa^{1,4}, José Miguel Juan², Antonio Rius³

(1)Geodetic Institute, Norwegian Mapping Authority, Honefoss, Norway

(2)Dept. Física Aplicada, UPC, Barcelona, Spain

(3)Centre d'Estudis Avançats de Blanes, CSIC, Blanes, Spain

(4)Now in DLR Remote Sensing Ground Station Neustrelitz, Germany

Abstract

The permanent geodetic VLBI network in Europe has produced some of the best data sets available in geodetic VLBI. In hardly four years, significant results about tectonic displacements in Europe have been obtained and published, following the standard strategies of VLBI analysis. Now, with an enlarged set of data, with seven years of regular high quality experiments, it is a good time to revisit parts of this data set with new analysis concepts.

In geodetic VLBI analysis, the normal approach is to use a constrained reference frame to determine the positions and velocities of the other stations. This is the method used to obtain the former results in Europe and, also, the standard approach of global solutions published by the Goddard VLBI group and others. However, techniques like GPS have been trying analysis concepts based on free network solutions and a-posteriori links to a global reference. We will present the application of a free network concept to a subset of European VLBI data. In a small network with few stations like the European, this method may have interesting advantages, because it permits to isolate the results from the a-priori constrained frame, and reliable displacements can be found for all the stations, with respect to an "average" frame.

Introduction

As opposed to satellite based geodetic techniques, which are "dynamical" in the sense that they are intimately referred to the Earth by the satellite orbits, VLBI is a "geometrical" technique. This means that the results are in principle independent of reference frames other than the celestial.

However, interpreting the VLBI results in real life requires that they are referred to a certain Earth based reference system. This is customarily accomplished by setting some constraints in the VLBI analysis. For example, fixing the position of one station and the Earth rotation parameters, or fixing one station plus two directions. Each option allows for some parameters to be determined, so depending what we are after, or the quality of the a-priori constraints, we can use one or the other.

In our work with European VLBI data already published (Zarraoa et al., 1994), the constraints were formed by the a-priori position of Wettzell, the direction Wettzell-Onsala and the vertical component of Madrid. With this constraints we have obtained excellent results in the horizontal components of the stations, yielding to the determination of motions at the 1 cm/year level in Southern Italy. Other groups may have used different sets of constraints, but following a similar approach (e.g. Ryan et al., 1993). Although some efforts to use a free-network approach to VLBI have been suggested (Plietker & Schuh, 1991), none has been applied in practice to real data analysis.

In a small network like the European, the number of constraints is significant compared with the total number of geodetic parameters. In the approach used in Zarraoa et al., (1994), the direction Wettzell-Onsala was chosen because it had shown good stability over a long VLBI data series, but the fixing of the vertical component of Madrid was only the result of the network geometry, and it was not based on a known stability of such component. Hence, any possible vertical deformation of Madrid might be contaminating the vertical and also (in a smaller scale) the horizontal results of the other stations.

In GPS analysis, we see a tendency to use a free network concept by several groups (e.g. Heflin et al.

1992, Rius et al., 1995). The advantages of the free network over the "fiducial" (or constrained) mode are several, but the two most important are that it does not depend on a-priori constraints with their possible errors and that all parameters can be obtained, giving positions or velocities for all the stations. The main disadvantage is that the result may not be referred to a standard terrestrial reference frame, so the a-posteriori adjustment to an existing reference frame may be necessary.

This transformation must be performed with the full covariance matrices. In results from free-network processes, the covariance matrix is not positive definite, because they are not full-ranked. Hence, a preliminary projection of the complete covariance matrix into a full-rank matrix must be performed prior to the transformation parameter estimation. The method is described in Koch (1988).

We are going to present the application of a free network analysis concept to the European geodetic VLBI data. We will present the results in terms of positions and velocities, and compare them with the standard analysis results.

The analysis of the European VLBI data

We have used a subset of the EUROPE series of VLBI experiments: 14 experiments from 1990 to 1994. In all of them the stations Wettzell, Onsala and Madrid were observed, so we could make a better comparison between the standard analysis and the free-network results.

All VLBI data has been analysed with OCCAM 3.3 (Zaragoza, 1993) using two strategies, the "standard" (i.e. fixing Wettzell, the direction Wettzell-Onsala and the vertical component of Madrid), and a "free-network", where loose constraints (100 meters) were set to the positions of the stations and also to the Earth rotation parameters.

In the standard analysis, all results and variances are reliable (referred to the constraints). In the case of a free adjustment, where all positions and the Earth rotation are loosely constrained the variances obtained for the station coordinates are very large (tens of meters). These large values do not mean that we have a bad result, but only that the actual values of the parameters are "floating" on an undefined space, due to the loose constraints. The baseline lengths, however, come out with the same results and variance level than in the standard analysis, showing that in fact, the data is consistent.

One would expect from the correct application of both procedures, that the results would be identical for the baseline lengths. However, this is not so. The explanation for the differences lays basically in a problem of over constraining in the standard analysis. Although one would expect the number of parameters to be constrained as 6, in fact we are using additional constraints to fix one direction and one vertical component, which may introduce distortions in the method. The free-network concept is not affected by these errors. Additionally, we can not discard that part of the difference is produced by the different correlation between parameters that can appear in one or other case, and that may produce differences in the actual estimation.

In order to compare different experiments analysed with the free-network concept, it is necessary to refer all of them to a common reference frame via a 6 or 7-parameter transformation (depending on whether we estimate scale changes or not). Such a frame may be external (e.g. the ITRF92, IERS Annual Report, 1993) or internal, either selecting one epoch as reference, using the a-priori values of the station positions or using an "average" of the results. In any case, the relative results can be compared via these transformations, and also velocities can be estimated for all the components.

In our case we have applied 7-parameter transformations. The scale parameter in the transformation does not have, in principle a clear justification between different VLBI experiments. However, the estimated scale factors were not negligible, and could contribute to an artificial improvement in the rms of the parameter determination. On the other hand, after testing the results obtained with a 6-parameter transformation, we found that they were at the same level than those obtained with the 7-parameter transformation.

We have chosen several options as a-priori reference frame to transform our results: first we chose as reference the results of our first epoch. Then we tried with an average of all results as the a-priori frame.

Results

In table 1 we present the comparison in the velocities estimated for each station component when we have used the standard approach and the free-network analysis (referred to an average positions of the stations). We include also the repeatabilities in both strategies.

The velocity results are referred to the NUVEL-1 a-priori model, where both Noto and Matera have been assumed in the African plate, based on the results of Zarraoa et al. (1994). We have to mention that the velocities obtained from the standard analysis, are obtained directly from the independent analysis of each experiment, and no transformation has been applied to them to solve for small deficiencies of the reference frame (such transformations were applied in Zarraoa et al. 1994).

Table 1. Velocities and repeatabilities obtained with the standard (ST) and free-network (FN) approaches

	Vert (ST)	Vert. (FN)	North (ST)	North (FN)	East (ST)	East (FN)
Madrid (repeatab.)	0.0 mm/y 0.0 mm	0.1 mm/y 1.0 mm	-2.6 mm/y 5.8 mm	1.1 mm/y 2.0 mm	0.3 mm/y 4.0 mm	-0.6 mm/y 1.4 mm
Matera (repeatab.)	0.3 mm/y 19.2 mm	1.0 mm/y 10.1 mm	-2.6 mm/y 5.8 mm	-2.0 mm/y 2.9 mm	7.7 mm/y 5.7 mm	3.5 mm/y 1.8 mm
Medicina (repeatab.)	-5.4 mm/y 6.7 mm	-3.7 mm/y 5.4 mm	1.5 mm/y 3.8 mm	1.8 mm/y 2.0 mm	2.4 mm/y 4.8 mm	0.9 mm/y 3.3 mm
Noto (repeatab.)	-2.1 mm/y 13.3 mm	2.7 mm/y 7.2 mm	-3.3 mm/y 7.2 mm	-1.0 mm/y 1.6 mm	2.7 mm/y 6.9 mm	0.1 mm/y 1.3 mm
Onsala (repeatab.)	0.0 mm/y 0.2 mm	0.4 mm/y 2.4 mm	0.0 mm/y 3.3 mm	-1.1 mm/y 1.9 mm	0.0 mm/y 0.9 mm	-0.5 mm/y 2.3 mm
Wettzell (repeatab.)	-	0.7 mm/y 3.7 mm	-	0.2 mm/y 2.2 mm	-	-1.6 mm/y 2.7 mm

The results of the free network adjustment show significantly better repeatabilities than the standard analysis. With respect to the velocities estimated, the results agree rather well, after the results of the standard approach are corrected by the estimated motion of Wettzell in the free-network. However, there are some exceptions to the good agreement, mainly the vertical component of Noto, where the standard analysis shows a negative value and the free-network a positive value. In the other components the differences are below the 3 mm/year level. If we compare the free-network results with those already published, we find an excellent agreement. Noto shows only a small disagreement with respect to the NUVEL-1 model, while Matera indicates a larger East component than what NUVEL-1 predicts, which was also present in our previous results.

Table 2. Velocities and repeatabilities (free-network) referred to the first epoch (FST) or to an average position (AVG)

	Vert (AVG)	Vert. (FST)	North (AVG)	North (FST)	East (AVG)	East (FST)
Madrid (repeatab.)	0.1 mm/y 1.0 mm	0.0 mm/y 0.3 mm	1.1 mm/y 2.0 mm	0.5 mm/y 2.3 mm	-0.6 mm/y 1.4 mm	-0.2 mm/y 1.0 mm
Matera (repeatab.)	1.0 mm/y 10.1 mm	5.3 mm/y 24.3 mm	-2.0 mm/y 2.9 mm	-1.9 mm/y 5.0 mm	3.5 mm/y 1.8 mm	3.8 mm/y 4.2 mm
Medicina (repeatab.)	-3.7 mm/y 5.4 mm	-1.8 mm/y 8.6 mm	1.8 mm/y 2.0 mm	1.4 mm/y 2.6 mm	0.9 mm/y 3.3 mm	1.2 mm/y 3.9 mm
Noto (repeatab.)	2.7 mm/y 7.2 mm	0.8 mm/y 2.5 mm	-1.0 mm/y 1.6 mm	-1.5 mm/y 2.3 mm	0.1 mm/y 1.3 mm	0.6 mm/y 1.9 mm
Onsala (repeatab.)	0.4 mm/y 2.4 mm	-0.2 mm/y 1.2 mm	-1.1 mm/y 1.9 mm	-0.6 mm/y 1.7 mm	-0.5 mm/y 2.3 mm	-0.1 mm/y 2.2 mm
Wettzell (repeatab.)	0.7 mm/y 3.7 mm	1.8 mm/y 3.1 mm	0.2 mm/y 2.2 mm	0.2 mm/y 2.5 mm	-1.6 mm/y 2.7 mm	-1.3 mm/y 2.2 mm

We also tried to use the first epoch as common reference for the free-network results. An the comparison between both free-network approaches is shown in Table 2. In that case we also improved the repeatabilities with respect to the standard model, but with the exception of Matera, which was not observed in the reference experiment. This produced a worse result for the station (and also somewhat to Medicina), with an rms in the vertical component of 2.5 cm, compared with the 1 cm rms we show in table 1. Also some of the velocities estimated are slightly different.

Conclusions

The application of a free-network strategy into VLBI analysis has been successfully accomplished. The single-experiment analysis using loose constraints was straight forward due to the Kalman filter approach using in OCCAM 3.3 for all parameters, and the subsequent reduction of all experiments to a unique reference frame via 7-parameter transformations has produced excellent results.

The estimated values for the velocities of the European stations are consistent with the results of the standard analysis of the same data set, with a maximum difference of 3 mm/year. The results are also in very good agreement with those already published by Zarraoa et al. (1994) with a different data set.

The repeatabilities obtained in the standard analysis are at the 5 mm level for the horizontal components and 1-2 cm for the vertical components. The application of the free network concept has improved in general the repeatability level to 3-4 mm in the horizontal and better than 1 cm in the vertical.

The improvement in the results achieved with the free network with respect to the standard must be interpreted as the result of avoiding the over constraining which occurs in the standard strategy, although the estimation of scale factor variations between experiments may also have contributed to a small decrease of the standard deviations of the parameters.

After the success in this initial application of the procedure, we plan to extend it to re-analyse all the geodetic VLBI data available from the European network, starting in 1988, using standard and free-network approaches, in order to refine the velocity models derived for the European stations, when we have almost 8 years of excellent data available.

References

- Heflin, M., W.I. Bertiger, G. Blewitt, A. Freedman, K. Hurst, S.M. Lichten, U.J. Lindqwister, Y. Vigue, F. Webb, T. Yunck, J. Zumberge. Global geodesy using GPS without fiducial sites. *Geoph. Res. Lett.* V. 19, No. 2. 131-134. 1992.
- Koch, K.R. Parameter estimation and hypothesis testing in linear models. *Springer Verlag*. 1988.
- Plietker, B., H. Schuh. Free network adjustment in VLBI data analysis. Proc. VIII European VLBI Meeting. Rep. MDTNO-R-9243. Survey Dep. of Rijkswaterstaat. Delft. 1991.
- Rius, A., J.M. Juan, M. Hernández-Pajares, A.M. Madrigal. Measuring geocentric radial coordinates with a non-fiducial GPS network. *Bulletin Géodésique*. In press. 1995.
- Ryan, J.W., C. Ma, D.S. Caprette. NASA Space Geodesy program-GSFC Data Analysis-1992. *NASA Tech. memo.* 104572. 1993.
- Zarraoa, N. OCCAM V3.2: Status report. Proc. IX European VLBI Meeting. Univ. Bonn Geod. Series, 81. Ed. J. Campbell & A. Nothnagel. 25-26. 1993.
- Zarraoa, N., A. Rius, E. Sardón, J.W. Ryan. Relative motions in Europe studied with a geodetic VLBI network. *Geophys. J. Int.* 117, No. 3 (763-768). 1994.

Geodynamical Parameters Determined by VLBI

Rüdiger HAAS ¹

James CAMPBELL ¹

Harald SCHUH ^{1,2}

¹ *Geodetic Institute of the University of Bonn (GIUB), Germany*

² *Deutsches Geodätisches Forschungsinstitut (DGFI), Abt. I, Munich, Germany*

Abstract. We show amplitudes of diurnal and subdiurnal UT1 and polar motion variations determined from IRIS-S VLBI data. A reason for the differences between empirically determined and theoretically predicted amplitudes are influences on the VLBI measurements from geodynamical phenomena with short term variations as for example the solid Earth tides. The solid Earth tides model used in standard VLBI data analysis only approximates to the first order the frequency dependence of the tidal deformation due to the free core nutation [FCN] resonance. We solved for frequency dependent second degree Love numbers from VLBI data and found good agreement with the theoretical model by J.Wahr and an indication for a change in the FCN period. By using a refined Earth tide model that includes the frequency dependence of the Love numbers in the VLBI data analysis the empirically determined amplitudes of diurnal and subdiurnal UT1 and polar motion variations change by 10% on the average.

1 Introduction

VLBI is being used as a precise geodetic technique that is capable of linking the terrestrial reference frame [TRF] and the celestial reference frame [CRF] with very high accuracy. One of the major goals is the measurement of the Earth orientation parameters [EOP] to obtain information on precession/nutation, polar motion and UT1.

In the standard procedure of data analysis mean values for the EOP from 24 hour geodetic VLBI experiments are estimated. However, theoretical models predict diurnal and subdiurnal variations in the Earth rotation parameters [ERP] polar motion and UT1 due to the ocean tides (Wünsch/Seiler 1992, Brosche/Wünsch 1994, Seiler/Wünsch 1995) and due to the inequality of the two equatorial moments of inertia of the Earth (Wünsch 1991). These variations could already be detected from geodetic VLBI data for example by estimating ERPs every 2 or 3 hours (Brosche et al. 1991) or by fitting a model to the VLBI data for the main diurnal and subdiurnal variations (Sovers 1993, Herring/Dong 1994).

Empirical determinations of diurnal and subdiurnal Earth rotation variations do not perfectly agree with theoretical predictions, showing remaining discrepancies on a level of several tens of μ as. The reason for these differences are the insufficient theoretical models on the one side and the influences of other short periodic effects on the empirical determination on the other side.

In the diurnal and subdiurnal frequency bands there are several other geodynamical effects and local physical effects at the VLBI sites that influence the VLBI measurements. Among these phenomena are the solid Earth tides, loading of the Earth's crust due to ocean tides and currents (ocean loading), loading of the Earth's crust due to the atmosphere (atmospheric pressure loading), local physical phenomena like thermal deformation effects of the VLBI antennas, variations of the troposphere, etc. Especially all phenomena raised by the tides have the same frequencies and therefore may influence the estimation of diurnal and subdiurnal variations in the Earth rotation parameters.

2 Theoretical models and empirical estimates of diurnal and subdiurnal Earth rotation variations

Based on a hydrodynamical numerical ocean model by Seiler (Seiler 1989, Seiler 1991) research groups in Bonn and Hamburg (Brosche/Seiler/Sündermann/Wünsch) developed the Bonn-Hamburg-Models [BHM] for the influence of ocean tides on UT1 and on polar motion using angular momentum balance computations. In the diurnal and semidiurnal frequency bands the predicted variations in UT1 (26 tides in the diurnal and semidiurnal frequency bands) get maximum amplitudes of 36 μsec and have a total effect of 155 μsec if added. In the diurnal and semidiurnal frequency bands the predicted variations in polar motion (37 tides in the diurnal and semidiurnal frequency bands) get maximum amplitudes of 0.3 mas in x_p and 0.4 mas in y_p and have a total effect of about 1.5 mas in x_p and 1.1 mas in y_p if added. Retrograde diurnal polar motion is assumed to be included in the estimates for nutation correction values in VLBI data analysis and thus is not considered in this study.

Wünsch (1991) published a model for UT1 variations due to the inequality of the equatorial moments of inertia of the Earth. The predicted semidiurnal variations in UT1 get a maximum amplitude of 2 μsec and have a total effect of 3.5 μsec if added.

Variations in UT1 and polar motion due to the ocean tides can be formulated by :

$$\Delta UT1 = \sum_{Tides} [B_1 \cdot \cos(\phi) + B_2 \cdot \sin(\phi)] \quad (1)$$

$$\Delta x_{Pole} = \sum_{Tides} [-A_{1p} \cdot \cos(\phi) + A_{2p} \cdot \sin(\phi) - A_{1r} \cdot \cos(\phi) - A_{2r} \cdot \sin(\phi)] \quad (2)$$

$$\Delta y_{Pole} = \sum_{Tides} [+A_{2p} \cdot \cos(\phi) + A_{1p} \cdot \sin(\phi) + A_{2r} \cdot \cos(\phi) - A_{1r} \cdot \sin(\phi)] \quad (3)$$

The argument ϕ is the astronomical argument of the specific tide which can be computed according to Bartels (1957). Polar motion variations are described by prograde (A_{1p} , A_{2p}) and retrograde amplitudes (A_{1r} , A_{2r}) of the cosine and sine of the astronomical argument of the specific tide. This way of modeling is equivalent to the alternative method of representation by amplitude and phase.

Several authors (e.g. Sovers 1993, Herring/Dong 1994 [HD]) have estimated amplitudes and phases of diurnal and subdiurnal variations in Earth's rotation at the tidal frequencies

directly from VLBI data. These determinations partly agree with the model amplitudes predicted by [BHM] but the amplitudes of the semidiurnal components are only about half the size of the predicted ones.

We estimated amplitudes of variations at 9 tidal frequencies for UT1 and 8 tidal frequencies for polar motion exclusively from IRIS-S VLBI data. The IRIS-S VLBI network formed by the stations Wettzell (Germany), Westford (USA), Hartrao (South Africa) and Fortaleza (Brazil) is well appropriate for the investigations of UT1 and polar motion due to its long East-West and North-South extension. Tables 1 to 4 in chapter 7 contain results of our analysis [IRIS-S], [IRIS-S-Recalculation] compared with those of the theoretical model [BHM] and of the empirical analysis by [HD]. The formal errors of our analysis (about 31000 observations in the IRIS-S network) are about 1.3-2.8 μsec for UT1 amplitudes and 12-18 μas for polar motion amplitudes. Herring/Dong [HD] achieved from their analysis (about 600000 observations) smaller formal errors but give scaled standard deviations of 14-16 μas for polar motion amplitudes and 1 μsec for UT1 amplitudes.

Figures 1 and 2 show two examples of ocean tidal variations in UT1 in vector representations. Figure 1 shows the P1 tide where the magnitude of the theoretical and empirical vectors is similar and the phases are slightly different. Figure 2 shows the M2 tide in UT1 where the phases of the theoretical and the empirical vectors are nearly identical but the magnitude of the theoretical vector is two times the magnitude of the empirical ones.

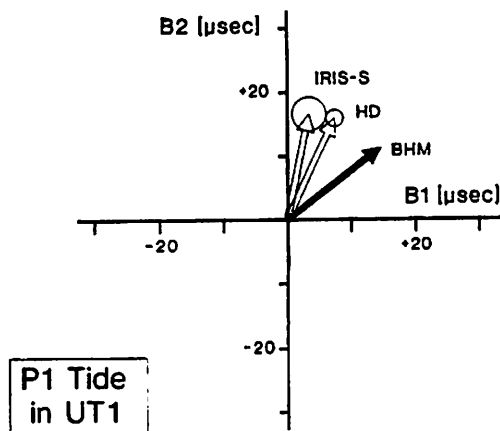


Fig. 1, theoretical and empirical variations in UT1 due to P1 tide

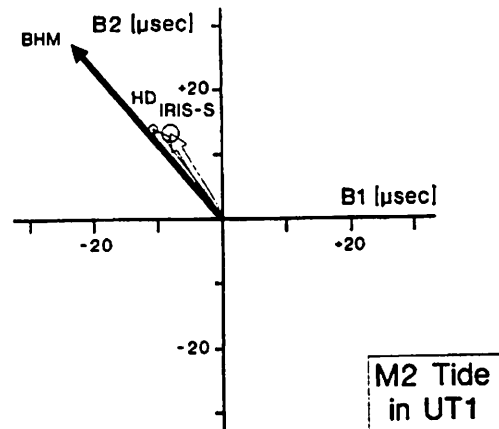


Fig. 2, theoretical and empirical variations in UT1 due to M2 tide

3 Other geodynamical and local effects in the diurnal and subdiurnal frequency bands

In the diurnal and subdiurnal frequency bands there is a variety of other geodynamical and local physical effects. The biggest ones are :

- solid Earth tides
- ocean loading
- atmospheric loading
- thermal deformation of the VLBI telescopes
- tropospheric variations

Models for the first two effects are included in the standard VLBI data analysis software as for instance the CALC/SOLVE package, but the ocean loading corrections strongly depend on the ocean tide models which need further improvement. Moreover, the model used for the solid Earth tides should be refined according to latest research. Atmospheric loading and local effects are not considered in standard VLBI solutions and the correct modeling of the tropospheric refraction of the radio signals still causes problems in VLBI data analysis.

Any mismodelling or neglect of an effect which shows short term variations will contaminate the determination of diurnal and subdiurnal Earth rotation variations. Especially the tidally driven effects have the same frequency dependence as the Earth rotation variations we are looking for. Thus, these effects must be modeled with the highest possible accuracy in order to avoid influences on the empirical determination of diurnal and subdiurnal variations in the Earth's rotation.

The first object of our investigations are the solid Earth tides.

4 Treatment of solid Earth tides in VLBI data analysis software CALC/SOLVE

In the VLBI data analysis software CALC/SOLVE used at the Geodetic Institute of the University of Bonn (GIUB) solid Earth tides are modeled in the time domain. The lunisolar tidal potential W_T is computed from the geocentric position vectors of the VLBI sites, the geocentric position vectors of the tide generating bodies, the site centered position vectors of the tide generating bodies, their masses and the universal gravitational constant. The JPL DE200 ephemerides are used for these calculations. For example the Sun's contribution to the tidal potential at a VLBI site is computed by :

$$W_{T(Sun)} = GM_{Sun} \cdot \left(\frac{1}{|\vec{x}_{SiSu}|} - \frac{1}{|\vec{x}_{GeSu}|} - \frac{(\vec{x}_{GeSu} \bullet \vec{x}_{GeSi})}{|\vec{x}_{GeSu}|^3} \right) \quad (4)$$

In this equation GM_{Sun} is the universal gravitational constant multiplied by the mass of the Sun, \vec{x}_{SiSu} is the site centered position vector of the Sun, \vec{x}_{GeSu} the geocentric position vector of the Sun and \vec{x}_{GeSi} the geocentric position vector of the VLBI site.

The topocentric vertical and horizontal displacements of the VLBI sites (ΔUp , $\Delta East$, $\Delta North$) due to the tidal potential W_T are then computed using frequency independent second degree Love numbers $h=0.609$ and $l=0.085$ as scaling values (equations 5 to 7). Only the radial displacement of the K1 tide is corrected with $h=0.516$ to account for the free core nutation resonance [FCN] of the solid Earth tides.

$$\Delta Up = h \cdot \frac{W_T}{g} + \text{K1-correction} \quad (5)$$

$$\Delta East = l \cdot \frac{\partial W_T}{\partial \lambda} \cdot \frac{1}{(g \cdot \cos(\phi))} \quad (6)$$

$$\Delta North = l \cdot \frac{\partial W_T}{\partial \phi} \cdot \frac{1}{g} \quad (7)$$

In these equations g is the Earth gravity at the VLBI site, ϕ is the geodetic latitude and λ is the east longitude of the VLBI site.

5 Solid Earth tide model by J.Wahr (1981)

Based on a harmonic expansion of the tide generating potential J.Wahr (1981) determined surface displacement models for different Earth models, e.g. the model 1066A by Gilbert and Dziewonski. By eigenfunction expansion for the displacements he derived Love numbers h and l and coupling coefficients for the tidal spectrum. The Love numbers for the diurnal frequency band show a frequency dependence due to the free core nutation [FCN] resonance of the Earth model. Wahr gives resonance models for the second degree Love numbers $h_0(\omega)$ and $l_0(\omega)$ in the diurnal frequency band (equations 8 and 9 and figures 5 and 6) :

$$h_0(\omega) = h_0(\omega_{O1}) + h_1 \cdot \frac{\omega - \omega_{O1}}{\omega_{FCN} - \omega} \quad (8)$$

$$l_0(\omega) = l_0(\omega_{O1}) + l_1 \cdot \frac{\omega - \omega_{O1}}{\omega_{FCN} - \omega} \quad (9)$$

In these models ω are the frequencies of the specific tides, ω_{O1} is the frequency of the O1 tide, ω_{FCN} is the frequency of the free core nutation (FCN) and h_1 and l_1 are amplitude factors.

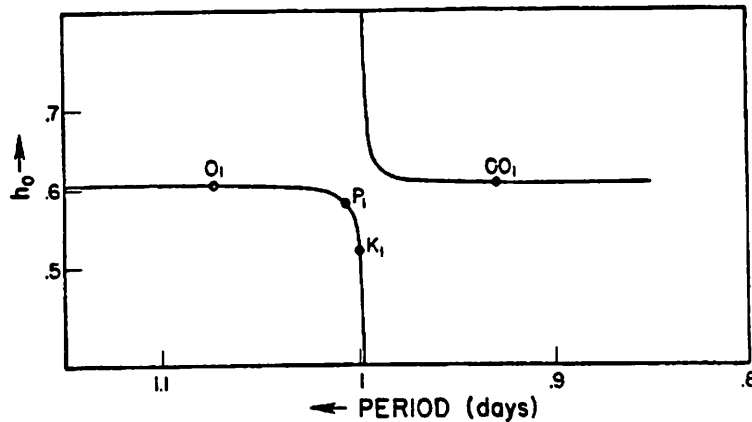


Fig. 3. Love number h_0 in the diurnal frequency band according to J.Wahr

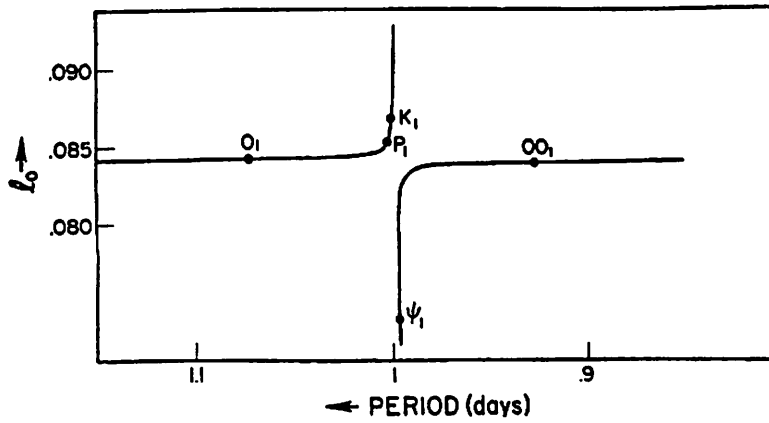


Fig. 4. Love number l_0 in the diurnal frequency band according to J.Wahr

6 Estimation of frequency dependent Love numbers from VLBI data

The idea was now to solve for frequency dependent Love numbers h and l for the main tides in the diurnal frequency band from VLBI data. The harmonic expansion of the tidal potential by Büllsfeld (1985) was used to calculate partial derivatives for a least squares analysis with CALC/SOLVE. Then about 300000 VLBI delay observables from 1986 to 1995 which is 25% of all VLBI data available, i.e. data from different VLBI networks (e.g. IRIS-S, IRIS-A, Europe, R&D) were combined for a final batch solution. Estimates for 20 discrete Love numbers h and l in the diurnal frequency band show a very good agreement with J.Wahr's model.

The estimates for h and l of those tides with a strong potential (e.g. Q1, O1, P1, K1) received small error bars and they lie close to the theoretical values of J.Wahr (see figures 5 and 6). The results for h and l of tides with weak potential are not that well determined and show larger discrepancies from the theoretical values. The estimate of h for Ψ_1 lies on the left branch of the theoretical curve although its place in the theoretical model is on the right branch. This is an indication for a smaller FCN period than J.Wahr used in his model (461 days), but further investigations are needed. The estimates of h and l for the S1 tide, which is known to be a thermal tide too, lie far off their theoretical values. Thus, h_{S1} and l_{S1} have to be fixed on the theoretical values. Overall it can be seen that the estimates for l corresponding to horizontal displacements are not that well determined than the estimates for h which represent the much larger radial displacement.

In figures 5 and 6 the solid lines show the theoretical model of J.Wahr. The discrete points show the estimated values for the Love numbers h and l .

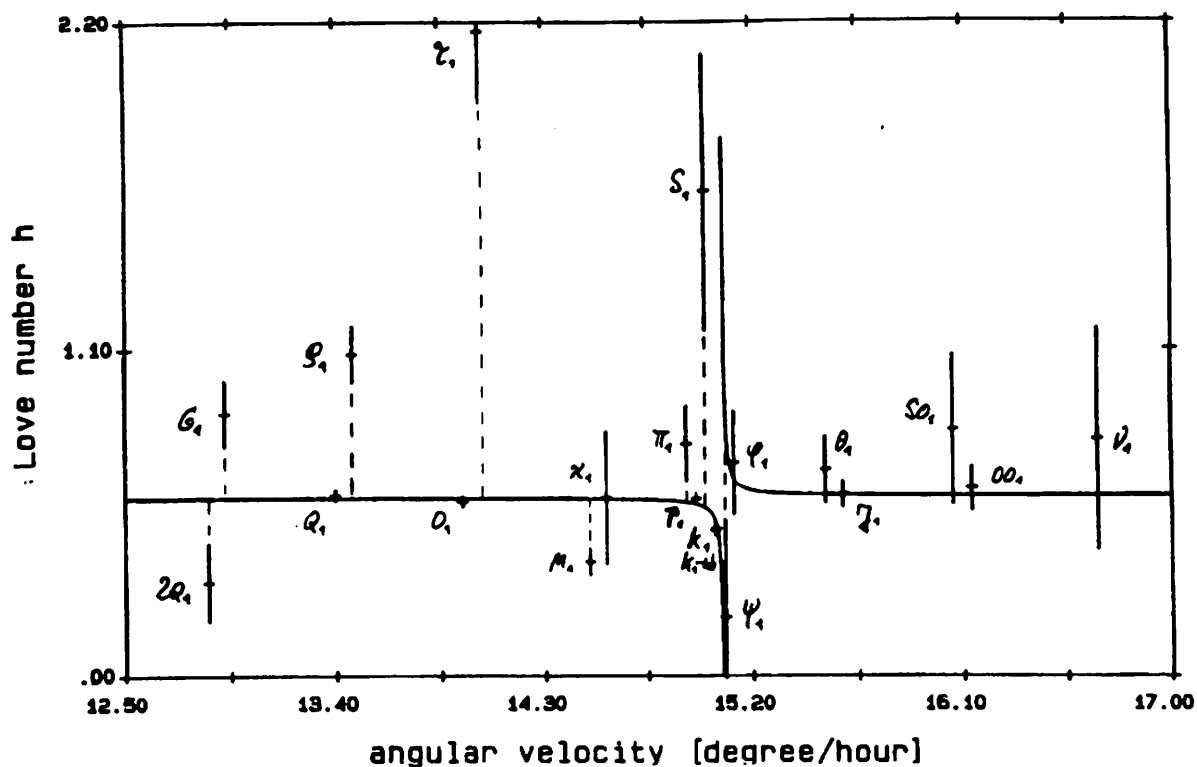


Fig. 5. Estimates of frequency dependent Love numbers h in the diurnal frequency band

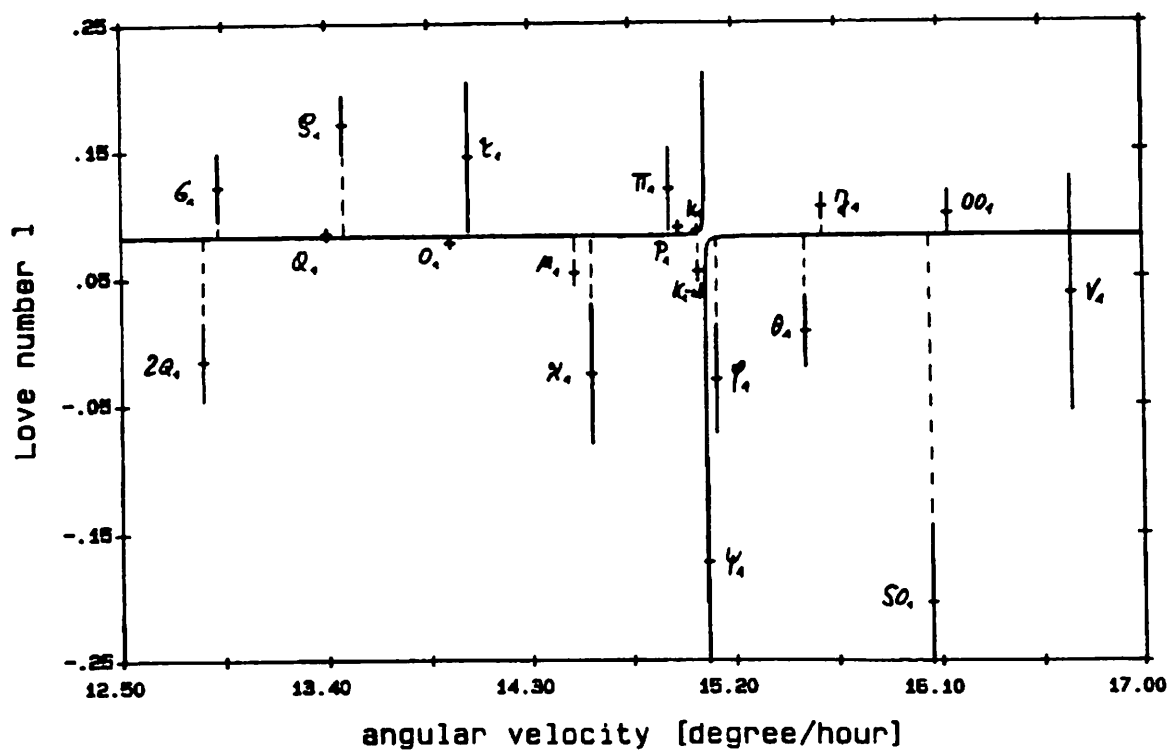


Fig. 6. Estimates of frequency dependent Love numbers l in the diurnal frequency band

In a second step, the five parameters of a frequency dependent model for the diurnal tides were estimated, i.e. $h_0(\omega_{O1})$, $l_0(\omega_{O1})$, h_1 , l_1 , ω_{FCN} in equations 8 and 9. As can be seen in figures 7 and 8, the results, i.e. the 'empirical' frequency model fits rather well with Wahr's theoretical model. The thin lines represent the theoretical model of J.Wahr while the thick lines including the error ranges show the 'empirical' frequency models for the Love number h and l . The estimates for the parameters of the frequency model again indicate a smaller FCN period than used by J.Wahr. Both h and l curves show a small shift in the total level with respect to the theoretical model. Again the Love numbers l are weaker determined than the Love numbers h .

These results show that VLBI data provide valuable information for the independent determination of frequency dependent Love numbers. In a first approach the analysis agrees in the whole with the theoretical model by J.Wahr for the resonance periods in the diurnal frequency band. A first consequence is to fully include this model for solid Earth tides rather than to use the simple model according to the IERS standards (McCarthy 1992) implemented in the CALC/SOLVE package where only for the K1 a frequency dependence is included.

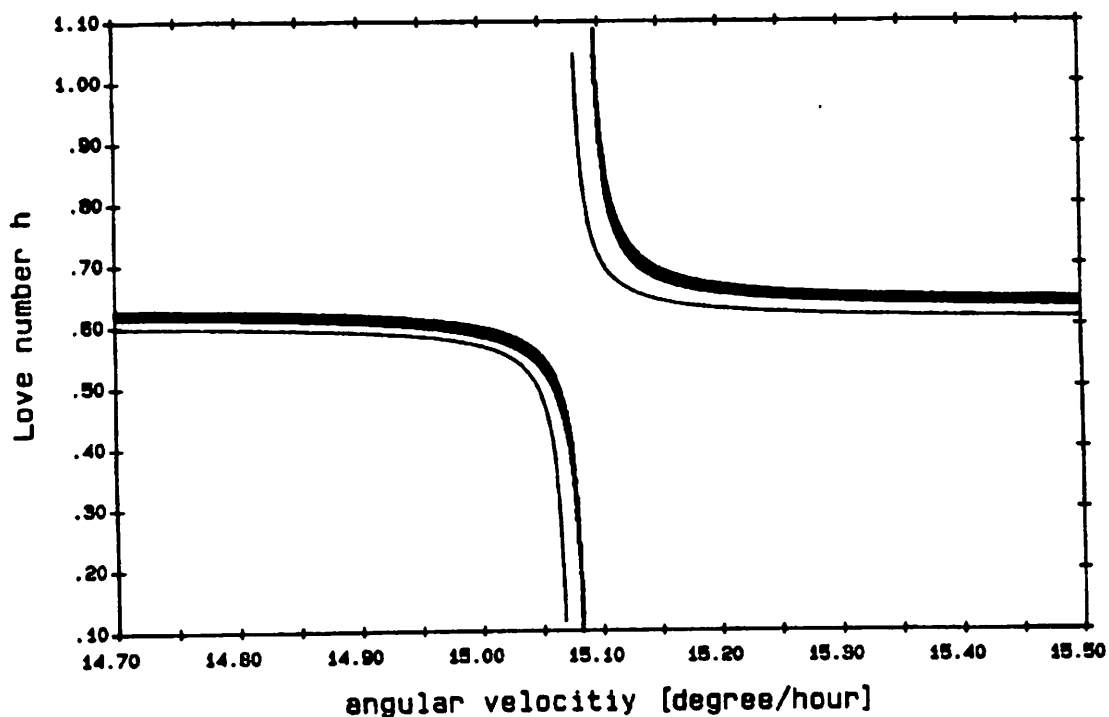


Fig. 7, Estimates of resonance model parameters for Love numbers h in the diurnal frequency band

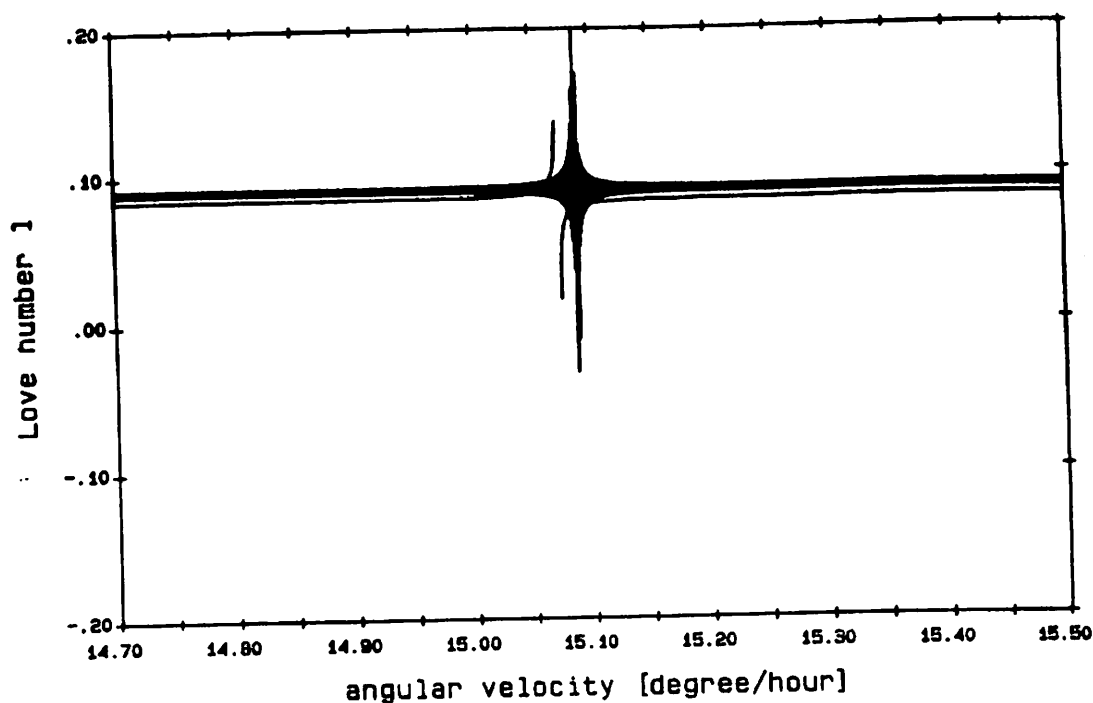


Fig. 8. Estimates of resonance model parameters for Love numbers 1 in the diurnal frequency band

7 Recalculation of diurnal and subdiurnal Earth rotation variations

Finally the effect of the usage of an expanded solid Earth tide model on the determination of diurnal and subdiurnal Earth rotation variations will be shown. Again amplitudes of diurnal and subdiurnal variations in the Earth rotation parameters were estimated from IRIS-S data. An expanded solid Earth tide model was used now. We chose a harmonic expansion of the tidal potential and the frequency dependent model for the Love numbers and the coupling coefficients according to J.Wahr. For the final run the period of the FCN in that model was changed from its value of 461 days (J.Wahr) to a value of 434 days which is a result from nutation observations and gravity tide measurements (Defraigne/Dehant/Hinderer 1994). Differences between the 'old' and the refined tidal deformation model are in the range of 2.3 mm for the vertical deformations and 0.8 mm for horizontal deformations.

A complete recalculation of the diurnal and subdiurnal polar motion and UT1 variation amplitudes was done after having corrected for the refined tidal deformation model. As can be seen from tables 1,2,3,4 the new results (IRIS-S-Recalculation) of polar motion and UT1 variation amplitudes change on the average by about 10% with maximum changes of 25-40% for K1 and K2 compared to those results (IRIS-S) where the 'old' tidal deformation model was used.

Tide		BHM	HD	IRIS-S	IRIS-S-Recalculation
K1	A_{1p}	160.18	133.	117.	112.
	A_{2p}	-65.37	-74.	-31.	-33.
P1	A_{1p}	-50.44	-49.	-2.	1.
	A_{2p}	21.93	35.	33.	30.
O1	A_{1p}	-177.89	-178.	-126.	-127.
	A_{2p}	38.46	89.	97.	97.
Q1	A_{1p}	-33.38	-33.	-65.	-66.
	A_{2p}	1.22	11.	4.	3.

Table 1, Theoretical and empirical amplitudes of diurnal prograde polar motion in μas

Tide		BHM	HD	IRIS-S	IRIS-S-Recalculation
K2	A_{1p}	-0.50	39.	-22.	-26.
	A_{2p}	-10.69	-5.	-35.	-35.
S2	A_{1p}	-11.67	2.	24.	23.
	A_{2p}	-29.47	-12.	-12.	-12.
M2	A_{1p}	26.92	1.	12.	15.
	A_{2p}	-103.35	-58.	-28.	-26.
N2	A_{1p}	12.30	12.	-39.	-37.
	A_{2p}	-18.24	-12.	-16.	-17.

Table 2, Theoretical and empirical amplitudes of semidiurnal prograde polar motion in μas

Tide		BHM	HD	IRIS-S	IRIS-S-Recalculation
K2	A_{1r}	-0.78	-26.	39.	49.
	A_{2r}	63.70	16.	72.	70.
S2	A_{1r}	-64.00	-67.	-29.	-31.
	A_{2r}	227.68	99.	84.	84.
M2	A_{1r}	164.95	-10.	-34.	-38.
	A_{2r}	258.92	265.	245.	246.
N2	A_{1r}	15.63	-10.	-5.	-5.
	A_{2r}	35.95	47.	75.	-77.

Table 3, Theoretical and empirical amplitudes of semidiurnal retrograde polar motion in μas

Tide		BHM	HD	IRIS-S	IRIS-S-Recalculation
K1	B_1	14.64	7.4	3.0	3.7
	B_2	11.48	16.0	16.9	17.1
P1	B_1	-6.09	-3.9	-2.3	-2.4
	B_2	-3.65	-5.9	-10.2	-10.2
M1	B_1	1.53	1.8	0.8	1.0
	B_2	1.58	2.3	2.3	2.8
O1	B_1	-12.90	-14.0	-11.2	-11.6
	B_2	-32.10	-15.6	-13.5	-13.4
Q1	B_1	0.23	-3.1	-5.0	-5.1
	B_2	-4.60	-4.3	-4.3	-3.9
K2	B_1	-1.18	0.8	-1.1	0.9
	B_2	3.72	3.7	3.5	5.1
S2	B_1	-3.58	-0.1	0.5	0.4
	B_2	18.25	8.6	9.3	9.3
M2	B_1	-23.34	-10.8	-8.4	-8.4
	B_2	27.14	14.3	13.6	13.3
N2	B_1	-4.75	-1.6	0.0	0.2
	B_2	5.93	2.8	5.9	5.6

Table 4. Theoretical and empirical amplitudes of semidiurnal UT1 in μsec

Columns 1 name the examined tide, columns 2 [BHM] give the theoretical amplitudes according to the Bonn-Hamburg-Models, columns 3 [HD] show the estimates of Herring/Dong and columns 4 [IRIS-S] and 5 [IRIS-S-Recalculation] show our estimates exclusively from IRIS-S data. Columns 5 give the estimates calculated using the expanded solid Earth tide model with frequency dependent Love numbers.

8 Conclusions

It has been shown that VLBI data can be used to determine the frequency dependence in the estimates of second degree Love numbers. There is an indication for a shorter FCN period than that used by J. Wahr (461 days). This has already been concluded from nutation observations and gravity tide measurements. The refined model for tidal deformations differs from that one used in standard VLBI data analysis by up to 2.3 mm for the vertical deformation due to the inclusion of frequency dependent Love numbers h , l for all periods close to the FCN resonance rather than for K1 only. After having entered the refined tidal deformation model in the data analysis the empirically determined amplitudes for diurnal and subdiurnal polar motion and UT1 variations change by 10% on the average. In order to avoid further influences on the empirical determination of diurnal and subdiurnal Earth rotation variations all other diurnal and subdiurnal effects should be modeled consistently. Thus, also effects of ocean loading, atmospheric loading, thermal deformation, have to be investigated thoroughly. For thermal deformations of the telescopes see Nothnagel/Pilhatsch/Haas (this issue).

9 References

- Bartels, J.** , "Gezeitenkräfte" in : Handbuch der Physik, Band XLVIII, Geophysik II, Springer-Verlag, 1957
- Brosche, P., Wünsch, J.** , On the 'rotational angular momentum' of the oceans and the corresponding polar motion, *Astr. Nachrichten* 315 (2), pp. 181-188, 1994
- Brosche, P., Wünsch, J., Campbell, J., Schuh, H.** , Ocean tide effects in Universal Time detected by VLBI. *Astron. Astrophys.* 245, pp. 676-682, 1991
- Büllesfeld, F.J.** , Ein Beitrag zur harmonischen Darstellung des gezeitenerzeugenden Potentials, *DGK Reihe C. Heft-Nr.* 314, 1985
- Defraigne, P., Dehant, V. Hinderer, J.** , Stacking gravity tide measurements and nutation observations in order to determine the complex eigenfrequency of the Nearly Diurnal Free Wobble, *JGR. Vol.* 99, NO. B5, pp. 9203-9213, 1994
- Herring, T.A., Dong, D.** , Measurement of diurnal and semidiurnal rotational variations and tidal parameters of Earth, *JGR, Vol* 99, NO. B9, pp. 18051-18071, 1994
- McCarthy, D.D.** , IERS Standards. IERS Technical Note 13, 1992
- Wünsch, J.** . Small waves in UT1 caused by the inequality of the equatorial moments of inertia A and B of the Earth, *Astr. Nachrichten* 312 (5), pp. 312-325, 1991
- Seiler, U.** . An investigation to the tides of the world ocean and their instantaneous angular momentum budget. *Mitt. Inst. f. Meereskunde, Univ. Hamburg.* Nr. 29. pp. 101, 1989
- Seiler, U.** . Periodic changes of the angular momentum budget due to the tides of the world ocean, *JGR, Vol.* 96. NO. B6, p. 10287-10300, 1991
- Sovers, O.J., Jacobs, C.S., Gross, R.S.** . Measuring Rapid Ocean Tidal Earth Orientation Variations With Very Long Baseline Interferometry, *JGR, Vol.* 98, NO. B11, pp. 19959-19971, 1993
- Wahr, J.M.** , Body tides on an elliptical, rotating, elastic and oceanless earth, *Geophys. J. R. astr. Soc.* 64, pp. 677-703, 1981

VLBI in the Far North. A closer look

Néstor Zarraoa^{1,2}

¹ *Geodetic Institute, Norwegian Mapping Authority, Honefoss, Norway*

² *Now in DLR Remote Sensing Ground Station Neustrelitz, Germany*

Abstract

There is a long history of geodetic VLBI experiments in the Northern hemisphere. However, this long history does not reach the northernmost areas, the Arctic, where interesting geophysical phenomena are still unexplained and where not much data is available for the research community. Until recently, only a few permanent stations were located close to the Arctic regions. Some mobile campaigns have provided interesting data in North America and Europe, reaching up to Tromsø (Norway), at 70 degrees north. Very recently, Yellowknife has become a permanent site for geodetic VLBI, and of more importance, the new permanent geodetic observatory in Ny Ålesund, at almost 80 degrees north has become a reality, opening a broader future for geodetic research in the Arctic. In this paper I will present the analysis of a large set of VLBI data with stations located far north. Problems like the appropriate reference frame and the repeatability that can be obtained with routine VLBI will be presented for this particular area. I will also show some of the trends that can be found in the long term VLBI data sets, with unexplained systematic behaviours at the few millimetre level. In addition, I will give a view about how we can conduct research based on space geodesy in the Arctic. Problems like global climatic change, post-glacial rebound effects and geodynamics, can be addressed with a proper combination of space geodetic techniques, where permanent VLBI and GPS sites in the region can play the role of backbone for a number of other techniques, like SAR interferometry, satellite altimetry, local GPS campaigns, gravity measurements and sea level studies.

Introduction

The Arctic region is a very interesting area for research, in particular for Far North countries like Norway. Plenty of investigation in different fields have been conducted in the Arctic environment in the last century, but from the point of view of space geodesy, the efforts have just started, and there are very little data available so far.

Regarding the use of geodetic VLBI, only three permanent stations are available today above 60° N: Fairbanks (Alaska, US), Yellowknife (Canada) and the new geodetic observatory in Ny Ålesund (Spitsbergen, Norway) at 79.8° North (Pettersen, 1993). The last two started routine operations very recently, so there is not much data available from them. In addition, some mobile campaigns have observed northern stations in Alaska and Canada (Ma et al., 1991) and in Norway and Iceland (Zarraoa and Danielsen, 1993).

The situation with other space geodetic techniques is also not good, but improving rapidly. Ny Ålesund also runs a permanent GPS receiver of the IGS network and has one of the Russian Sirius systems. It will host a PRARE receiver in the near future. At lower latitudes, Fairbanks and Yellowknife operate GPS receivers as well, and there is a dense GPS network in Scandinavia, as well as other sites in Canada. There are advanced plans for at least one permanent GPS receiver in Greenland and another one in Iceland. The coverage of satellite altimetry and gravity data is quite good in the region up to 80-85 degrees north. Unfortunately, the Russian side of the Arctic is still an empty zone for space geodesy. In figure 1, we show some of the stations around the North Pole, currently available with permanent VLBI or GPS equipment. Not all the available stations in dense areas like Central Europe or Scandinavia are shown.

Results of baseline length

Comprehensive reports on the results of VLBI analysis are regularly published by the Goddard Space Flight Center VLBI group (e.g. Ryan et al., 1993), with the inclusion of all available experiments. We will not reproduce the analysis here, but we must mention that the results achieved are of superb quality.

The repeatabilities obtained from our analysis are at the part per billion level and in figure 2 we can see the repeatabilities as a function of the baseline length. A line fitting the results shows a ground level noise of 1.6 mm plus 1.4 mm/1000 Km.

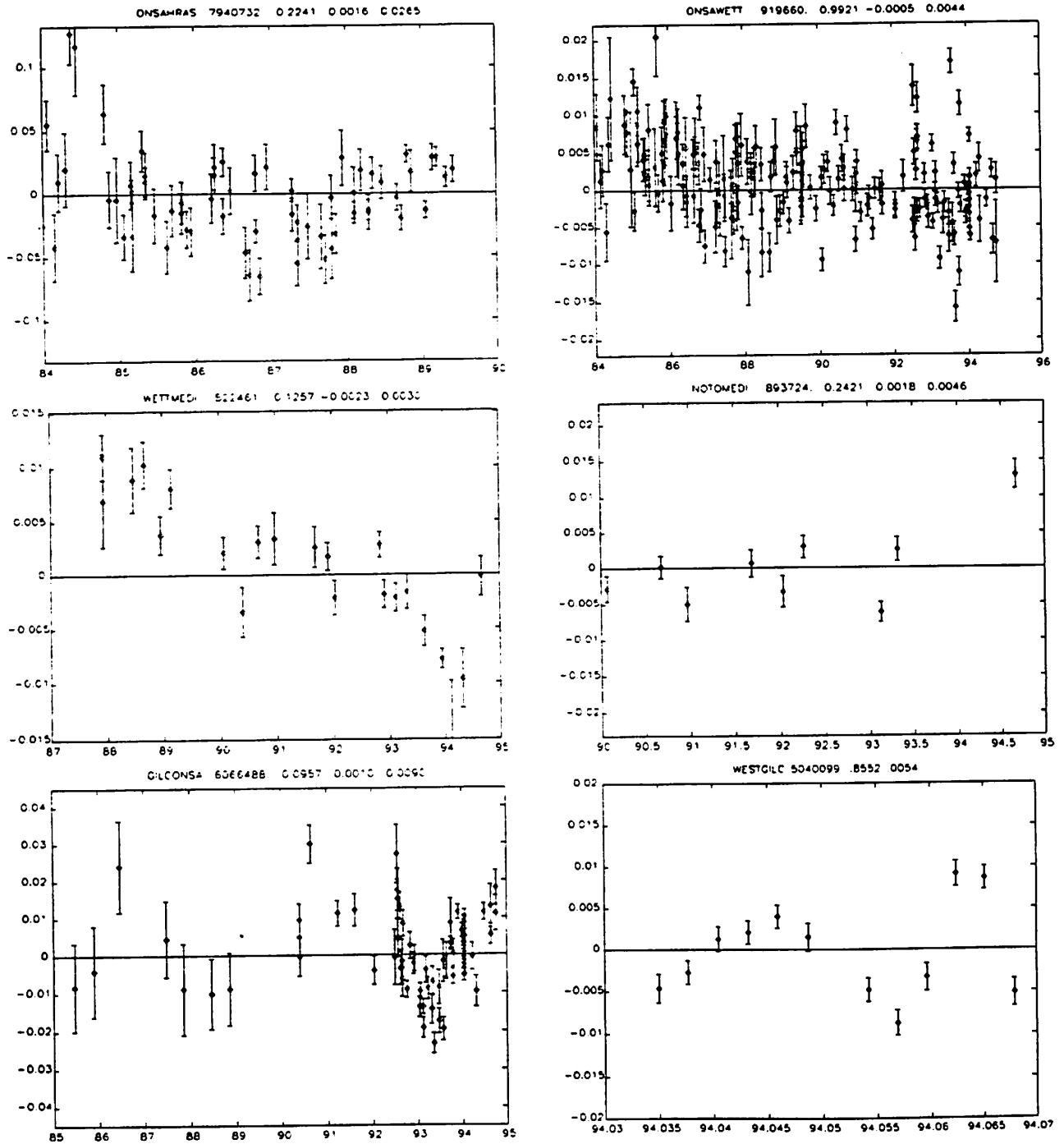


Fig. 3. Examples of systematic behaviour in VLBI baselines as function of time. Figures are numbered from 3a to 3f, left to right, top to bottom. All values are in meters.

Systematic trends in the baseline lengths

The ever increasing accuracy of VLBI permits now to glimpse signals that were not visible few years ago, and systematic behaviour at the millimetre level can be found in the baseline lengths evolution.

In several of the available baselines, the volume of data is rather high, and it spans for several years. In general we can see how the quality of the experiments has improved extraordinarily in the last years, following the major advances in hardware, software and experiment design. The result is that most of the recent data start to show some systematic behaviours at the few millimetre level, which can be traced back also to the past experiments.

However, it is not a simple task to identify the source for the systematics, as so many different unknowns are still playing a role in the VLBI analysis. In figure 3 we show some of the most remarkable features. In some cases we see that the data set is not sufficient to really prove the existence of a systematic effect, but it gives a hint of possible tasks for the future research. In all the plots, we are showing the residuals to the estimation of a regression line over the baselines, and in the figure title we can see, besides the baseline name, the length (two numbers, first the integer number of meters and second the remaining length in meters too), the rate (meters per year), and the repeatability of the estimation.

In figure 3a and 3b we can compare two different baselines, Onsala-Fort Davis and Onsala-Wettzell. Some years ago, the VLBI analysis showed that the Fort-Davis behaviour could not be attributed to linear motions, so this station became a special case in VLBI analysis. Some of the strange features can be seen in figure 3a (although they also extend to the period before 1984). But we can also see in figure 3b how in the Onsala-Wettzell baseline it is possible to find similar trends, although with a much smaller scale (the baseline is 8 times shorter).

Figure 3c and 3d refer also to the European network. In Wettzell-Medicina (3c), we might be seeing a non-linear trend over several years, which is obscured in the plot by the effect of the observations with smaller formal errors. Noto-Medicina, however, shows a rather peculiar alternance between larger and shorter baselines, more or less following the summer-winter periods. Are we seeing, perhaps, an effect of the temperature deformations in this short baseline?

With the improved quality of the R&D experiments, we do not need much time to see systematic trends. In figure 3e, we can appreciate the striking feature in the Onsala-Fairbanks baseline since 1992. And even more interesting, during the special January 1994 continuous R&D VLBI campaign, we can appreciate systematic trends over just 13 days in figure 3f (Westford-Fairbanks). In this last example, the repeatability during the 2 weeks period is impressive, 5 mm in a 5000 Km baseline, but if we could remove the systematic effect, we would have a remaining rms. of hardly 1-2 mm, 3 parts in 10^{-10} !

Some of these features may not correspond to real phenomena, but we are seeing more and more of them, and the number of possible loose ends at millimetre level in geodetic analysis is rather large, so we are probably in the need of a major software revision, to accommodate the improved capabilities of the current VLBI systems and of the coming MarkIV.

Evaluation of different reference networks

In order to study with some more detail which of the possible reference frame configurations provides the best results, we have selected a few of the triplets and processed for each all the experiments with at least the three stations of the triplet. Then we had the chance to intercompare the estimation of coordinates and earth rotation in addition to the baseline lengths. In table 1 we present the repeatability levels for two of the references selected, showing the mean and the worst rms. for all the stations with a significant number of epochs, and the station with the worst rms.

The best performance was found for the reference triplet Westford-Fairbanks-Onsala, that can be seen in table 1. The solid geometry of this reference has produced very good repeatability levels in all coordinates, better than 2 cm for the vertical components and better than 1 cm for the horizontal components of the stations. In general the worst results correspond to the Hawaiian stations, which are those who lay the furthest away from the three reference stations.

Some of the other reference triplets were not so good. For example, the use of the three North American stations: Westford-Algonquin-Fairbanks as reference was not possible because they are basically aligned, being thus insufficient to uniquely define the terrestrial reference frame.

Table 1. Repeatabilities of the results obtained with two different reference triplets

Ref. Network	Component	Mean RMS	Worst RMS	Station worst rms
Westford	Vertical	13.5 mm	28.7 mm	Kauai
Fairbanks	North	7.7 mm	11.7 mm	Kauai
Onsala	East	9.4 mm	16.4 mm	Kokee
Westford	Vertical	34.1 mm	70.1 mm	Kokee
Wettzell	North	28.7 mm	82.9 mm	Kokee
Onsala	East	34.7 mm	103.7 mm	Fairbanks

We have also tried the line Wettzell-Onsala along with an American station as reference. In these cases the results were not so good due to the short European baseline. When using them along with Westford (see table 1), the stations in the Pacific suffered from very low precision, and the overall repeatabilities were of several centimetres in all components. If Fairbanks was used instead of Westford then we had an additional problem in the determination of the polar wobble components, because the reference was aligned with the Pole. This led to unreliable results in the coordinates.

The current problems with the availability of Westford, will require a redesign of the best reference network. Yellowknife or Algonquin can play a very important role, specially along with the Onsala-Ny Ålesund baseline. From the results above, these seem the best candidates for a terrestrial reference in this strategy of geodetic VLBI analysis towards the North, although stations in Southern latitudes, or in the Asian-Pacific region may suffer from poorer results than those stations in the North.

The coordination of space geodetic research in the Arctic. A proposed plan.

In this paper we have presented some results of a dedicated analysis of the available VLBI data near the North pole, in order to evaluate the performance of the new northern VLBI stations for research purposes in the Arctic areas, in terms of precision and time scales for the detection of systematics.

But the real step ahead towards a proper research program with space geodesy in the Arctic is still to be done. In this section we present some of the topics that could be addressed with the use of space geodesy, and propose a sketch plan of how such a research could be conducted and coordinated.

Space geodesy has provided a direct insight into current tectonic motions. The study of the global geodynamics in the Arctic is still an interesting and unknown topic. Several tectonic plates meet in the Arctic and interact with each other. On top of that, the effects of the last glaciation period are still present in the form of post-glacial rebound land uplift, yet unmeasured in large areas. But even more than that, all these processes have a direct relation with global effects on the entire Earth, like climatic changes and their influence on ice caps and sea level. The Arctic is rapidly affected by those changes and it is more likely to measure their effects and possible consequences there than anywhere else.

Space geodesy is based in global reference frames that can be applied to global or local areas, but keeping always a common reference. For this, it is capable of merging into the same reference frame independent results from different areas or epochs, being also able to measure both horizontal and vertical displacements.

The initial goal of a coordinated project would be to make a global study of the area, by using a reduced number of geodetic points, but located on strategic areas and with the best coverage of the region. In addition to the global displacements that can be studied, such a network would provide a solid reference for a large variety of other projects related to local areas or for densification works. It could also be useful for other purposes, not the least, industrial (fisheries, oil platforms) or political (territorial waters boundaries). Such a project would require several stages:

1. Design an adequate network of observation considering the scientific interests and the available equipment. Establishment and monumentation of the geodetic points. The network should be as global as possible, but with a reduced number of points, which could be easily analysed in combination with existing networks like IGS.
2. GPS observation campaigns or installation of permanent sites. The latter are preferable, and in some cases can even be more cost effective. If that is not possible, frequent reoccupations would be necessary through the project duration in order to study the variations in the observed positions.
3. Analysis of the data to determine the coordinates and velocities of the sites in an International Terrestrial Reference Frame, to ensure a common reference for all the observing periods.

4. Comparative analysis of other data sets for calibration or comparison. Very Long Baseline Interferometry will be used as backbone network for calibration of the GPS system. Existing geophysical data of local displacements should be compared with the obtained results. Sea level measurements with tide gauges or satellite-borne altimetry would be linked to the earth-based GPS data to provide a global reference for the sea level measurements.
5. Interpretation of the results. Proposals for refinement or densification in areas of special interests.

Some of the stations that could be used already exist, as shown in figure 1. However, the task of implementing other stations and performing the observations, analysis and interpretation, would require a large international cooperation involving also other geophysical fields, not only geodesy, and relatively large funding. However, the scientific interest of a successful establishment of a permanent space geodesy network in the region is also considerable and it would also help to focus the work of different groups in Europe towards a major goal where both GPS and VLBI could participate.

Conclusions

The quality of the VLBI data has improved dramatically in the last years. With data from the last decade, we are approaching a precision level of 1 part per billion.

With the analysis of a large set of VLBI data we have shown that not only long-term horizontal displacements like plate tectonics can be detected, but also vertical motions and non-linear trends at the millimetre level could now be found in the data sets in short time scales. With the improved equipment that is currently available or will be in the immediate future (MarkIV) we can expect an extensive task towards the identification and modelling of those systematic trends, which may lead towards the 0.1 ppb precision level.

We have also shown that the available results support the extension of the geodetic VLBI network with new stations in the Arctic regions, which can provide reliable results about the conditions in the area in a very short time, compared with what was needed some years ago.

GPS is also sharing this improvement in the data quality, so this technique can also be used, with advantage, in combination and also as an extension of VLBI. Thus, we are in the position of proposing a coordinated project where the use of both techniques can establish a reference network in the Arctic to address different geophysical problems, like the global geodynamics and the sea level changes in the Arctic ocean, where other techniques can be calibrated and independent data sets properly merged by using such a reference network.

Acknowledgements. I would like to thank the staff of the Geodetic Institute of the Norwegian Mapping Authority (SKGD) for their support to my work and for our fruitful discussions about how to pursue a comprehensive research program in the Arctic. I also appreciate the support received from SKGD to finance my assistance to this meeting.

References

- Ma, C., J.M. Sauber, L.J. Bell, T.A. Clark, D. Gordon, W.E. Himwich, J.W. Ryan. Measurement of horizontal motions in Alaska using VLBI. *J. Geophys. Res.*, 95, 21,991-22,011. 1990.
- Pettersen, B.R. The Ny Ålesund VLBI Station. *Proc. IX European VLBI Meeting. Univ. Bonn Geod. Series*, 81. Ed. J. Campbell & A. Nothnagel. pg. 24. 1993.
- Ryan, J.W., C. Ma, D.S. Caprette. NASA Space Geodesy program-GSFC Data Analysis-1992. NASA Tech. memo. 104572. 1993.
- Zarraga, N. OCCAM V3.2: Status report. *Proc. IX European VLBI Meeting. Univ. Bonn Geod. Series*, 81. Ed. J. Campbell & A. Nothnagel. 25-26. 1993.
- Zarraga, N., J. Danielsen. Analysis of the European Mobile VLBI campaigns. *Proc. IX European VLBI Meeting. Univ. Bonn Geod. Series*, 81. Ed. J. Campbell & A. Nothnagel. 60-70. 1993.

Present Status of the VLBI Data Analysis Activities at the Matera Space Geodesy Center.

Roberto LANOTTE¹, Giuseppe BIANCO² and Marco FERMI³

¹ *Nuova Telespazio S.p.A., Centro di Geodesia Spaziale, Matera, Italy*

² *Agenzia Spaziale Italiana, Centro di Geodesia Spaziale, Matera, Italy*

³ *Nuova Telespazio S.p.A., Dipartimento di Geodesia Spaziale, Rome, Italy*

Abstract. The VLBI data analysis activities at the CGS of Matera is at the present addressed towards two directions: the analysis of the VLBI data acquired within the EUROPE project and that of the world wide VLBI network.

The results coming from the EUROPE analysis show the capability for this campaign to detect site motion on short time range.

The analysis of the global VLBI network is at the present to be considered as preliminary.

1 Introduction

The VLBI data analysis activities at the Space Geodesy Center (CGS) of Matera is at the present addressed towards two directions: the analysis of the VLBI data acquired within the EUROPE project and that of the world wide VLBI network.

With respect the analysis presented in the last Working Meeting [Lanotte, 1993], the analysis presented in the following uses a longer time range (from 1990 up to 1994). The obtained results show the capability of VLBI regional network to detect site motions on short time range and prove the good quality of the data acquired by the stations participating to the EUROPE campaign.

2 Data analysis of the EUROPE campaign

Since 1990 regular VLBI experiments have been performed using purely European fixed stations with a frequency of at least three experiments per year. Table 1 reports the antenna size, location and managing agency of the stations that participated, in the period covered by this analysis, to the Europe campaign.

The network covers the western part of the Eurasian plate including the Mediterranean area and allows to estimate the motion of the Italian sites which are believed to be near at the border between the Eurasian and the African plates.

Site	Antenna Diameter (m)	Agency	Location
DSS65	34	Deep Space Network	Madrid, Spain.
EFLSBERG	100	Max Planck Institute for Radioastronomy	Effelsberg, Germany
MATERA	20	Italian Space Agency (ASI)	Matera, Italy
MEDICINA	32	University of Bologna	near Bologna, Italy
NOTO	32	University of Bologna	Noto, Sicily, Italy
ONSALA	20	Onsala Space Observatory	Onsala, Sweden.
WETTZELL	20	German Institute for Applied Geodesy (IfAG)	Bavaria, Germany.

Table 1: Description of the chief stations participating to the Europe campaign

2.1 Data processing

For this analysis we used the geodetic Mark III [Rogers, 1983, Clark, 1985] VLBI experiments from the EUROPE campaign correlated at the Max Planck Institute for Radio Astronomy in Bonn.

Figure 1 schematically shows the steps of the data processing.

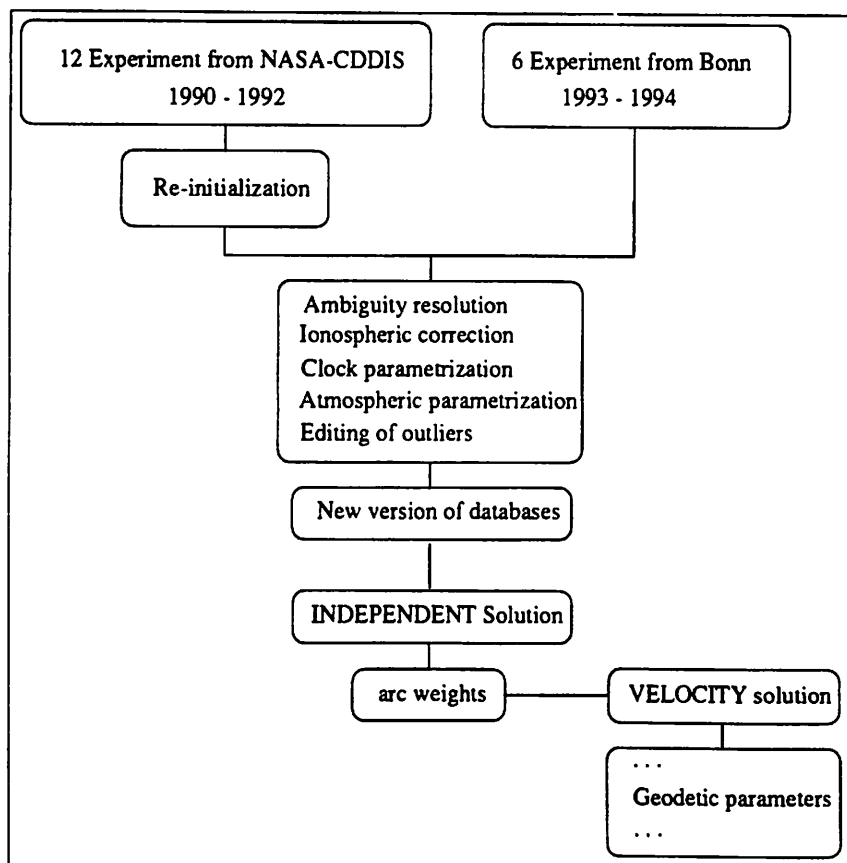


Figure 1: Data processing scheme.

The databases used have been acquired from NASA-CDDIS (Crustal Dynamic Data Information System) up to 1992 and from the Bonn correlator for the period 1993-1994.

The analysis have been carried out by means of the CALC/SOLVE software system developed at the NASA Goddard Space Flight Center, on an HP755 workstation.

Since the databases coming from the CDDIS held also informations about previous analysis, in order to be fully confident on our results, we re-initialized those databases and then the whole set of experiments has been processed for ambiguity resolution and ionospheric correction, using the data acquired on the S-band (2.3 GHz) and X-band (8.4 GHz), and then for clock and atmospheric parameterization and editing of outliers.

Two solutions, using SOLVE in GLOBL mode [Ma, 1990], were computed: the first was an *independent* solution to generate the arc weights used in the following *velocity* solution, where site positions and velocities were estimated as global parameters. The independent solution differs from the velocity solution for the absence of global parameters so that all the sessions are treated independently.

2.2 Data statistics

The analysis include 18 experiments of 24 hours belonging to the EUROPE campaign since 1990 up to 1994. Table 2 summarizes the site participation to the experiments.

		D	E	K	M	M	N	O	W	T
		S	F	A	A	E	O	N	E	O
		S	L	R	T	D	T	S	T	U
		6	S	L	E	I	O	A	T	L
		5	B	B	R	C	L	Z	O	
		E	U	A	I		A	E	U	
		R	R		N		6	L	S	
		G	G		A		O	L	E	
1	90JAN26X	*	-	-	-	*	*	*	*	-
2	90SEP05X	*	-	-	-	*	*	*	*	-
3	90DEC20X	*	-	-	-	*	*	*	*	-
4	91JAN06X	*	-	-	-	*	-	*	*	-
5	91SEP08X	*	-	-	-	*	*	*	*	-
6	91DEC01X	*	*	-	-	*	-	-	*	-
7	92JAN14X	*	-	-	-	*	-	*	*	-
8	92APR08X	*	-	-	-	*	*	*	*	-
9	92MAY12XA	*	-	-	-	*	-	-	-	*
10	92JUL07X	*	-	-	-	*	-	*	*	-
11	92NOV03X	*	-	-	-	*	-	*	*	-
12	92DEC01X	*	*	-	-	*	-	*	*	-
13	93FEB16XA	*	-	-	-	*	*	*	*	-
14	93APR27XA	*	-	-	-	*	*	-	*	-
15	93AUG18XA	*	-	-	-	*	-	*	*	-
16	93DEC11XE	*	*	-	-	*	-	*	*	-
17	94FEB09XD	-	-	-	-	*	-	*	*	-
18	94APR27XA	*	*	-	-	*	-	*	*	-

Table 2: Summary of sessions by database and site. The asterisk represent the participation of the site to a particular experiment.

The sites KARLBURG and TOULOUSE participated to one experiment only and then they will not be considered in the results.

The solution uses 33130 group delays.

2.3 Adopted models

The models used are implemented in the CALC/SOLVE program and are based on the IERS standards [McCarty, 1985]. In particular our solution adopts the following:

- Reference frames:
 - Earth Rotation Parameters and Nutation from the IERS series 90C04 [IERS A.R., 1992].
 - Source positions fixed at the value of the IERS Celestial Reference Frame ICRF92.
 - The solution is constrained moving the Wettzell site according to the NUVEL1A model [DeMets, 1994] and fixing its position to the value of the IERS Terrestrial Reference Frame ITRF92 [Bouchier, 1993] at the epoch January 1, 1988.
- Processing options:
 - Dry tropospheric zenith delay estimated using the Saastamoinen model and mapped to the elevation of the observation with the MTT dry model.
 - Wet tropospheric delay estimated using a continuous, piecewise linear function with duration of the linear sections of 60 minutes and 50 ps/h constrained in slope.
 - Clocks are estimated using a reference station (different arc by arc) and modeling the difference between the reference clock and the other with a second order polynomial plus a piecewise linear function with duration of the linear sections of 60 minutes and $5 \cdot 10^{-14}$ constrained in slope.
 - Cable calibrations are applied where available, they are always absent for DSS65.

The choice of 60 minutes for the length of the linear sections derive from a preliminary work. Since the inspection of the post fit residuals does not provide immediately the values for length and constraint of the segments, in order to obtain some indication about these values, we performed, for a few experiments used in this analysis, a series of solutions in which a parameter was changed fixing the others and then we investigated the behaviour of statistical and geodetic parameters.

Fig. 2 is an example of the results. Each point in these figures represents a solution in which the length of the linear sections for the troposphere change from a point to the other by 1 minute while the segments are 50 ps/h constrained in slope; clocks are parameterized with a 60 minutes interval and $5 \cdot 10^{-14}$ constrained in slope.

The results of this work are at the present under investigation but we concluded that the choice of 60 minutes for the length of the segments forming the piecewise function for the troposphere and clocks are adequate. A choice of a shorter length would increase the number of parameters giving no improvement on the estimate of geodetic results as showed in fig. 2(a). On the other hand a longer length could not adequately model troposphere as showed in fig. 2(b).

The selected values seem to be adequate also for the global solutions as investigated by J.W. Ryan, C. Ma and W.E. Himwich [Ryan *et al.*, 1991].

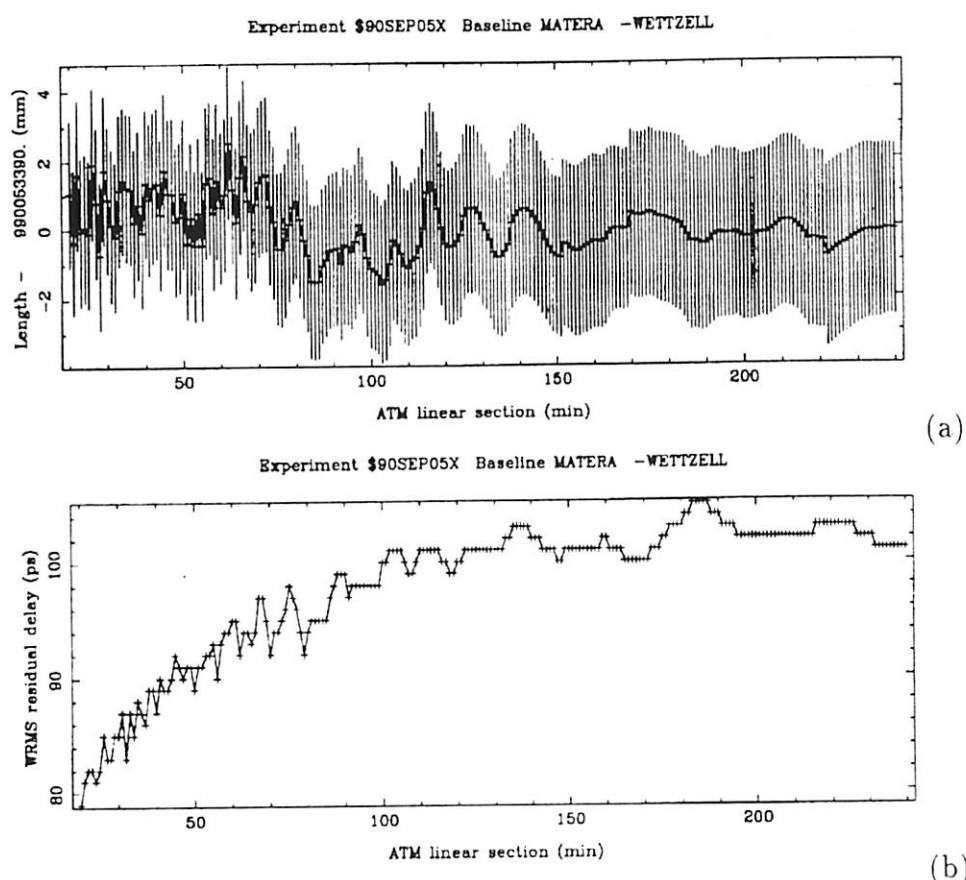


Figure 2: Behaviour of the change of length with errors (a) and of the WRMS residual delay (b) with respect to the length of the linear sections forming the piecewise function used to model the wet tropospheric delay for the baseline Matera-Wettzell in one of the experiments.

2.4 Presentation of the analysis results

There were 4475 arc parameters and 51 global parameters. The weighted RMS fit was 38.5 ps and the reduced χ^2 was 1.054.

Table 3 shows the estimated topocentric Up, East and North rates. Table 2.4 reports the estimated horizontal velocities.

Figure 3 shows the estimated motions with 3 standard deviations error ellipses. For Matera, both NUVEL1A values are reported assuming this station on the African or Eurasian plate.

The Up rates are affected with higher variances and are generally four times the variances of the horizontal rates. There is no evidence for vertical motion higher than 1 cm/yr for all the stations.

For Noto the magnitude of the horizontal velocity is bigger than that predicted by the model, at the 3σ confidence level, otherwise it exhibits African behaviour.

Medicina and Matera show clear disagreement with respect to the model.

Table 5 reports the three orthogonal components length, transverse and vertical rates

of the baselines. On the same table, the results from the solution GLB908 [Ma, 1990] are shown with the number of sessions in which the baseline is present and the span in years. The GLB908 uses data from 1979 to 1992 and includes nearly all Mark III geodetic VLBI experiments taken by any agency. Owing to the fairly recent installation of most of the European VLBI stations, half of the baseline have in GLB908 only two observing sessions or their time series does not cover more than one year and than their rates are not present in that solution.

The remaining baselines have an observatory story comparable between the two solutions with the exception of Eflsberg-Wettzell and, in particular, of Onsala-Wettzell that, in the GLB908, is present in 158 sessions. Both solutions exhibit the contraction existing between Noto and the stations in North Europe.

Confirmation of the Matera motion can be found comparing the VLBI rate for the baseline Matera-Wettzell with that obtained from other space geodesy techniques. Both stations can be considered as fundamental for space geodesy since they are occupied by VLBI, GPS and SLR.

The VLBI length rate of -6.5 ± 0.4 mm/yr for Matera-Wettzell is fully in agreement with the geodesic SLR rate of -6 ± 2 mm/yr achieved by our SLR data analysis group using 10 years of SLR data.

Site	Up rate (mm/yr)	East rate (mm/yr)	North rate (mm/yr)	NUVEL 1A			Assigned Plate
				Up rate	East rate	North rate	
DSS65	6.8 ± 1.3	19.9 ± 0.3	16.5 ± 0.3	0.0	18.7	15.6	Eurasian
EFLSBERG	4.9 ± 2.1	19.1 ± 0.4	15.1 ± 0.4	0.0	19.0	14.3	Eurasian
MATERA	-1.9 ± 1.4	23.2 ± 0.3	19.8 ± 0.4	0.0 0.0	19.2 22.0	20.5 12.7	African Eurasian
MEDICINA	-1.2 ± 1.2	22.5 ± 0.3	16.7 ± 0.3	0.0	20.8	13.6	Eurasian
NOTO	5.3 ± 1.7	21.9 ± 0.4	22.9 ± 0.5	0.0	19.8	20.5	African
ONSALA	5.5 ± 1.2	17.8 ± 0.3	13.7 ± 0.3	0.0	18.7	13.6	Eurasian
WETTZELL	0.0	20.4	13.4	0.0	20.4	13.4	Eurasian

Table 3: Topocentric rates. The estimated Up, East and North rates are compared with that predicted by the NUVEL 1A model. Matera shows disagreement with respect to the values predicted by the model assuming this site either on the African plate or on the Eurasian one.

Site	Horizontal Amplitude Rate (mm/yr)	Horizontal Azimuth (deg)	NUVEL 1A		Assigned Plate
			Horizontal Amplitude Rate (mm/yr)	Horizontal Azimuth (deg)	
DSS65	25.8 ± 0.4	50.3 ± 0.6	24.4	50.1	Eurasian
EFLSBERG	24.4 ± 0.4	51.8 ± 1.0	23.8	53.0	Eurasian
MATERA	30.5 ± 0.4	49.6 ± 0.8	28.1 25.5	43.1 60.0	African Eurasian
MEDICINA	28.1 ± 0.3	53.4 ± 0.7	24.9	56.8	Eurasian
NOTO	31.7 ± 0.4	43.6 ± 0.8	28.5	44.1	African
ONSALA	22.4 ± 0.3	52.3 ± 0.8	23.1	54.0	Eurasian
WETTZELL	24.4	56.7	24.4	56.7	Eurasian

Table 4: Horizontal rates.

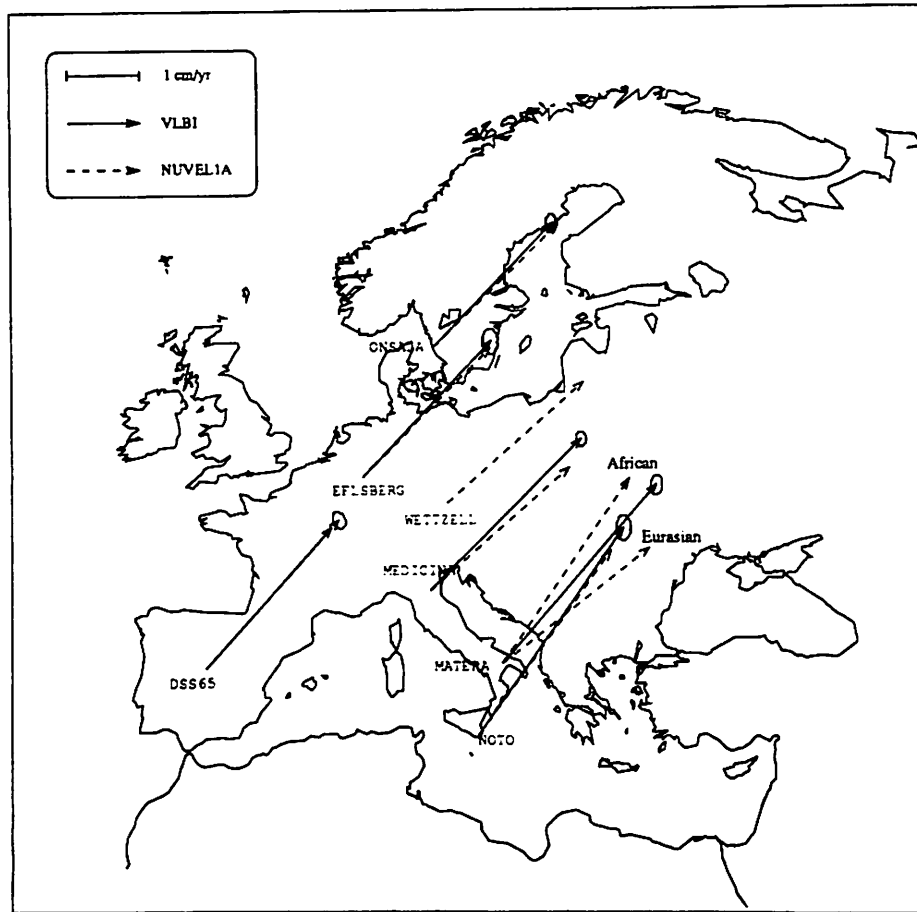


Figure 3: Horizontal motions for the sites participating to the Europe campaign. The ellipses are 3 scaled standard deviations. For the MATERA site, the estimated horizontal vector doesn't agree with the one predicted by the NUVEL1A model assuming the site either on the African plate or on the Eurasian plate.

Baseline	Length rate (mm/yr)	Transverse rate (mm/yr)	Vertical rate (mm/yr)	N. of sessions	Span (years)
DSS65 -EFLSBERG	.6± .5	-3.1± .4	7.3±2.3	4	2.4
				2	1.0
DSS65 -MATERA	-.2± .4	-8.4± .3	14.6±1.6	16	3.6
				10	1.9
DSS65 -MEDICINA	1.5± .4	-4.1± .3	13.5±1.4	16	4.2
	0.8± .5	-3.3± .5	13.6±3.1	16	4.2
DSS65 -NOTO	-2.9± .5	-10.0± .4	5.7±1.8	7	3.2
	-6.1±1.9	-8.1± .9	5.6±10.0	7	2.9
DSS65 -ONSALA	.4± .4	-5.2± .3	9.2±1.5	14	4.2
	-2.1± .9	-6.4± .5	10.6±3.4	15	4.1
DSS65 -WETTZELL	-.6± .4	-2.5± .3	13.2±1.3	14	4.2
	-1.2± .7	-3.3± .5	11.1±2.7	15	4.2
EFLSBERG-MATERA	-4.5± .6	-5.8± .5	6.3±2.3	4	2.4
				2	1.0
EFLSBERG-MEDICINA	-1.3± .5	-3.5± .4	5.6±2.2	4	4.2
				9	1.9
EFLSBERG-NOTO	-7.3± .6	-4.7± .5	-2.8±2.5		
EFLSBERG-ONSALA	-.3± .5	-2.2± .4	2.1±2.2	3	1.4
	-1.5± .2	-3.0± .2	-1.6± .8	7	12.3
EFLSBERG-WETTZELL	.3± .4	.1± .4	5.8±2.1	4	2.4
				2	1.0
MATERA -MEDICINA	-3.6± .3	-2.8± .3	-.9±1.5	16	3.6
				9	1.9
MATERA -NOTO	-2.1± .5	1.8± .4	-9.1±1.9	6	2.6
				5	1.3
MATERA -ONSALA	-5.8± .5	-5.7± .4	-3.5±1.6	13	3.6
				8	1.9
MATERA -WETTZELL	-6.5± .4	-4.2± .3	-.5±1.4	14	3.6
				23	2.0
MEDICINA-NOTO	-6.8± .4	-.9± .4	-8.2±1.7	7	3.2
	-5.6±1.0	-1.3±2.1	-6.1±10.3	6	2.2
MEDICINA-ONSALA	-2.5± .4	-4.8± .3	-3.2±1.4	13	4.2
	-2.4± .5	-5.8± .5	-.5±2.4	20	5.6
MEDICINA-WETTZELL	-3.4± .3	-1.8± .3	.3±1.2	14	4.2
	-2.2± .3	-2.3± .3	0.1±1.9	25	5.6
NOTO -ONSALA	-7.5± .6	-4.4± .4	5.7±1.8	6	3
	-7.8±2.8	-2.9±1.5	1.5±5.7	9	2.9
NOTO -WETTZELL	-9.2± .5	-2.3± .4	8.6±1.7	6	3.2
	-6.7±1.2	-1.1±1.0	1.2±3.8	22	2.6
ONSALA -WETTZELL	.6± .3	-2.4± .3	3.7±1.2	12	4.2
	-.4± .1	-3.0± .2	2.8± .7	158	9.3

Table 5: Baseline rates results and comparison with the GLB908 NASA solution.

3 Future plans

- Continue the analysis of the Europe campaign as new experiments will become available.
- Better understand the behaviour of Medicina, Noto and Matera.
- The parameterization for clocks and atmospheres requires a more detailed analysis in order to establish the duration of the linear sections of the piecewise function and the values for the slope constrains.
- As soon as GPS and SLR results will be available for more European sites, we plan to extend the comparison of the baseline rates.

4 Data analysis of the global network: the CGS95 solution

The purpose of the CGS95 solution is to analyse a world wide VLBI network and to produce:

- Time series of the Earth Orientation Parameters.
- Time series of the Nutation.
- Terrestrial Reference Frame.
- Celestial Reference Frame.
- Velocity field.

As first step we wish to compare the TRF and the time series of the EOP with that obtained by the SLR analysis performed at the CGS. A similar analysis is beginning at the CGS using GPS data and will produce a comparison using all the geodetic techniques.

At the present a total of 412 experiments have been used. Some baseline results are in figures 4 and 5

Campaign	N. of experiments
IRIS-A	181
NAVNET	118
NAVEX	39
IRIS-P	34
IRIS-S	30
Intra-Europe	10
Total	412

Table 6: Experiments used in the CGS95 solution. subdivided by campaign.

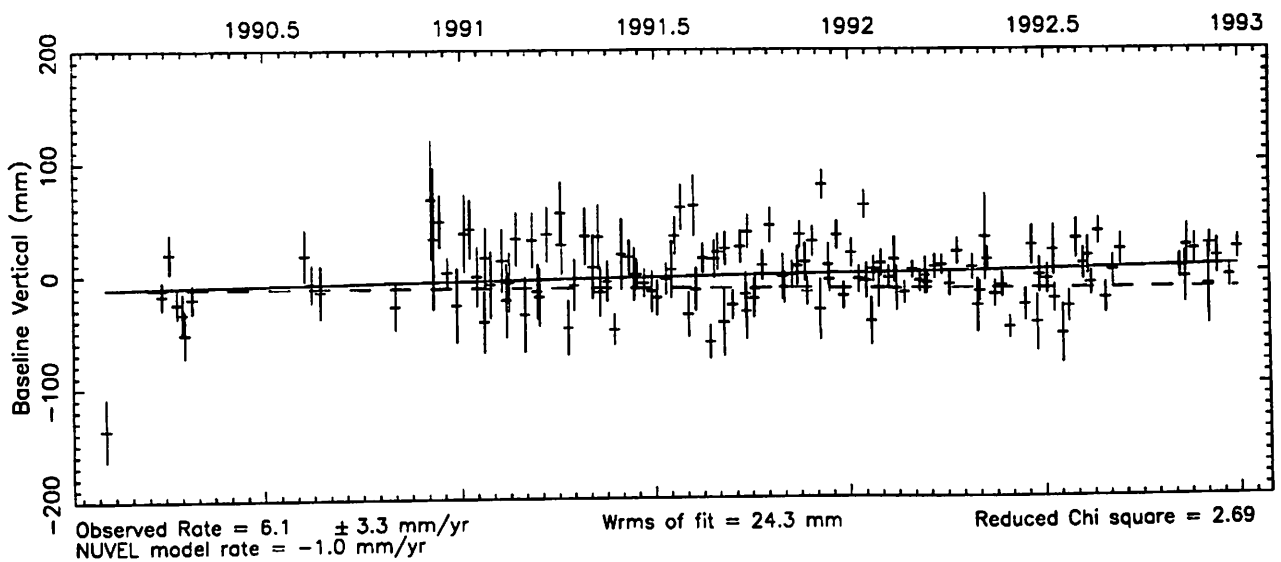
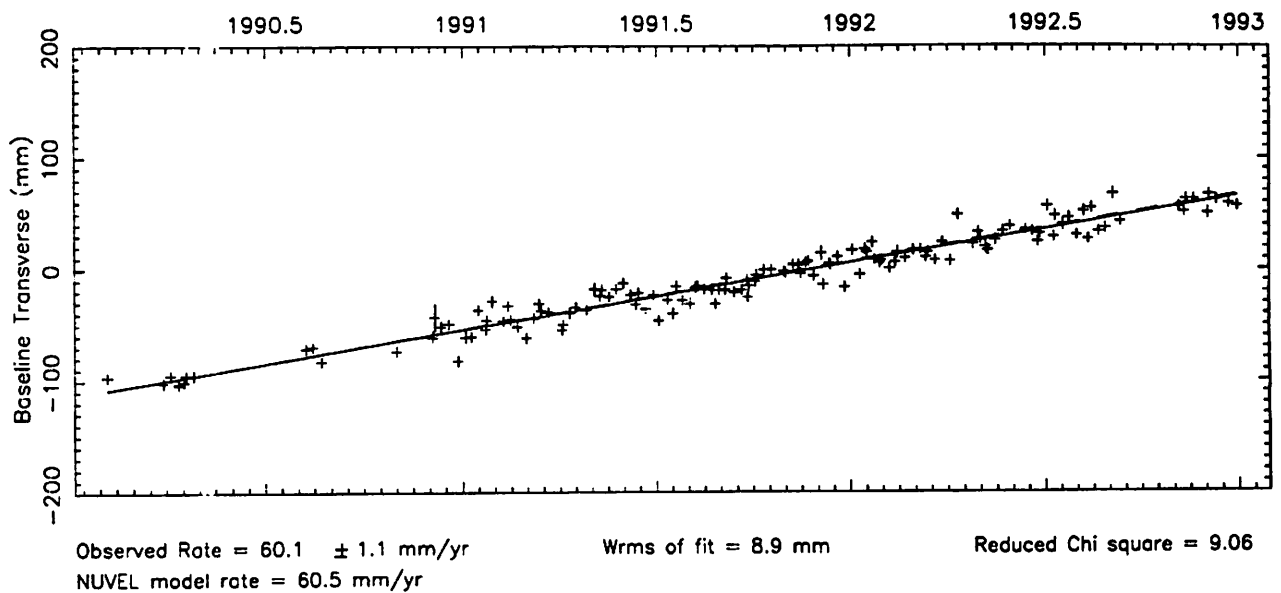
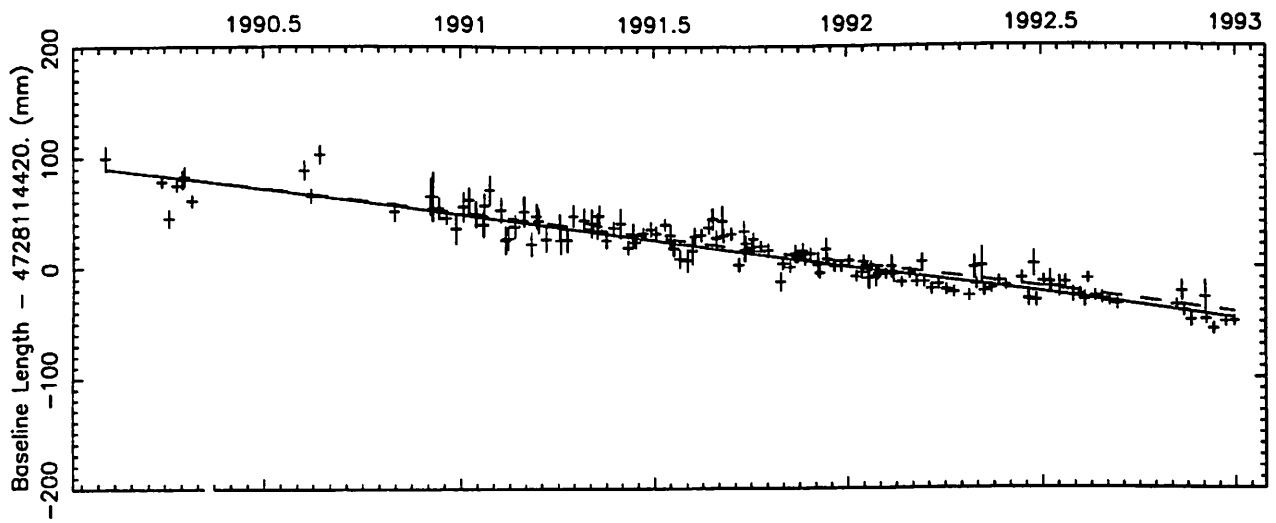
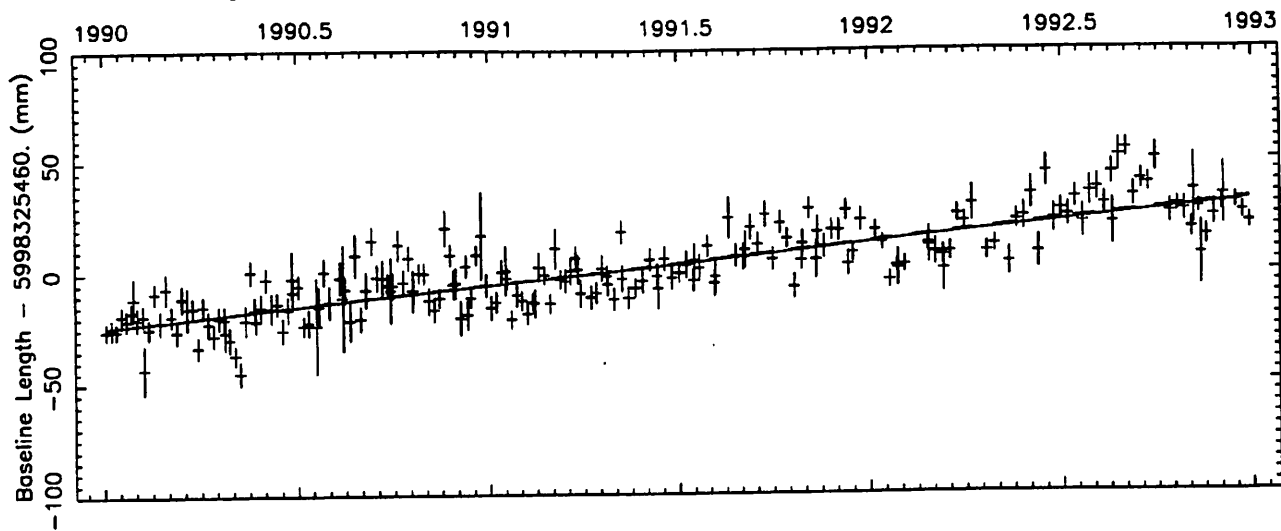


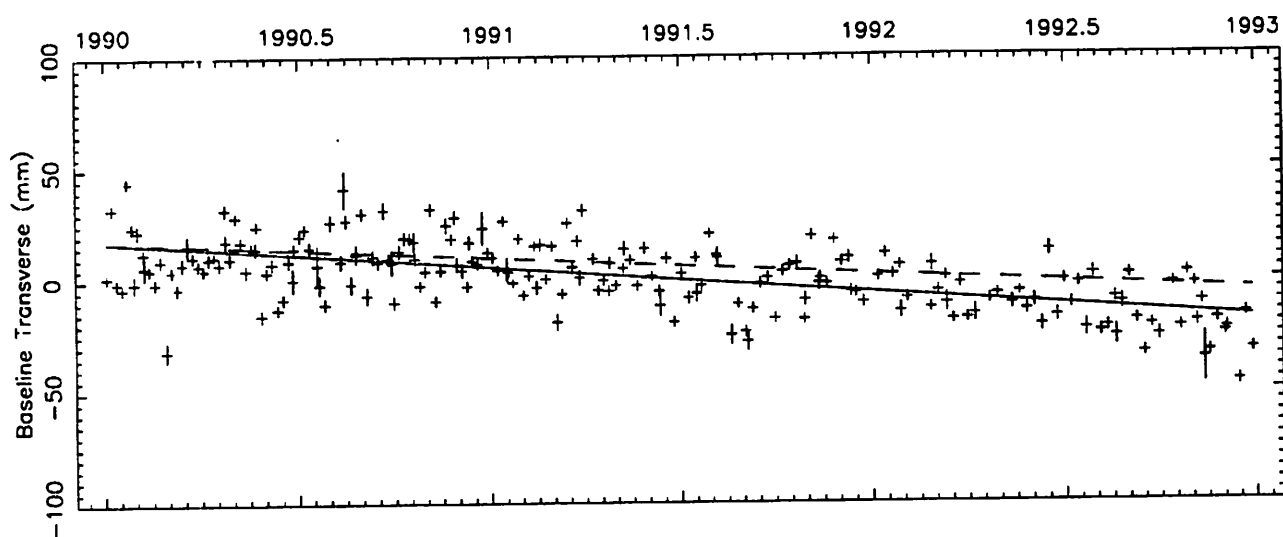
Figure 4: Vector baseline plots for CILCREEK-KAUAI



Wrms of fit = 9.6 mm

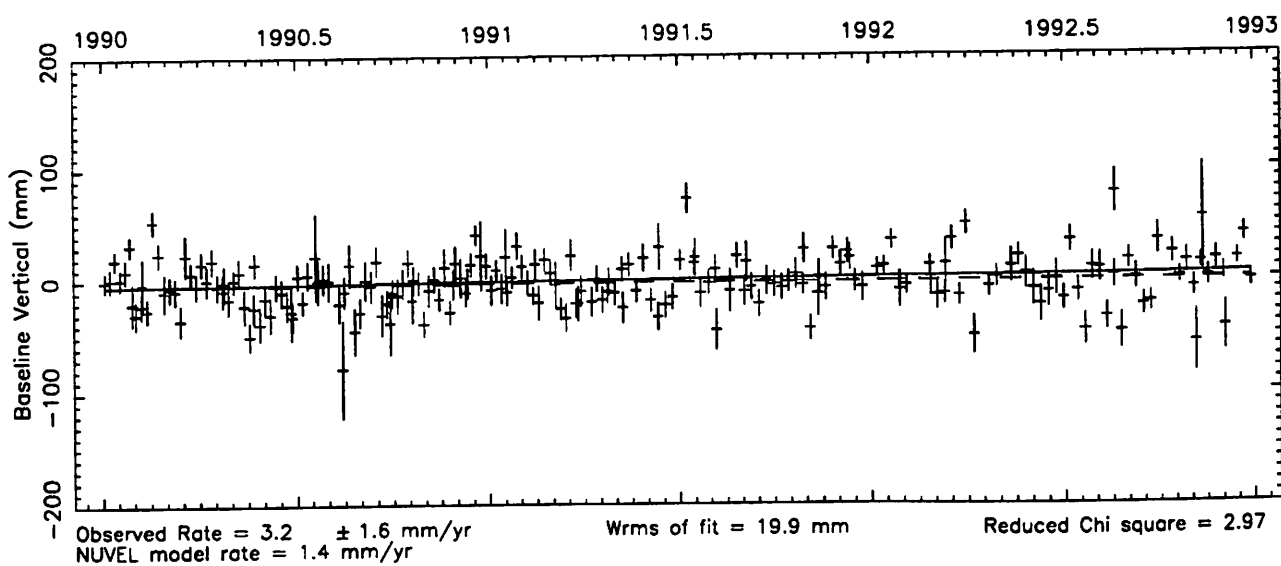
Reduced Chi square = 3.51

Weighted mean length = 5998325462.6 mm



Wrms of fit = 12.0 mm

Reduced Chi square = 26.42



Wrms of fit = 19.9 mm

Reduced Chi square = 2.97

Figure 5: Vector baseline plots for WESTFORD-WETTZELL

References

- Boucher, C.Z. Altamini, and L. Duhem, ITRF92 and its associated velocity field, Central Bureau of IERS, Paris Observatory, October 1993.
- Clark, T.A., B.E. Corey, J.L. Davis, G. Elgered, T.A. Herring, H.F. Hinteregger, C.A. Knight, J.I. Levine, G. Lundqvist, C. Ma, E.F. Nesman, R.B. Phillips, A.E.E. Rogers, B.O. Ronnang, J.W. Ryan, B.R. Schupler, D.B. Shaffer, I.I. Shapiro, N.R. Vandenberg, J.C. Webber, and A.R. Whitney, Precision Geodesy Using the Mark-III Very Long Baseline Interferometry System, *IEEE Transactions on Geoscience and Remote Sensing*, GE-23, 438, 1985.
- DeMets, C., R.G. Gordon, D.F. Argus, and S.Stein, Effect of recent revisions to the geomagnetic reversal time scale on estimates of current plate motions, *Geophys. Res. Lett.*, in press.
- IERS Annual Report 1992, Central Bureau of IERS, Paris Observatory, July 1993.
- Lanotte, R., G. Bianco, M. Fermi, and L. Garramone, VLBI Activities at the Matera Geodesy Center, *Proceedings of the 9th Working Meeting on European VLBI for Geodesy and Astrometry*, edited by J. Campbell and A. Nothnagel, pp. 27-35, Bonn, 1993.
- Ma, C., J.M. Sauber, L.J. Bell, T.A. Clark, D. Gordon, W.E. Himwich, and J.W. Ryan, Measurement of Horizontal motions in Alaska Using Very Long Baseline Interferometry, *J. Geophys. Res.*, 95, 21, 991-22, 011, 1990.
- Ma, C., J.W. Ryan, and D.S. Caprette, NASA Space Geodesy Program - GSFC Data Analysis - 1993. VLBI Geodetic Results 1979-92, *NASA Technical Memorandum 104605*, June 1994.
- McCarty, D.D., IERS Technical Note 3 - IERS Standards (1989), Central Bureau of IERS, Paris Observatory, November 1989.
- Rogers, A.E.E., R.J. Cappallo, H.F. Hinteregger, J.I. Levine, E.F. Nesman, J.C. Webber, A.R. Whitney, T.A. Clark, C. Ma, J.R. Ryan, B.E. Corey, C.C. Counselman, T.A. Herring, I.I. Shapiro, C.A. Knight, D.B. Shaffer, N.R. Vandenberg, R. Lacasse, R. Mauzy, B. Rayhrer, B.R. Schupler, and J.C. Pigg, Very Long Baseline Radio Interferometry: The Mark III system for geodesy, astrometry, and aperture synthesis, *Science*, 219, 51-54, 1983.
- Ryan, J.W., C. Ma and W.E. Himwich, Proceedings of the AGU Chapman Conference on Geodetic VLBI: Monitoring Global Change, *NOOA Technical Reports NOS 137 NGS 49*, 1991.

Investigations of Thermal Height Changes of Geodetic VLBI Radio Telescopes

Axel NOTHNAGEL, Martin PILHATSCH, Rüdiger HAAS

Geodetic Institute of the University of Bonn, Nußallee 17, D-53115 Bonn, Germany

Abstract. Radio telescope construction components are subject to temperature changes due to long and short term weather conditions. Consequently thermal deformations occur which have an impact on the location of the geodetic VLBI reference point and on the delay observable. So far calibration of these effects was hampered by the unknown response of the steel structures on changes of the air temperature.

In order to investigate the behaviour of telescope steel structures observations of the height variations of the VLBI reference point of the Hartebeesthoek (HartRAO) radio telescope were made and thoroughly analysed. An average time constant of 2 hours and 15 minutes was found as a best fit to the height and air temperature data gathered. On this basis a first simple model for a local height calibration at the Hartebeesthoek radio telescopes was developed which may provide the basis for a complete calibration of VLBI observations for thermal expansion effects.

In parallel to these investigations an attempt was made to estimate thermal parameters from VLBI data. Apparently the quality of the data and the complicated structure of the radio telescopes at present inhibit a direct estimate of the expansion coefficients.

1 Introduction

In recent years the internal accuracy of baseline length determinations by geodetic VLBI observations has reached the sub-centimeter level at intercontinental distances (Ryan et al. 1993). However, long time series of frequently observed baselines still display systematic variations with periods close to one year. Uncalibrated variations of station height components are conceivable causes for baseline length variations especially for long baselines. One of the main causes for local height changes is the thermal expansion of the telescope structure which may show both seasonal and daily variations.

McGinnis (1977) computed a 6.1 mm height displacement of the VLBI reference point of the 64 m DSS14 antenna as a result of mean daily ambient temperature changes of 22.5°C . His calculations were based upon temperature measurements and a theoretical thermal expansion coefficient of $1.06 \cdot 10^{-5} [1/^{\circ}\text{C}]$. McGinnis assumed that two hours are needed for 75% of the ambient temperature to transfer into height changes. Although the DSS14 antenna is much larger than most radio telescopes used in geodetic VLBI applications the computations show the extent of error which may be accumulated if calibrations are omitted.

Jacobs (1991) assumed a negligible time lag (Δt) between change of temperature and

height change together with a thermal expansion coefficient (γ) of $1.2 \cdot 10^{-5} [1/^{\circ}\text{C}]$ using a simple equation for the height change (Δh) found in Sovers (1991):

$$\Delta h = h \cdot \gamma \cdot (T - T_{Ref}) \quad (1)$$

with T_{Ref} being the reference temperature, T the metal temperature and h the effective length of the beams. Considering the importance of thermal height change calibrations the sometimes contradictory assumptions of earlier publications initiated further investigations into the response time of radio telescopes to ambient temperature changes. In this presentation the time lag is determined from geodetic height measurements and ambient temperature monitoring. Subsequently the height component of the expansion of steel structures is modelled as a function of ambient temperature and time lag.

2 Ground Survey

In order to determine the response time of a typical steel structure on temperature changes a series of terrestrial antenna height measurements at the Hartebeesthoek Radio Astronomy Observatory (HartRAO) in South Africa was performed. For a few days we observed the elevation angles of a concentric survey mark mounted at the telescope structure very close to the VLBI reference point (Figure 1).

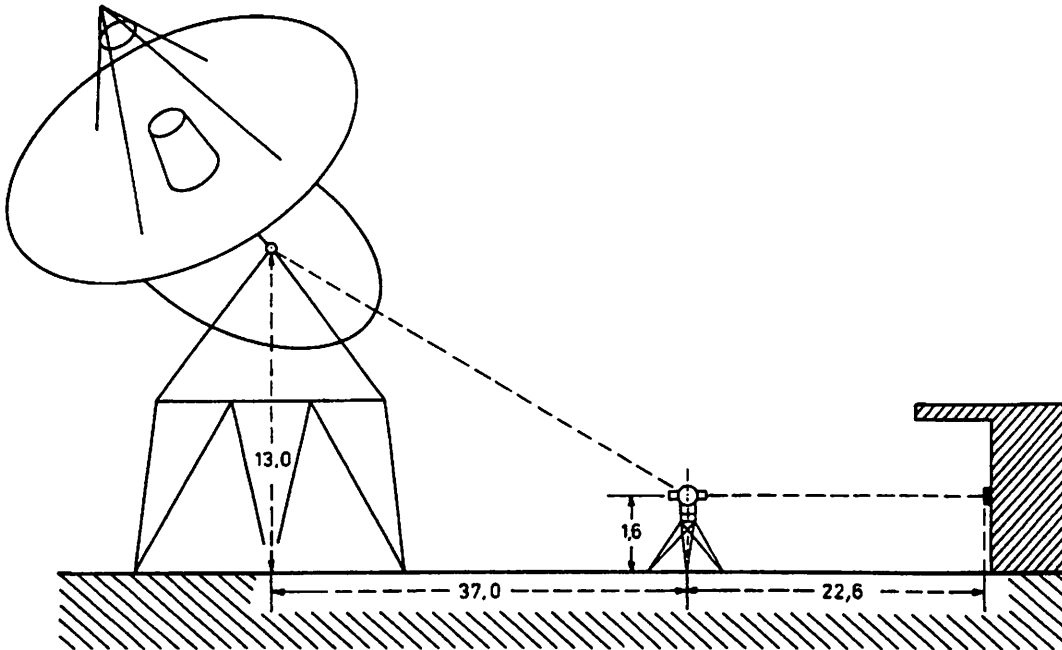


Fig. 1 Measurement Setup

In general, the VLBI reference point is the intersection of the telescope rotation axes (azimuth and elevation or hour angle and declination). In the case of an offset antenna

where both axes do not intersect it is the point where the secondary axis (elevation or declination) is projected onto the primary axis (e.g. Ma 1978). A second mark was fixed at level height of the theodolite at the wall of the control building which was supposed to be stable within fractions of millimeters during the observing period. Since the height of this survey mark was only about two meters off the ground thermal expansion of the building was considered negligible. This mark therefore served as the height reference which controlled the height of the tripod.

Each set of measurements consisted of one reading of the zenith distance towards each of both survey marks in both faces together with a temperature reading. During the first two days the readings of the zenith distances of both survey marks were taken in short intervals while in the last 5 days they were taken rather irregularly.

In the analysis of the zenith distances special emphasis was put on possible refraction effects which may have been arising from vertical temperature gradients. Brocks (1948) has determined refraction index profiles for a period of 24 hours between 0 and 14 m height. Figure 2 shows an average of several analyses of clear days in June. Since the time of year of the measurements agrees fairly well with these conditions and the environment of the Hartebeesthoek site is not suspect for anomalies, this profile should represent the actual refraction at any temperature sufficiently.

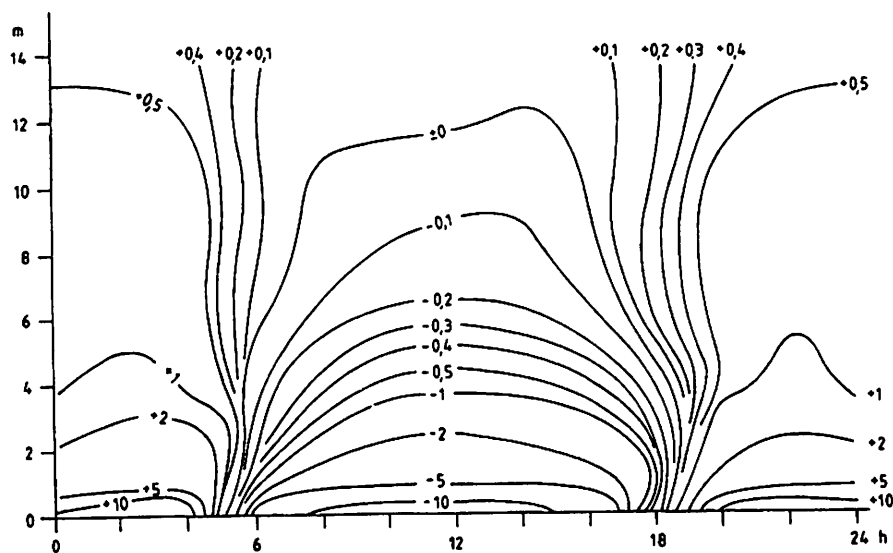


Fig. 2, Average refraction coefficients on clear days in June (northern hemisphere) from Brocks (1948)

Of special importance is the integrated refraction for the ray path between 1.6 and 13 m height. Integration of the profile at different hours of the day and a subsequent conversion into height changes produced 0.11 mm peak-to-peak variations for the height determination of the antenna target and, due to the stronger refraction near the ground, 0.12 mm for the

reference height. In the absence of true gradients both variations are considered to be small enough to be neglected in the computations of the telescope height variations. Without any further consideration of the refraction, the height (h) of the VLBI reference point at each epoch was then calculated from

$$h = h_w - s_w \cdot \cot(\beta_1) + s_t \cdot \cot(\beta_2) \quad (2)$$

(h_w = height of reference mark, s_i = distances, β_i zenith distances)

Considering all error sources the theoretical formal error of a single height determination is ± 0.8 mm. Figure 3 depicts the results of the height determinations of the two markers together with the respective air temperatures. In general the measurements appear fairly stable. Most of the individual data points are confirmed by neighbouring measurements with acceptable scatter where the measurements are taken frequently. The scatter in fact supports the validity of the formal error as a good representation of the individual height errors.

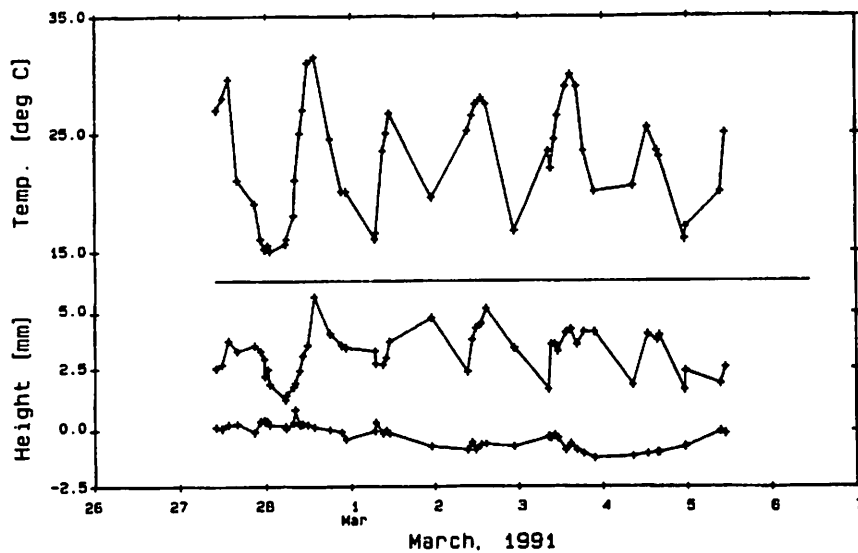


Fig. 3, plot of temperature and height variations, top line = temperatures in [$^{\circ}\text{C}$], middle line = telescope reference point height variations in [mm], bottom line = height variations of tripod in [mm]

The line at the bottom represents the height changes of the theodolite which is deduced from a constant height of the control building wall. It is obvious that the tripod has lowered by about one millimeter at the third day. The settling of the tripod is, of course, included in the height results of the telescope survey mark by referring all results to the stable reference marker.

At first glance it appears already that the height variations follow the temperature variations. Different correlation methods were tested to numerically determine a correlation between the two series (Pilhatsch 1994). Due to the sparse distribution of the data at the

later days of the series it was necessary to find a model representation of the data which provided a better signal-to-noise-ratio for the determination of the time lag than the individual data points. Pelzer (1987) concluded that ambient temperature induced deformations often behave periodically with a period of one day. Both series were therefore fitted with the following periodic model:

$$x(t) = A \cdot \sin\left(2\pi \frac{t}{t_p} + \varphi\right) + \text{offset} \quad (3)$$

where A is the amplitude, t the epoch, t_p the period and φ the phase angle.

An initial least squares adjustment yielded periods of 24h 08min. Since one would expect ideal periods of 24 hours due to the cycle of the sun, the hypothesis was tested whether the period would exactly match 24 hours. With a 95% confidence interval this hypothesis was accepted and the periods were fixed at 24 hours in the subsequent adjustments. After the elimination of a few outliers the following parameters were estimated:

Temperature	Amplitude	7.3	±	0.34	°C
	Phase	0.32	±	0.04	rad
	Offset	21.3	±	0.21	°C
Height variation	Amplitude	1.31	±	0.36	mm
	Phase	-0.27	±	0.19	rad
	Offset	0.54	±	0.22	mm

with a Chi Squared of 1.42 .

As one would expect from the data the determination of the deformation parameters is somewhat poorer than that of the temperature, the reason being the higher uncertainty in the height determination. The adjustment easily permits to compute a phase difference between the two series of 2h 15min ± 45 min. The main contribution to the high error of this time lag can be attributed to the phase error of the height variation. In order to check the time lag the data sets were reduced to the first 37 hours of the measurement series where the data points were taken in short intervals. The following parameters were estimated:

Temperature	Amplitude	7.5	±	0.58	°C
	Phase	0.41	±	0.07	rad
	Offset	21.5	±	0.37	°C
Height variation	Amplitude	1.49	±	0.66	mm
	Phase	-0.32	±	0.30	rad
	Offset	0.38	±	0.37	mm

with a Chi Squared of 2.93 and a time lag of 2h 47min ± 72 min.

Although one would expect a better fit of the model to the shorter data set, the formal errors of the parameters are higher. This is a strong indication that the adjustment stabilises with longer observing and the model indeed represents the physical behaviour of the expansion. Figure 4 displays the data together with the model providing an impression of the fit. The phases of both, the temperature and the height variations, seem to represent the data satisfactorily for the purpose of determination of the timelag.

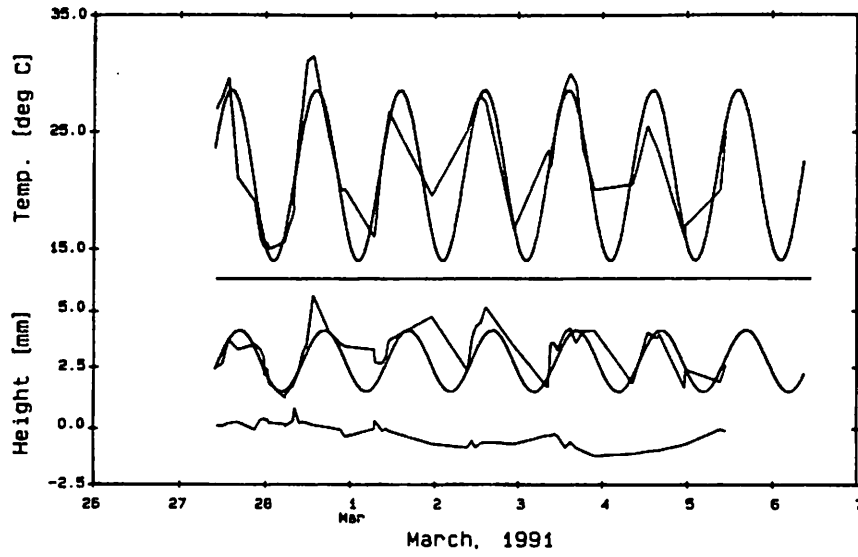


Fig. 4, plot of temperature and height variations with periodic model

As a final check a direct cross correlation was performed with the temperature and height variation series using a cubic spline interpolation. This method yielded a maximum correlation coefficient of 0.5 at exactly 2 hours time lag. Due to the spacing of the data at 30 minutes intervals a maximum resolution of 15 minutes was considered reasonable. Both control computations confirm the time lag of 2h 15min within its uncertainty which agrees very well with the theoretical figure of 2 hours of McGinnis (1977). Using a reference temperature of 20° C as is common practice in engineering and composing formula (3) for both temperature and height change into one yields the following expression as a model for temperature induced height changes of the VLBI reference point at HartRAO:

$$\Delta h = 0.18 \cdot (T(t - \Delta t) - T_{Ref}) \quad (4)$$

with Δh in [mm] and T in [°C] at 135 minutes before current epoch. For a 10° C temperature change this formula produces a height change of 1.8 mm. Using formular (1) and an effective height of the VLBI reference point of 12.73 m yields a height change of 1.5 mm. A possible reason for the difference of 20% is that the actual expansion coefficient of the steel used at HartRAO is not exactly known. Considering that stainless steel has a coefficient of $1.6 \cdot 10^{-5} [1/°C]$ a 20% higher value than $1.2 \cdot 10^{-5} [1/°C]$ is not impossible. Therefore, these results are a good indication of the validity of formula (4).

3 Models for Selected VLBI Telescopes

In the following paragraph simple models are developed for alt-azimuth and equatorially mounted radio telescopes for the calibration of VLBI delay observables (formula 5). The di-

mensions are taken from drawings and other information provided by the agencies operating the telescopes.

In general, the models consist of several parts representing the different components of the telescope structure and their effect on the geodetic VLBI delay observable. The main figures of models for alt-azimuth antennas are the height of the elevation axis above the ground h_p which scales with the elevation of the observation. Of lesser importance is the distance between the elevation axis and the vertex of the parabola h_v .

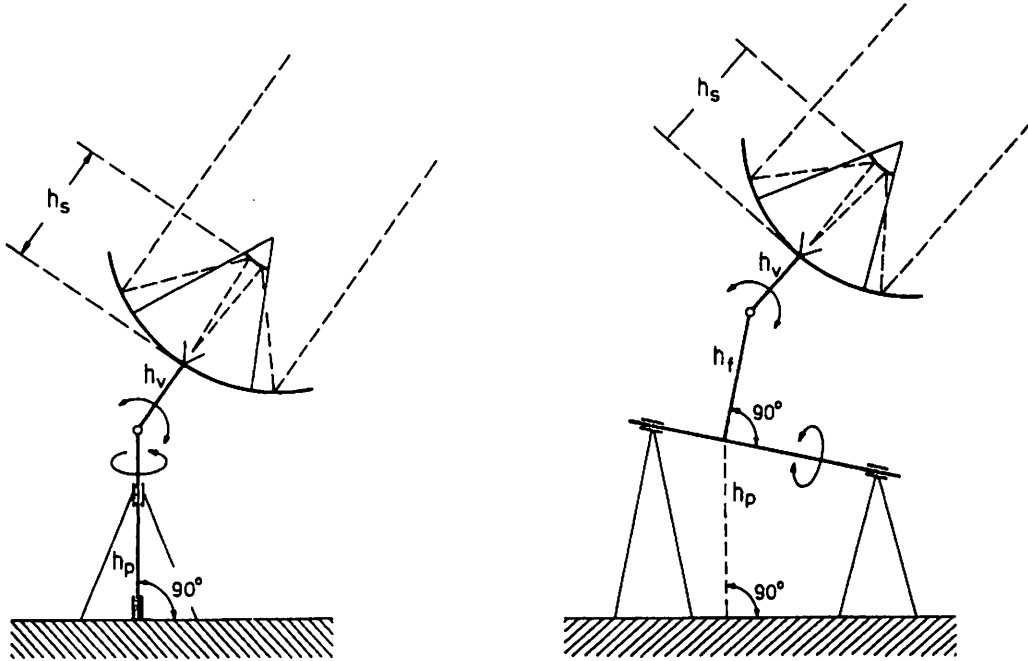


Fig. 5. Schematic drawings of alt-azimuth and polar antenna mounts

In addition to the purely structural changes there are RF pathlength changes along the path from the main reflector via the subreflector to the phase center of the feed horn h_s . Otoshi and Young (1982) determined that a subreflector height variation changes the pathlength linearly by a factor of 1.8. The height changes of the quadrupods are calculated applying the steel expansion coefficient to the effective height of the subreflector h_s above the intersection of the quadrupod and the main reflector assuming that any steel expansion within the quadrupod is symmetric and effectively only results in height variations. Changes in the shape of the paraboloid due to thermal deformation are considered small compared to gravitational deformation and are neglected in these models.

It is assumed that the time lag of the expansion measured at the Hartebeesthoek telescope is representative for all other steel structures as well. The expansion of the steel structures is, therefore, modelled as a function of the ambient temperature at 2h 15min (Δt) before the

time of observation and the steel expansion coefficient (γ) of $1.2 \cdot 10^{-5} [1/^\circ\text{C}]$. For equatorial telescopes formula 5 has to be extended for the metal component between Hour Angle and Declination shaft h_f which scales with the cosine of the declination (dec).

$$\Delta\tau = \frac{1}{c} \gamma (T(t - \Delta t) - T_0) \cdot (h_p \sin(el) + h_v + 1.8 \cdot h_s [+ h_f \cos(dec)]) \quad (5)$$

c is the velocity of light, T the ambient temperature, T_0 the reference temperature of 20°C , and el being the effective elevation angle of the observation. The structure variations above the elevation or declination axis will predominantly be compensated in the clock parameters of the least squares adjustments due to their clock-like effects. All other variations, however, do not easily coincide with standard parameters and should, therefore, increase the scatter of the residuals.

As an example of a standard alt-azimuth antenna we can describe the properties of the 100m telescope of the Max-Planck-Institute for Radio Astronomy at Effelsberg. The instrument has a Gregorian focus and pillars of exactly 50.00 m height (h_p) bearing the elevation axis. The distance between elevation axis and the vertex of the parabola (h_v) is 8.50 m while the effective subreflector height (h_s) is 28.00 m. Assuming a day to night temperature variation of only 10°C which is quite common in this area, the total delay correction of an observation in zenith direction amounts to 40 psec on a daily timescale. Annual temperature differences between summer and winter of 20 to 25°C cause systematic height variations of 12 - 15 mm which generally do not show up in the delay residuals.

Table 1 contains the dimensions of a few selected radio telescopes from which delay corrections can be computed. A number of telescopes are mounted on concrete pedestals which are above the ground and are thus exposed to temperature changes as well. Since concrete has an expansion coefficient similar to steel ($1.0 \cdot 10^{-5} [1/^\circ\text{C}]$) possible seasonal variations cannot be neglected. The problem with concrete, however, is the transfer of heat into extended foundations, a phenomenon which will be the topic of further studies. For completeness the first column contains the heights of the concrete foundations in addition to the proportions of the steel structures.

All dimensions in [m]	Concrete Base	h_p	h_v	h_s	h_f
Effelsberg	0.0	50.0	8.5	28.0	-
Hartebeesthoek (HartRAO)	0.0	12.7	2.3	9.4	6.7
Madrid (DSS45)	3.0	16.8	2.7	10.8	-
Matera	3.0	10.5	3.8	5.7	-
Medicina	2.3	15.5	4.3	4.3	-
Noto	2.2	15.7	4.2	5.0	-
O'Higgins	1.0	6.2			-
Onsala	12.0	3.0	3.4	5.5	-
Westford	16.9	2.0	3.0	3.6/4.9	-
Wettzell	8.0	4.0	3.7	7.9	-

Table 1. Dimensions of telescopes

4 Deformation estimates from VLBI data

In parallel to the investigations to calibrate the effect of thermal deformation of VLBI telescopes, we tried to detect these effects through estimating thermal expansion coefficients of VLBI telescopes from VLBI data.

Basis for these investigations is equation (1) describing the height change (Δh) of the VLBI reference point as a function of metal temperature. In absence of metal temperatures the air temperatures T monitored at the stations and a time lag Δt for the heat transfer to the telescope structure were used. The modified equation is :

$$\Delta h = \gamma \cdot (T(t - \Delta t) - T_{Ref}) \cdot h \quad (6)$$

The effect on the VLBI observable τ from variations in the topocentric height components at stations 1 and 2 forming a baseline is :

$$\Delta \tau = \frac{1}{c} \cdot [\Delta h_1 \cdot \sin(\epsilon l_1) - \Delta h_2 \cdot \sin(\epsilon l_2)] \quad (7)$$

Δh_i in [m] is the height change at station i , ϵl_i in [rad] is the Elevation of the radio source observed at station i and c in [m/s] is the velocity of light.

The partial derivatives of the VLBI observable with respect to the unknown thermal expansion coefficient γ_i for the least-squares-estimation were formed according to the model above. For example the partial derivative of the VLBI observable with respect to the thermal expansion coefficient γ_1 at station 1 is :

$$\frac{\partial \Delta \tau}{\partial \gamma_1} = \frac{1}{c} \cdot \sin(\epsilon l_1) \cdot \frac{\partial \Delta h_1}{\partial \gamma_1}$$

$$= \frac{1}{c} \cdot \sin(\epsilon l_1) \cdot (T_1(t - \Delta t) - T_{Ref}) \cdot h_1 \quad (8)$$

A time lag Δt of for example 2 hours means that the partial derivative of the observation τ with respect to the unknown expansion coefficient γ_i is computed using the air temperature of 2 hours prior to the observation. VLBI databases, however, only include air temperatures measured at the epochs of the observations and generally there are no measured air temperatures in the databases prior to the start of the experiment. Therefore, some back-extrapolating scheme must be used for the first observations.

This problem was solved assuming similar temperature profiles for 24 hour VLBI experiments for days following each other. If it is not possible to take a measured temperature value the partial derivative is computed with the temperature value of exactly 24 hours later corrected for a daily offset. This back-extrapolating scheme was tested with the continuous CONT94 VLBI data. Continuous VLBI experiments were treated as single 24 hour experiments. The back-extrapolated temperature values of these experiments were compared to the real measured temperatures of the VLBI databases of the days before. The comparisons (see figure 6) show a good agreement in the range of 1 to 2 degree Celsius for 6 hours of back-extrapolation. The arrows in the graph indicate the back-extrapolation epochs.

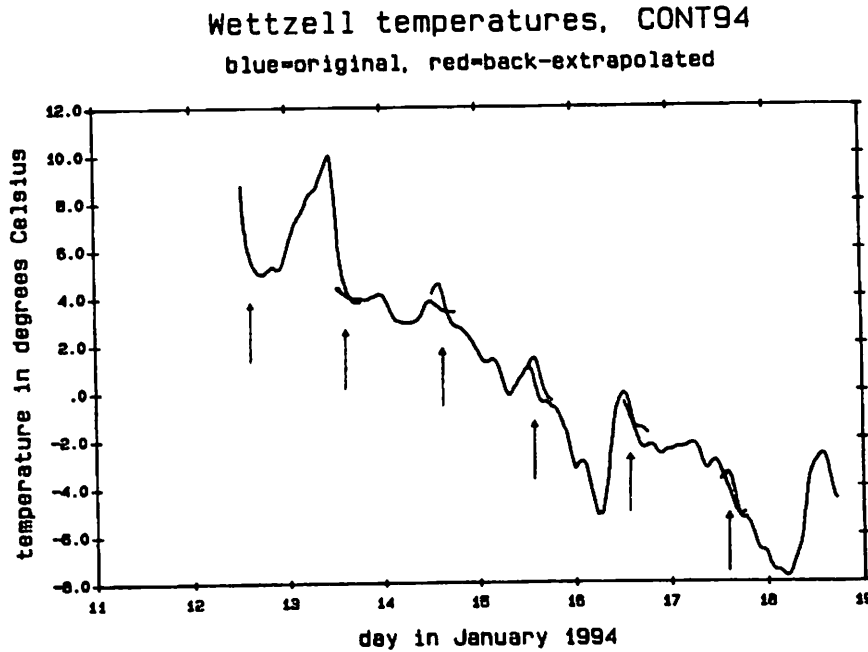


Fig. 6, example for the back-extrapolation scheme

Using the partial derivatives (7) in the CALC/SOLVE VLBI analysis software package thermal expansion coefficients for the stations Wettzell and HartRAO were estimated. Data from 50 experiments in the IRIS-S network with about 31000 observations were used in batch solutions. The time lag Δt was varied from 0.0 hours to 9 hours. Figure 7 and 8 show the estimates for Wettzell and HartRAO. Along the x-axis the time lag Δt used for the batch solutions is shown while along the y-axis the estimated expansion coefficient is shown for the

estimation with that specific time lag Δt .

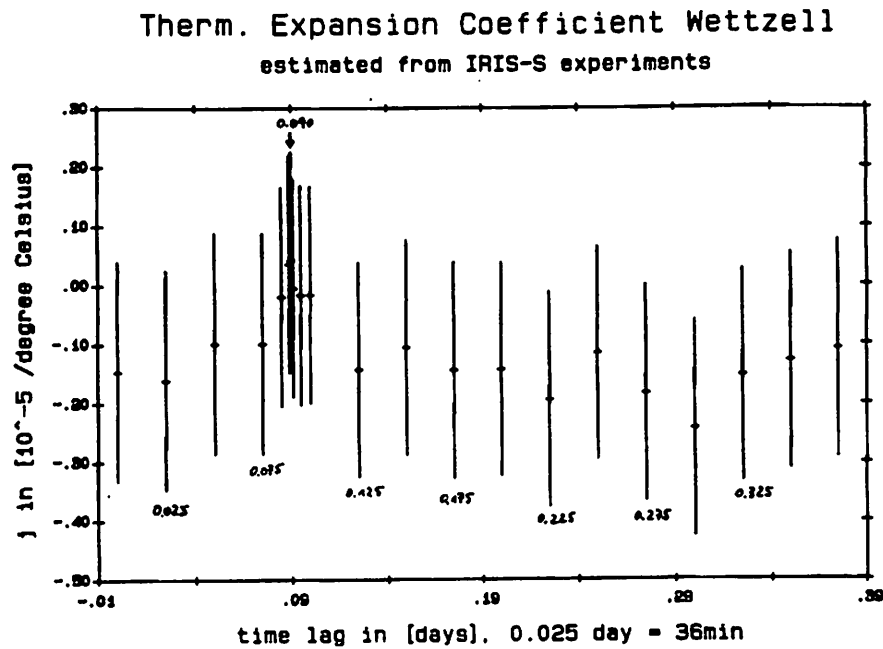


Fig. 7, estimates of thermal expansion coefficients for Wettzell

The results for Wettzell show a peak for Δt of 0.09 day (2h 9min 36sec). This agrees with the investigations in chapter 2. However, the estimated value for Wettzell ($+0.43 \cdot 10^{-06}$ [1/°C]) is 25 times smaller than the expansion coefficient of steel. In this investigation the antenna support structure has been assumed to be of one material only. It has to be investigated, if a more sophisticated approach taking into account the different materials of the telescope support structure (e.g. pedestal of concrete, other parts steel) and its isolation leads to more realistic values. However, independent measurements with invar wires measuring the height variation of the reference point of the Wettzell telescope showed only all small variation of 0.5 mm on a daily timescale (R. Kilger, pers. communication).

The results for HartRAO do not show a real peak for any time lag Δt , but the values estimated (about $+0.9 \cdot 10^{-05}$ [1/°C]) are in the range of the expansion coefficient of steel.

It seems that the quality of the data and the complicated structure of the radio telescopes in the IRIS-S network at present inhibits a direct estimate of the expansion coefficient.

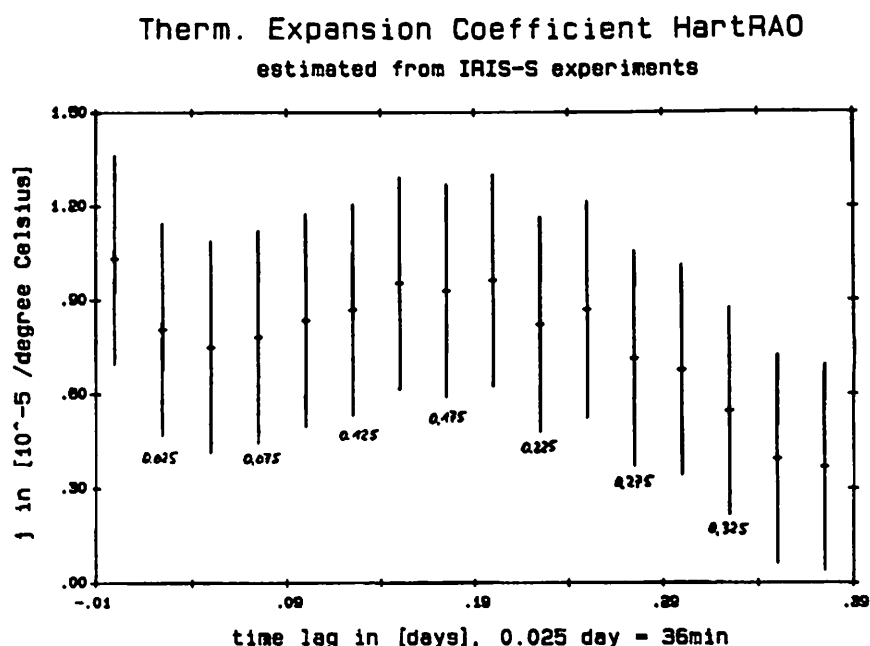


Fig. 8. estimates of thermal expansion coefficients for HartRAO

5 Conclusion and Outlook

The work presented here is the first step towards a complete calibration of geodetic VLBI observations for telescope thermal expansion effects. It shows that their contributions are not negligible and calibrations are necessary to achieve the 1 mm accuracy goal. Test computations are in progress applying the model reported here to VLBI data.

The contribution of solid concrete pedestals has still to be tackled. First investigations revealed that a long term model will probably be sufficient. Horizontal variations are another conceivable error source but pointing error analyses and tilt meter measurements at Hartebeesthoek indicate that the telescope expands symmetrically. For this reason it seems to be plausible that horizontal motions of the telescope structures are rather minor. In the absence of adequate models of differential heat transfer in various structure components horizontal movements of the VLBI reference points can therefore be neglected at the current accuracy level. Further geodetic monitoring of the horizontal behaviour similar to the vertical survey reported in this paper is necessary to provide a detailed insight.

6 Acknowledgements

We should like to thank all the individuals who provided informations on the construction of their telescopes. Arthur Niell provided earlier measurements done at Westford and with Richard Kilger we had numerous fruitful discussions on the behaviour of concrete and of the Wettzell telescope in particular.

7 References

- Brocks, K. (1948)** , Die terrestrische Refraktion. ein Grenzgebiet der Meteorologie und Geodäsie; Annalen der Meteorologie, Vol. 9/11. p. 329-336, Hamburg
- Jacobs, C. (1991)** , Modeling Antenna Effects for mm Level VLBI; Carter, W.E. (Convenor): Proceedings of the AGU Chapman Conference on Geodetic VLBI: Monitoring Global Change held at Washington. D.C. Apr. 22-26. 1991. NOAA Technical Report NOS 137 NGS 49, US Dept. of Commerce. NOAA/NOS, Rockville, MD
- Ma, C. (1978)** , Very Long Baseline Interferometry Applied to Polar Motion, Relativity and Geodesy: Ph.D. Thesis: NASA Technical Memorandum 79582; Greenbelt , USA
- McGinnis (1977)** , Estimated Displacements for the VLBI Reference Point of the DSS 14 Antenna: DSN Progress Report 42-41. pp. 218 - 225
- Otoshi, T.Y., Young, L.E.** . An Experimental Investigation of the Changes of VLBI Time Delays Due to Antenna Structural Deformations: TDA Progress Report 42-68, pp. 8 - 16. 1982
- Pelzer, H. (1987)** . Ingenieurvermessung. Ergebnisse des Arbeitskreises 6 des DVW, Verlag Konrad Wittwer. Stuttgart
- Pilhatsch, M. (1994)** . Auswertung von Deformationsmessungen an einem Radioteleskop : Unpublished Diploma Thesis. Geodetic Institute of the University of Bonn, FRG
- Sovers, O.J. (1991)** . Observation Model and Parameter Partial for the JPL VLBI Parameter estimation Software "MODEST". JPL Publication 83-39 Rev. 4, Pasadena

Tropospheric delays estimated from VLBI, WVR and GPS. A comparative study

Antonio Rius^{1,2}, Gunnar Elgered³, Jan M. Johansson³,
Stephen Keihm⁴ and Néstor Zarraoa⁵

¹ Centre d'Estudis Avançats de Blanes, CSIC, Spain

² LAEFF, INTA, Spain

³ Onsala Space Observatory, Chalmers University of Technology, Sweden

⁴ Jet Propulsion Laboratory, California Institute of Technology, USA

⁵ DLR Remote Sensing Ground Station, Neustrelitz, Germany

Abstract

The water vapor contained in the troposphere produces delays in Very Long Baseline Interferometry (VLBI) and Global Positioning System (GPS) observables which limit the accuracy of extracting geodetic signals in the analysis of VLBI and GPS data. It also produces increases in the sky brightness temperature which are measurable with water vapor radiometers. Presently, among the facilities participating in the European geodetic VLBI project, there is VLBI, WVR and GPS instrumentation at the Onsala Space Observatory and at the NASA Madrid Deep Space Communications Complex. In this paper we compare and discuss the zenith delays due the water vapor obtained with these three techniques from the analysis of the data gathered during the 1994 EUROPE geodetic VLBI experiments.

1 Introduction

We have used three techniques which provide estimates of the tropospheric delays: Very Long Baseline Interferometry (VLBI), Global Positioning System (GPS), and Water Vapor Radiometry (WVR). The purpose of this paper is to study the data gathered simultaneously at the European VLBI sites during the experiments EUROPE which took place during 1994. Comparing the results obtained at different places with different weather regimes using complementary techniques could be of utility for improving the analysis of VLBI observables.

2 Available data

GPS and WVR data are taken continuously and archived as part of different projects at some of the sites participating in the EUROPE project. Because of the exploratory nature of this work, we have concentrated our analysis on data obtained at places in which the three techniques were available: Onsala and Madrid. For this study, we have restricted ourselves to the analysis of the data gathered during the 1994 EUROPE 2.3 and 4 geodetic VLBI

experiments. The rest of the experiments have not been analyzed due to severe weather conditions which degraded the quality of the WVR data or to instrumental problems. In summary, we have used the available data sets as indicated in Table 1,

TABLE 1 Instrumental availability								
Experiment	Madrid			Onsala			Starting epoch	
	GPS	VLBI	WVR	GPS	VLBI	WVR		
EUROPE 2	yes	yes	yes	yes	yes	yes	27 April 1994	20:00
EUROPE 3	yes	yes	yes	yes	yes	yes	29 June 1994	14:00
EUROPE 4	yes	yes	yes	yes	yes	no	30 August 1994	20:00

where for each experiment we indicate the availability of the GPS , VLBI and WVR data for Madrid and Onsala as well as the epoch in which the experiments started. Each VLBI experiment spanned 24 hours, which is the data window used for the comparison. The GPS set consisted of data gathered during two consecutive days overlapping the period of the experiment.

The WVRs measure the sky brightness temperature at two separate frequencies (20.7 GHz and 31.4 GHz for the Madrid WVR and 21.0 GHz and 31.4 GHz for the Onsala WVR) to retrieve the delay produced by the integrated water vapor content along the observing direction of the radiometer. The expected accuracies of the WVR zenith delay estimates are of the order of 0.5 cm. For the Madrid WVR data, only the 20.7 GHz channel was used due to spurious interference effects at the 31.4 GHz channel. The 20.7 GHz channel alone can be used for path delay measurements when clouds are absent. Consequently, we have used Madrid data only when the meteorological conditions were adequate.

3 Data analysis

In this section we describe the generalities of the different processing strategies. The details of the processing procedures are outside the scope of this paper. They can be found in the given references.

For the VLBI data, the analysis has been made using OCCAM [1] with the standard OCCAM strategy. The GPS data has been analyzed using GIPSY II, a software package developed at JPL [2] with a strategy implemented at Onsala Space Observatory for the analysis of the data acquired in the Swedish GPS Network (SWEPOS).

The VLBI and GPS analysis provide measurements of the total tropospheric delay, which is comprised of two components: wet and hydrostatic. The hydrostatic component is larger than the wet, but is predictable with better accuracy using appropriate models and surface meteorological measurements. We have used meteorological data obtained at these two sites to compute the corresponding hydrostatic delays, which are subtracted from the VLBI and GPS total delay measurements to obtain the VLBI and GPS vapor-induced delay components.

The conversion of WVR brightness temperature measurements to path delay was accomplished using standard statistical correlation techniques [3], [4]. Using site-specific radio-sonde data, computed brightness temperature and path delays are correlated to produce linear algorithms relating the delay to the observables. The estimated WVR retrieval accuracy (0.5 cm) includes the effects of WVR calibration and vapor absorption model uncertainties.

TABLE 2 Summary of the analytical approach		
Technique	Tools	Models
VLBI	OCCAM	Saastamonien for the dry component applied to the observables Random walk process for the wet component forward Kalman initial value equals 0 cm Power Spectral Density equals 0.1 ps ² /s Davies mapping function
GPS	GIPSY II	Saastamonien for the dry component applied to the estimates Random walk process for the wet component forward+backward Kalman Power Spectral Density equals 2 ps ² /s Lanyi mapping function Precise orbits Antenna phase center variations not included Batches of 24 hours starting at 00:00 UT
WVR(Onsala)	OSO Soft.	Retrieval algorithms based on radiosonde data gathered at Goteborg-Landvetter Airport
WVR(Madrid)	JPL Soft.	Retrieval algorithms based on radiosonde data gathered at the Madrid Airport

In the Table 2 we summarize aspects of the analytical tools used in the reduction of the data acquired, which are candidates for explanations of the variations of results across the techniques. In general, the approach taken in this phase of the work is to use in all the cases the standard processing strategy. Therefore the results obtained should be considered as a first step. In general, VLBI and GPS share parts of the physical and mathematical models for the tropospheric segment of the delays, with the exception of the mapping function. Nevertheless, it should be noted that GPS is able to sample the troposphere in different directions simultaneously while VLBI is able to sample the troposphere at lower elevations. Other aspects which should be taken into account are the effects of the inaccuracies in the determination of the GPS orbits and the effects induced by multipath and the differential delays in the GPS antennas as a function of the propagation path.

4 Discussion

In figures 1 and 2 we have plotted the VLBI, GPS and WVR wet delays as a function of time for the experiments EUROPE-2 and -3. The results for EUROPE-4, being similar, have not been included in this report. We expect that the WVR radiometer estimates are the most accurate, not only because of the quoted expected accuracy (0.5 cm) but also because the VLBI and GPS estimates are produced through a Kalman filter approach in which the geocentric radial position of the satellites and antennas are strongly correlated with the zenith tropospheric delay and other elevation dependent effects. As a consequence we have represented the histograms of the differences between the VLBI and WVR and the GPS and WVR in figure 3.

These figures elicit the following comments and suggest areas in which more work should be done:

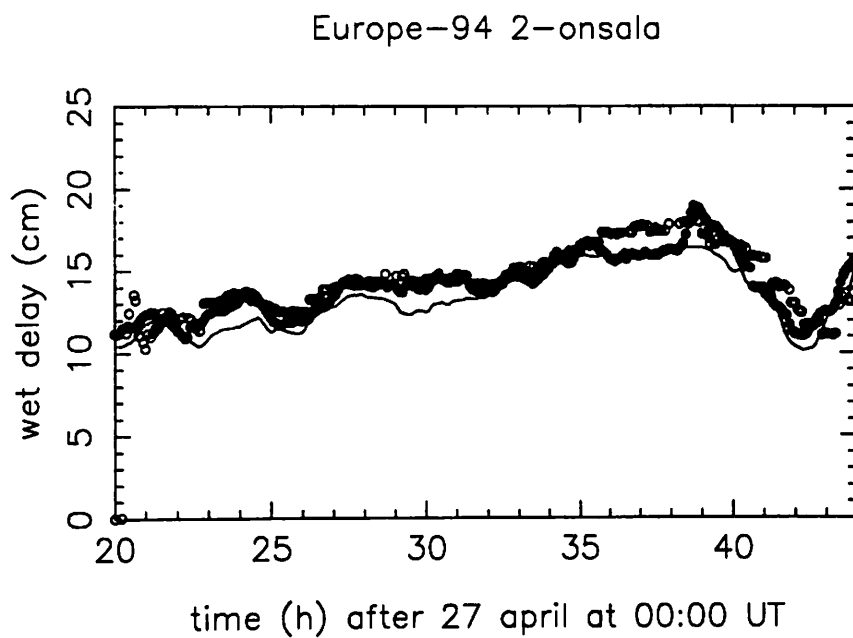
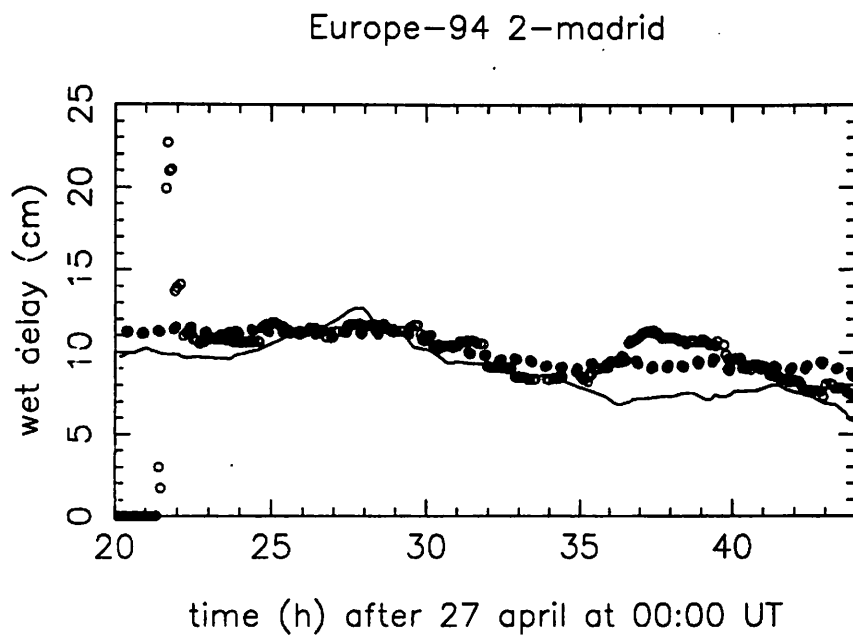


Figure 1: Measured zenith wet delay with VLBI (empty dots),GPS (continuous line) and WVR (filled dots) for the experiment EUROPE-94 2

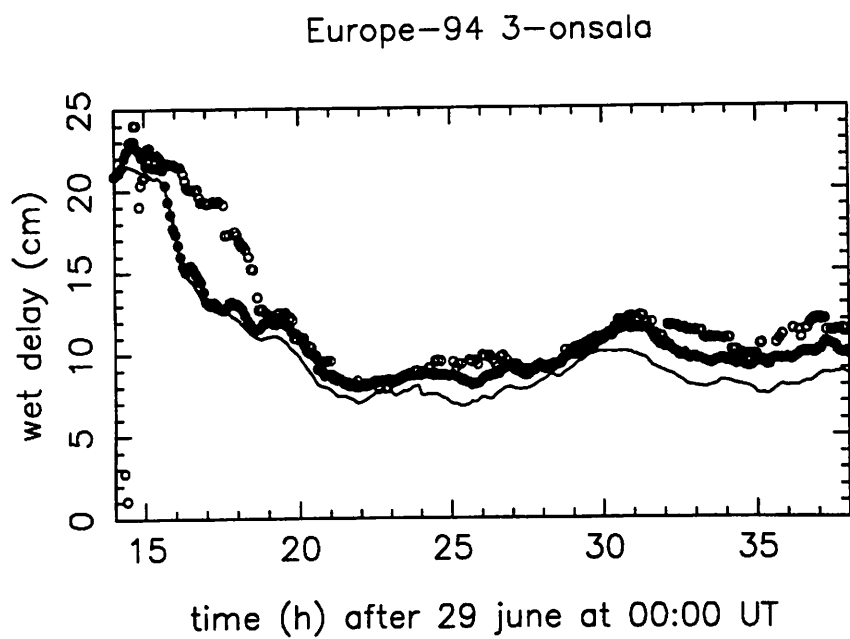
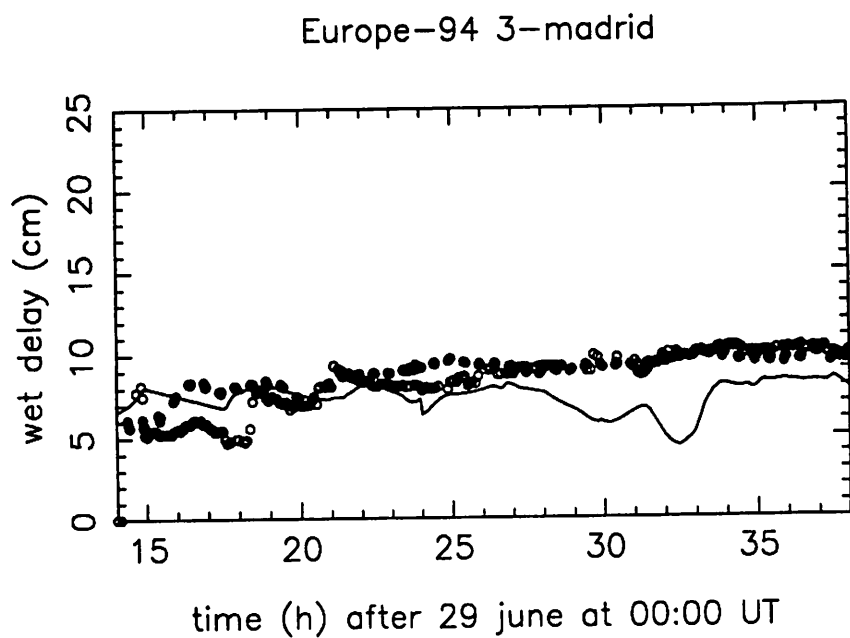


Figure 2: Measured zenith wet delay with VLBI (empty dots),GPS (continuous line) and WVR (filled dots) for the experiment EUROPE-94 3

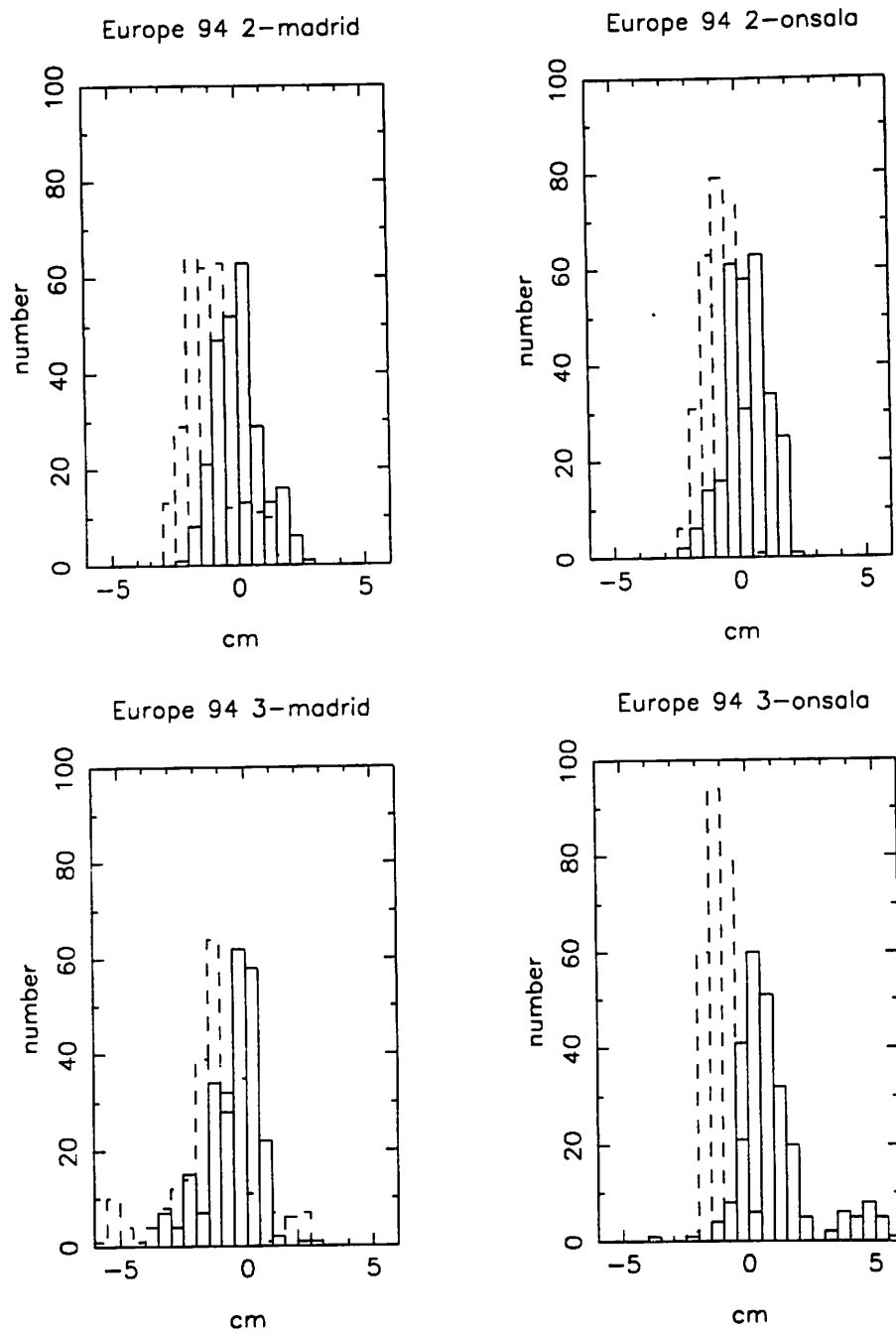


Figure 3: Histograms of the estimate differences: VLBI-WVR (solid line) and GPS-WVR (dashed line)

- a) At the beginning of the VLBI estimates there are large errors due to the initial value taken in the Kalman filter process.
- b) At the end of the experiment the VLBI results tends to be closer to the WVR than the GPS results. This could be a consequence of the sensitivity of the GPS results to errors in the orbits. A similar problem is the jump at the level of 1 cm present in the data of EUROPE-3 at Onsala and Madrid at 24:00 UT.
- c) The VLBI results are slightly noisier than the GPS results, but their bias is smaller.
- d) The WVR zenith delay results are based on zenith brightness temperature measurements. The VLBI and GPS zenith delay estimates are derived from residual delays from a range of azimuth and elevation positions using a mapping function which assumes horizontal stratification in the atmospheric vapor distribution. Realistic inhomogeneities in the vapor distribution could account up to 1 cm differences in the VLBI, GPS and WVR zenith delay estimates.
- e) Future effort is clearly required to generate comprehensive error budgets for intercomparative wet path delay measurements based on WVR, GPS, and VLBI techniques. Uncertainties due to instrumental calibration, processing algorithms, and vapor spatial structure must be quantified to determine the expected levels of agreement using the three techniques.

5 Acknowledgments

The VLBI data has been obtained from the European VLBI project funded by the SCIENCE program of the European Union. Goddard Space Flight Center provided support to these experiments through the NASA Dynamics of the Solid Earth Program. Jet Propulsion Laboratory has provided support for use of the NASA Madrid Deep Space Communications Complex.

The GPS data has been obtained through the following members of the IGS consortium: Onsala Space Observatory (Sweden), Wettzell Fundamental Station (Germany), Agenzia Spaziale Italiana (Italy) and Jet Propulsion Laboratory (USA).

References

- [1] Zarraoa, N. (1993). OCCAM 3.2: Status Report. Proceedings IX Working Meeting on European VLBI for Geodesy and Astrometry. Bonn
- [2] Lichten, S. and J.S. Border (1987) "Strategies for High-Precision Global Positioning System Orbit Determination", Journal of Geophysical Research, Vol. 98, No. B3 pp. 4611-4617
- [3] Elgered, G. (1993), "Tropospheric Radio-Path Delay from Ground-Based Microwave Radiometry", in Atmospheric Remote Sensing by Microwave Radiometry, M.A. Jenssen, Ed., Ch. 5, Wiley, New York.
- [4] Westwater, E.R. (1993), "Ground-Based Remote Sensing of Meteorological Variables", in Atmospheric Remote Sensing by Microwave Radiometry, M.A. Jenssen, Ed., Ch. 4, Wiley, New York.

GPS as a tool for estimating the ionospheric effects on the VLBI observables

Antonio Rius^{1,2}, J.Miguel Juan³,
Manuel Hernández-Pajares⁴, Esther Sardón⁵ and
Antonio Alberdi²

¹ Centre d'Estudis Avançats de Blanes, CSIC, Spain

² LAEFF, INTA, Spain

³ Dept. Física Aplicada, UPC, Barcelona, Spain

⁴ Dept. Matemàtica Aplicada i Telemàtica, UPC, Barcelona, Spain
Universitat Politècnica de Catalunya, Barcelona, Spain

⁵ DLR Remote Sensing Ground Station, Neustrelitz, Germany

Abstract

The ionosphere produces delays in the propagation of radio waves which are frequency dependent. This electronic distribution is far from being uniform in space and in time, and the models available only represent a crude approximation to the reality. In this paper we continue our exploration towards the optimum use of GPS data obtained in global networks such as the International Service for Geodynamics. As an example of this approach we analyze the data gathered at 35 GPS stations distributed worldwide using tomographic techniques.

1 Introduction

We will consider, in this paper, the ionosphere as "that part of the upper atmosphere where sufficient ionization exist to affect the propagation of radio waves" (see K. Davies, 1990, for details on the different effects of the ionosphere on the radio propagation). These effects are a consequence of the interaction of the free electrons in the ionosphere with the radio signals. The distribution of electrons could be modeled defining the electron density as a random process function of the time and the position. Their parameters are measured with a variety of instruments which, in a large extension, are remote sensing techniques. Among these techniques we could include the VLBI and the GPS observations.

Due to its importance in the VLBI analysis, as well as in other techniques like GPS or radar altimetry in which the observables are differences of arrival time of electromagnetic (EM) signals, we will concentrate our study on the effects of the ionized media on the phase and group delay of these signals.

For the Global Positioning System the satellites, which are orbiting ~ 20000 km above the Earth surface, transmit codes within two carriers: L1 ($f_1 \sim 1.6$ GHz) and L2 ($f_2 \sim 1.2$ GHz). Then, each GPS code and phase observation between a given receiver i and a satellite j (P_{ki}^j and L_{ki}^j , respectively in the frequency L_k) is affected by a ionospheric delay, which depends

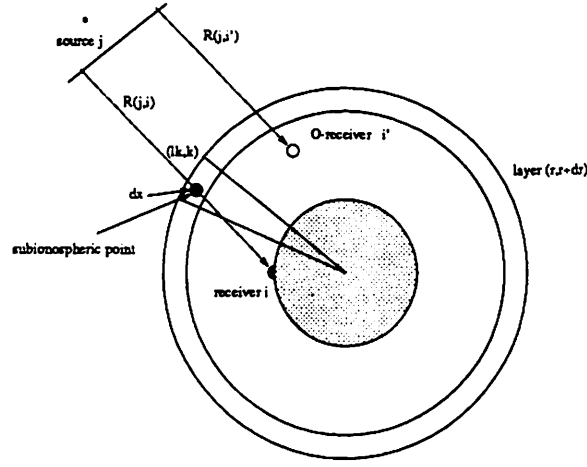


Figure 1: A signal from a VLBI source j propagates to ground receiver i (and an orbiting receiver i') along rays R crossing an ionospheric layer.

on the frequency. This dependence allows to eliminate these delays using the *ionospheric-free combination* of L1-L2 observations.

Following the strategy of [7], and after detecting and repairing the *cycle-slips* of the phases, we obtain:

$$\bar{T}_i^j = \frac{L_{1i}^j - L_{2i}^j}{\alpha_2 - \alpha_1} = I_i^j + K_i + K_j^j \quad (1)$$

where

$$\alpha_k = \frac{40.3}{f_k^2} \text{ (m} \cdot \text{Hz}^2/\text{electrons/m}^2\text{)} \quad (2)$$

This equation can be rewritten in terms of the electronic density n , obtaining a standard expression of the tomographic problems (see for instance [6] and figure 1):

$$\bar{T}_i^j = \int_{R(i,j)} n \, dx + K_i + K_j^j \equiv \int_{R(i,j)} \bar{n} \, dx \quad (3)$$

being $R(i,j)$ the ray between the satellite j and receiver i , and \bar{n} a distribution which accounts for the electron density n and the instrumental delays K_i, K_j .

The inversion of this integral equation could be made in different manners. In our case, given the spherical shape of the ionosphere, we have divided it in spherical layers, each one subdivided in a large number of cells. There are two choices to define the shape of each cell: 1) to use a regular grid and 2) to use a grid in which each cell is crossed by a similar number of rays. The discussion of the relative merits of both approaches is outside the scope of this communication. We will only indicate that both methods have given similar results (see more details in [4]).

2 Estimates of the VLBI ionospheric delays

Usually, in the VLBI context, the ionospheric contribution is modeled by considering a single layer [8]. If we want to take into account the protonosphere (see reference [5]) we need to perform a more complex analysis including outer shells. The effect of one additional shell can be qualitatively understood in terms of Fig. 2. Indeed, if we note d_k as the TEC along

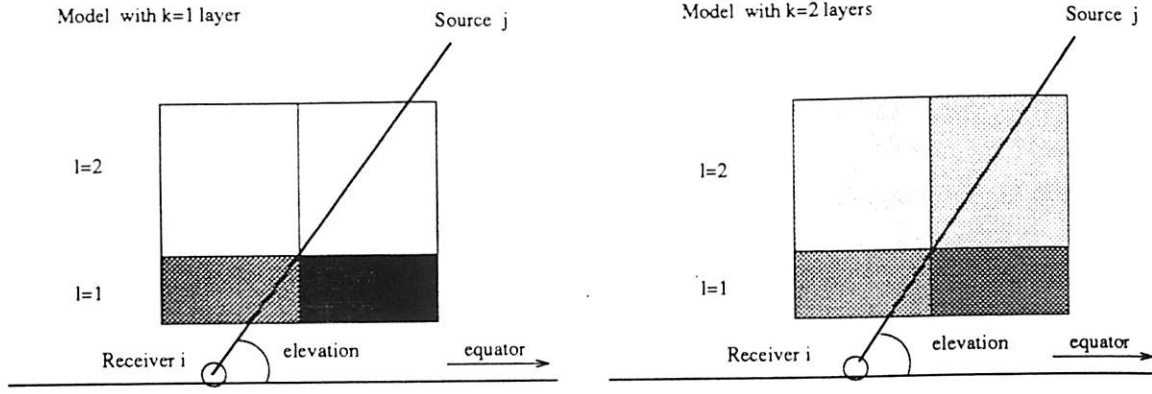


Figure 2: The ionospheric delay for a given ray from transmitter j and receiver i is better explained with two shells instead of one, especially at low elevations (the gray dot density represents approximately the electron density).

0 WETTZELL	1 GRAZ	2 KOOTWIJK	3 ONSALA	4 MATERA
5 METSAHOVI	6 MADRID	7 KIRUNA	8 TROMSO	9 NY ALESUND
10 MASPALOMAS	11 ST JOHN'S	12 ALGONQUIN	13 BERMUDA	14 YELLOWKNIFE
15 GSFC	16 FAIRBANKS	17 NORTH LIBERTY	18 FORTALEZA	19 KOUROU
20 PENTICTON	21 ALBERT HEAD	22 HARTEBEESTHOEK	23 PIE TOWN	24 USUDA
25 QUINCY	26 MACDONALD	27 TAI SHAI	28 GOLDSTONE	29 JPL MESA
30 VANDENBERG	31 KOKEE	32 SANTIAGO	33 YARRAGADEE	34 TIDBINBILLA

Table 1: List of the GPS stations plotted in Fig. 5.

the ray $R(i, j)$ with a model with k shells, then

$$d_2 - d_1 = M_1 T_1^2 + M_2 T_2^2 - M_1 T_1^1 = M_1 (T_1^2 + T_2^2 - T_1^1) + (M_2 - M_1) T_2^2 \quad (4)$$

being T_l^k the vertical TEC obtained within the k -shell model for one cell of the layer l , and M_l the geometrical factor that relates the vertical with the slant TEC. From Eq. 4 we get differences of predicted TEC between 2-shell and 1-shell model which for low elevations are dominated by the second term, which is negative. However for high elevations, the first term approximates well such difference. Figures 3.4 represent the *total electron content along the ray* I (10^{17} e/m²) as a function of the UT and the elevation respectively, estimated with 1 and 2 shell models. The observations corresponds to rays from a VLBI source at right ascension $\alpha = 0$ deg and declination $\delta = 30$ deg, to a station at longitude $\lambda = 0$ deg and latitude $\phi = 40$ deg. The delays for different frequencies f (in Hz) could be computed using (for the phase):

$$\Delta s_i^j = -40.3 \frac{I_i^j}{f^2} \quad (5)$$

We have analyzed GPS data obtained during the period 15 Nov 1993- 19 Nov 1993 at the IGS sites as indicated in figure 5 and in table 1 (see more details in [9]).

The correction of the cycle slips have been made along the lines discussed in [1],[3],[7].

In the analysis presented here we have assumed that the ionosphere is composed of two geocentric spherical shells ($k=2$), with boundaries placed at 50-600-5000 km above the earth mean radius.

In figure 6 we have the TEC distribution as a function of right ascension and declination of the subionospheric point for the first shell. Each box represents the mean distribution each

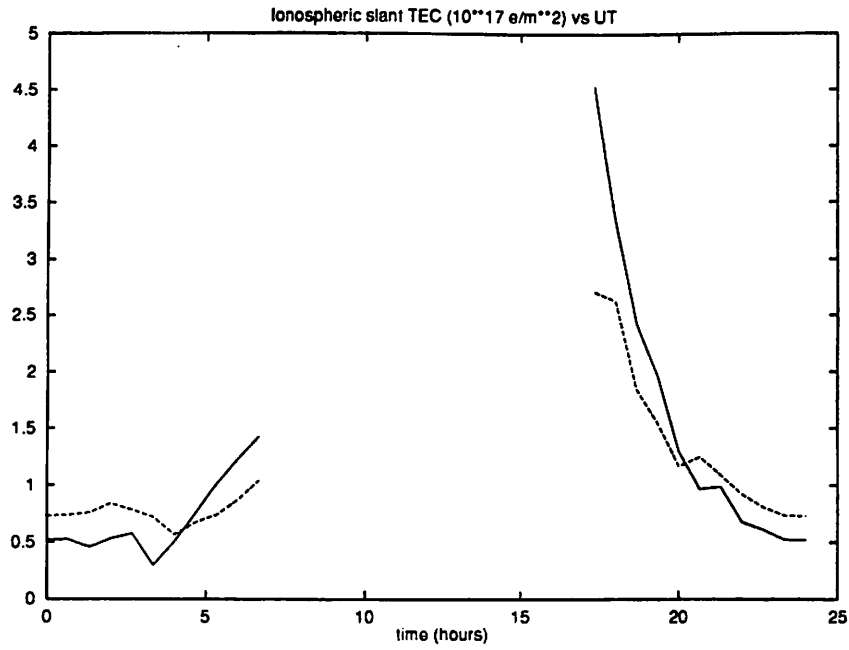


Figure 3: Integrated electron content along the VLBI source direction as a function of UT, using one-shell model (continuous line) and two-shell model (dashed line)

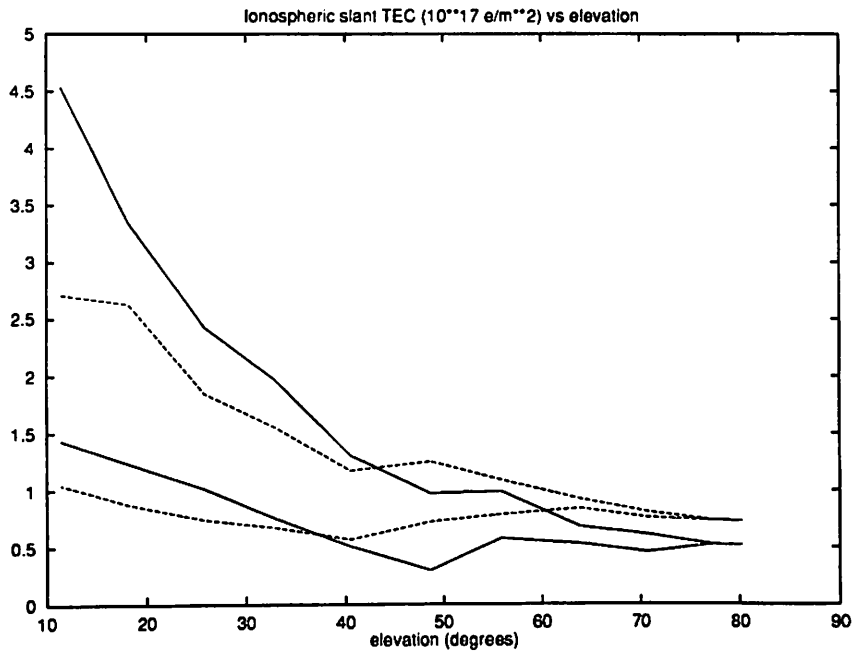


Figure 4: Integrated electron content along the VLBI source direction as a function of elevation, using one-shell model (continuous line) and two-shell model (dashed line)

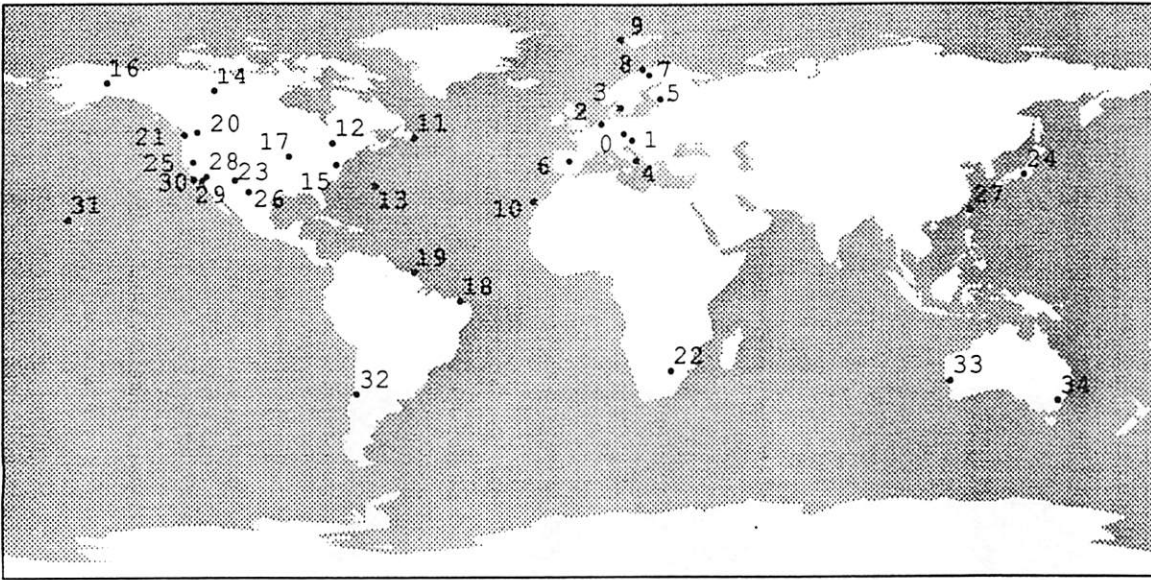


Figure-5: Map with the IGS stations used in the analysis. The station names are listed in table 1

12 hours, and in figure 7 we have plotted the estimates of the TEC for the second layer as a function of the declination of the subionospheric point.

3 Conclusions

We have developed techniques to model the 3-D structure of the ionospheric electron density. It has been shown that this more realistic model produces significant variations in the estimate of the slant TEC to be used in the calibration in the VLBI experiments.

4 Acknowledgments

This work has been partially supported with funds from the Spanish government project PB93-1235 (DGICYT). The GPS data has been obtained through the IGS consortium.

References

- [1] Blewitt G., 1990. An automatic editing algorithm for GPS data. *Geophysical Research Letters*, Vol.17, No.3, pages 199-202.
- [2] Davies K., 1990. *Ionospheric Radio*. IEE ElectroMagnetic Waves Series 31, Peter Perigrinus Ltd., London.
- [3] Freymueller J.T., 1993. PhasEdit version 1.1: An automatic data editing program for dual-frequency codeless GPS receivers. An Introduction to GIPSY/OASIS-II (notebook). eds. F.H.Webb & J.F.Zumberge, JPL, Colorado.

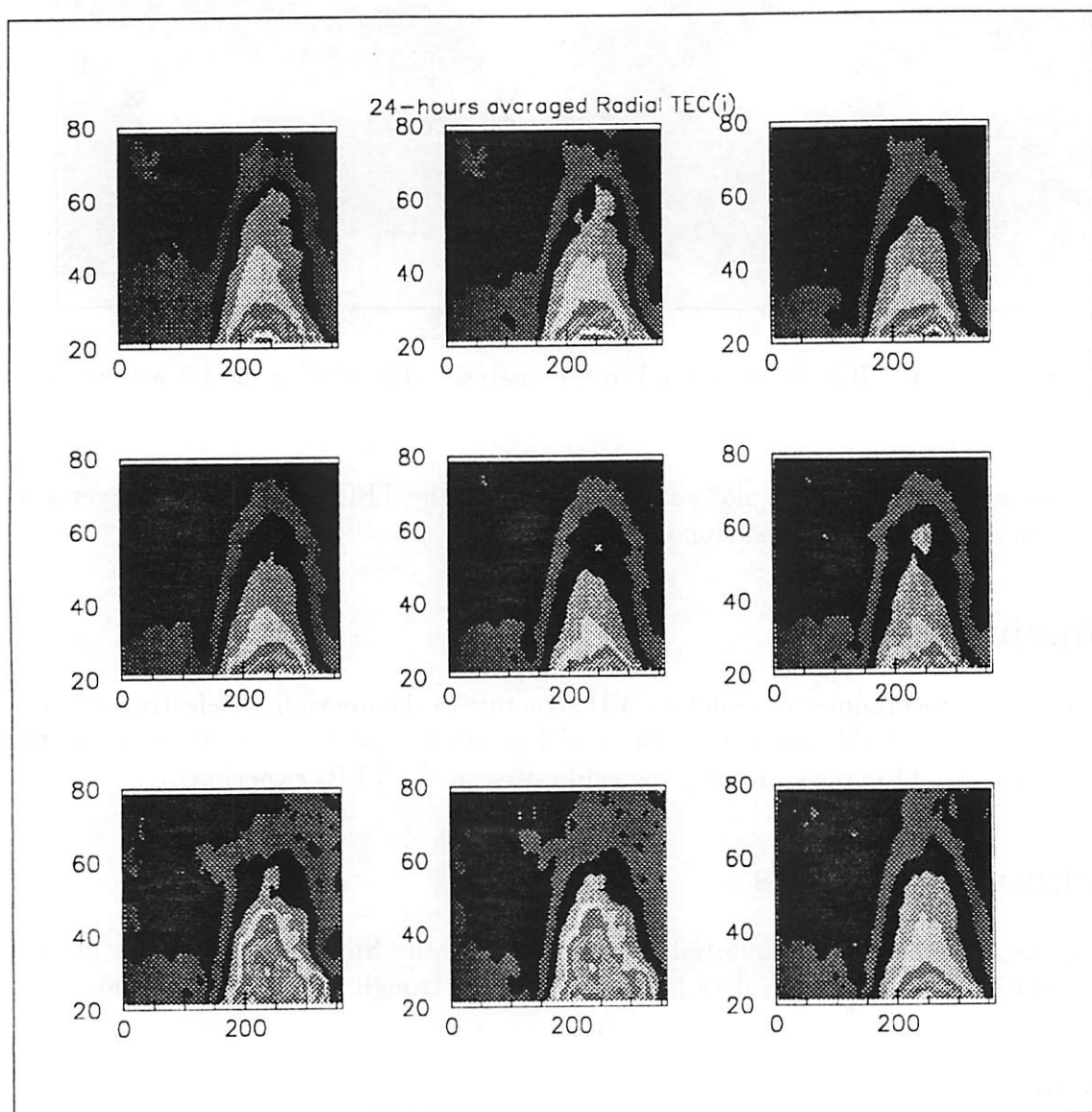


Figure 6: Sequence of ionospheric radial TEC plots, computed each 12 hours including data during 24 hours. The first one corresponds to 0-24 h of Nov. 15 and the last plot to 0-24 h of Nov. 19. Each *color* level corresponds to an increase of $4 \cdot 10^{16}$ electrons/m² starting with a minimum range of $0 - 4 \cdot 10^{16}$ electrons/m² achieved in the North Pole.

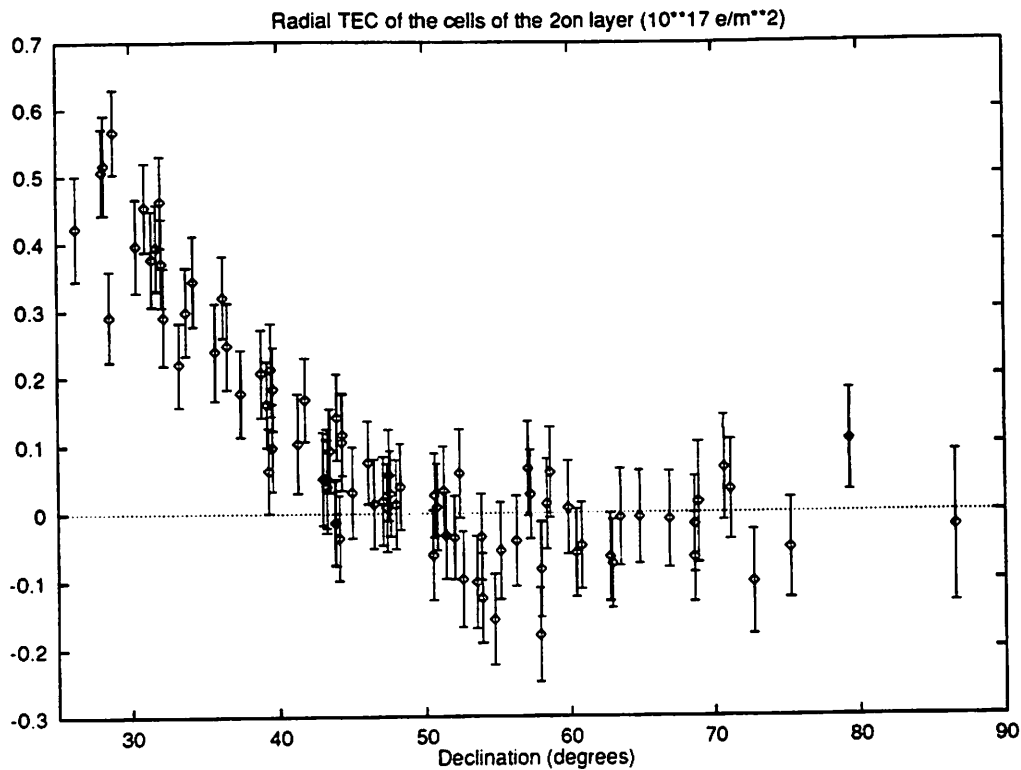


Figure 7: TEC of the different cells of the second layer of the ionosphere as a function of the declination (0-12 hours of November 15th 1993).

- [4] Hernández-Pajares. M: The Kohonen networks as a tool to perform TEC estimation of the Ionosphere. Technical Memorandum 11/95, CSIC/UPC, available by anonymous ftp in maite125.upc.es (147.83.39.125). /pub/incoming/tm11.ps.
- [5] Klobuchar J.A., Doherty P.H., Bailey G.J., Davies K., 1994. Limitations in Determining Absolute Total Electron Content from Dual-Frequency GPS Group Delay Measurements. Beacon Satellite Symposium, Aberystwyth, July 11-15 1994.
- [6] Nolet G., 1987. Seismic tomography with applications in Global Seismology and Exploration Geophysics, D.Reidel Publishing Company.
- [7] Sardon E., Rius. A., Zarraoa N., 1994a. Estimation of the transmitter and receiver differential biases and the ionospheric total electron content from Global Positioning System observations. *Radio Science*, Vol.29. No.3. pages 577-586.
- [8] Sardon E., Rius, A., Zarraoa N., 1994b. Ionospheric calibration of single frequency VLBI and GPS observations using dual GPS data. *Bulletin Geodesique*, 68:230-235.
- [9] Zumberge J., Neilan R., Beutler G., Gurtner W., 1994. The International GPS Service for Geodynamics-Benefits to Users. ION GPS-94. Salt Lake City, Utah.

External wet tropospheric corrections during a two-week-long VLBI campaign

T. Ragne Carlsson, Gunnar Elgered, and Jan M. Johansson
Onsala Space Observatory, Chalmers University of Technology
S-439 92 Onsala
Sweden

Abstract

Data from two weeks of continuous Very-Long-Baseline-Interferometry (VLBI) measurements in January 1994 have been used to evaluate methods using external estimates of the propagation delay caused by atmospheric water vapor. Three possible methods to correct for this "wet delay" have been compared, (1) the standard estimation of the wet delay using the VLBI data themselves, (2) measuring the water vapor with the microwave radiometer at the Onsala Space Observatory, and (3) using the independent estimates of the propagation delay from the Global Positioning System (GPS) data. For a short term (twelve 24 hour experiments) repeatability study we found the two latter methods showing an improvement compared to the standard method. Baseline length weighted root mean square (wrms) about a straight line fit for the single baseline Onsala–Wettzell was reduced to 63% of the standard solution with wet delay estimates from the VLBI data when the tropospheric path delay was corrected for using GPS data at both ends.

Introduction

Since the start of intercontinental Very-Long-Baseline-Interferometry (VLBI) measurements the precision of the measurements has clearly improved [Rogers et al., 1993]. This improvement is due to both a hardware evolution, *e.g.*, the RF bandwidth upgrade [Corey and Clark, 1991] and better mapping functions for the atmospheric delay [MacMillan and Ma, 1994]. However, the variations in the wet delay is still considered one of the main error sources in VLBI. A well known fact is that a varying amount of water vapor in the atmosphere affects the propagation time of the radio signals used in space geodetic techniques like VLBI and the Global Positioning System (GPS). A common way to correct for the extra path delay due to the atmospheric water vapor is to assume a horizontally stratified atmosphere to estimate the equivalent zenith wet delay from the data themselves using mapping functions to estimate values at appropriate elevation angles. This correction may be modeled as a piece wise linear function or a

stochastic process. An other method is to independently measure the water vapor using a Water Vapor Radiometer (WVR) [Elgered, 1993]. In the present paper we have used three different methods to correct for the tropospheric path delay in the VLBI solutions. The first is the standard procedure to solve for the wet delay from VLBI data. The second is to use the measured water vapor from the Onsala WVR. Finally, the third method is to use the GPS estimates of the wet delay from the analysis of the permanent Swedish GPS network SWEPOS. The data set used in this work is the Cont94 campaign.

Experiment description

The Cont94 campaign in January 1994 was a series of twelve 24 hour long VLBI experiments conducted over a period of 13 days. Seven stations, Onsala, Fairbanks, Kokee Park, Westford, Wettzell and the VLBA sites Fort Davis and Los Alamos, usually involved in the monthly R&D experiments formed 21 baselines.

The WVR at Onsala is a dual frequency microwave radiometer measuring the atmospheric emission at 21.0 and 31.4 GHz. For a more detailed description see [Elgered et al., 1991]. The distance between the WVR and the 20 m VLBI antenna at Onsala is approximately 80 m and the height difference is around 13 m. During Cont94 the WVR was running continuously in a "sky mapping mode" [Davis et al., 1993] with a cycle of approximately 10 minutes.

SWEPOS is a permanent network of GPS receivers established in Sweden by Onsala Space Observatory and the National Land Survey of Sweden [Johansson et al., 1993]. The network consists of 20 stations operating continuously with a present sample rate of 0.33 s^{-1} . One of the receivers is located at Onsala where the longest of the distances between the VLBI antenna, the WVR and the GPS antenna is approximately 80 m.

Solution procedure

The VLBI experiments from Cont94 were processed with the least squares estimation program SOLVE [Ma et al., 1990]. The clock error was estimated as a continuous piece-wise linear function. Three different

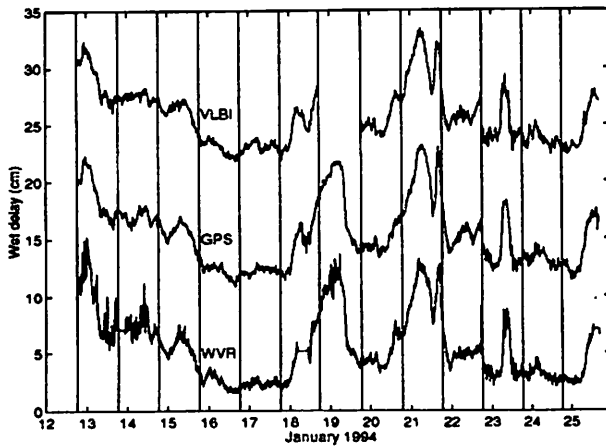


Figure 1: Estimated zenith wet delay for the Onsala site from VLBI, GPS and WVR, where in order to make it easier to compare results biases of +20 and +10 cm have been added to the VLBI (upper curve) and GPS (middle curve) results respectively.

techniques were used correcting for the wet delay, (1) the wet delay was estimated from the VLBI data, (2) the inferred water vapor was measured with the microwave radiometer at Onsala, and (3) the wet delay was estimated from GPS data. The MTT [Herring, 1992] dry and wet mapping functions were used.

During Cont94 the WVR was always observing above an elevation angle of 23.6 degrees. The equivalent zenith wet delays were calculated from the observed using the cosecant law. It should be pointed out that the WVR data used in the VLBI solution were not taken in the observing direction of the VLBI antenna, but in the sky mapping mode mentioned earlier. The equivalent zenith wet delays from the WVR were grouped according to difference in angle of observation between the WVR and the VLBI antenna. The groups were then ranked and the data from the best ranked group were averaged over the time of each VLBI observation resulting in the zenith wet delay used in the VLBI solution.

The GPS data were analyzed with the GIPSY software [Lichten and Border, 1987] using a Kalman filter technique. Observations down to an elevation angle of 15 degrees were used in the solution. The Lanyi [Lanyi, 1984] mapping function was used to estimate the total tropospheric path delay. The wet delay was obtained by subtracting the hydrostatic delay, which is known from the pressure readings at the sites, from the total estimate. The GPS estimates correcting for the wet tropospheric delay in the VLBI solutions were then obtained by averaging the wet delays over the time of each VLBI observation.

Results

When analyzing the Cont94 VLBI experiments we compared the baseline length rms errors using three

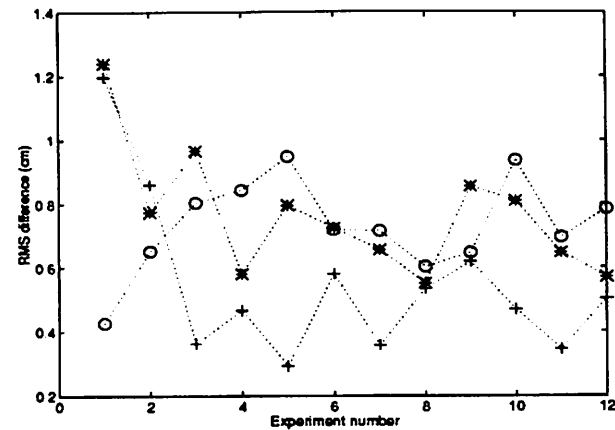
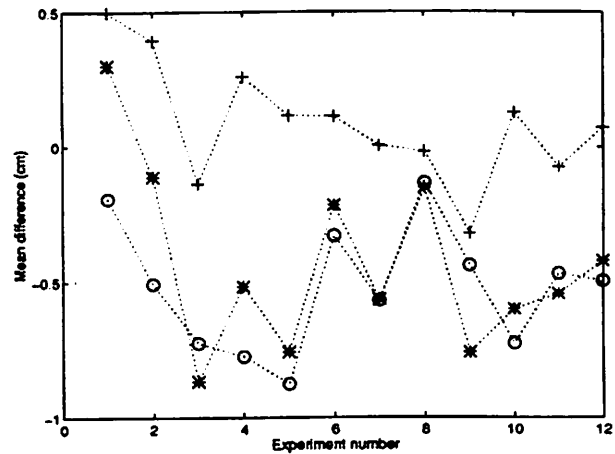


Figure 2: (a) Mean differences and (b) RMS difference between the wet delay estimates for WVR - GPS (pluses), WVR - VLBI (stars) and GPS - VLBI (circles). The curve showing the rms difference between the measured wet delay by the WVR and the GPS estimates is apparently lower than the rms difference for WVR - VLBI and GPS - VLBI. This is due to the offset of about 5 mm in the VLBI estimate compared to the other estimates. This does not hold for the first two experiments, when there were periods of rain increasing the noise in the WVR measurements.

different methods correcting for the wet tropospheric path delay.

The first method used continuous piecewise linear functions in segments of 10 minutes duration in estimating the wet delay at all sites. Observations down to an elevation angle of 6 degrees were used in the analysis. We will take a look at the baselines from the solution by this method, but first however a discussion about the VLBI estimate of the wet delay.

From this solution a comparison of the estimated equivalent zenith wet delay between VLBI, WVR and GPS measurements has been conducted. Figure 1 shows the estimated zenith wet delay from VLBI, GPS and WVR at the Onsala site. In order to make it easier to compare results biases of +20 and +10 cm have been added to the VLBI and GPS results respectively.

Table 1: Mean value and rms scatter for the VLBI equivalent zenith wet delay estimates during Cont94 for all the stations in the network.

Station	Average (cm)	RMS (cm)
Onsala	5.70	2.62
Fairbanks	2.78	1.64
Fort Davis	3.36	2.52
Kokee Park	8.50	3.79
Los Alamos	1.51	0.84
Westford	2.85	2.56
Wetzell	5.21	2.70

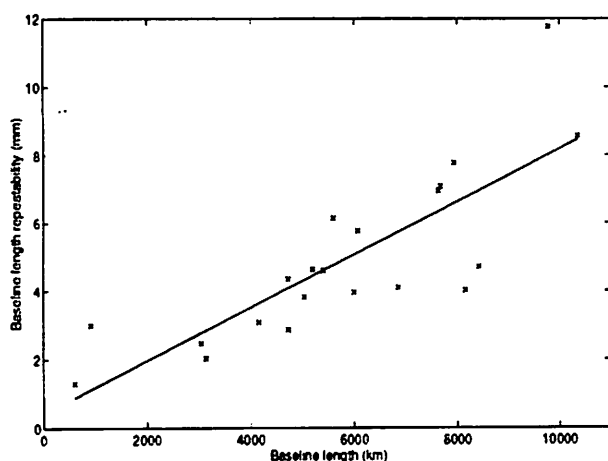


Figure 3: Baseline repeatability as a function of baseline length for the 21 baselines in the network. The best fit in least square sense shown is $0.41 \text{ mm} + 0.78 \text{ ppb}$.

Although the agreement between the three different methods looks good the VLBI estimate have a mean bias of about 5 mm, over the period, compared to the two other estimates. This can be seen in Figure 2 where the differences and the rms differences between the wet delays from the different methods are displayed. The results for the first two days in the series differ from those for the other days mainly due to periods of rain which increases the noise in the WVR measurements. An overview for all the sites in the network can be found in Table 1, showing the mean value and rms scatter of the equivalent zenith wet delay estimates from the VLBI data at each site for the two week period.

For the overall performance of the VLBI solution Figure 3 shows the baseline length repeatability as a function of baseline length for all seven stations in the network. For the full range of baselines the best fit of a straight line is $0.41 \text{ mm} + 0.78 \text{ ppb}$.

In the second type of VLBI solution the equivalent zenith wet delay derived from the WVR measurements

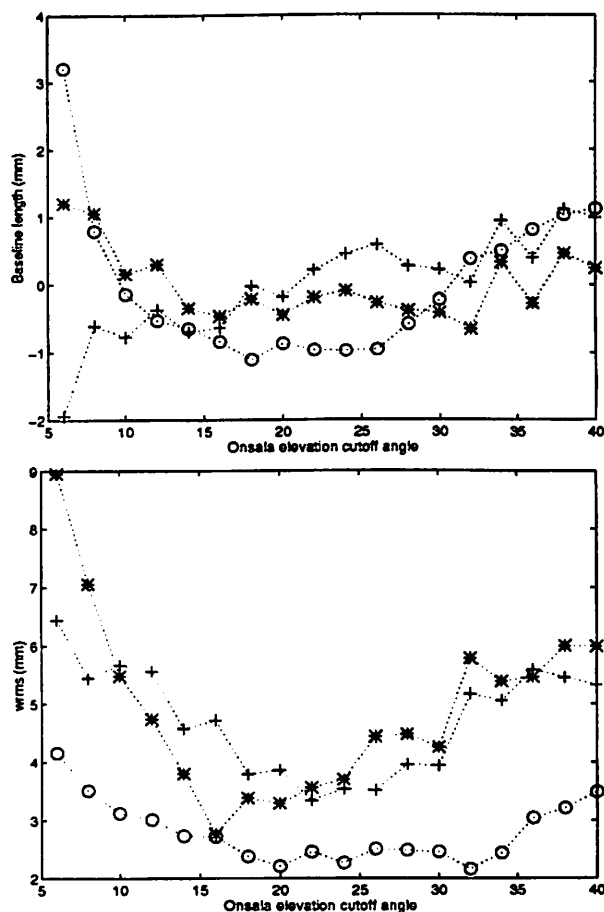


Figure 4: (a) Baseline length deviations from a mean value and (b) baseline length wrms as a function of elevation cutoff angle at the Onsala site for baselines Onsala-Fort Davis (stars), Onsala-Fairbanks (pluses) and Onsala-Wetzell (circles). WVR data have been added for the Onsala site.

(see Figure 1) was used to correct for the tropospheric path delay at the Onsala site. At the other sites in the network the wet delay was estimated in piecewise segments of 10 minutes duration and observations down to an elevation angle of 6 degrees were used. To evaluate the impact on the VLBI solution when adding WVR data we did 18 solutions with the elevation cutoff angle at Onsala varying from 6 to 40 degrees. Figure 4 shows baseline length deviations from a mean value and baseline length wrms as a function of elevation cutoff angle at the Onsala site for the baselines Onsala-Fort Davis (7940 km), Onsala-Fairbanks (6066 km) and Onsala-Wetzell (919 km). According to Figure 4 elevation cutoff angles of 15 to 30 degrees give the lowest wrms. Similar results were obtained by [Elgered and Davis, 1993] in a study including about a hundred experiments over a ten year period. Figure 5 shows a baseline repeatability plot based on the solution with an Onsala cutoff angle of 20 degrees with baseline length wrms as a function of baseline length. This time the best fit of a straight line is described by

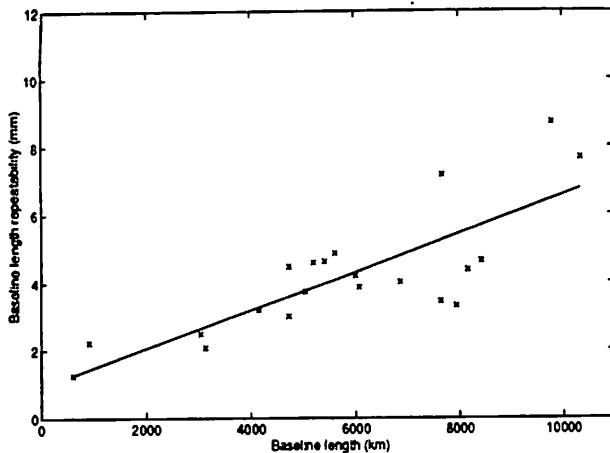


Figure 5: Baseline repeatability as a function of baseline length for the 21 baselines in the network with WVR atmosphere added for the Onsala site. The best fit in least square sense shown is $0.92 \text{ mm} + 0.56 \text{ ppb}$.

$0.92 \text{ mm} + 0.56 \text{ ppb}$. A decrease in wrms compared to the standard solution for the baselines involving Onsala can be seen (*c.f.* Figure 3).

GPS estimates of the wet delay for the Onsala site were used in the third type of solution. Figure 6 shows baseline length deviations from a mean value and baseline length wrms as a function of elevation cutoff angle at the Onsala site for the baselines Onsala–Fort Davis, Onsala–Fairbanks and Onsala–Wetzell. For the solution having an elevation cutoff angle of 26 degrees the best fit of the straight line for the baseline length repeatability as a function of baseline length is $0.96 \text{ mm} + 0.55 \text{ ppb}$.

A fourth solution was finally made by adding the GPS estimates of the wet delay for the Wetzell site as well. The result of a cutoff test at Wetzell is similar to that of Onsala. With 26 degrees elevation cutoff angle the repeatability plot is shown in Figure 7. The best fit of a straight line is $0.83 \text{ mm} + 0.57 \text{ ppb}$. Because variations in the wet delay at Kokee Park are large (see Table 1) a best fit for the subset of 15 baselines created when the baselines including the Kokee Park site are excluded is displayed. This lower line is described by $1.8 \text{ mm} + 0.25 \text{ ppb}$.

Conclusions and future work

We have studied different methods for improving the baseline length repeatability by using different kinds of wet delay correction techniques in the VLBI solutions. For the entire network the repeatability improved by 10% when WVR or GPS data were added for the Onsala site. This improvement is probably due to the stronger solution obtained by using wet delay estimates independent of the VLBI data. Further, according to Figures 1 and 2 the WVR and GPS estimates of the Onsala wet delay have a better agreement than that of WVR and VLBI or GPS and VLBI due to

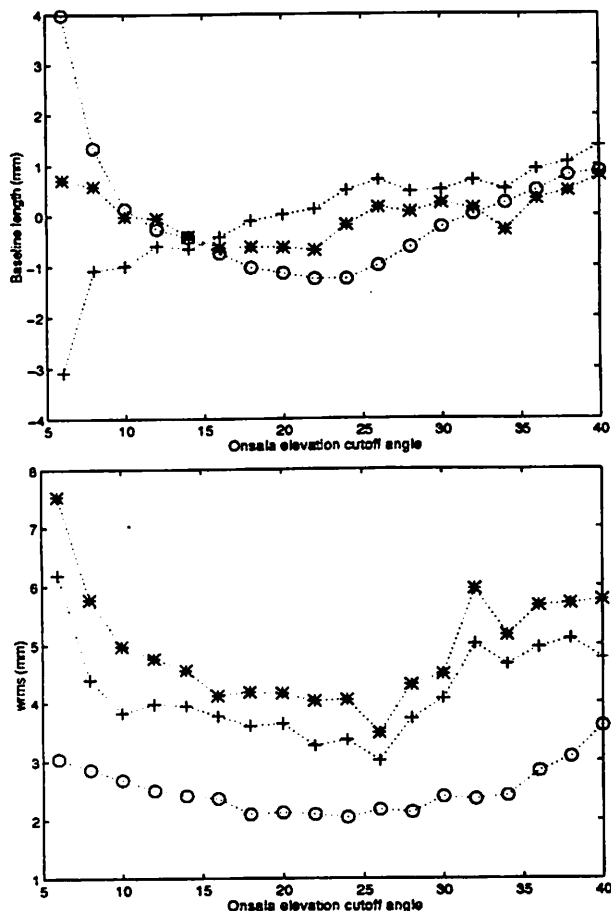


Figure 6: (a) Baseline length deviations from a mean value and (b) baseline length wrms as a function of elevation cutoff angle at the Onsala site for baselines Onsala–Fort Davis (stars), Onsala–Fairbanks (pluses) and Onsala–Wetzell (circles). GPS data have been added for the Onsala site.

the offset of about 5 mm in the VLBI estimate compared to the other two methods.

The adding of GPS data to the Wetzell site did not have as much impact on the baseline repeatability as the adding of GPS data to the Onsala site. One possible reason for this is the lower rms difference between the wet delay estimates from VLBI and GPS at Wetzell, 6.3 mm compared to Onsala 7.4 mm. Further for the Wetzell site we had no independent instrument, *e.g.*, a WVR for estimating the wet delay. Thus making it harder to evaluate the comparison between the VLBI and GPS estimates of the wet delay.

Table 2 shows the weighted rms for the baseline Onsala–Wetzell for the four different solution methods presented in this paper. This baseline is so far the only baseline with GPS data processed and included in the VLBI database at both sites. The solution with WVR data included at the Onsala site uses data from Onsala down to an elevation of 20 degrees. The two solutions using GPS data for Onsala and Wetzell use data down to 26 degrees at the stations using the GPS

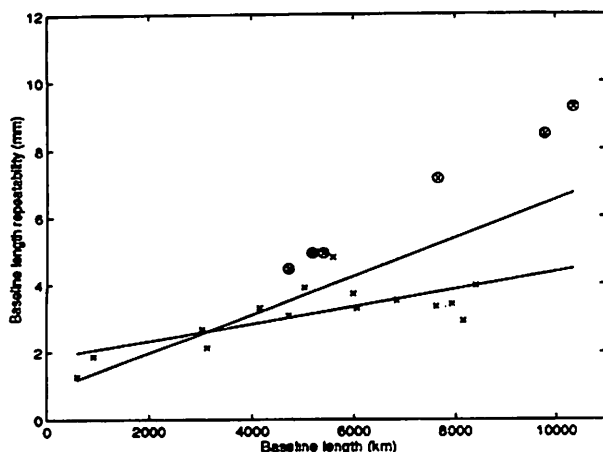


Figure 7: Baseline repeatability as a function of baseline length for the 21 baselines in the network with GPS atmosphere added for the Onsala and Wettzell sites. The best fit in least square sense shown is $0.83 \text{ mm} + 0.57 \text{ ppb}$. The lower line shows the best fit for the subset of 15 baselines created when the baselines including the Kokee Park site are excluded. This best fit is $1.8 \text{ mm} + 0.25 \text{ ppb}$. Baselines including the Kokee Park site are surrounded by rings.

data. Notable is that the wrms of the baseline length is 37% lower with GPS corrections for the wet troposphere added at both ends compared to the standard solution with the wet delay estimated from the VLBI data.

Notable is also the fact, recalling Figure 7, that the outliers from the least square fit are all baselines involving Kokee Park. Table 1, showing mean value and rms scatter around that value for the VLBI equivalent zenith wet delay, implies a more variable atmosphere at the Kokee Park site as was the case at Onsala. Further improvements in the precision of the baseline length might therefore be obtained by using GPS estimates of the wet delay at stations like Kokee Park.

Finally it should be stated that more than the twelve experiments conducted during the Cont94 campaign are needed to evaluate the effect on the short term repeatability using the methods presented here. If we have n experiments we can for simplicity assume $(n-1) \cdot \text{wrms}^2 / \sigma^2$ to be χ^2 distributed with $n-1$ degrees of freedom as being $(n-1) \cdot \text{rms}^2 / \sigma^2$. Then almost 40 experiments are needed to separate the 95% confidence intervals for the wrms for the standard VLBI solution and the wrms for the solution having GPS data added for both Onsala and Wettzell (see Table 2).

Another work that is yet to be done is a long term repeatability study with the same methods as presented here, where we have seasonal effects that might affect both the VLBI solutions and the GPS estimates of the wet delay.

Table 2: Baseline length wrms for the baseline Onsala-Wettzell using four different methods to correct for the wet delay.

Solution Method	WRMS (mm)
Standard VLBI	3.0
WVR data used for the Onsala site only	2.2
GPS data used for the Onsala site only	2.2
GPS data used for the Wettzell site only	2.2
GPS data used for the Onsala and Wettzell sites	1.9

Acknowledgements

We wish to thank the VLBI group at NASA Goddard Space Flight Center for the help with Solve and especially Jim Ryan for assistance and fruitful discussions during RC's visit at Goddard.

References

- Corey, B. E., and T. A. Clark, "The RF bandwidth upgrade: doubling the X-band spanned bandwidth of geodetic VLBI receiving systems", *NOAA Technical Report NOS 137 NGS 49*, Proceedings of the AGU Chapman Conference on Geodetic VLBI: Monitoring Global Change, pp. 15-23, U.S Department of Commerce, Rockville, Maryland, 1991.
- Davis, J. L., G. Elgered, A. E. Niell, and C. E. Kuehn, "Ground-based measurement of gradients in the "wet" radio refractivity of air", *Radio Sci.*, 28, 1003-1018, 1993.
- Elgered, G., J. L. Davis, T. A. Herring, and I. I. Shapiro, "Geodesy by Radio Interferometry: Water Vapor Radiometry for Estimation of the Wet Delay", *J. Geophys. Res.*, 96, 6541-6555, 1991.
- Elgered, G., "Tropospheric Radio Path Delay from Ground-Based Microwave Radiometry in", *Atmospheric Remote Sensing by Microwave Radiometry*, ed. M. Janssen, Wiley and Sons, pp. 215-258, 1993.
- Elgered, G., and J. L. Davis, "Microwave Radiometry for Correction of Atmospheric Path-Length Variations in VLBI: Recent Results." *Proc. of the 9th Working Meeting on European VLBI for Geodesy and Astrometry*, Bad Neuenahr, 98-108, 1993.

Herring, T. A., "Modeling atmospheric delays in the analysis of space geodetic data, in" *Symposium on Refraction of Transatmospheric Signals in Geodesy*, ed. J. C. De Munk and T. A. Spoelstra, pp. 157-164, Netherlands Geod. Comm., Delft, 1992.

Johansson, J. M., B. O. Rönnäng, T. R. Carlsson, T. M. Carlsson, G. Elgered, R. T. K. Jaldehag, P. O. J. Jarlemark, B. I. Nilsson, and H.-G. Scherneck, "VLBI and GPS Measurements of the Fennoscandian Uplift" *Proc. of the 9th Working Meeting on European VLBI for Geodesy and Astrometry*, Bad Neuenahr, 49-54, 1993.

Lanyi, G., "Tropospheric delay affecting radio interferometry" *TDA Progress Report 42-78*, 152-159, Jet Propul. Lab., Pasadena, Calif., 1984.

Lichten, S. M., and J. S. Border, "Strategies for high-precision Global Positioning System orbit determination" *J. Geophys. Res.*, 92, 12751-12762, 1987.

Ma, C., J. Sauber, L. Bell, T. Clark, D. Gordon, W. Himwich, and J. Ryan, "Measurements of horizontal motions in Alaska using very long baseline interferometry", *J. Geophys. Res.*, 95, 21991-22011, 1990.

MacMillan, D. S., and C. Ma, "Evaluation of very long baseline interferometry atmospheric modeling improvements", *J. Geophys. Res.*, 99(B1), 637-651, 1994.

Rogers, A. E. E., R. J. Cappallo, B. E. Corey, H. F. Hinteregger, A. E. Niell, R. B. Phillips, D. L. Smythe, A. R. Whitney, T. A. Herring, J. M. Bosworth, T. A. Clark, C. Ma, J. W. Ryan, J. L. Davis, I. I. Shapiro, G. Elgered, K. Jaldehag, J. M. Johansson, B. O. Rönnäng, W. E. Carter, J. R. Ray, D. S. Robertson, T. M. Eubanks, K. A. Kingham, R. C. Walker, W. E. Himwich, C. E. Kuehn, D. S. MacMillan, R. I. Potash, D. B. Shaffer, N. R. Vandenberg, J. C. Webber, R. L. Allshouse, B. R. Shupler, and D. Gordon, "Improvements in the Accuracy of Geodetic VLBI", *Contributions of Space Geodesy to Geodynamics: Technology*, ed. D. E. Smith, and D. L. Turcotte, AGU Geodynamics Series, 25, 47-63, 1993.

A VLBI Survey with the European Geodetic Network: preliminary results

F. Mantovani¹, W. Alef², M. Bondi³ and D. Dallacasa⁴

¹ Istituto di Radioastronomia del CNR, Bologna, Italy

² Max-Planck-Institut für Radioastronomie, Bonn, Germany

³ Nuffield Radio Astronomy Labs., Jodrell Bank, UK

⁴ Joint Institute for VLBI in Europe, Dwingeloo, The Netherlands

Abstract

We report on the results of snap-shot observations with the European Geodetic Network (Onsala, Medicina, Noto, Wettzell and Matera + Effelsberg) on ~ 29 Compact Steep-spectrum Sources. The sources were selected with Spectral Index > 0.5 , Flux Density > 0.2 Jy at λ 6 cm and Dec. $> -25^\circ$. Fringes were found for 27 sources at both S- and X-band. About 75% of the data set has been analysed and the maps produced for most of the sources. On the bases of the present data we can confirm a significant correlation between the overall radio spectrum and the VLBI morphology.

Introduction

In a flux-density-limited sample of radio sources like the 3CR and the Peacock and Wall (1982), $\sim 30\%$ of the sources with redshift $z > 0.2$ show angular dimensions $\theta < 2$ to 3 arcsec, which correspond to linear size $L \leq 10$ to 15 kpc. These sources also have a steep optically thin Spectral Index ($\alpha > 0.5$: flux $S \propto \nu^{-\alpha}$). They form a separate class of powerful radio objects ($P_{178} \leq 10^{26.8}$ W/Hz) known as Compact Steep-spectrum Sources (CSSs).

Most of the CSSs show a double-lobed radio structure at the milli-arcsecond scale. This is found in more than 50% of the CSSs quasars and in $\sim 90\%$ of the galaxies. A structure dominated by a radio jet – infrequent in galaxies – is quite common in quasars. The radio core is detected in 70% of the quasars and in 40% of the galaxies. The core fractional luminosity of CSSs is similar to those of large size radio sources, namely $\sim 3\%$ in quasars and $\leq 0.4\%$ in galaxies. When CSSs are dominated by jet emission, the jet itself often shows a distorted structure.

The nature of CSSs is still under discussion. Lobe-dominated CSSs are thought to be the young objects ($\leq 10^6$ years) precursors of the large size double-lobed radio sources (see Fanti et al. 1995), while asymmetric jet-dominated CSSs are thought to

be brightened either by Doppler boosting or by interaction with an inhomogeneous ambient medium. For more details on this class of objects see for example Fanti et al. (1990), Spencer et al. (1991), Sanghera et al. (1995), Dallacasa et al. (1995).

In order to increase the sample of CSSs considering objects with lower luminosities, we started a 'filler' project with the European VLBI Network, involving in the observations the available European Geodetic Stations.

The ED3 Project: observations and data processing

A list of CSS candidates taken from the compilation by Dallacasa & Stanghellini (1990) not yet observed in VLBI was defined with the following selection criteria: optically thin spectral index ($\alpha > 0.5$), flux density > 0.2 Jy at λ 6 cm and Dec. $> -25^\circ$. The aims of the observations were:

- detect the source
- compare the structures with those found for more powerful CSSs
- obtain spectral information (i.e. identify the cores of the sources)
- evaluate the physical parameters in the centres of CSSs

We observed with an array of 5 telescopes: Matera, Medicina, Noto, Onsala and Wettzell. Effelsberg also joined the network for 37.5 hours. The total observing time of 48.5 hours was split into 3 sessions (network codes: ED3A, B and C). The sources were observed with the snap shot technique, tracking each of them for at least 4 widely spaced scans each 13 minutes long. The data were recorded with the MK3A data acquisition system in the standard geodesy setup, i.e. dual frequency observing (S/X), but with twice the bandwidth (mode A) with 32 MHz for X-band and 24 MHz for S-band.

The data were cross-correlated with the MK3A processor at the Max-Planck-Institut für Radioastronomie in Bonn and analysed in the standard way with AIPS. The results of the source imaging at both S- and X-band are reported in Tab. 1 which contains the relevant information collected so far.

Preliminary results

In the ED3 project 29 sources were observed. All but 2 were detected in both bands. The analysis is completed for about 75% of the objects. Examples of the more interesting brightness distributions are shown in Fig. 1.

The images we could make are generally rather 'crude' due to the poor coverage of the aperture plane (UV coverage). The observing array is mainly oriented north-south and the observing time for each source was quite short. The rms noise we achieved is

at best ~ 1 mJy/beam. The observed morphologies can be summarized as follows: 8 sources are point like with the resolution we achieved (3.5×9 mas² and 12×30 mas² for the X- and S-band respectively); 10 sources are resolved: 6 sources were found with a double-lobe morphology; 2 are core-jet and 1 shows a more complex structure. On the bases of the present data we can confirm a significant correlation between the overall radio spectrum and the VLBI morphology. In particular, for unresolved sources the the radio spectrum peaks at frequencies as high as 5 GHz or even higher.

Acknowledgements. The authors wish to thanks the staff at the stations for their collaboration during the observations and the correlator staff for the data processing.

References

- Dallacasa & Stanghellini (1990) *Compact Steep-Spectrum & GHz-Peaked Spectrum Radio Sources*. Workshop held in Dwingeloo, ed. by C. Fanti, R. Fanti, C.P. O'Dea and R. Schilizzi
- Dallacasa et al. (1995) *Astron.Astrophys* **295**, 27
- Fanti et al. (1990) *Astron.Astrophys* **231**, 333
- Fanti et al. (1995) *Astron.Astrophys* in press
- Peacock J.A. & Wall J.V. (1982) *Monthly Notices Roy. Astron. Soc.*, **198**, 843
- Sanghera et al. (1995) *Astron.Astrophys* **295**, 629
- Spencer et al. (1991) *Monthly Notices Roy. Astron. Soc.*, **250**, 225

IAU Name	LAS mas	Morph.	S_{CDF} Jy	X_{CDF} Jy
0201+113	10	P	0.56	0.31
0237-027		S	0.26	0.42
0237-233		S?	3.27	0.90
0500+019		S	1.56	1.02
0511-220		S-P	0.33	
0743-006		P	0.70	
0922+055		S? C-J?	0.45	
0941-080		D?	0.92	
0941+261		ND	-	-
1143-245	-	S	1.11	
1237-101		S	0.82	
1317-005		P	0.18	
1502+036		P-S	0.51	
1518+047		D	1.69	
1607+268		D	2.39	1.07
1629+120		D	0.29	
1848+283		P	0.24	
2044-027		S	0.29	
2053-201	-	ND	-	-
2126-158	60	P	0.56	
2128+048		D?	2.25	1.28
2137+209		S	0.63	
2210+016		T-CPLX	1.20	0.40
2223+210		S	0.79	
2351-006		P	0.29	
1402-012		P	0.49	0.30
1602+576		D?	0.56	0.34
1629+680		C-J	0.79	0.20
1801+010	120	P	1.64	1.05

P = pointlike; S = single component, resolved either at S or at X band (or both);
D = double; C-J = core-jet; T = triple; CPLX = complex. ND = Not Detected!

Table 1.

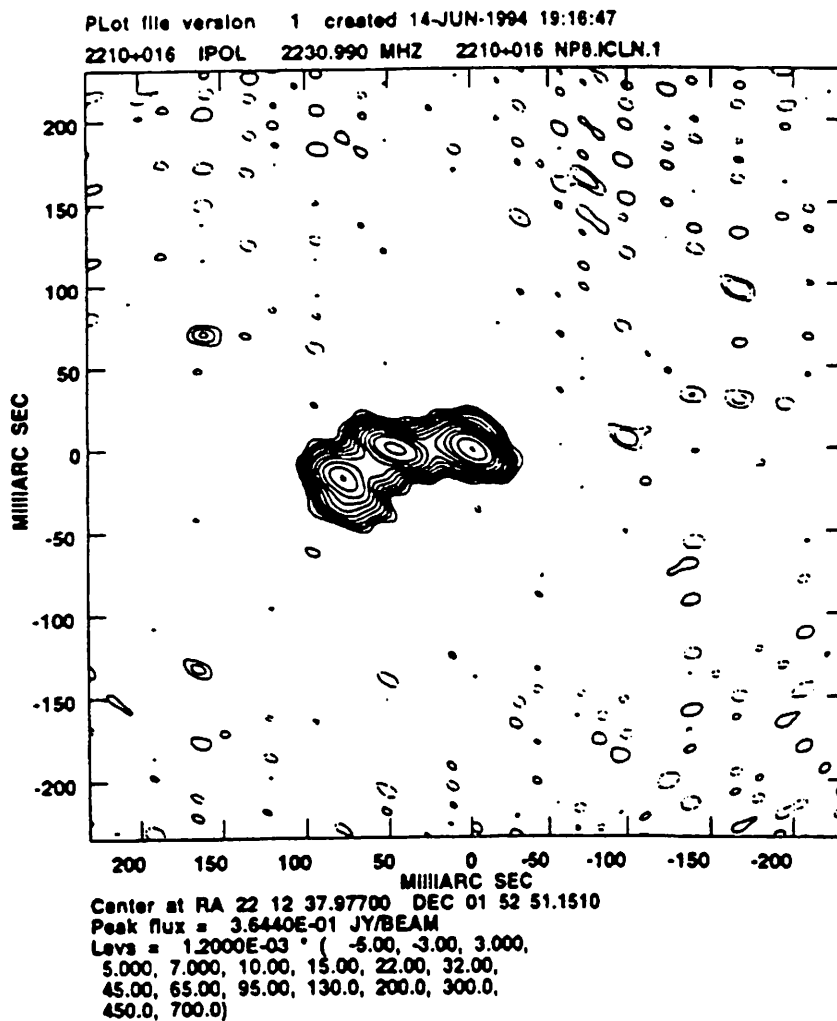
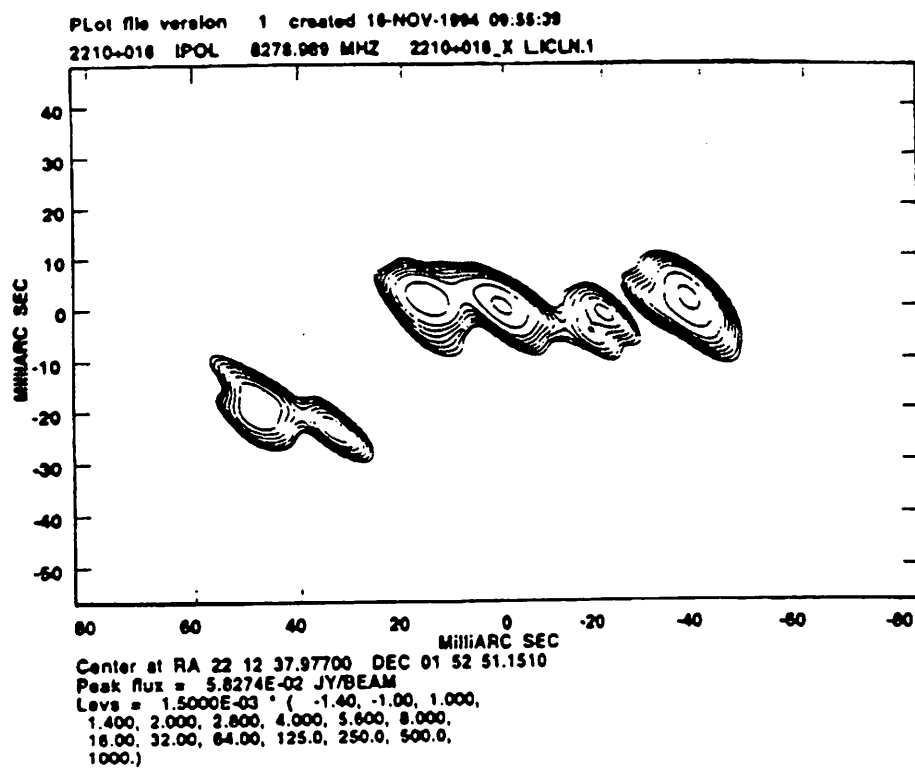


Figure 1

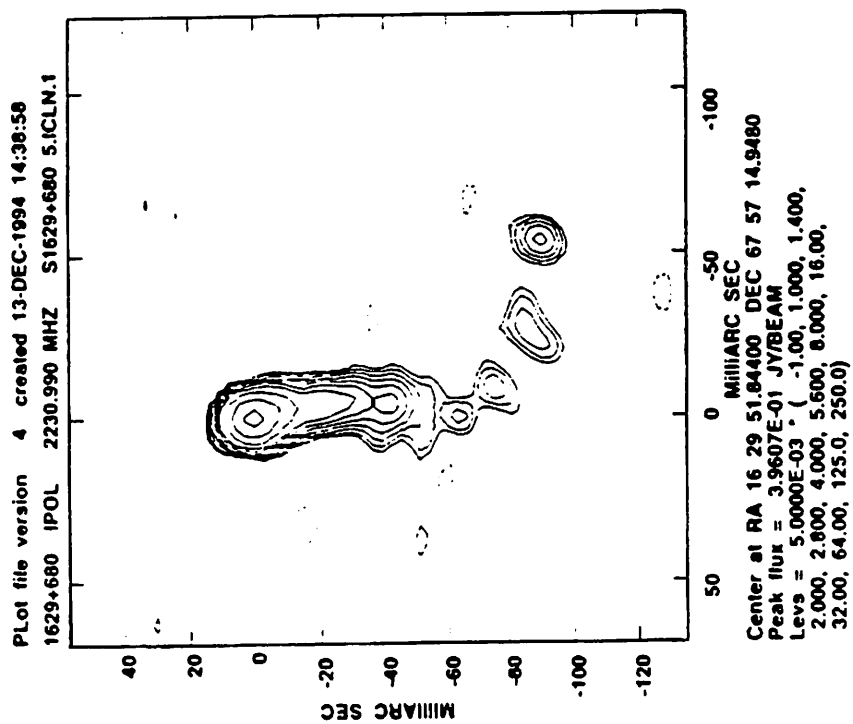
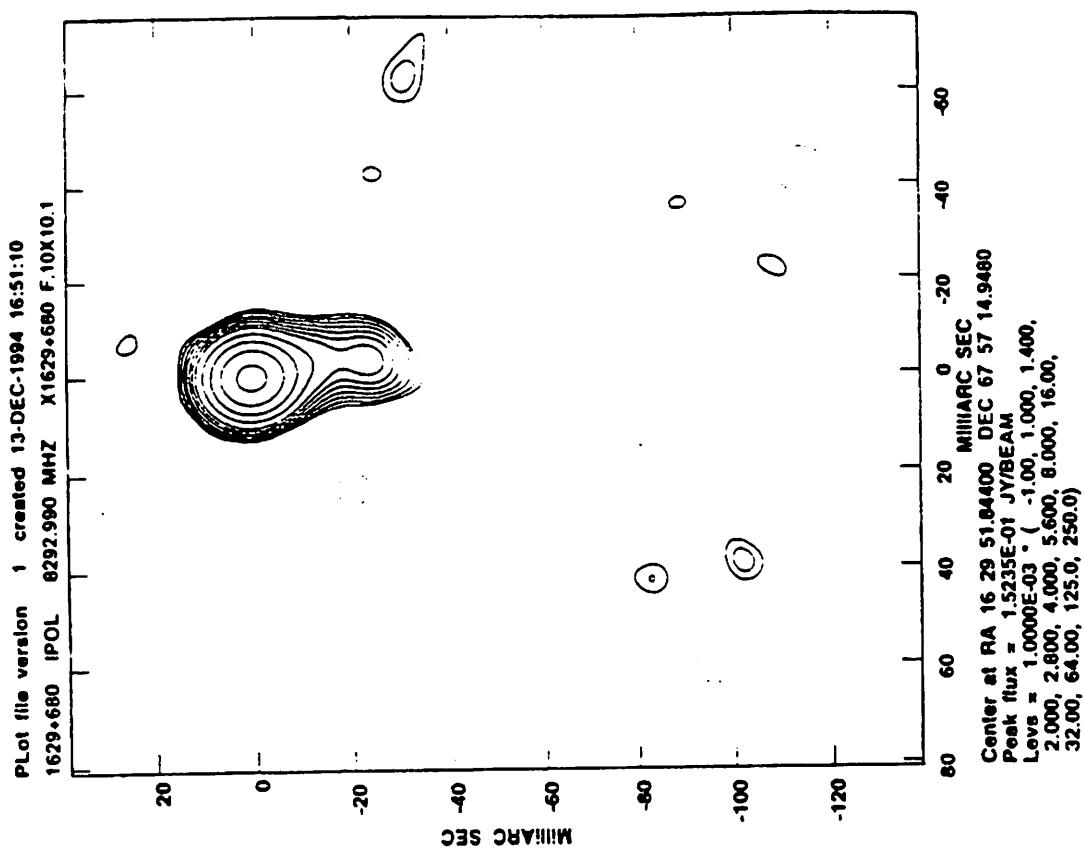


Figure 1 cont.

A “CLUSTER-CLUSTER” VLBI EXPERIMENT

M.J. Rioja^{1,4}, L.I. Gurvits^{1,2,3}, R.T. Schilizzi¹, A. van Ardenne², A.-J. Boonstra², J. Bregman²,
H.R. Butcher², A.R. Foley², H. Kahlmann², T.A.Th. Spoelstra², H. van Someren Greve²,
W. Alef⁴, M.J. Claussen⁵, E.B. Fomalont⁵, Y. Asaki⁶, T. Sasao⁶

¹*Joint Institute for VLBI in Europe, Dwingeloo, The Netherlands*

²*Netherlands Foundation for Research in Astronomy, Dwingeloo, The Netherlands*

³*Astro Space Center of P.N. Lebedev Physics Institute, Moscow, Russia*

⁴*Max-Planck-Institut für Radioastronomie, Bonn, Germany*

⁵*National Radio Astronomy Observatory, Socorro, U.S.A.*

⁶*Mizusawa Observatory, Japan*

Abstract: VLBI between sites with multiple antenna elements holds out the prospect of solving for certain geodetic parameters in a new way. By making simultaneous observations of 4 sources on the separate ‘sub-baselines’ between sub-elements from one site to the other, quasi instantaneous determinations of EOP and station locations can be made. We describe the results of the first test observations using this technique with the Westerbork and VLA arrays.

1 Introduction

The Cluster-Cluster (Cl-Cl) or multiview VLBI technique is a development of the observational capability of the VLBI technique applied to geodesy and astrometry. It presumes simultaneous use of a group of identical antennas, equipped with a phase stable signal transmission system and a precise phase calibration system, fed from a common frequency standard at each end of a VLBI baseline. The relative positions of the antennas should be precisely monitored by ground geodetic measurements.

As is shown by Sasao and Morimoto (1991) and Kawano et al. (1994), the particular case of four antennas in each group allows:

- To determine the 3 spatial components of the baseline vector and the clock offset at once, by simultaneous observations of 4 radio sources with known position.
- To measure radio source positions in direct reference to other sources, without invoking any precession-nutation model or equatorial system.
- To yield precise relative positions and proper motions of close radio sources, using the differential VLBI and phase-referencing technique.
- To derive the Earth orientation parameters at a high rate by combining the Cluster-Cluster and the traditional geodetic VLBI technique.

The Cl-Cl VLBI is a natural development of a so called “dual baseline interferometry” demonstrated with two antennas at NRAO (Green Bank, West Virginia) and two antennas at the Owens Valley Radio Observatory (California) in 1972 (Hemenway 1974), and, in another experiment, with two antennas at NRAO/Green Bank and two antennas at Haystack (Counselman et al. 1974). The

application of the phase-referencing techniques in the analysis of Cl-Cl observations benefits from the simultaneous observations of the reference and target sources. Otherwise, it generally requires a switching cycle of the single telescope between the sources. The same applies to differential VLBI astrometric techniques. Moreover, in observations of weak sources, the collecting area may be increased simply re-distributing the number of telescopes pointing to each source. The multidirectional character implicit to this technique helps to a better modeling of the spatial structure of the propagation medium contribution in the analysis of astrometric and geodetic observations, in the same way as the GPS technique does.

As discussed in several recent publications, the Cl-Cl VLBI technique can accomplish the tasks above better (more accurately and faster) than any other known technique (Sasao et al. 1994, Hara et al. 1994). At present the WSRT and VLA are the only multi-antenna telescopes equipped with compatible VLBI instrumentation. However, the use of WSRT and VLA in Cl-Cl VLBI regime requires a few special non-standard technical features. An observational detection test has been carried out in order to demonstrate the feasibility of the technique and to verify the implementation of these non-standard instrumental features.

2 Instrumental implementation at the WSRT and VLA

The following features must be implemented at WSRT and VLA in order to conduct Cl-Cl VLBI observations with N antenna subarrays at each VLBI site:

- The ability to point N subarrays in different directions and to apply fringe stopping and delay control.
- To form N independent RF and IF signals and to convert the latter into a format compatible with a standard MK3 video converter (VC).
- To form N parallel MK3 baseband signals from N subarrays and to record them in one of the standard Mk3 modes on one tape.

At the WSRT, most of these hard- and software requirements were implemented in preparation for the 21/92 cm observational campaign on for the comet Shoemaker-Levy 9 encounter with Jupiter in July 1994.

3 Verification test of the Cl-Cl VLBI technique

A fringe verification test observation was run on 5 January 1995, for 4.5 hours, between the WSRT and the VLA. At the WSRT 12 antennas were combined in 4 subarrays designated as "Green" (G), "Red" (R), "blue" (E), and "black" (K). Fig. 1 shows the assignment between telescopes, Digital Continuum Backend (DCB) and MK3 video converters (VC) used at the WSRT. At the VLA two individual antennas participated, VLA_A and VLA_B. For scheduling convenience, the entire test was arbitrarily divided into two simultaneous "experiments", Cl_01, and Cl_02. The combination of "(G + E) & VLA_A" constituted experiment Cl_01, while the combination "(R + K) & VLA_B" constituted experiment Cl_02. The schedules of experiments Cl_01 and Cl_01 were organized as

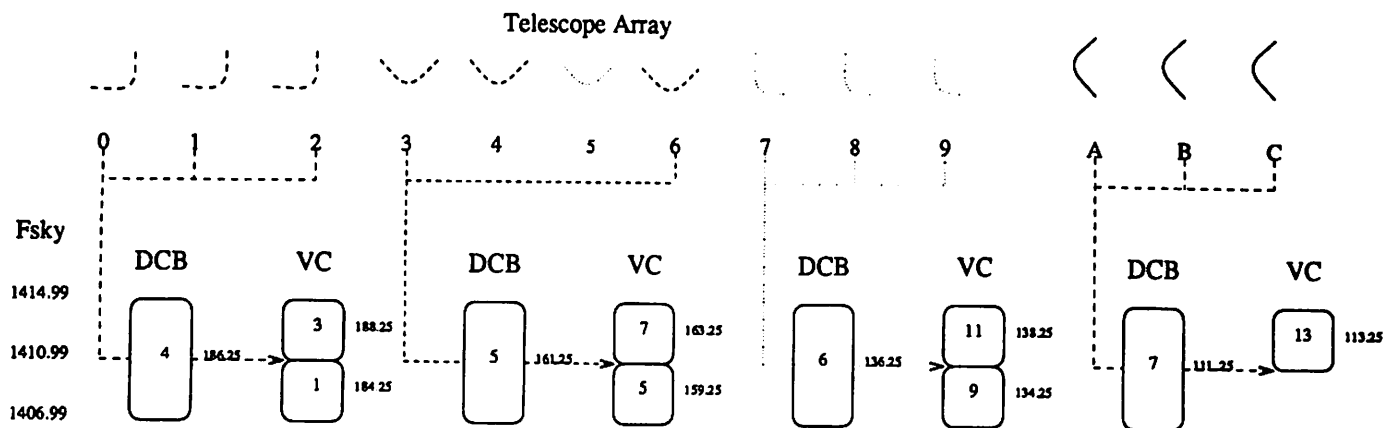


Figure 1: Observational scheme used at the WSRT in Cl-Cl mode. All DCB bands were set to the same frequency. The telescopes were combined in 4 subarrays: Green (telescopes 0, 1 and 2), Red (3, 4 and 6), blueE (7, 8 and 9) and black (A, B and C). Telescopes 5 and D were not used.

alternating observations on the same sources. The duration of a single scan was about 13 min. In addition, during three of the scans, both experiments (i.e. all telescopes) observed the same source, NRAO 140, simultaneously. This schedule allowed to achieve a comprehensive cross-examination of all parts of the instrumentation involved.

The correlation was done using the MPfR correlator. The correlation of scans for which the subarrays were looking at different sources in the sky had to be done in separate passes, as the MK3 correlator can only process data with a single sky position in one run. The setup for the correlation had to reflect the particular tracks on the MK3 tape used for the source to be correlated, as well as the reference positions of the VLA antenna/WSRT subarray. The capability of the MK4 playback units to switch tape tracks to different output tracks had to be used to correlate all 4 possible combination of sub-elements when all the telescopes observed NRAO 140.

Interference fringes have been successfully detected for all sources in both experiments and all available scans. Fig. 2 shows an example of the alternating registration of fringes in Cl_01 and Cl_02 for the sources 3C84 and 0300+470.

4 Conclusions and future plans

The verification test has demonstrated that the WSRT and the VLA are capable to carrying out Cl-Cl VLBI observations. Further elaboration of the technique will concentrate on particular scientific tasks, such as the astrometry of weak continuum and spectral line radio sources and phase-referencing VLBI observations of weak sources.

Another run of Cl-Cl VLBI observations was conducted on June 1995. At present, the data are waiting to be correlated. The aim of this latter project is to measure the isoplanatic patch size and related effects on wave front perturbations.

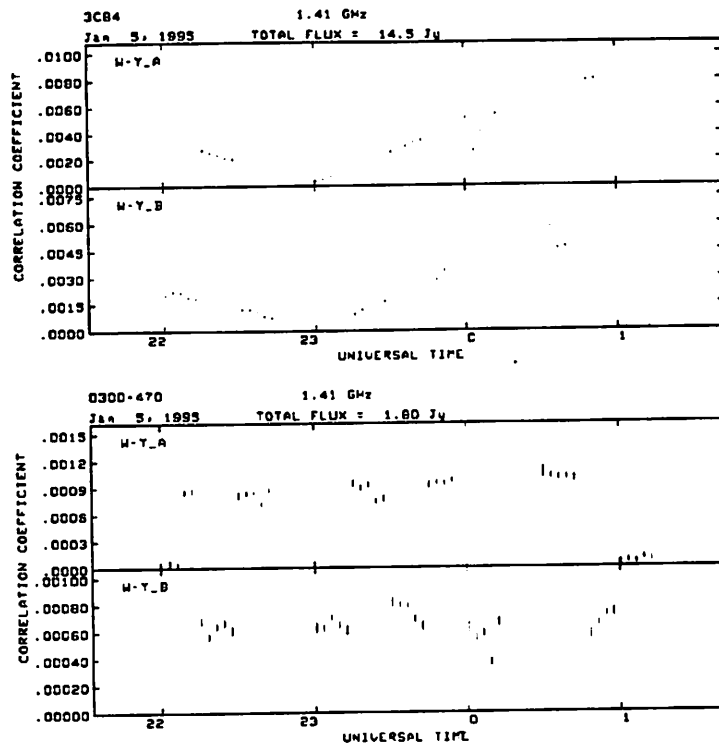


Figure 2: An example of the correlated (uncalibrated) amplitude of the verification test experiments CL01 (*W-Y_A*) and CL02 (*W-Y_B*) for the sources 3C84 and 0300+470.

5 References

- Counselman III C.C. et al. 1974, Phys. Rev. Lett. 33, No. 27, 1621
- Hara T. et al. 1994, in the Proceedings of the Symposium "VLBI Technology: Progress and Future Observational Possibilities", eds. T.Sasao, S.Manabe, O.Kameya, M.Inoue, Universal Ac. Press, 264
- Hemenway P.D. 1974, PhD Thesis "The measurement of position, baseline, and time using 4-antenna interferometry", University of Virginia
- Kawano N., Sasao T., Hara T., Sato K.-H., Iwadata K., Asaki Y., 1994, in the Proceedings of the Symposium "VLBI Technology: Progress and Future Observational Possibilities", eds. T.Sasao, S.Manabe, O.Kameya, M.Inoue, Universal Ac. Press, 232
- Sasao T. et al. 1994, in the Proceedings of the Symposium "VLBI Technology: Progress and Future Observational Possibilities", eds. T.Sasao, S.Manabe, O.Kameya, M.Inoue, Universal Ac. Press, 254
- Sasao T. and Morimoto M. 1991, Proceedings of Chapman Conference on Geodetic VLBI: Monitoring Global Change, 48

Success and Limitations of X- and S/X-band Astronomical Observations with the EVN and The Geodetic VLBI Network

Walter ALEF¹ and Maria RIOJA^{1,2}

¹ *Max-Planck-Institut für Radioastronomie, Bonn, Germany*

² *Joint Institute for VLBI in Europe, Dwingeloo, The Netherlands*

Abstract. We recently conducted several VLBI observations at X- and S/X-band using telescopes of the European VLBI Network, affiliated telescopes and geodetic telescopes in Europe, Africa and Asia. We discuss the potential of such an array for astronomical and astrometric work. We report about our experience with different frequency and recording setups, and give suggestions of how to make the astronomical frequency standard for X- and S/X-band observations more compatible with geodetic modes.

1 Introduction

VLBI observing at X-band (8.4 GHz) offers high sensitivity and high resolution, and suffers little from atmospheric and ionospheric disturbances. In combination with simultaneously recorded S-band (2.3 GHz) data the influence of the ionosphere can even be removed to better than 90%, which is a very important prerequisite for high precision astrometric observations.

In contrast to the importance of X- and S/X-band observations, there are only a few telescopes in the EVN which support this frequency pair. Therefore the coverage of the aperture plane (UV-plane) for EVN-only observations at these frequencies is poor (see fig. 1 for original EVN and fig. 2 for present EVN), which means low resolution, low sensitivity and low map fidelity for any astronomical observation at X- or S/X-band. Map fidelity, resolution and map sensitivity can only be increased further in the EVN by adding more telescopes. The coverage of the UV-plane should be as complete as possible.

In order to be able to perform state of the art X-band observations with the EVN a possible solution is the addition of geodetic antennas in Europe, Africa, and Asia: Wettzell, Matera, Madrid (34 m or 70 m), Ny Ålesund, Hartebeesthoek, Crimea, and Kashima. The resulting coverage is impressive (see fig. 3); the achievable sensitivity is on the order of $45\mu\text{Jy}$ (1σ noise level) in 6 to 8 hours observing. This is comparable to what can be achieved with the VLBA, while its coverage and resolution are superior to than of the VLBA (see fig. 4)

The disadvantage of using such a hybrid array of EVN plus geodetic stations is that the participation of geodetic antennas has to be organized outside of the network. The user has to ask for observing time, organize the tape shipments, and has to make sure that the geodetic stations receive the schedules and that the logs are sent to the correlator. A normal user of the EVN cannot fulfil these requirements without help from people at the correlator. This limits these kind of observations to a small community.

DA193

BONN BOLOGNA ONSALA NOTO

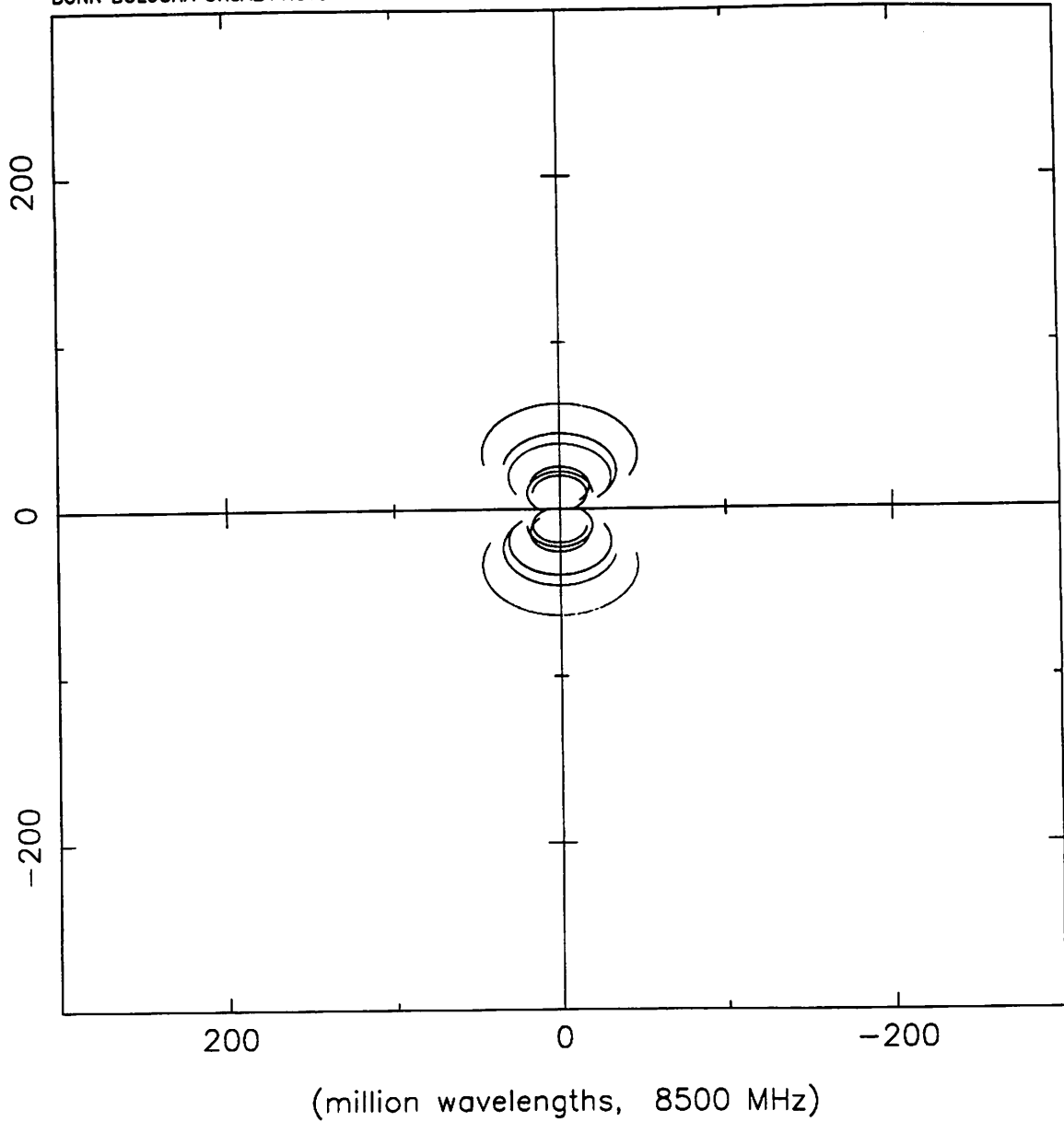


Figure 1: Full-track coverage of the aperture plane (UV-plane) for DA193 ($\delta = 39^\circ$) for the original EVN (up to 1993) with Effelsberg, Onsala, Medicina and Noto. The diameter of the earth corresponds to nearly 300 Mega-waves at X-band.

DA193

BONN BOLOGNA ONSALA NOTO SESHAN URUMQI

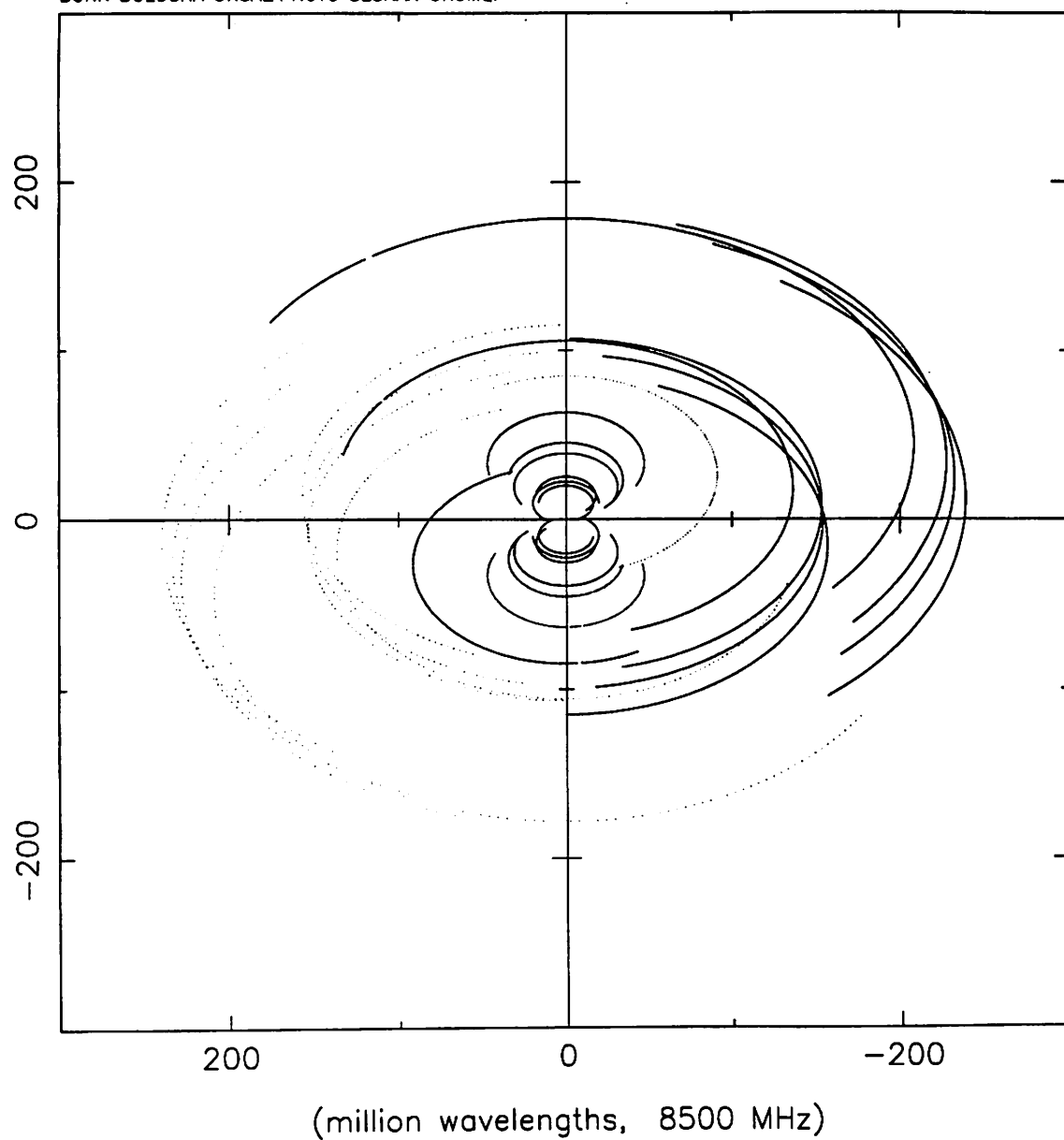


Figure 2: Full-track coverage of the aperture plane for DA193 with the present EVN: includes Shanghai and Urumqi. The coverage is already improved.

DA193

BONN BOLOGNA ONSALA NOTO SESHAN CRIMEA WETZELL MATERA URUMQI DSS63 NYALES20 KASHIMA

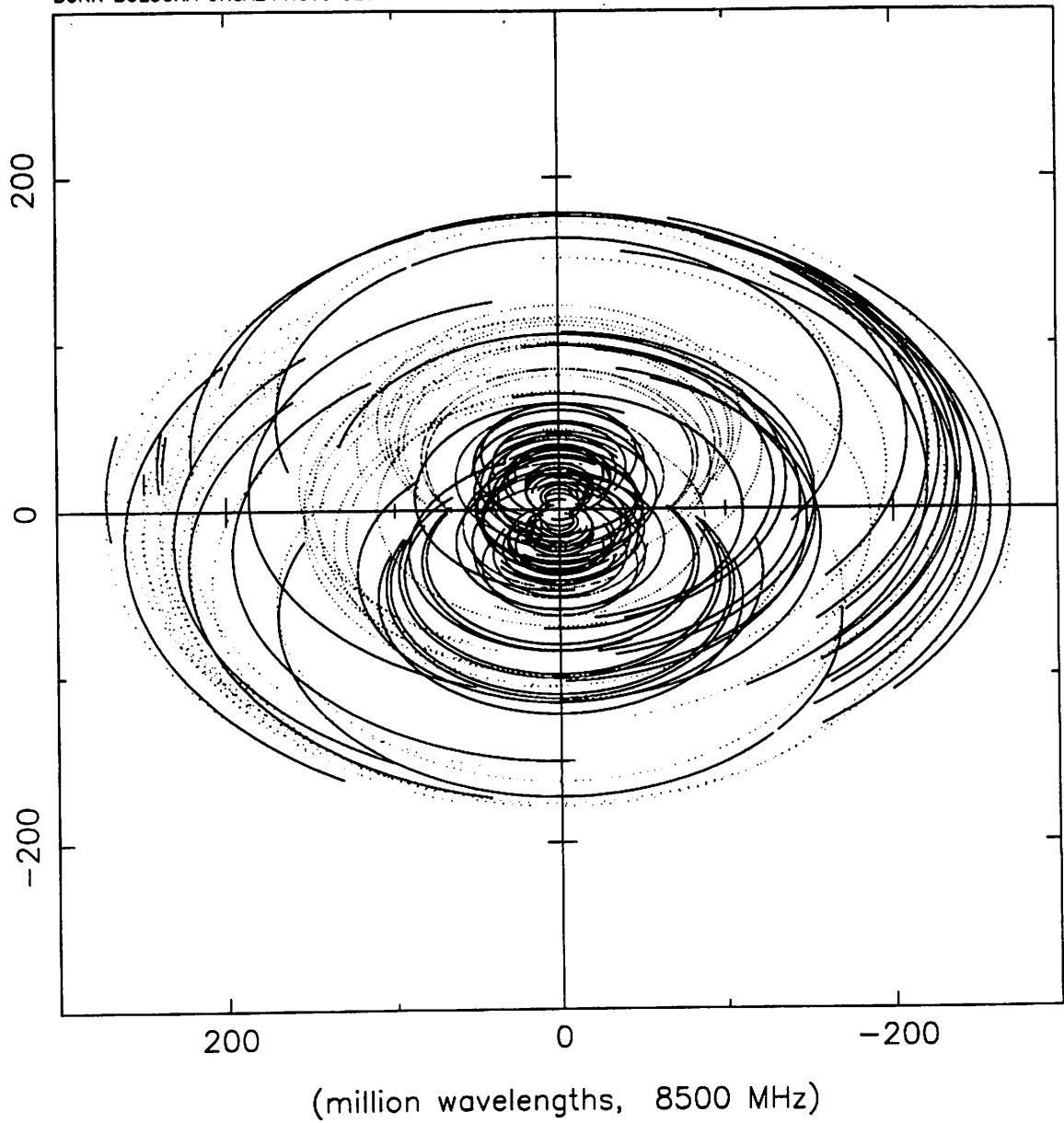


Figure 3: Full-track coverage of the UV-plane for DA193 for the EVN combined with the geodetic telescopes Wettzell, Matera, Madrid, Ny Ålesund, Crimea, and Kashima.

DA193

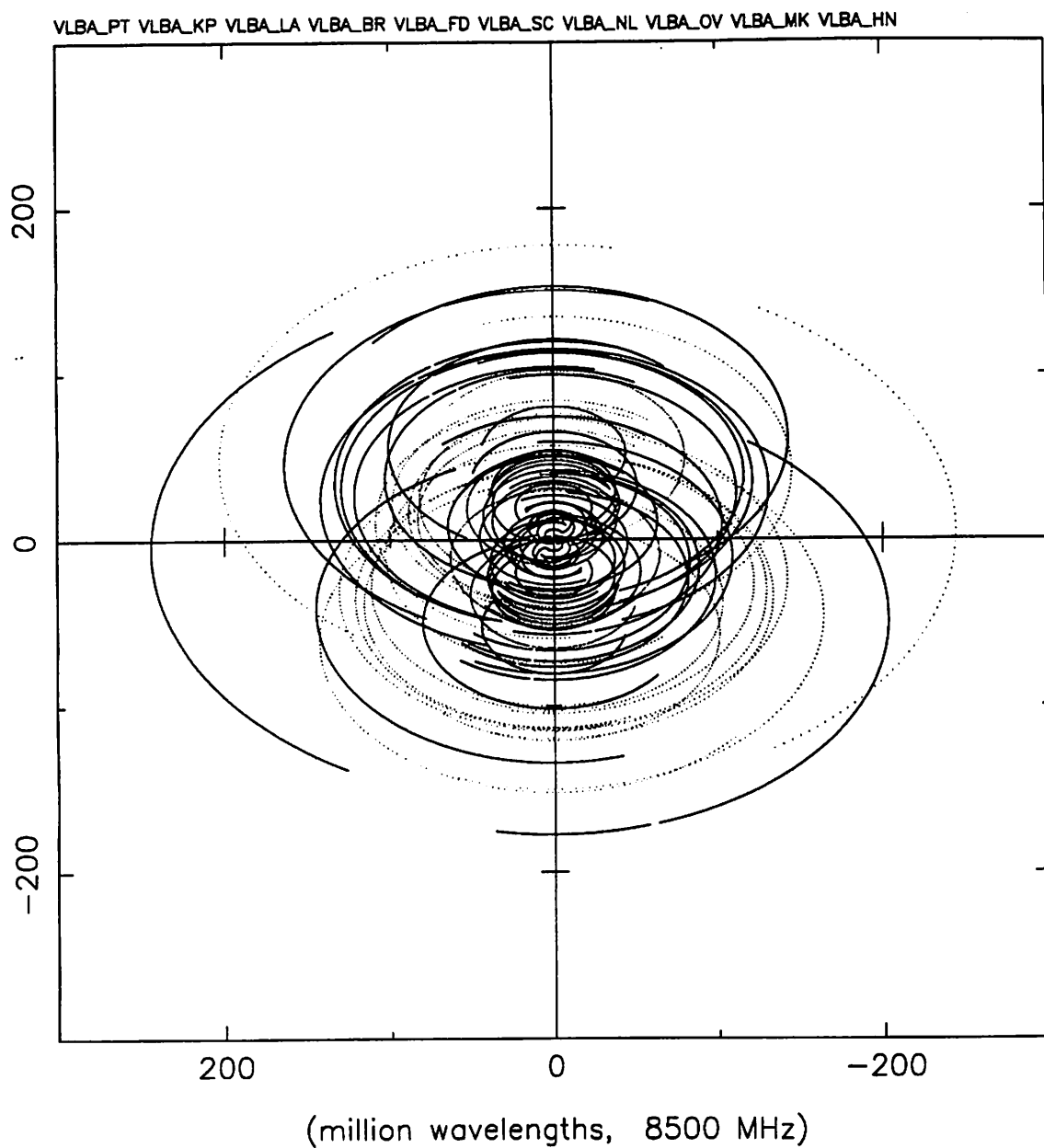


Figure 4: Full-track coverage of the aperture plane for DA193 with the 10 telescopes of the VLBA.

2 Types of astronomical observations

Various kinds of astronomical observations can profit from the large EVN/Geo array. In the standard mapping projects better maps can be made due to the improved coverage and sensitivity. If both S- and X-band are observed simultaneously the instantaneous spectral index of the observed object can be determined. Astrometric observations like phase-referencing astrometry are ideal for the EVN/Geo array, because the technique of observing employed is very similar to the standard geodetic observing mode. Finally, the so-called phase-reference mapping projects, where very weak objects are mapped with rapid switching between a strong nearby phase-calibrator and the source of interest, need all the sensitivity available to get the target source above the noise in the map.

3 History of EVN/Geo observations

Even before 1990 a few observations were performed with a mixed array of astronomical and geodetic antennas. Typically these observations were conducted outside the standard network session. Since 1990 the number of such observations has increased.

The most recent successful observations were mostly conducted in official EVN observing sessions.

- ED3A and ED3B in September 1993 using S/X band in astronomical setup, recorded in MK3 Mode A with the 4 European EVN stations plus Wettzell and Matera (see article by F. Mantovani et al. in these proceedings).
- BQ1A in March 1994 using S/X band in astronomical setup, recorded in MK3 Mode C with 6 EVN telescopes, some VLBA stations and Matera and Wettzell.
- ED3C: third part of ED3 in May 1994; same setup as ED3A/B.
- EA6A/B in February 1995. This phase-reference mapping project used only X-band in Mode A to achieve highest sensitivity. All available telescopes were used: the 5 EVN stations, Wettzell, Matera, Madrid (34 m), Hartrao, Ny Ålesund, Kashima and Crimea.
- ER1 also in February 1995. A standard phase-referencing project using S/X in Mode A (same as ED3) with the same telescopes as EA6 except for Madrid.

4 Incompatibilities

The geodetic requirement of a wide synthesized bandwidth is in conflict with the astronomical requirement to have a contiguous band of as much bandwidth as possible. This leads to incompatibilities in how the local oscillators and MK3 record terminals are set up. In order to switch between astronomical and geodetic observing modes, the IF to video converter

patching in the MK3 terminals, and sometimes also the local oscillator frequencies, have to be changed.

The standard geodetic setup has video converters 1 to 8 assigned to X-band and the remaining converters 9 to 14 assigned to S-band. The recorded band is sampled between 8182 and 8863 MHz for X-band and 2212 and 2323 MHz at S-band¹. The recording mode is usually 'C'.

There are a number of astronomical setups on the other hand, which makes astronomical observing at geodetic stations more difficult. Standard astronomical observing and recording modes are:

- 7 X-band frequencies in 1 block in the range 8390 to 8440 MHz. The recording modes can be B (28 MHz bandwidth) or E (14 MHz bandwidth).
- 14 X-band frequencies in 1 block in the interval from 8408 to 8422 MHz. Both polarizations are recorded in either mode 'A' or 'C'. The odd video converters are connected to RHC (right hand circular) and the even ones to LHC. Left circular polarization (LHC) is usually not available at pure geodetic telescopes.
- 14 X-band frequencies spanning the range from 8386 to 8442 MHz. Recording mode is 'A' (56 MHz), RHC only.
- 7 X-band (odd VCs) and 7 S-band (even VCs) frequencies with recording modes 'A' or 'C'. No mode 'C' standard has been defined.
- 8 X-band (VCs 1 to 8) and 6 S-band (VCs 9 to 14) frequencies again with modes 'A' or 'C' and right circular polarization. The frequency ranges are 8276 to 8308 MHz and 2218 to 2242 MHz respectively. This is the mode most compatible with geodetic observing. It is not an official standard, but has been used successfully since the ED3 observations. This setup needs re-patching at the astronomical sites.

5 How to improve EVN/Geo observing

The most urgent improvement needed follows from the description of the different observing setups in the previous section. As the re-patching and LO frequency incompatibilities are the most annoying problems, we recommend a change of the astronomical standards for X- and S-band such that the frequency bands will be 8270 to 8326 MHz for X-band and 2215 to 2271 MHz for S-band. This would allow working with minimal re-patching and without LO frequency changes. In addition, non-standard frequency to track assignments can allow special recording schemes for some stations, which can now be decoded at the correlators with the help of the advanced MK4 tape electronics.

¹This frequency range is being used for IRIS observations

As one of the prime observables of the astronomers is the interference amplitude, the knowledge of the gain curves of the participating telescopes is absolutely essential for achieving competitive results. In order to measure the gain curves of the geodetic telescopes, we offer help to create a SNAP schedule which just does ON/OFF measurements while tracking a strong source.

The standard EVN schedule and log distribution via the ASTBO1 computer in Bologna should be no problem for geodetic stations. They are all connected to Internet (except Crimea) and are used to sending and receiving logs and schedules from NASA's CDDIS computer.

It would also help if we astronomers provided more general information about astronomical observing to the geodetic stations. Their participation in EVN committees would help them to stay well informed about technical and other developments in the EVN, e.g. new observing modes like 'continuous tape motion' for phase-referencing observations in the near future.

6 Other minor problems

If the astronomical observer finally tries to conduct an experiment with the EVN/Geo array he/she may find other minor problems that are unknown with other instruments.

Wettzell may have to interrupt an astronomical project for 2 to 3 hours to observe the so-called 'intensive'.

It may be totally impossible to get time in Madrid as they may be busy observing other space projects. In addition the observer is responsible for supervising the observations.

Kashima seems to record on a K4 system with subsequent copying to MK3A. The pass positions may not be correct, as this is not done regularly in Kashima. They are not accustomed to the different MK3 recording modes. Of course no standard field system logs will be available, which will make correlation painful. The schedule transmission is not well tested yet. The K4 system has a phase offset between lower (LSB) and upper sideband (USB) of each video converter which is different from both MK3 and VLBA acquisition hardware.

7 Final remarks

The experiments that were observed with the EVN/Geo network in February 1995 show that this approach is very promising. Even though initial failures at some geodetic stations resulted in significant loss of data, the overall coverage and sensitivity is still quite remarkable. The geodetic stations which participate regularly in geodetic observations and have already observed astronomical projects in the past have given an impressive and a reliable performance. If more EVN telescopes can be equipped with S/X-band receivers the potential of the network can even be increased. Unfortunately, the additional efforts and the expert knowledge needed for combining the EVN with the geodetic telescopes does not make it easily accessible for the standard user.

Structure and Astrophysics of Geodetic VLBI Sources

Silke BRITZEN and Thomas P. KRICHBAUM

Maz-Planck-Institut für Radioastronomie, Auf dem Hügel 69, 53121 Bonn, Germany

Abstract. Geodetic VLBI observations of quasars and BL Lacertae objects, designed to determine earth rotation parameters and plate tectonic effects, provide a powerful database also for astrophysical investigations of source structures and their variability on mas-scales.

With geodetic VLBI data it is possible to monitor the kinematics of AGN-cores on a monthly timebasis. Here we present preliminary results for two sources, covering an observing period of 1986 to 1993. The BL Lac object 1803+78 shows a complex – possibly bent – jet with embedded stationary and superluminally moving components.

The data obtained for the γ -ray bright blazar PKS 0528+134 allow to investigate correlations between its broad-band flux density activity and its structural variability.

1 Introduction

With the operation of the VLBA, now it will become possible to monitor the structural evolution of AGN with considerably improved time resolution. However such observations just have started. Quite complementary to the VLBA monitoring, the geodetic VLBI campaigns provide a data base, which covers an observing period starting in the mid eighties, thus providing regularly sampled VLBI data also at times before the VLBA was put into operation.

With a time sampling of up to one observation per month, the analysis of the geodetic VLBI data could reveal a much more detailed picture of the kinematics in compact radio sources. On the basis of geodetic VLBI data maps with a typical dynamic range of 50 – 75:1 it will be possible to determine the trajectories and velocities of the VLBI jet components with much higher accuracy, required in particular with regard to the complex motion patterns seen in an increasing number of radio sources ([9], [16]).

VLBI-monitoring data obtained in the past sometimes suffered from non-unique cross identifications of VLBI components visible in maps obtained at different observing epochs, in particular if these components were moving faster than a few tens of a milliarcsecond per year. The probability of such mis-identifications is dramatically reduced in densely sampled monitoring data, e.g. the geodetic data base.

Preliminary analysis showed that at least 7 sources of the IRIS-S sample can be reliably mapped. Here we present an intermediate status report of our ongoing data analysis for two objects. For the BL Lac object 1803+78 the X-band (8.4 GHz) data shown here span the period 1986.21 to 1992.34 (43 maps), for 0528+134 results covering the period 1991 to 1993 are shown.

2 The short-time structural variability of 1803+784

The BL Lac object 1803+78 ($z=0.68$) is a member of the S5-VLBI sample and is regularly observed at all available frequencies and angular resolutions since the late 1970's ([3], [4], [15]). On mas-scales the source shows a pronounced jet with prominent jet components located at relative core separations of 1.4, 5, and 12 mas ([3]). Geodetic and astronomical VLBI data gathered between 1979 – 1985 revealed apparent stationarity of the component located at 1.4 mas ([14]). High frequency VLBI observations at 22 & 43 GHz allowed to monitor the motion of jet components located at smaller core separations ($r < 1.4$ mas) ([8]). These inner jet components move superluminally with possibly variable speed $\beta_{app} \leq 4$ ($H_0 = 100 km s^{-1} (Mpc)^{-1}$, $q_0 = 0.5$) along a curved path, suggesting helical motion ([9]). Such curved jet morphology is found also at

larger core separations from VLBI-maps obtained at S & X-band ([1]).

The data obtained so far suggest the existence of a spatially curved helical jet in 1803+78. A more detailed investigation of the complex kinematics (coexistence of moving and stationary components, curved trajectories) clearly is required to improve our understanding of astrophysical jets.

Here we present 43 X-band maps obtained mainly from the IRIS and IRIS-S observing campaigns. Details of the observations are summarized in table 1. After data export from the correlator, amplitude calibration, and removal of bad data (for details see [13]), the data were analysed using the standard procedures provided within the CalTech VLBI-package.

From the total of all IRIS & IRIS-S VLBI observations performed on 1803+784, we selected 43 data sets with at least 3 antennas participating. A second aspect in this selection was the aim of an almost uniform distribution of observations over the 6 year observing period from 1986 to 1992.

The data analysis of each observation was done in several steps. Starting from a point source model we mapped the source using the standard phase-selfcalibration and CLEAN algorithm. In parallel we fitted elliptical Gaussian components to the visibilities. Starting in each case from a single component model, the agreement between model and data was improved by adding further components to the model. Depending on data quality and uv-coverage models with typically 5–8 Gaussian components were obtained, providing final component parameters and error estimates for the individual features all of them seen also in the CLEAN-maps: flux density, position relative to the VLBI-core, component size and orientation. The errors of the individual parameters were estimated from a comparison between alternative Gaussian component models fitted to the same data set and from comparison between model fits and maps: as typical relative errors we obtained $\sim 20\%$ for the flux density, ± 0.15 mas for the relative core separation, $\sim 15\%$ for the component size, and $(5 - 10)^\circ$ for position angle relative to the core.

Consistent with observations at other frequencies ([3], [4], [12], [15]) we obtained a one sided core-jet structure of 1803+78, consisting of 5-8 components oriented mainly along $P.A. \simeq 270^\circ$. The identification of the components seen in the models at different times was done stepwise. First, a component located at $r = 1.3$ mas could be identified with the so called *stationary* component, already observed earlier ([14]). We labeled this component A. The prominence in flux density of the VLBI-core of 1803+78 and A (A is about 5 times brighter than the remaining jet components) facilitated then in a second step the identification of the remaining jet components on the basis of their relative positions. In figure 2 we summarize these results and show the structural evolution of 1803+78 based on Gaussian model fits to the observed visibilities.

Two inner jet components B and C seem to separate from the core with an apparent speed of $\beta_{app} \sim 6$. Whereas for the outer jet component F located at $r \simeq 2$ mas no significant motion could be detected, significant deviations from apparent stationarity now are seen for component A (located at $r \sim 1.3$ mas) and component E (located at $r \sim 1.5$ mas), with position shifts between $r \sim 0.7$ mas and $r \sim 1.5$ mas for A and $r \sim 1.2$ mas and $r \sim 1.5$ mas for E (see figure 2). Obviously the improved time sampling of the geodetic VLBI data lead to the detection of systematic position variations for components regarded as stationary on the basis of less frequently performed earlier observations.

At present it is still unclear, whether the apparent oscillations of A and E are due to intrinsic motion, blending of components unresolved by the interferometer beam at X-band or apparent shifts of the center of gravity of the brightness distribution of the component used as reference, namely the synchrotron self-absorbed flat spectrum VLBI core. The apparent correlation of two of the ‘minima’ of core separation observed for A and evident also for E with the appearance of the components B in ~ 1988.5 and C in ~ 1990.5 (see fig.2) seems to support the hypothesis of a shift of the core position. If the core shifts due to blending effects caused by the emergence of new jet components, this position offset, however, must be visible for all components. A more detailed analysis of the motion of B and C and of the somewhat ‘ill-constrained’ stationarity of F will help in clarifying this question.

3 0528+134: Variability in Radio and γ -ray regimes

The blazar PKS 0528+134 recently attracted special attention due to its extreme brightness and variability in the γ -ray regime ([5]).

The evaluation of five IRIS-S epochs revealed a bent core-jet structure of up to 10 mas length and confirmed the results from [17] for the inner few mas. Furthermore, the combination of the deduced component separations with observations at 22.2 GHz lead to the detection of superluminal motion of at least one jet component C1 [11].

Figure 3 shows a Clean-map of 0528+134 at X-band from 1991.23 obtained from IRIS-S observations.

Adding the results of two 86 GHz observations to the previously mentioned datasets, the jet of 0528+134 can be investigated at sub-mas scales as well ([6]).

Similar as in the case of 1803+784 the jet seems to be composed of moving (N1, N2, C1) and stationary components (C3, C4, see figure 3). Back-extrapolation of the motion of the most recent jet component N2 leads to 1992.9 ± 0.3 as time of ejection from the core ([6]). This date is close to the time of a prominent flare observed in the γ -ray bands (EGRET), with its maximum located at $1992.86 \leq t \leq 1993.3$ ([10]).

This date strongly suggests that N2 was ejected after the γ -flare. Clearly more data are needed to follow the motion of N2 and establish such a correlation. Geodetic VLBI monitoring could help to investigate the correlation between broad-band flux density activity (from γ - to radio-bands) and component ejection in considerably improved detail.

Acknowledgements. This work would not have been possible without the help of many people at the observatories and at the Mk III correlator. Special thanks are due to Dr. A. Witzel who initiated this project and accompanied it scientifically in every stage of progress. We also wish to thank Prof. Dr. J. Campbell for his continuous support, Dr. C. Schalinski for communicating valuable information concerning the reduction of geodetic VLBI data, and Dr. A.-M. Gontier for making the data exports and improvements of the export routine. Thanks are also due to Drs. W. Alef and K. Standke for critical discussions and Dipl. Ing. A. Müskens for his assistance at the correlator in Bonn.

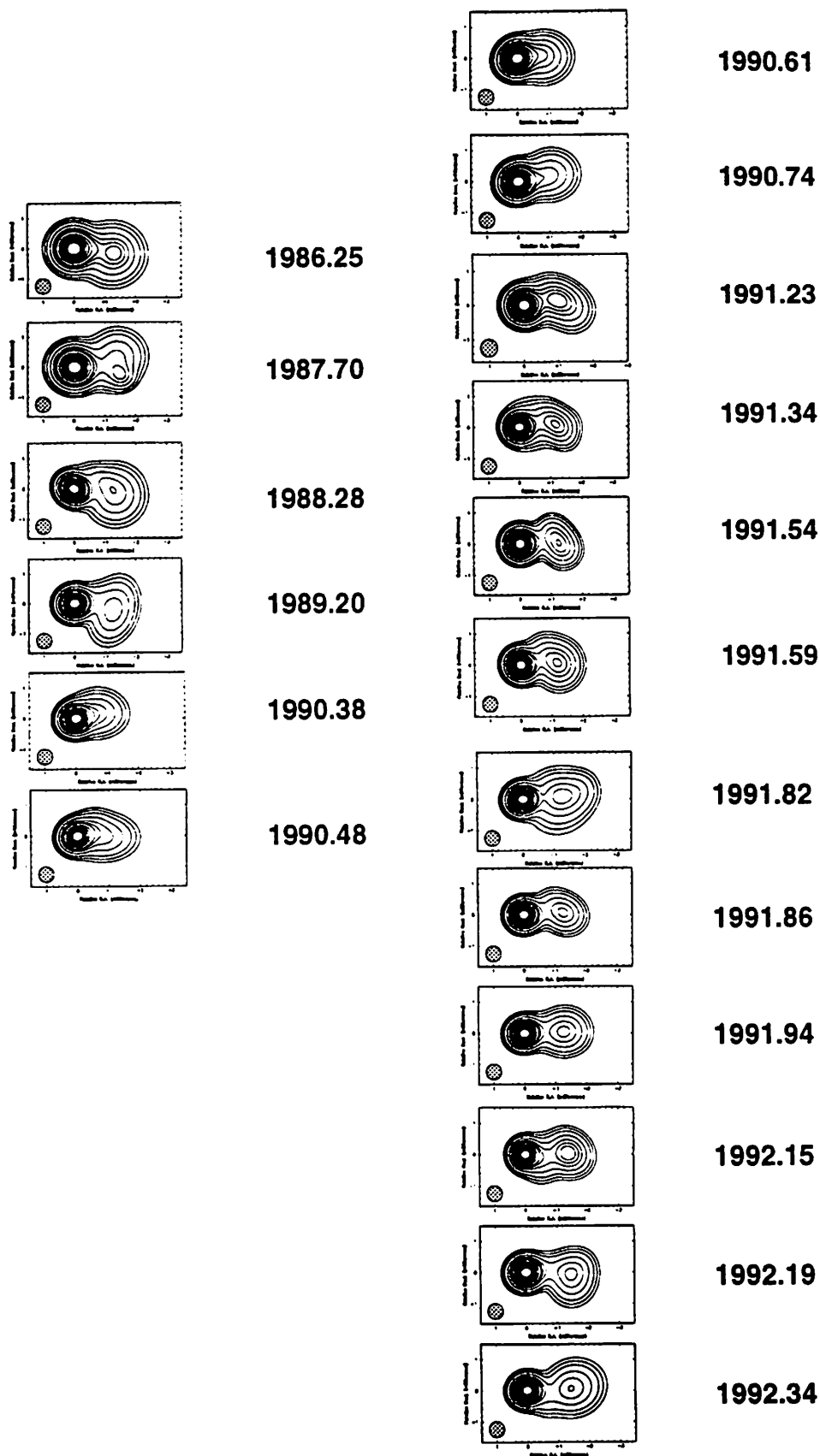
References

- [1] Britzen, S., Krichbaum, T.P., Steffen, W., Witzel, A., Schalinski, C.J., 1994, in: *Compact Extragalactic Radio Sources*, eds. Zensus, J.A. and Kellermann, K.I., NRAO-workshop, Socorro, p.251.
- [2] Britzen, S., Gontier, A.-M., Witzel, A., Schalinski, C.J., Campbell, J., (1993) in: *Proceedings of the 9th Working Meeting on European VLBI for Geodesy and Astrometry*, p.157.
- [3] Eckart, A., Witzel, A., Biermann, P., Johnston, K.J., Simon, R., Schalinski, C.J., Kühr, H., 1986, *A&A*, **168**, p.17.
- [4] Eckart, A., Witzel, A., Biermann, P., Johnston, K.J., Simon, R., Schalinski, C.J., Kühr, H., 1987, *A&A Suppl. Ser.* **67**, p.121.
- [5] Hunter, S.D., Bertsch, D.L., Dingus, B.L., et al., 1993, *ApJ*, **409**, p.134.
- [6] Krichbaum, T.P., Britzen, S., Standke, K.J., Witzel, A., Zensus, J.A., 1995, in: *Quasars and AGN: High Resolution Radio Imaging*, eds. Cohen, M. and Kellermann, K.I., *Proc. Nat. Acad. Sci., USA*, in press.

- [7] Krichbaum T.P., Standke, K.J., Graham, et al., 1994, in: *Multi-Wavelength Continuum Emission of AGN*, eds. Courvoisier, T.J.-L. and Blecha, R.A., p.187.
- [8] Krichbaum, T.P., Witzel, A., Graham, D.A., Schalinski, C.J., Zensus, J.A., 1993, in: *Subarcsecond Radio Astronomy*, eds. Davies, R.J. and Booth, R.S., p.181.
- [9] Krichbaum, T.P., Witzel, A., Standke, K.J., Graham, D.A., Schalinski, C.J., and Zensus, J.A., 1994, 'MM-VLBI: Bending of Jets in the Vicinity of AGN', in: *Compact Extragalactic Radio Sources*, eds. Zensus, J.A. and Kellermann, K.I., NRAO-workshop, Socorro, p.39-44.
- [10] Montigny, C. von, Bertsch, D.L., Chiang, J., et al., 1995, *ApJ*, **440**, p.525.
- [11] Pohl, M., Reich, W., Krichbaum, T.P., Standke, K., Britzen, S., Reuter, H.P., Reich, P., Schlickeiser, R., Fiedler, R.L., Waltman, E.B., Ghigo, F.D., Johnston, K.J., 1995, *A&A*, in press.
- [12] Schalinski, C.J., 1990, Dissertation, Universität Bonn.
- [13] Schalinski, C.J., 1985, Diplomarbeit, Universität Bonn.
- [14] Schalinski, C.J., Alef, W., Witzel, A., Campbell, J., Schuh, H., 1987, in: *The Impact of VLBI on Astrophysics and Geophysics*, Proc. of the IAU Symp. No. 129, Cambridge, Mass., USA, p.359.
- [15] Witzel, A., Schalinski C.J., Johnston K.J., Biermann, P.L., Krichbaum, T.P., Hummel, C.A., Eckart, A., 1988, *A&A*, **206**, p.245.
- [16] Zensus, J.A., Krichbaum, T.P., and Lobanov, A.P., 'Morphology of High-Luminosity Compact Radio Sources', 1995, in: *Quasars and AGN: High Resolution Radio Imaging*, eds. M. Cohen and K. Kellermann, *Proc. Nat. Acad. Sci., USA*, in press.
- [17] Zhang, Y.F., Marsher, A.P., Aller, H.D., et al., 1994, *ApJ*, **432**, p.91.

<i>Experiment</i>	<i>Epoch</i>	<i>Telescopes</i>	<i>N</i>
IRIS313	1986.21	WS/HR/O/WT	308
IRIS316	1986.25	WS/HR/O/WT	404
IRIS345	1986.65	WS/HR/O/WT	293
IRIS359	1986.84	WS/HR/O/WT	348
IRIS366	1986.94	WS/HR/O/WT	338
IRIS390	1987.26	WS/HR/O/WT	373
IRIS422	1987.70	WS/HR/O/WT	318
IRIS457	1988.18	WS/HR/O/WT	455
IRIS464	1988.28	WS/HR/O/WT	464
IRIS468	1988.33	WS/HR/O/WT	443
IRIS477	1988.46	WS/HR/O/WT	181
IRIS492	1988.66	WS/HR/O/WT	251
IRIS496	1988.72	WS/HR/O/WT	250
IRIS506	1988.85	WS/HR/O/WT	262
E.ATL-5	1988.95	D/ME/WT/O/WS	295
IRIS513	1988.95	WT/HR/WS	78
IRIS531	1989.20	WS/WT/O/HR	231
IRIS540	1989.32	WS/WT/HR/O	259
IRIS-P30	1989.72	K/G/M	69
IRIS-S26	1990.08	WT/M/WS	37
IRIS-S29	1990.31	WT/M/WS	97
IRIS-S30	1990.38	WT/M/WS	104
SHAWE90A	1990.25	K/WT/SE	99
IRIS-S31	1990.48	WT/M/WS	65
IRIS-S32	1990.54	WT/M/WS	43
IRIS-S33	1990.61	WT/M/WS	42
IRIS-S34	1990.74	WT/M/WS	23
IRIS-S37	1990.94	WT/HA/WS/R/M	65
IRIS-S39	1991.12	WT/M/WS	100
IRIS-S40	1991.23	WT/M/WS	103
IRIS-S41	1991.31	WT/M/WS	106
IRIS-S42	1991.34	M/N/WS/WT	43
IRIS-S43	1991.44	WT/M/WS	89
IRIS-S44	1991.54	M/N/WS/WT	127
IRIS-S45	1991.59	M/N/WS/WT	148
IRIS-S46	1991.67	M/N/WS/WT	123
IRIS-S47	1991.82	WT/M/WS	131
IRIS-S48	1991.86	WT/M/WS	130
IRIS-S49	1991.94	WT/M/WS	110
IRIS-S51	1992.15	WT/M/WS	111
IRIS-S52	1992.19	WT/M/WS	104
IRIS-S54	1992.34	WT/M/WS/SE	176

Figure 1: The table above lists the geodetic VLBI campaigns analyzed so far, the dates of the observations, the antennas and the number of scans. Column 4 shows the number of scans observed for 1803+784 which should serve as a crude measure of the uv-coverage. Abbreviations have been used for the participating telescopes: *D*: Spain (DSN-Madrid, 34 m), *K*: Japan (Kashima, 26 m), *G*: Alaska (Gilcreek, 25 m), *M*: USA (Mojave, 12 m), *ME*: Italy (Medicina, 32 m), *N*: Italy (Noto, 32 m), *O*: Sweden (Onsala, 20 m), *HA*: South-Africa (Hartebeesthoek, 26 m), *HR*: USA (Ford Davis, 25 m), *R*: USA (Richmond, 18 m), *SE*: China (Seshan, 25 m), *WS*: USA (Westford, 18 m), *WT*: Germany (Wettzell, 20 m).



The figure shows 18 modelfits of 1803+784, calculated for the inner 2 mas on the basis of IRIS and IRIS-S VLBI data. Contours are 1, 2, 5, 10, 17, 25, 35, ..., and 95 % of the peak brightness. The convolving circular beam is 0.5 mas, the rectangles are 5 mas \times 3 mas in size.

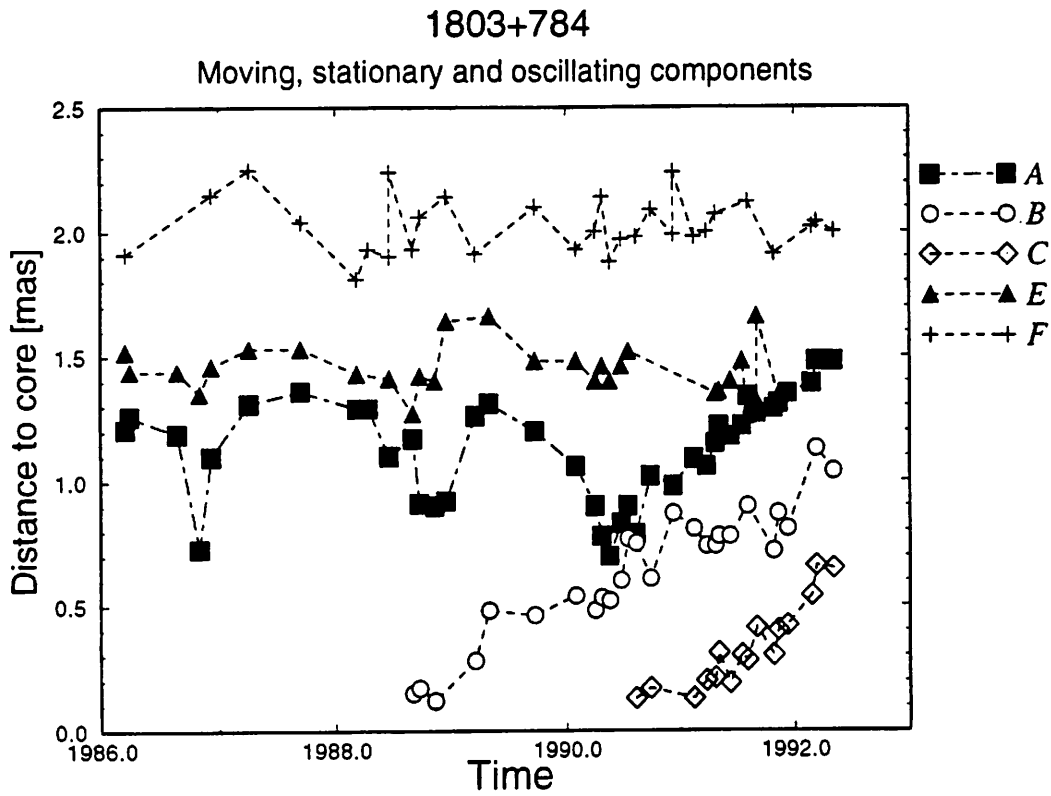


Figure 2: The structural evolution of the inner 2 mas separation to the core of 1803+784 shown for the period of 1986.21 to 1992.34. Individual components are marked by different symbols: the filled symbols (square and triangle) represent the oscillating components A and E respectively, 'plus' marks the stationary component F and circle and diamond demonstrate the movement of component B and C respectively. The error of the relative core separations is typically ± 0.15 mas.

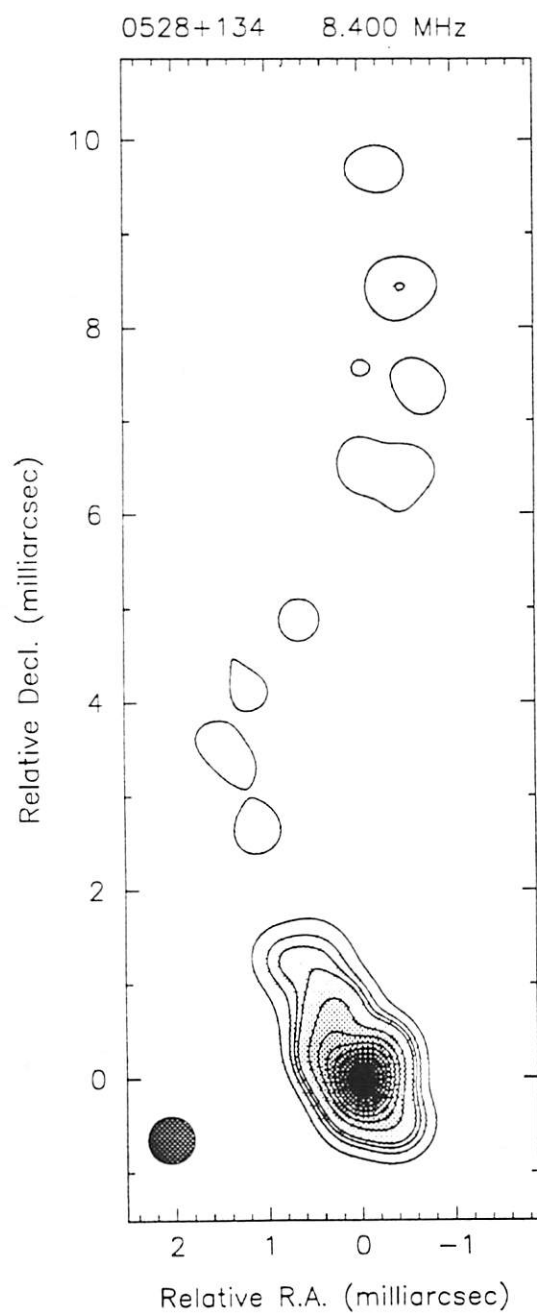


Figure 3: Clean-Map of 0528+134 restored with a circular beam of 0.5 mas. Contour levels are 2, 5, 7.5, 10, 20, ... and 80% of the peak flux density (0.60 Jy/beam). Five telescopes participated in this IRIS-S observations which took place on March 25, 1991. The underlying grey-scale denotes for the intensity ranging from black at the brightest, to white at zero intensity.

Superluminal motion in 0528+134

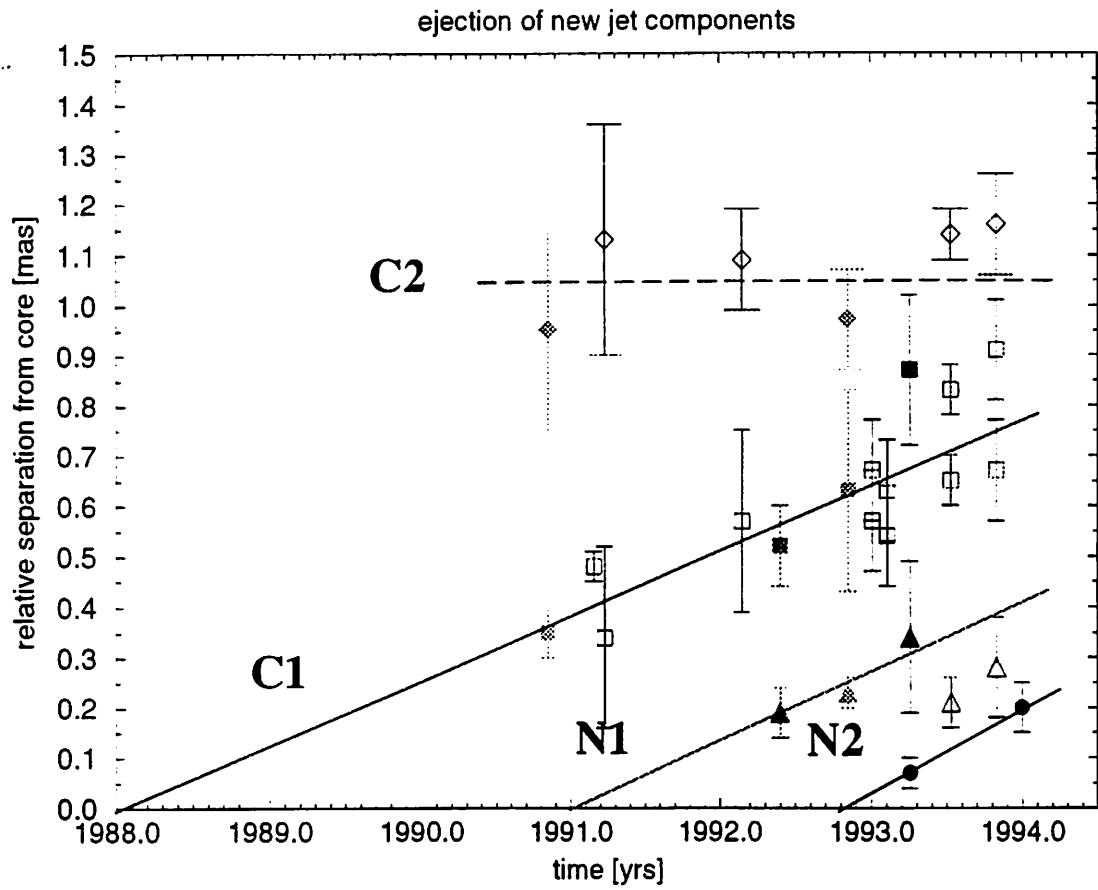


Figure 4: The motion of the inner jet components is shown for 0528+134. The plot results from VLBI measurements at mm-wavelengths (22, 43 & 86 GHz, filled symbols) by [6] and geodetic VLBI measurements (8.4 GHz, open symbols).

Absolute Proper Motion in the Quasar 4C39.25

J.C. GUIRADO¹, A. ALBERDI² and J.M. MARCAIDE³

¹ *Jet Propulsion Laboratory, California Institute of Technology, California 91109, USA*

² *Laboratorio de Astrofísica Espacial y Fundamental, INTA, 28080 Madrid, Spain*

³ *Departamento de Astronomía, Universidad de Valencia, 46100 Burjassot, Valencia, Spain*

Abstract. From a series of simultaneous 8.4 and 2.3 GHz VLBI observations of the quasar 4C39.25 phase-referenced to the radio source 0920+390 we have measured an eastward proper motion of component b in 4C39.25 of $90 \pm 43 \mu\text{s/yr}$. This proper motion is consistent with previous VLBI hybrid mapping results, which showed an internal proper motion of this component with respect to other structural components. Our differential astrometry analyses clarify the kinematics of 4C39.25, showing component b to be the one in motion and not the other as permitted by previous results from hybrid mapping.

1 Introduction

The radio source 4C39.25 (0923+392) is an 18th magnitude quasar with a redshift of 0.699 (Hewitt & Burbidge 1980). The milliarcsecond (mas) angular scale of 4C39.25 at cm-wavelengths consists of four components, labelled a, b, c, and d, from east to west. Since the early VLBI observations of Shaffer *et al.* (1977), components a and c have remained stationary with respect to each other, while component b (first identified by Marcaide *et al.* 1985) has been moving superluminally from near c towards a (Shaffer *et al.* 1987; Marscher *et al.* 1987; Schalinski *et al.* 1988; Marcaide *et al.* 1989; Marscher *et al.* 1991; Alberdi *et al.* 1993a). None of these three components had the inverted or flat spectrum associated with the core of a superluminal source. However, component d, detected via sensitive 22 GHz VLBI observations (Marcaide *et al.* 1990; Alberdi *et al.* 1993a), remains stationary with respect to a and c and possesses an inverted spectral index (Alberdi *et al.* 1993a,b) indicating that it could be the core of 4C39.25.

Based on these observational facts, Marcaide *et al.* (1989), Marscher *et al.* (1991), and Alberdi *et al.* (1993a) suggested a model for this source which has a relativistic bent jet; the knots a and c are associated with bends of the jet and b with a shock wave travelling along the jet from c towards a. In this model d is considered as the core of the radio source. Since this model is based on the assumption that both a and c are stationary, a much stronger constraint than existing observational evidence for relative stationarity would be evidence for (or against) stationarity with respect to an external reference (Marcaide *et al.* 1990).

With this purpose we carried out simultaneous 8.4/2.3 GHz VLBI observation on 4C39.25 phase-referenced to the nearby radio source 0920+390 (separated only by $0^{\circ}75$). While conventional VLBI mapping provides information only about the relative position between different features of a given radio source, phase-reference observations can provide precise positional information with respect to the external reference. The array was composed by the antennas at Westford (18m, USA), Wettzell (18m, Germany), Medicina (32m, Italy), Noto (32m, Italy), and the NASA tracking antenna at Madrid (70m, Spain); the data were correlated at the MPIfR correlator. This European interferometer (with the addition of the Westford antenna to gain intercontinental resolution in right ascension, the coordinate along b is seen to be moving in the hybrid maps) proved to be exceptional for astrometric purposes; its only drawback is the poor uv -coverage, which translates into maps with limited dynamic range (both 4C39.25 and 0920+390 are pointlike to our array at any of the observed frequencies). We overcame, in part, this problem with the help of high quality maps of 4C39.25 from a ten-station VLBI experiment on 4C39.25.

2 Astrometric Analysis

Our astrometric analysis of the data from each observing epoch is similar to that of previous astrometric studies that used phase delay, the most precise VLBI observable (Shapiro *et al.* 1979; Bartel *et al.* 1986; Guirado *et al.* 1995) that we outline briefly here:

- We corrected the phase delays for the 2π -ambiguities (the so-called “phase-connection” process), by comparison of the measured phases, with predictions from our high-accurate astrometric model for the geometry of the array (based on IERS values).
- We selected a reference point on the structure of the radio sources at each epoch and frequency.
- Using the previously selected reference point on each map of the radio sources as phase center, we removed the structure contribution to the phase delays.
- We used the unstructured- and connected- phase delays at both frequencies to remove the plasma effects.
- We formed the differenced phase delays between the two sources by subtracting the ionosphere-free phase delays from one of the sources to those of the other.
- Finally, we estimated the relative position at each epoch from a weighted-least-squares fit to the differenced phase delays.

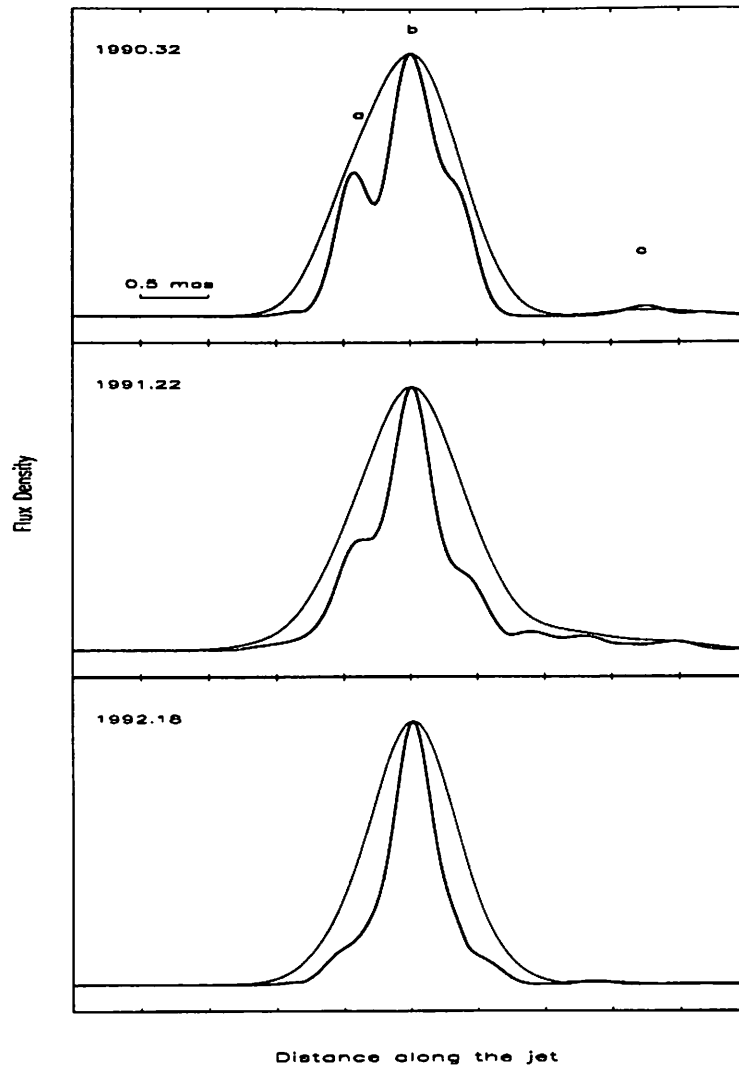


FIGURE 1. Flux-density profiles of 4C39.25 at 8.4 GHz for a position angle of 90° . For each epoch, we show the profiles constructed by using the synthesized beams and, superimposed, the profiles constructed by using a restoring beam (thick line) whose dimensions are twofold smaller than those of the synthesized beam. The peak of brightness (i.e. reference point for proper motion measurements) corresponds to the maximum of the over-resolved profiles. The components a and b can be distinguished in the first epoch, but appear partially and totally blended in the second and third epoch, respectively. Therefore, the reference-point location is approximately the brightness centroid of components a and b. Flux-density units are arbitrary.

The previous astrometric analysis is fully described in Guirado *et al.* (1995b). We emphasize that the reference-point selection is, by far, the most difficult step of our astrometric analysis, given the limited dynamic range of our maps. This selection process is crucial at 8.4 GHz: to determine proper motion, or to place a stringent bound on it, we should select as the reference point the same physical feature of the radio source at all the observing epochs (see Fig. 1): a wrong selection in one of the epochs may caused misleading estimates of the proper motion.

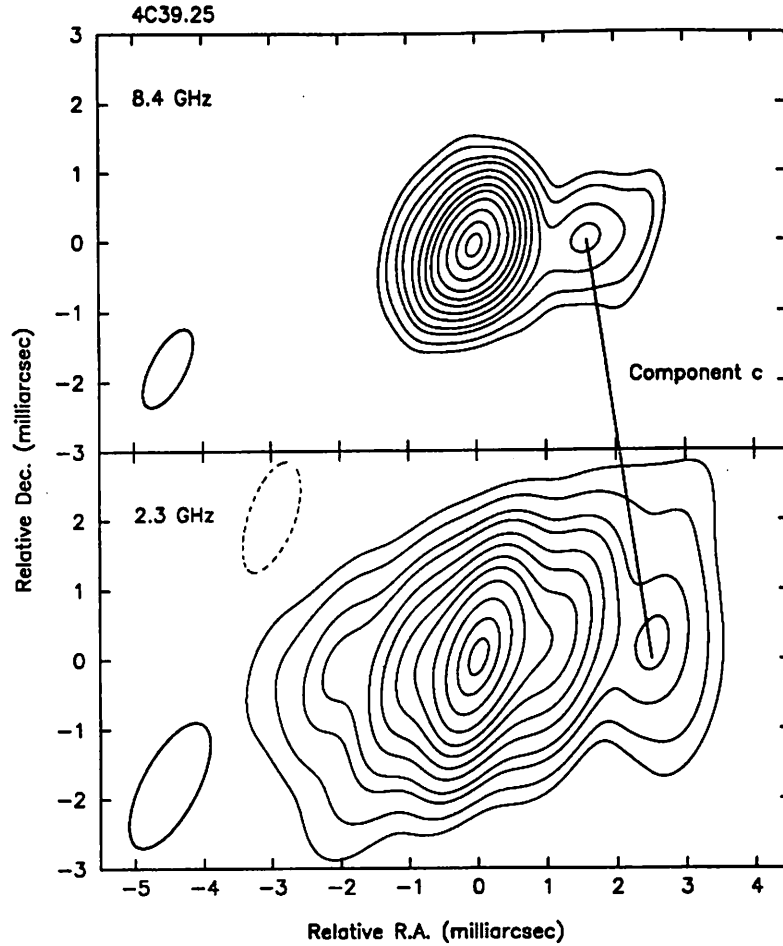


FIGURE 2. We used high-quality 8.4 and 2.3 GHz maps of 4C39.25 at epoch 1990.55 (Rioja 1993) to find their proper registration at 8.4 GHz and 2.3 GHz. We obtained this alignment by superimposing the region of 4C39.25 less affected by opacity effects, component *c* in this case. Contours are -1, 1, 2, 4, 6, 10, 15, 22, 30, 42, 60, 80, 95% of the peak of brightness of each map, 4.23 and 2.08 Jy/beam, respectively. Dashed lines correspond to negative contours. The sizes of the restoring beams, shown at the bottom left corners, are 1.21×0.62 mas with a major axis position angle of -18° for the 8.4 GHz map and 2.15×0.90 mas with a major axis position angle of -18° for the 2.3 GHz map (note that the latter map is over-resolved by a factor two with respect to the dimensions of the corresponding main lobe of the synthesized beam of the array).

The selection process at 2.3 GHz is not less important: since we combined the 8.4 GHz and 2.3 GHz data, as if the source positions were identical at the two frequencies, in order to estimate and remove the plasma contribution, the phase delays should be referred to the same points on the radio source structure (see Fig. 2). The sensitivity of our astrometric results to the uncertainty in selecting the reference points on the radio structures is shown (among other effects) in Table 1.

6. RESULTS

We used the relative coordinates and their associated standard errors (Table 1) in two separate weighted-least-squares analyses to estimate the proper motion in each coordinate (see Fig. 3):

$$\begin{aligned}\mu_\alpha &= 90 \pm 43 \text{ } \mu\text{as/yr} \\ \mu_\delta &= 7 \pm 68 \text{ } \mu\text{as/yr}\end{aligned}$$

where each error corresponds to one standard deviation. The proper motion obtained in right ascension between the adopted reference points in the two sources is significant at the two-standard-deviation level. In declination, the estimate of proper motion is not significantly different from zero; its uncertainty is larger than that of the right ascension, as expected from the geometry of our array.

The proper motion of the reference point of 4C39.25 with respect to that of 0920+390 is consistent with a motion of the component b along the jet of 4C39.25 from c towards a. This proper motion is compatible with the results inferred from the hybrid mapping of 4C39.25 (Marcaide *et al.* 1989; Marscher *et al.* 1991; Alberdi *et al.* 1993a) and together with them it shows that component b is moving from west to east, while the separation of components a and c remains fixed.

TABLE 1. Contributions, $\delta\Delta\alpha$ and $\delta\Delta\delta$, to the standard errors of the dual-frequency estimates of the sky coordinates of 4C39.25 with respect to those of 0920+390 obtained from the sensitivity study

Effect/Parameter	Epoch					
	1990.32		1991.22		1992.18	
	$\delta\Delta\alpha$ (μas)	$\delta\Delta\delta$ (μas)	$\delta\Delta\alpha$ (μas)	$\delta\Delta\delta$ (μas)	$\delta\Delta\alpha$ (μas)	$\delta\Delta\delta$ (μas)
8.4 GHz reference point identification	41	50	15	14	28	40
8.4/2.3 GHz map registration ¹	40	40	40	40	40	40
Earth's nutation	1	2	1	3	1	2
Statistical standard error ²	25	84	24	72	17	48
Root-sum-square of the above contributions	63	106	49	84	52	74

¹ Contribution due to the uncertainty in selecting the same reference point on the radio structure for the maps from the two frequency bands.

² Note that these uncertainties contain the contributions of the standard errors of the tropospheric zenith delays, site coordinates, reference source coordinates, Earth's pole coordinates, and UT1-UTC as they were estimated in our weighted-least-squares fits through the use of a priori covariances.

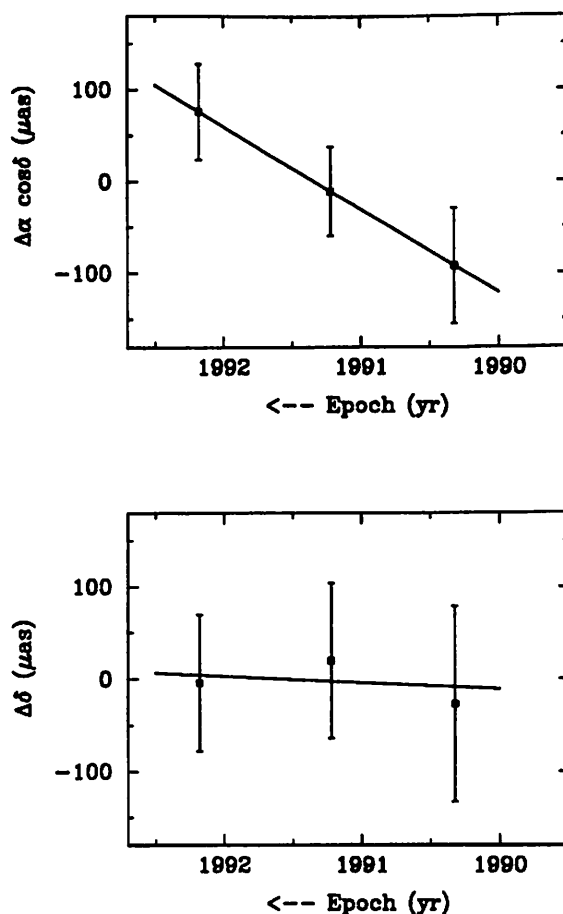


FIGURE 3. Proper motion of component b in 4C39.25 with respect to 0920+390. Values of proper motion in 4C39.25 are shown for three epochs. The straight lines shown represent the results of weighted-least-squares fits to the data for each coordinate separately. The origin for the relative right ascension (declination) is the weighted-mean of the relative right ascensions (declinations) from the three epochs: $3^m 48^s.5609770$ ($12' 40''.941822$).

However, none of the hybrid-map measurements determines, for example, whether a and c are stationary components and b a travelling one or vice versa. Our proper-motion measurements clarify the kinematics of component b, which has a proper motion in right ascension of 90 ± 43 $\mu\text{as/yr}$ relative to an external reference, 0920+390. In addition, the consistency of our measurement with the hybrid mapping results, and the stationarity of components a and c relative to each other (to within 30 μas ; Alberdi *et al.* 1995) implies that a and c are stationary with respect to the external reference, at least at the level of the combination of the uncertainties of both measurements.

With this determination of the proper motion of component b of 4C39.25 we have demonstrated the validity of an essential aspect of the phenomenological and numerical model for 4C39.25 proposed by Marcaide *et al.* (1989), Marscher *et al.* (1991), and Alberdi *et al.* (1993a). The moving character of component b is an argument in favor of its interpretation as a travelling shock wave.

REFERENCES

- Alberdi, A., Marcaide, J.M., Marscher, A.P., Zhang, Y.F., Elósegui, P., Gómez, J.L., and Shaffer, D.B. 1993a, *ApJ*, 402, 160
- Alberdi, A., Krichbaum, T.P., Marcaide, J.M., Witzel, A., Graham, D.A., Inoue, M., Morimoto, M., Booth, R.S., Rönnäng, B.O., Colomer, F., Rogers, A.E.E., Zensus, J.A., Readhead, A.C.S., Lawrence, C.R., Vermeulen, R., Bartel, N., Shapiro, I.I., and Burke, B.F. 1993b, *A&A*, 271, 93
- Bartel, N., Herring, T.A., Ratner, M.I., Shapiro, I.I., and Corey, B.E. 1986, *Nature*, 319, 733
- Guirado, J.C., Marcaide, J.M., Elósegui, P., Ratner, M.I., Shapiro, I.I., Eckart, A., Quirrenbach, A., Schalinski, C.J., and Witzel, A. 1995, *A&A*, 293, 613
- Hewitt, A., and Burbidge, G. 1980, *ApJS*, 43, 57
- Marcaide, J.M., Bartel, N., Gorenstein, M.V., Shapiro, I.I., Corey, B.E., Rogers, A.E.E., Webber, J.C., Clark, T.A., Romney, J.D., and Preston, R.A. 1985, *Nature*, 314, 424
- Marcaide, J.M., Alberdi, A., Elósegui, P., Schalinski, C.J., Jackson, N., and Witzel, A. 1989, *A&A*, 211, L23
- Marcaide, J.M., Alberdi, A., Elósegui, P., Marscher, A.P., Zhang, Y.F., Shaffer, D.B., Schalinski, C.J., Witzel, A., Jackson, N., and Sandell, G. 1990. In: *Parsec-scale Radio Jets*, Zensus, J.A., and Pearson, T.J. (eds.), Cambridge: Cambridge University Press, p. 236
- Marscher, A.P. 1987. In: *Superluminal Radio Sources*, Zensus, J.A., and Pearson, T.J. (eds.), Cambridge: Cambridge University Press, p. 280
- Marscher, A.P., Zhang, Y.F., Shaffer, D.B., Aller, H.D., and Aller, M.F. 1991, *ApJ*, 371, 491
- Rioja, M.J. 1993, Ph.D. thesis, Universidad de Granada
- Schalinski, C.J., Alberdi, A., Elósegui, P., and Marcaide, J.M. 1988. In: *The Impact of VLBI on Astrophysics and Geophysics*, IAU Symposium 129, Reid, M.J., and Moran, J.M. (eds.), Dordrecht: Kluwer Academic Publishers, p. 39
- Shaffer, D.B., Kellerman, K.I., Purcell, G.H., Pauliny-Toth, I.I.K., Preuss, E., Witzel, A., Graham, D., Schilizzi, R.T., Cohen, M.H., Moffet, A.T., Romney, J.D., and Niell, A.E. 1977, *ApJ*, 218, 353
- Shaffer, D.B., Marscher, A.P., Marcaide, J.M., and Romney, J.D. 1987, *ApJ*, 314, L1
- Shapiro, I.I., Wittels, J.J., Counselman III, C.C., Robertson, D.S., Whitney, A.R., Hinteregger, H.F., Knight, C.A., Rogers, A.E.E., Clark, T.A., Hutton, L.A., and Niell, A.E. 1979, *AJ*, 84, 1459

Gravitational Lens Image Astrometry

R.W.Porcass¹ and A.R.Patnaik¹

¹ Max-Planck-Institut für Radioastronomie, Auf dem Hügel 69, D-53121, Bonn, Germany.

Abstract

A standard astrometric problem is the registration of VLBI images of a radio source, from observations either at different epochs in proper motion studies, or at different frequencies in studying the spectral distribution across the source structure. Using normal astronomical mapping techniques, a certain amount of arbitrariness ('physical intuition'!) is involved, because absolute position information is not preserved. The technique of phase-referencing for close pairs (e.g. 1038+52A,B) can increase the objectivity of the registration. In the special case of gravitational lens images, however, the registration can be made in a completely objective way in certain circumstances. When one image is used as a phase reference for the other, there is the additional constraint that the 'target' and 'reference' source structures are the same, and are related by a 2×2 linear magnification matrix. The elements of the matrix (which are related to the gravitational potential distribution of the lensing object) can be determined if particular points within one image can be recognised in the other. Using this matrix, determined from one epoch (or frequency), maps at other epochs (or frequencies) can be registered, provided that the relative position between corresponding features in the two images can be measured in them. The process relies on the achromaticity of the gravitational lensing effect (for frequency registration) and on the stability of the lens gravitational field (for temporal registration). Some preliminary results from the gravitational lens system B0218+357 are presented.

1 Introduction

For VLBI geodesists, the ideal radio sky would consist of point radio sources, with stable positions, co-located at X- and S-band. Fortunately for astronomers, radio sources do not resemble GPS beacons in this way but generally consist of seething jets of plasma, whose study can be made into a respectable career. The X-band structures of sources observed during geodetic campaigns can be sufficiently complex that they introduce errors into geodetic delay measurements (Charlot et al. 1988, Gontier et al. 1993). The S-band structure may be different, and is often much more extended. A further (small) error in geodetic analysis arises if the X- and S-band mean 'positions' of a source do not coincide. Because the difference between the X- and S-band delays is assumed to arise in the ionosphere, and is used to correct the X-band delay, the resultant derived source position will be offset from the true X-band position, in the direction away from the S-band position by a fraction $\lambda_X^2 / (\lambda_S^2 - \lambda_X^2)$ of the X/S-band position offset.

In normal astronomical VLBI analysis, the hybrid mapping procedure used to reconstruct an image of the source results in the loss of the absolute position of the source structure. Thus the registration of maps made at different frequencies, or different epochs, requires some degree of physical insight. One method of solving this problem is to make phase-referencing observations, from which the map coordinates relative to a nearby reference source can be fixed. However, the reference source itself may have frequency- or time-dependent structure. The work of Marcaide and Shapiro (1984) and Rioja (1993) on the quasar pair 1038+52A,B made use of the interesting property that the 'target' and reference source structures were extended in roughly orthogonal directions; this makes it much easier to select the physically reasonable interpretation of the registration of the target and reference source maps at different frequencies and epochs. An interesting result from this study is that the position of the emission peak in the core of 1038+52A differs by 0.8 mas between S-and X-band.

2 VLBI observations of the gravitational lens B0218+357

The phenomenon of gravitational lensing provides an interesting opportunity to extend the 'objectivity' of map registrations at different frequencies and epochs. When the radiation from a distant source passes close to a massive galaxy on its path to an observer, it may be deflected by the gravitational field of the galaxy. In some cases multiple images of the source are seen by the observer. These will preserve the basic structure of the object, but may be magnified or demagnified, and can be stretched and distorted in a manner which depends on the gravitational potential experienced by the radiation, and its spatial derivatives. Studies of the relationship between two gravitational lens images of the same object provide a powerful tool for investigating the mass distribution of the intervening galaxy.

Although the chance of a favourable source-galaxy-observer alignment is small, there are about 10 known cases where a compact radio source is multiply imaged by the action of an intervening gravitational lens. We have been making a multi-frequency VLBI study of one of these systems, B0218+357 (Patnaik et al., 1993). In this system there are two images of the background source, separated by only 0.335 arcsec. We observed at 15 GHz using the VLBA (Patnaik et al., 1995), and at 5 and 1.7 GHz using a 'global' array of EVN and US antennas. The 'A' and 'B' 15 GHz images of B0218+357 are shown in Fig. 1. It is apparent that the basic source morphology is the same in both images, consisting of 2 components with a flux ratio of 1.7. We label the western and more compact component in both images as component 1. Component 2 lies to the east and is more resolved. The orientation of the source structure is different in the images, however. The A image covers a larger area (it also has a higher flux density) and the two components appear stretched in PA -40° , compared to their counterparts in the B image.

The effect of the gravitational field upon the rays making up the two different images is summarised by the image relative magnification matrix, M , which describes the mapping of one image into the other. We take as reference points the positions of component 1 (the 'core') in the B0218+357 images A and B. For every other point in B, its position (x_b, y_b) w.r.t. the core is transformed by M to the corresponding point (x_a, y_a) w.r.t. the core in A. The elements of M can be determined if one can identify many pairs of corresponding points in the two images. In addition, the determinant of M is given by the ratio between corresponding areas in A and B. One property of gravitational lenses is that the surface brightness of the unlensed source is preserved by the lens, and so the resolved components must appear with the same surface brightness in both the lensed images. Thus the determinant of M is also given by the flux density ratio, S_a/S_b , of

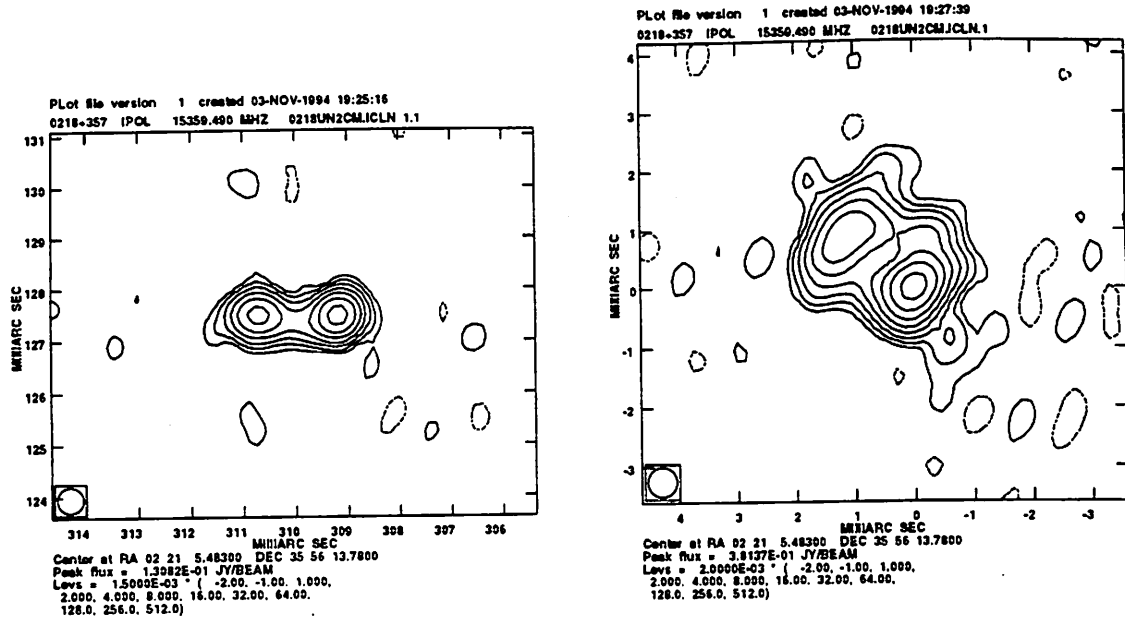


Figure 1: 15 GHz VLBA maps of B0218+357 images A (right) and B (left) with a resolution of 0.5 mas. The contour levels for image B are 1.5 mJy/beam \times (-1, 1, 2, 4, 8, 16, 32, 64, 128) and the peak flux density is 130.8 mJy/beam. The contour levels for image A are 2.0 mJy/beam \times (-1, 1, 2, 4, 8, 16, 32, 64, 128, 256) and the peak flux density is 381.4 mJy/beam. The CLEAN beam of 0.5 mas is drawn in the bottom left hand corner of each panel.

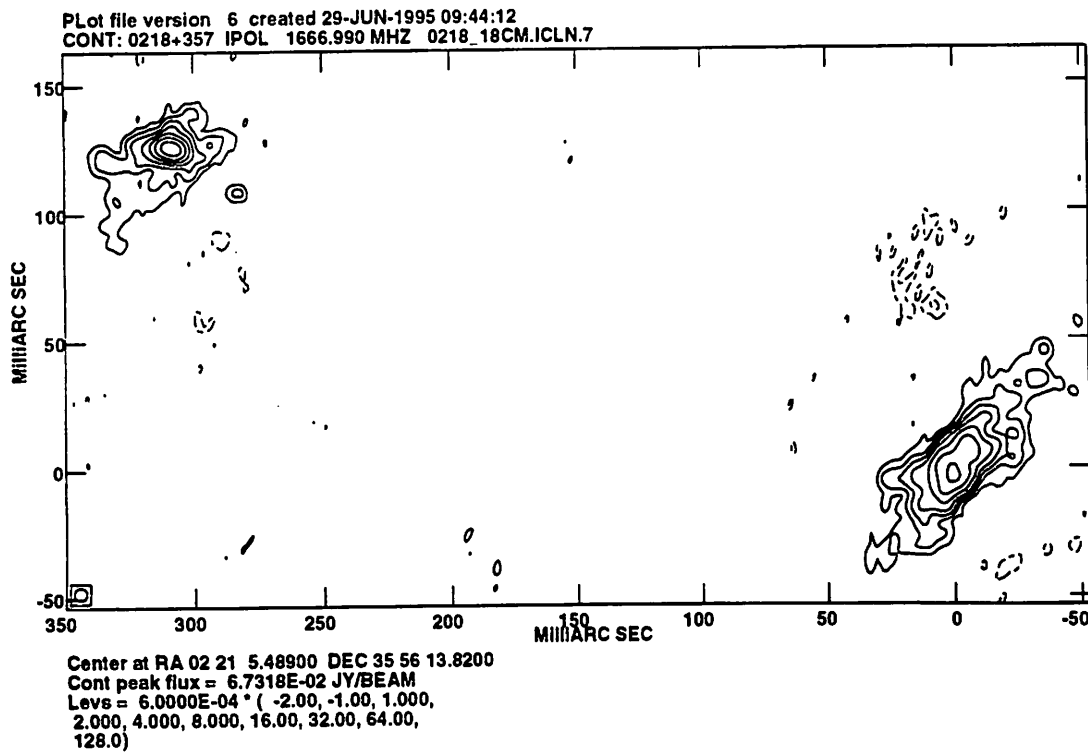


Figure 2: VLBI map of B0218+357 with a resolution of 5mas at 1.7GHz.

corresponding features.

We have used the positions of component 2 in A and B, the flux density ratio ($A/B = 3.7$) and the angle of an off-axis extension of the core (which is above the source axis line in A and below it in B, because of the opposite parities of the two images) to calculate the 4 elements of M : $m_{11} = 0.730$, $m_{12} = 2.137$, $m_{21} = 0.591$, $m_{22} = -3.232$. Note that the matrix eigenvectors are in PA 82.1° (transforms to 82.1°) and 153.5° (transforms to -26.5°). These elements are a property of the gravitational field of the lens only. Since gravitational lensing is an achromatic process, the elements can also be used to relate pairs of images at different frequencies.

Now we return to the topic of image astrometry. Because the image separations in gravitational lens systems are small (ranging from 0.3 to 6 arcsec in known systems) the relative separation between images can be measured to high accuracy using VLBI phase-referencing, or equivalently, simply making a map containing both images. For example, we measure the separation between the A and B images of the core in B0218+357 at 15 GHz as $\Delta X_c = -309.2$ mas, $\Delta Y_c = -127.5$ mas ($A - B$). Because the two images have different sizes and orientations, the separations between other pairs of corresponding points in the images (e.g. component 2) are different. For a point at position (x_b, y_b) in B, the separation from its corresponding point in A is given by:

$$\Delta X = \Delta X_c + x_a - x_b = \Delta X_c + (m_{11} - 1) x_b + m_{12} y_b$$

$$\Delta Y = \Delta Y_c + y_a - y_b = \Delta Y_c + (m_{21} - 1) x_b + m_{22} y_b$$

or in vector notation: $\Delta \mathbf{X} = \Delta \mathbf{X}_c + (M - I)\mathbf{x}_b$ (where I is the unit matrix). Thus, for every point (x_b, y_b) in B there corresponds a unique separation $(\Delta X, \Delta Y)$ from its corresponding point in A, and conversely, every measured value of a separation between corresponding points in the two images can be converted into a unique location in the B image.

Now we can use the time stability and achromaticity properties of the lens gravitational potential to register maps at different epochs and frequencies. We must first locate a pair of corresponding points in the second map, e.g. a map of B0218+357 at 1.7 GHz, and measure their separation $\Delta X, \Delta Y$. Then, using the above relation we can calculate the position (x_b, y_b) of this point in B, w.r.t. the 15 GHz core location. In fact, the 1.7 GHz VLBI images of B0218+357 are rather amorphous (Fig 2) and there is no obvious feature which can be clearly identified in both the A and B images. However, we have calculated the centroid positions of both the A and the B image brightness distributions: these are relatively stable to variations of the lowest brightness level considered, and can be estimated to an accuracy of ca. 0.3 mas. It is easy to show that the centroids are corresponding points in the images. Their separation is $\Delta X = -309.5$ mas, $\Delta Y = -126.6$ mas, and this corresponds to a point roughly 2 mas to the east of the 15 GHz core in B, i.e. very close to component 2 at 15 GHz. One should perhaps treat this result with caution, because the image sizes at 1.7GHz are larger than at 15 GHz, and the relative magnification between the images can change if their sizes are not \ll the scale size of the lens. However, it does illustrate the principle of this method of registration.

In this example we used the achromatic property of gravitational lensing to register maps made at different frequencies. The same technique can be used to register maps made at the same frequency but at different epochs. We hope to do this for future 15 GHz observations of B0218+357; if there are structural changes, and in particular a change of separation between the two major components, we will be able to determine which, if any, of the radio components is stationary. In this case we make use of the stability of the gravitational potential of the lens over the time scale

of the separation between the observing epochs.

Acknowledgements We wish to thank Ian Browne and Sunita Nair for many interesting discussions.

3 References

- Charlot, P., Lestrade, J-F., and Boucher, C., 1988, Proc. IAU Symp. 129, eds. Reid and Moran, Kluwer, p33
- Gontier, A-M., Britzen, S., Witzel, A., Schalinski, C.J., and Campbell, J., 1993, Proc. 9th Working Meeting, Bonn, p167
- Marcaide, J.M. and Shapiro, I.I. 1984, Ap.J., 276, 56
- Patnaik, A.R. et al., 1993, MNRAS, 261, 435
- Patnaik, A.R., Porcas, R.W. and Browne, I.W.A., 1995, MNRAS, 274, L5
- Rioja, M.J. 1993, Proc. 9th Working Meeting, Bonn, p152

Did the Matera Radiotelescope Really Observe the Jupiter/SL9 "T" impact?

Giuseppe Bianco¹, Luciano Garramone² and Roberto Lanotte²

¹ Agenzia Spaziale Italiana, Centro di Geodesia Spaziale "G. Colombo", Matera, Italy

² Nuova Telespazio S.p.A., Centro di Geodesia Spaziale "G. Colombo", Matera, Italy

Abstract. We report evidence of the possible detection of a radio outburst in the X-band emission from Jupiter in close proximity with the expected time for the impact of the fragment T of the comet Shoemaker-Levy 9.

1. Introduction

In the second half of July, 1994, mankind has had the opportunity to witness an extremely rare event, such as the crash of the comet 1993e, named Shoemaker-Levy 9 after its discoverers, on the biggest planet of the solar system, Jupiter. In that period, virtually every available astronomical instrument, both from the space and from the surface of the earth, has been monitoring the phenomenon in several regions of the electromagnetic spectrum.

The event has gone far beyond the expectations in the visible and in the infrared, where huge fireballs, plumes and spots have dramatically modified the appearance of Jupiter's surface for many days.

In the region of centimetric wavelengths, a steady increase of Jupiter's flux has been observed in the period of the crash, but no abrupt events in conjunction with the single crashes have been reported to date.

2. Observations

Our radiotelescope was available for observations only at the end of the impact period, when the major fragments had already crashed onto Jupiter's atmosphere. Nevertheless, we decided to try to monitor Jupiter's emission in the X-band in a short period around the expected time for the T impact, namely July 21st, 1995, 18:23 UT.

To do that, we set up the 20-m Cassegrain radiotelescope in "single dish" configuration; we have been observing the emission in the whole X-band (8180-8580 MHz) by measuring the total power over 400 MHz, using the Mark-III Field System command TPI (*Total Power Integrator*).

The observing sequence has been the following:

Cold sky - Jupiter - Cold sky - (calibrator) - ...

in order to "sandwich" each observation between two sky background readings.

The calibrator has been 3C-273, whose X-band flux density is about 30-40 Jy, because it was close enough to Jupiter in the sky to allow a reasonably fast switching. Each single measurement was obtained by averaging 3 consecutive readings (one every

5 sec) for each "object" in the sequence. The duty cycle between sources and cold sky has been 50%. The first part of the observing session has been plagued by a strong thunderstorm which fortunately vanished about one hour before the expected impact time. The remaining observations have been carried out under clear sky conditions; the stability of the atmosphere is confirmed by the measured values of the main meteorological parameters (temperature T, pressure P and humidity H) in the period of interest:

$$T \approx 20^{\circ}\text{C} \pm 0.5^{\circ}\text{C}$$

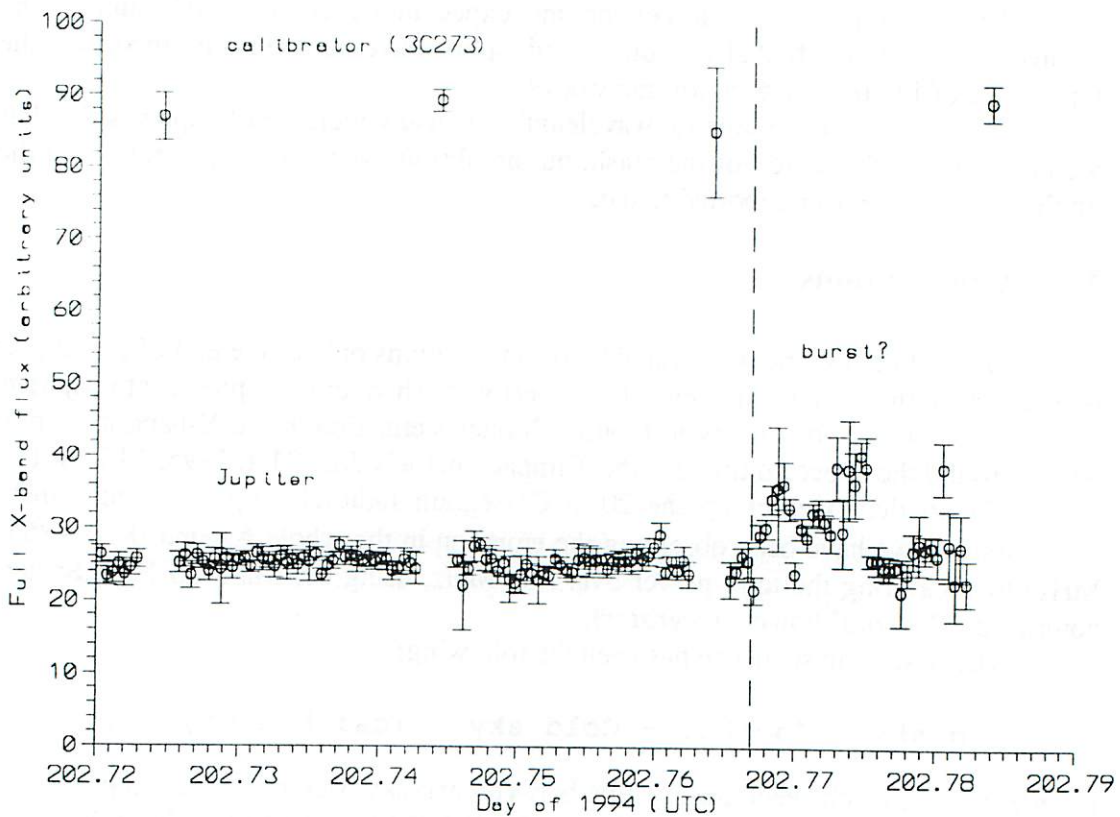
$$P \approx 953.5 \text{ mB} \pm 0.5 \text{ mB}$$

$$H \approx 82\% \pm 2\%$$

3. Results

Each 3-readings sequence on each object has been averaged to obtain a normal point. Then, the interpolated value of the sky background emission has been subtracted from each observation on Jupiter and 3C-273; the error propagation has been taken into account in a quite conservative way.

The figure below shows the complete series of corrected normal points on Jupiter and 3C-273. The error bars indicate the propagated 1- σ formal error, while the vertical dashed line indicates the expected T impact time.



3. Conclusions

The most important feature in our observations is the coincidence between the expected impact time and the start of the observed burst. The observed X-band flux from Jupiter had an apparent increase of about 30% with respect to the “steady” level observed before; the apparent duration of the phenomenon has been about 15 minutes.

The T impact has been one of the very few which have not been reported from visual or infrared monitoring. Since it was known to be one of the smallest fragments of the comet, the relatively small impact energy could have caused an emission in a longer wavelength region of the spectrum than in the infrared or in the visual.

Theoretical calculations and simulations could eventually corroborate this hypothesis, since the observation do not seem to allow to draw any firm conclusion.

Author Index

Alberdi, A., 22, 141, 181
Alcolea, J., 27
Alef, W., 11, 154, 160, 164
Ardenne, A. van, 160
Asaki, Y., 160

Barcia, A., 27
Bregman, J., 160
Bianco, G., 49, 109, 193
Bondi, M., 154
Boonstra, A.-J., 160
Britzen, S., 172
Butcher, H.R., 160

Campbell, J., 79, 91
Carlsson, T.M., 32
Carlsson, T.R., 32, 69, 148
Cenci, A., 49
Claussen, M.J., 160
Colomer, F., 27
Colucci, G., 49

Dallacasa, D., 154
Del Rosso, D., 49

Elgered, G., 32, 69, 134, 148

Fermi, M., 109
Foley, A.R., 160
Fomalont, E.B., 160

Gómez-González, J., 27
Galledo, J.D., 27
Garramone, L., 49, 193
Garrido, J.E., 27
Greve, H. van S., 160
Guirado, J.C., 181
Gurvits, L.I., 160

Haas, R., 91, 121
Hase, H., 57
Hernández-Pajares, M., 141

Jaldehyag, R.T.K., 32
Jarlemark, P.O.J., 32
Johansson, J.M., 32, 134, 148
Juan, J.M., 87, 141

Kalmann, H., 160
Keihm, S., 134
Krichbaum, T.P., 172

López-Fernández, I., 27
Lanotte, R., 109, 193
Liechti, S., 27

Müskens, A., 11
Maccaferri, G., 45
Mantovani, F., 16, 154
Marcaide, J.M., 181
Mariotti, S., 45
Morsiani, M., 45

Nilsson, B.I., 32
Nothnagel, A., 121

Orfei, A., 16, 45

Parea, J.A., 22
Patnaik, A.R., 188
Pettersen, B.R., 29
Pilhatsch, M., 121
Porcas, R.W., 38, 188

Rönnäng, B.O., 32
Reinhold, A., 66
Rioja, M.J., 160, 164
Rius, A., 22, 87, 134, 141

Sardón, E., 141
Sasao, T., 160
Scherneck, H.G., 32
Schilizzi, R.T., 160
Schuh, H., 51, 91
Spoelstra, T.A.Th., 160
Standke, K., 1

Thorandt, V., 68
Tomasi, P., 16
Tornatore, V., 39

Ullrich, D., 68

de-Vicente, P., 27

Wojdziak, R., 66

Zacchioli, G., 45
Zarraoa, N., 87, 103, 134

List of Participants

Antonio Alberdi (Colaborador Cientifico)	LAEFF - INTA P.O. Box 50727 28080-Madrid Spain	Phone: -34-1-813 1267 Fax: -34-1-813 1160 Internet: alberdi@laeff.esa.es
Walter Alef (Astronomer, friend of) the MK3 correletor in Bonn)	Max-Planck-Institut fuer Radioastronomie Auf dem Huegel 69 D-53121 Bonn Germany	Phone: (49)-228-525-289 Fax: (49)-228-525-229 Internet: walef@mpifr-bonn.mpg.de
Giuseppe Bianco (Space Geodesy Program Manager)	Agenzia Spaziale Italiana Centro di Geodesia Spaziale Contrada Terlecchia P.O. Box 11 75100 Matera Italy	Phone: +39-835-377209 Fax: +39-835-339005 Internet: bianco@asimt0.mt.asi.it
Agata Buemi (Scholarship holder)	Istituto di Radioastronomia CNR Stazione radioastronomica di Noto Contrada Renna Bassa Localita' Case di Mezzo C.P.169 I-96017 Noto (SR) Italy	Phone: +39 931 835622 +39 931 835002 +39 931 835042 Fax: +39 931 573265 Internet: abuemi@ira.noto.cnr.it
Silke Britzen (Ph.D. student)	Max-Planck-Institute fuer Radioastronomie Auf dem Huegel 69 53115 Bonn Germany	Phone: +49 228 525217 Fax: +49 228 525229 Internet: p660sil@mpifr-bonn.mpg.de
James Campbell	Geodetic Institute of the University of Bonn Nussallee 17 D-53115 Bonn Germany	Phone: +49 (228) 733562 Fax: +49 (228) 732988 Internet: jcampbell@kuestner.geod.uni-bonn.de
Ragne Carlsson (Phd student)	Onsala Space Observatory 439 92 Onsala Sweden	Phone: +46-31-7725575 Fax: +46-31-7725590 Internet: rtc@gere.oso.chalmers.se
Alberto Cenci	Nuova Telespazio S.p.A. Via Tiburtina 965 00156 Roma Italy	Phone: +39-6-40793861 Fax: +39-6-40793638 Internet: tpz3@icnucevm.cnuce.cnr.it
Patrick Charlot	Observatoire de Paris 61 Avenue de l'Observatoire 75014 Paris France	Phone: 33 1 40 51 22 30 Fax: 33 1 40 51 22 91 Internet: charlot@mesioa.obspm.fr DECnet: mesioa::charlot
Francisco Colomer (VLBI coordinator)	Observatorio Astronomico Nacional Centro Astronomico de Yebes Apartado de Correos 148 E - 19080 Guadalajara Spain	Phone: 34-49-290311 Fax: 34-49-290063 Internet: colomer@cay.es
Giuseppe Colucci	Nuova Telespazio S.p.A. Centro di Geodesia Spaziale Contrada Terlecchia P.O. Box 155 75100 Matera Italy	Phone: +39-835-377291 Fax: +39-835-334951 Internet: colucci@geodaf.mt.asi.it
Domenico Del Rosso	Nuova Telespazio S.p.A. Centro di Geodesia Spaziale Contrada Terlecchia P.O. Box 155 75100 Matera Italy	Phone: +39-835-377230 Fax: +39-835-334951 Internet: laser@asimt0.mt.asi.it
Gunnar Elgered	Onsala Space Observatory Chalmers University of Technology S - 439 92 Onsala Sweden	Phone: +46 31 772 5565 Fax: +46 31 772 5590 Internet: kge@oso.chalmers.se

Marco Fermi	Nuova Telespazio S.p.A. Via Tiburtina 965 00156 Roma Italy	Phone: +39-6-40793862 Fax: +39-6-40793638 Internet: tpz3@icnucevm.cnuce.cnr.it
Luciano Garramone	Nuova Telespazio S.p.A. Centro di Geodesia Spaziale Contrada Terlecchia P.O. Box 155 75100 Matera Italy	Phone: +39-835-377272 Fax: +39-835-334951 Internet: vlbi@asimt0.mt.asi.it
Jose Carlos Guirado	Jet Propulsion Laboratory (MS 238-332) 4800 Oak Grove Dr Pasadena, CA 91106 USA	Phone: 818 393 2657 Fax: 818 393 6890 Internet: jcg@fora.jpl.nasa.gov
Ruediger Haas	Geodetic Institute of the University of Bonn Nussallee 17 D-53115 Bonn Germany	Phone: +49 (228) 733562 Fax: +49 (228) 732988 Internet: haas@kuestner.geod.uni-bonn.de
Hayo Hase (Geodetic Engineer)	Institute for Applied Geodesy Fundamental Station Wettzell D-93444 Koetzing Germany	Phone: +49-9941-603-0 +49-9941-603-104 Fax: +49-9941-603-222 Internet: hase@wettzell.ifag.de DECnet: WVAX1::HASE
Richard Kilger (Staff member)	Technical University Munich Fundamental Station Wettzell 93444 Koetzing Germany	Phone: +49-9941-603-0 +49-9941-603-263 Fax: +49-9941-603-222 Internet: kilger@wvax1.dnet.nasa.gov DECnet: WVAX1::VLBI
Roberto Lanotte (Geodynamics data analyst)	Nuova Telespazio S.p.A. Centro di Geodesia Spaziale Contrada Terlecchia P.O. Box 155 75100 Matera Italy	Phone: +39-835-377238 Fax: +39-835-334951 Internet: lanotte@hp755.mt.asi.it
Franco Mantovani (Scheduler, Medicina Station)	Istituto di Radioastronomia Via P. Giobetti 101 I-40129 Bologna Italy	Phone: +39 51 6399377 +39 51 6399385 Fax: +39 51 6399431 Internet: fmantovani@astbo1.bo.cnr.it
Arno Mueskens	Geodetic Institute of the University of Bonn Nussallee 17 D-53115 Bonn Germany	Phone: +49 (228) 733562 Fax: +49 (228) 732988 Internet: am@hp.mpifr-bonn.mpg.de
Nikolai Nesterov (Leading Research Worker, VLBI Friend)	Simeiz Station Crimean Astrophysical Observatory Laboratory of Radio Astronomy RT-22 Katsiveli Crimea 334247 Ukraine	Phone: +7-0654-727952 Fax: +7-0654-727961 Internet: nesterov@rt22.crimea.ua
Axel Nothnagel	Geodetic Institute of the University of Bonn Nussallee 17 D-53115 Bonn Germany	Phone: +49 (228) 733562 Fax: +49 (228) 732988 Internet: nothnagel@uni-bonn.de
Alessandro Orfei	Istituto di Radioastronomia Via P. Giobetti 101 I-40129 Bologna Italy	Phone: Fax: Internet: orfei@astbo1.bo.cnr.it
Bjorn Ragnvald Pettersen (Chief of the Space Related Research Group)	Geodetic Institute, Statens kartverk Kartverksveien N-3500 Honefoss Norway	Phone: +47 32 11 83 15 +47 32 11 81 00 Fax: +47 32 11 81 01 Internet: bjornrp@gdiv.statkart.no
Richard Porcas (Staff Scientist)	Max-Planck Institut fuer Radioastronomie Auf dem Huegel 69 D 53121 Bonn Germany	Phone: +49-228-525288 Fax: +49-228-525229 internet: porcas@mpifr-bonn.mpg.de

Maria Jose Rioja (Support Scientist)	Joint Institute for VLBI in Europe Radio Observatory P.O. Box 2 Germany Max-Planck Institut fuer Radioastronomie Auf dem Huegel 69 53121 Bonn Germany	Phone: +31 (0)5219 7244 Fax: +31 (0)5219 7332 Internet: rioja@nfra.nl Phone: (+49) 228 525-0 / -245 Fax: (+49) 228 525 229 Internet: rioja@mpifr-bonn.mpg.de
Antonio Rius (Investigador Cientifico)	Consejo Superior de Investigaciones Cientificas Instituto Nacional de Tecnica Aeroespacial Centre de Estudis Avancats de Blanes Cami de Santa Barbara s/n Blanes Spain	Phone: 34-72-336102 Fax: 34-72337806 Internet: rius@mach.laef.es
Harald Schuh	Deutsches Geodaetisches Forschungsinstitut Marstallplatz 8 D-80539 Muenchen Germany	Phone: +89 23031 214 Fax: +89 23031 240 Internet: schuh@dgfi.badw-muenchen.de
Kurt Standke	Geodetic Institute of the University of Bonn Nussallee 17 D-53115 Bonn Germany	Phone: +49 (228) 733562 Fax: +49 (228) 732988 Internet: p621kst@mpifr-bonn.mpg.de
Carlo Stanghellini (Scholarship holder)	Istituto di Radioastronomia CNR Stazione radioastronomica di Noto Contrada Renna Bassa Localita' Case di Mezzo C.P.169 I-96017 Noto (SR) Italy	Phone: +39 931 835042 Fax: +39 931 573265 Internet: carlo@eloro.ira.noto.cnr.it
Oleg A. Titov (Scientific researcher)	Institute of Applied Astronomy Saint-Petersburg Russia, 197042	Phone: 123-44-52 Fax: 230-74-13 Internet: titov@ipa.ioffe.rssi.ru
Paolo Tomasi (Scientist)	IRA CNR Via Gobetti 101 40129 Bologna Italy	Phone: 39 51 6399388 Fax: 39 51 6399431 Internet: tomasi@boira6.bo.cnr.it
Vincenza Tornatore (Research worker)	Istituto di Radioastronomia CNR Stazione radioastronomica di Noto Contrada Renna Bassa Localita' Case di Mezzo C.P.169 I-96017 Noto (SR) Italy	Phone: +39 931 835622 +39 931 835002 +39 931 835042 Fax: +39 931 573265 Internet: tornatore@astbol.bo.cnr.it
Alexandre Evgen'evich Volvatch (Junior research worker)	Simeiz station Laboratory of Radio Astronomy of Crimean Astrophysical Observatory RT-22 Yalta, Katzively 334247, Crimea Ukraine	Phone: +7 0654 727991 Fax: +7 0654 727961 Internet: volvatch@rt22.crimea.ua
Nestor Zarraoa (Researcher)	DLR Fernerkundungsstation Neustrelitz Kalkhorstweg 53 17235 Neustrelitz Germany	Phone: Fax: +49-3981-480299 Internet: zarraoa@nz.dlr.de